PREDICT TB

Prevention of Resistance, Evaluation of Diagnostics and
Intensified or Custom-made Treatment of Tuberculosis

JURRIAAN E.M. DE STEENWINKEL

PREDICT TB

Prevention of Resistance, Evaluation of Diagnostics and Intensified or Custom-made Treatment of Tuberculosis

Voorkomen van resistentie, evaluatie van diagnostiek en
intensivering van de behandeling van Tuberculose

Proefschrift

ter verkrijging van de graad van doctor aan de
Erasmus Universiteit Rotterdam
op gezag van de rector magnificus
Prof.dr. H.G. Schmidt
en volgens besluit van het College voor Promoties

De openbare verdediging zal plaatsvinden op
vrijdag 16 november 2012 om 11.30 uur

door

Jurriaan Evert Mathijs de Steenwinkel
geboren te Brussel

CONTENTS

Chapter 1

General introduction and outline of the thesis

Tuberculosis (TB) caused by *Mycobacterium tuberculosis* (Mtb) is still a global health problem of immense proportion. Indeed, TB is considered the second most frequent cause of infectious disease-related death worldwide (after HIV-AIDS). The World Health Organization (WHO) is increasing its efforts to reduce the global threat of TB. Nevertheless, the morbidity and mortality statistics for TB remain shocking. For example, the WHO estimates that the global burden of disease caused by TB in 2010 comprised 8.8 million incident cases, including 1.1 million deaths from TB among HIV-negative individuals, and an additional 0.35 million deaths from HIV-associated TB.[1]

Additional to these impressive figures is the underlying problem of latent TB infections, with as many as one-third of the world's population being thought to be latently infected with this bacterium, an immense pool of potential patients around. Further, all current treatment programs tend to be specifically aimed towards the treatment of active TB infection, leaving the huge underlying problem of latent TB infections untouched, essentially meaning that the worldwide elimination of TB is still a distant dream.

The **diagnosis** of TB can be complex and challenging. Differentiating between latent TB infection and active TB is of vital importance, though not always easy for the clinician. The tools available for diagnosing TB infections are diverse and available in several different combinations. First and most important remains the direct detection of Mtb in sputum and other fluids, for example via the microscopic determination of bacilli, bacterial culture, or amplification of Mtb-specific genes, which are considered the "gold" standard techniques for TB diagnosis. Secondly, diagnosis can be made via the recognition of TB in terms of disease presentation e.g. patient anamnesis or chest radiography, or the detection of a TB-specific host immune response e.g. the tuberculin skin test (TST) or interferon gamma (IFN-γ) release assays (IGRA). Both TST and IGRA are based on detection and recognition of Mtb antigens by cells of the immune system and a subsequent immune response. Unfortunately, one major limitation of the use of gold standard techniques for TB diagnosis is that these tests may take as long as 6 weeks to produce a result. This means that more rapid TB detection is urgently required in order to begin effective treatment as soon as possible. Several studies are currently ongoing to try to identify and validate biomarkers for the detection of active TB infection, among which IFN-γ (detected via the IGRA technique) is one of the most promising potential biomarkers. All these efforts to make a correct diagnosis are most important because if left untreated, TB can be a fast developing, lethal infection. However, it should be remembered that the treatment of TB is lengthy, complicated and not without side-effects, such that anti-TB therapy should ideally only be given to those who need it.

The current six-month standard **treatment** of TB, as recommended by the WHO, and incorporated into numerous national and international guidelines, consists of an initial phase

of therapy which is then followed by a continuation phase of treatment.[2] During the first two months (initial phase), the **first-line anti-TB drugs**; isoniazid, rifampicin, ethambutol and pyrazinamide are administered, whereas in the subsequent four months (continuation phase) only isoniazid and rifampicin are prescribed.

The mode of action of the anti-TB drugs is (in short); isoniazid inhibits the synthesis of mycolic acid, a component of the mycobacterial cell wall; rifampicin inhibits bacterial DNA-dependent RNA synthesis; ethambutol acts by obstructing the formation of the cell wall; pyrazinamide inhibits the enzyme fatty acid synthase, required to synthesize fatty acids.

Isoniazid, in the multidrug combination therapy, is regarded as the most potent drug available in reducing Mtb load and acts primarily by killing extracellular Mtb.[3-4] The extraordinary killing capacity of isoniazid is clearly demonstrated by its high early bactericidal activity (EBA).[5] In fact, the bacterial load is dramatically reduced in the first days of isoniazid treatment, greatly decreasing the risk of selecting resistant bacteria. Rifampicin and pyrazinamide become more effective in their bactericidal activity after the first few days of therapy. The major role of rifampicin is to "sterilize" the infected tissues, helping to ensure that persistent (low active / slow dividing) Mtb is killed. These persistent Mtb are considered to be responsible for relapses in infection, thus requiring lengthy duration of treatment to eliminate all infecting Mtb. The role of ethambutol is to prevent selection and/or growth of drug-resistant Mtb at the start of TB treatment when the susceptibility pattern of the infecting Mtb is still unknown and there exists the possibility of Mtb resistance to isoniazid, rifampicin or pyrazinamide. Once it is known that the Mtb is susceptible to isoniazid, rifampicin and pyrazinamide, the ethambutol can be stopped, since its use is then of no added value in the killing of a susceptible Mtb.

In cases of single- or multidrug resistance of Mtb towards the first-line anti-TB drugs, an alternative to the standard treatment regimen is required. These alternative treatments comprise a combination of any of the still active first-line anti-TB drugs, combined with additional second- or even third-line anti-TB drugs. Among the **second-line anti-TB drugs** are: aminoglycosides (e.g. streptomycin, amikacin or kanamycin), fluoroquinolones (e.g. moxifloxacin or levofloxacin), thioamides (e.g. ethioamide), para-aminosalicylic acid and polypeptides (e.g. capreomycin). The most prominent drugs in the group of **third-line anti-TB drugs** are linezolid, clarithromycin, amoxicillin-clavulanic acid and clofazimine. These anti-TB drugs are classified as second- or third-line choices of TB therapy rather than standard treatments per se, the reasons for this being the fact that; 1) there is (still) insufficient clinical experience when using these antibiotics; 2) these drugs possess a less potent pharmacokinetic profile in comparison to first-line drugs; and/or 3) there is an increased incidence and severity of adverse events or toxicity by these drugs.[6] Crucially, as a consequence of the increased

treatment duration and expenses of these second- and third-line antibiotics, the total cost of treating multidrug resistant Mtb (MDR-TB) exceeds the costs of treating drug-sensitive TB therapy by 30-40 fold.[7] It is clear that second- and third-line anti-TB drugs are only indicated when there is proven resistance towards first-line drugs.

Attempts to realize **shortening of treatment duration** are of high importance as this will improve patient compliance and thereby reduce the risk of resistance selection. There is also an urgent need for **new drugs** that will enable (more effective) treatment of drug-resistant TB. Fortunately, after a gap of several years, there are currently several new promising anti-TB drugs in development.[8] Currently, a promising anti-TB drugs is moxifloxacin, one of the newer fluoroquinolones. Although at present not (yet) officially registered as a first-line anti-TB drug, moxifloxacin is already a prominent drug in the treatment of (MDR-) TB. Moxifloxacin is currently undergoing evaluation in a phase III trial, where its capacity as a replacement for either ethambutol or isoniazid in a first-line treatment regimen is being investigated. Aim of these studies is to shorten treatment from 6 to 4 months.[8-10] A second novel drug under development is called TMC207. TMC207 is a mycobacterial adenosine triphosphate (ATP) synthase proton pump inhibitor. Due to its unique mode of action of TMC207 on Mtb, no cross-resistance is expected. In vitro assays and *in vivo* models using this new drug have shown promising results.[11-12] Other new drugs that are under investigation for the treatment of (MDR-) TB include; SQ-109 [13], PA-824 [14-15], and PNU-100480 [16]. However, even with the eventual introduction of these newly developed drugs, there will still be room for improvement in the use of the current range of anti-TB drugs. For example, the currently used therapeutic dose of rifampicin (10 mg/kg) may not actually be optimal for killing Mtb, and studies exploring the use of higher dosages of rifampicin, or the use of rifamycin derivatives, are ongoing.[17] Ultimately, the aim of all of these studies is to shorten TB treatment duration from 6 to less then 4 months.[8-10] All of these new treatment approaches are extremely important in helping prevent the spread of (MDR-) TB. Unfortunately however, more time, effort and funding are required before these new drugs become available to those who desperately need them, especially relevant for those individuals suffering from TB in poorer regions of the world.

The emergence of **drug-resistant** Mtb has greatly increased in the last decade [1, 18], with several drug-resistant phenotypes now circulating globally. Multidrug resistant TB (MDR-TB) is defined as resistance to isoniazid and rifampicin, while extensively-drug resistant TB (XDR-TB) is defined as being resistance to both isoniazid, rifampicin, as well as additional resistance to at least one of the fluoroquinolones and at least one of the second-line injectable agents (e.g. aminoglycosides such as amikacin, kanamycin or capreomycin). Recently also, totally-drug resistant TB (TDR-TB) has been described in India. [19]. Each of these different levels of resistance have a dramatic effect on the expected therapeutic outcome of different antimicrobial treatment regimens.[18]

In fact, several factors promote the **development of resistance** to anti-TB drugs, including factors associated with patient therapy per se, and factors associated with the infecting Mtb genotype strain. The factors promoting the development of Mtb resistance and associated with individual patient therapy include: the unregulated availability of anti-TB drugs; unprofessional prescribing practices, patient non-compliance; malabsorption of the anti-TB drugs; and inter-individual variability in the pharmacokinetics of anti-TB drugs. However, the extent of involvement of each of these various factors, or combinations of factors, in determining the selection of resistant Mtb isolates and the accompanying emergence of resistant TB is not well understood, though patient non-compliance is considered to be one of the leading factors.[1, 20-21] Besides these different factors on the host side contributing to drug-resistance, there are also factors on the mycobacterial side that drive the development of drug-resistant Mtb. It is known that different Mtb genotype strains can exhibit different degrees of virulence, [22] and that different genotype strains are particularly associated with treatment failures.[23] For example, TB infection caused by the Beijing Mtb genotype strain is strongly correlated to the development and transmission of MDR-TB and even XDR-TB.[24-27]. The mechanism by which this Mtb genotype-associated resistance is regulated is unclear. Interestingly in this respect is also the geographical distribution of different genotype strains, since the majority of MDR-TB is currently found in the Former Soviet Union States (FSU) and in Asia.[1].

A wide range of *in vitro* **assays** is currently used to elucidate the different mechanisms of Mtb resistance against anti-TB drugs. The frequently used assays, including the Minimal Inhibitory Concentration determination (MIC) and Mycobacteria Growth Indicator Tube (MGIT, BD BACTEC MGIT 960 System) assays, provide endpoint data that are obtained only after several weeks of Mtb exposure to anti-TB drugs; in addition these tests only determine the inhibition of Mtb growth.[28] In comparison, the Time-Kill Kinetics assay used in the present thesis is performed over a 6-day period and is more informative with respect to the concentration-dependent or time-dependent activity of anti-TB drugs, whilst also determining the killing of Mtb.[29] Another assay, the Hollow Fiber Model, allows investigation of the dynamics of drug activity by simulating the fluctuating drug concentrations likely to be achieved during antibiotic therapy in TB patients.[30] Additional to these *in vitro* assays, which investigate the action of drugs acting on extracellular Mtb, there are also assays available using *in vitro* macrophage systems harbouring Mtb that also mimic the intracellular behaviour of Mtb,[31]. These assays add an extra therapeutic dimension to the analysis of the activity of anti-TB drugs.

One of the key (translational) steps in anti-TB drug development and research is the use of **animal models**, as these models represent a dynamic test system in which the therapeutic effect of anti-TB drugs can be measured, taking into account the biological availability of these anti-TB drugs as observed in patients. One of the major merits of using animal models is that these models enable comparative therapeutic studies at similar conditions of severity

and duration of infection, which is difficult to standardize in actual clinical patients due to their different underlying disease conditions. Several different animal models of TB infection have been developed including models using zebra fish, mice, rats, guinea pigs and monkeys. These animal models are diverse (with respect to costs and equipment required) and their predictive value for clinical trial outcomes is sometimes uncertain. Recently, several large research consortia, including the Critical Path to TB Drug Regimens and IMI joint undertaking entitled - "Model-based preclinical development of anti-tuberculosis drug combinations", have been formed in order to compare the predictive value of different animal models. The limitations of animal models for research into human TB infection should also be emphasized. Limitations include the artificial induction of infection, differences in bacterial virulence and immunological host responses, and differences in pharmacokinetics and toxic side effects of anti-TB drugs in experimental animals. As a result, comparative therapeutic studies in animal TB models may only serve as a basis for studies in TB patients. Nonetheless, despite these limitations, animal models for TB are needed as they provide the only rational basis for the design of therapeutic clinical trials in TB patients.

In all, there is a need to further understand the selection of drug-resistant Mtb mutants and the mechanisms of development of drug resistance. Also, more insight into the value of the new diagnostic tools might be helpful in restricting the burden of TB. Ultimately, as the current treatment for TB is complicated by its length and complexity, which has led to inadequate response and emergence of MDR-TB and even XDR-TB, there is very urgent need for new powerful TB regimens and strategies to minimize mortality and/or morbidity of TB.

OUTLINE OF THE THESIS

The aim of this thesis is to answer the following questions:

– What are the important factors that determine the translational value of an animal model of TB?

  In **chapter 2,** we describe, characterize and validate our mouse respiratory TB model, using Mtb strain H37Rv. In **chapter 3,** we discuss the role of the route of infection in influencing the course of murine TB and the observed therapeutic response. In **chapter 6,** we describe the course of infection and therapy response in "relapse episode of TB" versus "primary TB", in order to provide an insight into dissimilarities between those two infection types.

– What are the limitations of current TB diagnostics and are additional assays useful?

  Chapter 4 illustrates the difficulties of accurately diagnosing TB using a case of possible congenital transmission of Mtb. In **chapter 5,** the value of the Interferon Gamma Release Assay (IGRA) in diagnosing active murine TB caused by H37Rv is determined, and the role of cytokines as potential biomarkers in TB is explored.

– Which novel *in vitro* assays for the measurement of the dynamics of anti-TB drug killing activity and for selection of Mtb drug-resistance are more informative than currently used *in vitro* assays?

  In **chapter 7,** we show that the Time-Kill Kinetic assay is required to investigate the *in vitro* time- and concentration dependent killing activity of anti-TB drugs and the selection of drug-resistant mutants in Mtb H37Rv. In **chapter 8,** micro-array analysis is used to genetically characterize selected rifampicin-resistant Mtb mutants.

– Is a lower intrinsic susceptibility of Beijing genotype Mtb strains to anti-TB drugs correlated to epidemiologically observed treatment failures and the emergence of resistance in TB?

  In **chapter 9**, we compare the *in vitro* activity of anti-TB drugs towards clinically relevant Beijing genotype and East-African/Indian genotype Mtb strains. We focus on the measurement of mutation frequencies, the mutant prevention concentration, and the concentration-window within which only drug-resistant mutants are selected. In **chapter 10,** two prominent Beijing genotype and East-African/Indian genotype Mtb strains are used to further develop murine TB infection models and to determine the impact of the infecting strain on the course of infection and on therapeutic efficacy, during treatment compliance and treatment non-compliance.

– Can we improve the therapeutic efficacy of the current treatment regimen by optimizing the use of rifampicin?

In **chapter 11,** we describe the effect of increasing dosage of rifampicin on its tolerability, pharmacokinetics and efficacy in a mouse model of TB caused by the Beijing genotype Mtb strain, and investigate the consequences with respect to the duration of therapy required in order to ensure successful treatment of TB.

REFERENCES

1. WHO. Global tuberculosis control 2011, Annual Report WHO. WHO Library Cataloguing-in-Publication Data 2011: 1-258.
2. WHO. Treatment of Tuberculosis guidelines, fourth edition. WHO Library Cataloguing-in-Publication Data 2010; WHO/HTM/TB/2009.420.
3. Mitchison DA. Role of individual drugs in the chemotherapy of tuberculosis. Int J Tuberc Lung Dis 2000; 4: 796-806.
4. Mitchison DA. Antimicrobial therapy of tuberculosis: justification for currently recommended treatment regimens. Semin Respir Crit Care Med 2004; 25: 307-15.
5. Donald PR, Diacon AH. The early bactericidal activity of anti-tuberculosis drugs: a literature review. Tuberculosis (Edinb) 2008; 88 Suppl 1: S75-83.
6. Blumberg HM, Burman WJ, Chaisson RE *et al*. American Thoracic Society/Centers for Disease Control and Prevention/Infectious Diseases Society of America: treatment of tuberculosis. Am J Respir Crit Care Med 2003; 167: 603-62.
7. Diel R, Rutz S, Castell S *et al*. Cost of illness of tuberculosis in Germany. Eur Respir J 2012.
8. Ginsberg AM. Drugs in development for tuberculosis. Drugs 2010; 70: 2201-14.
9. Nuermberger E, Tyagi S, Tasneen R *et al*. Powerful bactericidal and sterilizing activity of a regimen containing PA-824, moxifloxacin, and pyrazinamide in a murine model of tuberculosis. Antimicrob Agents Chemother 2008; 52: 1522-4.
10. Rosenthal IM, Zhang M, Almeida D *et al*. Isoniazid or moxifloxacin in rifapentine-based regimens for experimental tuberculosis? Am J Respir Crit Care Med 2008; 178: 989-93.
11. Ibrahim M, Truffot-Pernot C, Andries K *et al*. Sterilizing activity of R207910 (TMC207)-containing regimens in the murine model of tuberculosis. Am J Respir Crit Care Med 2009; 180: 553-7.
12. Diacon AH, Pym A, Grobusch M *et al*. The diarylquinoline TMC207 for multidrug-resistant tuberculosis. N Engl J Med 2009; 360: 2397-405.
13. Nikonenko BV, Reddy VM, Protopopova M *et al*. Activity of SQ641, a capuramycin analog, in a murine model of tuberculosis. Antimicrob Agents Chemother 2009; 53: 3138-9.
14. Ahmad Z, Peloquin CA, Singh RP *et al*. PA-824 exhibits time-dependent activity in a murine model of tuberculosis. Antimicrob Agents Chemother 2011; 55: 239-45.
15. Singh R, Manjunatha U, Boshoff HI *et al*. PA-824 kills nonreplicating *Mycobacterium tuberculosis* by intracellular NO release. Science 2008; 322: 1392-5.
16. Williams KN, Brickner SJ, Stover CK *et al*. Addition of PNU-100480 to first-line drugs shortens the time needed to cure murine tuberculosis. Am J Respir Crit Care Med 2009; 180: 371-6.
17. Ruslami R, Nijland H, Aarnoutse R *et al*. Evaluation of high- versus standard-dose rifampicin in Indonesian patients with pulmonary tuberculosis. Antimicrob Agents Chemother 2006; 50: 822-3.
18. WHO. Towards universal access to diagnosis and treatment of multidrug-resistant and extensively drug-resistant tuberculosis by 2015, WHO progress report 2011. WHO Library Cataloguing-in-Publication Data 2011: 1-127.
19. Udwadia ZF, Amale RA, Ajbani KK *et al*. Totally Drug-Resistant Tuberculosis in India. Clin Infect Dis 2011.
20. Sharma SK, Mohan A. Multidrug-resistant tuberculosis: a menace that threatens to destabilize tuberculosis control. Chest 2006; 130: 261-72.
21. van den Boogaard J, Boeree MJ, Kibiki GS *et al*. The complexity of the adherence-response relationship in tuberculosis treatment: why are we still in the dark and how can we get out? Trop Med Int Health 2011; 16: 693-8.

22. Dormans J, Burger M, Aguilar D *et al*. Correlation of virulence, lung pathology, bacterial load and delayed type hypersensitivity responses after infection with different *Mycobacterium tuberculosis* genotypes in a BALB/c mouse model. Clin Exp Immunol 2004; 137: 460-8.

23. Buu TN, Huyen MN, Lan NT *et al*. The Beijing genotype is associated with young age and multidrug-resistant tuberculosis in rural Vietnam. Int J Tuberc Lung Dis 2009; 13: 900-6.

24. European Concerted Action on New Generation Genetic M, Techniques for the E, Control of T. Beijing/W genotype *Mycobacterium tuberculosis* and drug resistance. Emerg Infect Dis 2006; 12: 736-43.

25. Parwati I, van Crevel R, van Soolingen D. Possible underlying mechanisms for successful emergence of the *Mycobacterium tuberculosis* Beijing genotype strains. Lancet Infect Dis 2010; 10: 103-11.

26. Devaux I, Kremer K, Heersma H *et al*. Clusters of multidrug-resistant *Mycobacterium tuberculosis* cases, Europe. Emerg Infect Dis 2009; 15: 1052-60.

27. Devaux I, Manissero D, Fernandez de la Hoz K *et al*. Surveillance of extensively drug-resistant tuberculosis in Europe, 2003-2007. Euro Surveill 2010; 15.

28. Woods GL, Brown-Elliot BA, Desmond EP *et al*. Susceptibility testing of mycobacteria, nocardiae, and other aerobic actinomycetes. Approved standard. National Committee for Clinical Laboratory Standards 2003; M24-A, volume 23: 1-69.

29. Bakker-Woudenberg IA, van Vianen W, van Soolingen D *et al*. Antimycobacterial agents differ with respect to their bacteriostatic versus bactericidal activities in relation to time of exposure, mycobacterial growth phase, and their use in combination. Antimicrob Agents Chemother 2005; 49: 2387-98.

30. Srivastava S, Gumbo T. In vitro and *in vivo* modeling of tuberculosis drugs and its impact on optimization of doses and regimens. Curr Pharm Des 2011; 17: 2881-8.

31. Rey-Jurado E, Tudo G, Borrell S *et al*. Impaired fitness of *Mycobacterium tuberculosis* resistant isolates in a cell culture model of murine macrophages. J Antimicrob Chemother 2011; 66: 2277-80.

Chapter 2

Immunological parameters to define infection progression and therapy response in a well-defined tuberculosis model in mice

J.E.M. de Steenwinkel, G.J. de Knegt, M.T. ten Kate, A. van Belkum, H.A. Verbrugh, R. Hernandez-Pando, D. van Soolingen, I.A.J.M. Bakker-Woudenberg

ABSTRACT

To evaluate novel approaches for tuberculosis (TB) diagnostics and treatment, well-validated animal TB models are needed. Especially the emergence and spread of drug resistant TB requires innovative therapy and accurate parameters for monitoring success or failure of therapy.

We developed a TB model in BALB/c mice, in which *Mycobacterium tuberculosis* (Mtb) infection was induced through the natural respiratory route, mimicking human TB infection. The lung showed a mild inflammatory infiltrate consisting of granulomas in the first phase of infection, followed by progressive increase of pneumonic lesions resulting in extensive lung consolidation in the chronic phase. Dissemination to the extra-pulmonary sites was observed. The model was validated in terms of therapeutic outcome. The 26-weeks standard therapy, administered in human pharmacokinetic-equivalent doses, resulted in complete elimination of Mtb in all infected organs, without relapse of infection in the post-treatment period. However, a 13-weeks therapy duration, simulating patient non-adherence resulted in relapse of infection.

In our quest to find biomarkers for monitoring success or failure of therapy, the concentrations of various cytokines in serum and lung, determined by the Cytometric Bead Array (CBA), were evaluated in relation to the in situ cytokine expression in the lung, assessed by immunohistochemistry. The IFN-γ concentration in serum increased with infection progression, and decreased during effective therapy, and as such appeared to be an appropriate immunological parameter for success or failure of therapy. Relapse of infection, after inappropriate therapy manifested as an increase in the serum IFN-γ concentration.

INTRODUCTION

Tuberculosis (TB) remains one of the leading causes of morbidity and mortality worldwide, especially the middle- and low-income countries. About one third of the world's population is currently (latently) infected with *Mycobacterium tuberculosis* (Mtb), of which nine million develop TB and almost two million die.[1] Together with the increasing amount of TB-HIV co-infection and ever-increasing emergence of resistance to anti-tuberculosis drugs, TB constitutes a global threat. This prompted the World Health Organisation (WHO) to declare improved diagnosis and enhanced treatment of TB as one of their top priorities. One of the WHO's millennium development goals is "to have halted TB by 2015 as well as reverse the incidence of TB".[2] In order to achieve this ambitious goal, there are many challenges among which the development of new anti-tuberculous drugs as well as rapid and low-cost diagnostic tests.[2]

For evaluation of innovative therapeutic approaches, in TB patients only a few parameters are available, including sputum smear, general clinical observations, chest X-ray and laboratory infection parameters. The value of cytokines in serum of patients to assess the progression of infection and the efficacy of anti-tuberculosis treatment in the first month of therapy was investigated in previous clinical studies.[3-7] However, at present it is not yet clear whether immunological parameters in serum may be indicative in this respect and by that can possibly be useful markers.

In the present study, we developed an infection model of TB in BALB/c mice that resembles human TB. We induced the infection through the natural respiratory route, as such mimicking infection in patients, and we started treatment when the infection had achieved a late progressive phase. Anti-tuberculosis drugs currently used, were administered in human pharmacokinetic-equivalent doses [8] and treatment duration was identical to the WHO guidelines (26 weeks). To simulate patient non-adherence, a treatment regimen of only 13 weeks was applied. Efficacy of both treatment regimens was assessed at various intervals during treatment, as well as 13 weeks after termination of treatment, to evaluate potential relapse of infection in the post-treatment period. To characterize infection progression and to monitor therapy response microbiological, immunological and histopathological parameters were used. To recognize treatment failure at an early stage, which is of high importance from the clinical point of view, we investigated whether immunological parameters in serum are appropriate for monitoring therapy efficacy. Therefore the concentrations of various cytokines in serum and infected lung homogenates were determined by the Cytometric Bead Array (CBA), and evaluated with respect to the in situ cytokine expression in the infected lung, assessed by immunohistochemistry.

MATERIALS AND METHODS

Bacteria

The *Mycobacterium tuberculosis* (Mtb) strain used in this study was the H37Rv strain, kindly supplied by C.W. Wieland (Academic Medical Centre, University of Amsterdam, The Netherlands). The H37Rv strain is a clinical isolate and nowadays the strain most commonly studied *in vitro* as well as in animal models.[9] Mycobacteria were cultured on Middlebrook 7H10 agar medium [Difco Laboratories, Detroit, MI] supplemented with 10% oleic acid-albumin-dextrose-catalase enrichment [OADC; Baltimore Biological Laboratories, Baltimore, MD] for 21 days at 37°C and 5% CO_2. Mtb suspensions were prepared in Middlebrook 7H9 broth [Difco Laboratories, Detroit, MI] supplemented with 10% OADC, 5% glycerol [BDH laboratory supplies, Poole, England] and 0.05% Tween 20 [Sigma Chemical Co, St. Louis, MO]. Vials containing Mtb suspensions were stored at -80°C.

Animals

Specified pathogen-free female BALB/c mice were obtained from Charles River [Les Oncins, France]. At the day of infection, the animals were 10-12 weeks old and weighted 20-25 grams. The experimental protocols adhered to the rules specified in the Dutch Animal Experimentation Act (1977) and the published Guidelines on the Protection of Experimental Animals by the Council of the EC (1986). The Institutional Animal Care and Use Committee of the Erasmus MC Rotterdam approved the present protocols.

Infection

A suspension of Mtb, stored at -80°C was defrosted at room temperature and centrifuged for 10 min at 14,000x*g*. The Mtb pellet was resuspended in phosphate-buffered saline (PBS) and centrifuged again for one min at 1,900x*g* to eliminate any aggregated bacteria. The Mtb suspension was diluted in PBS to obtain a concentration of $2.4x10^6$ CFU/mL. To establish the pulmonary infection, a 22-Gauge mouse gavage feeding needle, with a 1.25 mm diameter tip [Fine Science Tools; Foster City, CA], a 1 ml syringe and a repeating dispenser [Hamilton company; Bonaduz, Switzerland] were used. Mice were infected by intratracheal instillation of 40 µL of Mtb suspension, containing $9.5x10^4$ Mtb, under general anaesthesia using a mixture of medetomidine [Domitor®, 0.5 mg/kg; Orion Corporation; Espoo, Finland], midazolam [Dormicum®, 5 mg/kg; Roche; Basel, Switzerland] and fentanyl [Fentanyl, 0.05mg/kg; Janssen Pharmaceuticals; Beerse, Belgium]. After inoculation mice were kept in a vertical position for 5 min to ensure proper inhalation of the inoculum. Mice were antagonized using a mixture of atipamezol [Antisedan®, 2.5 mg/kg; Orion Corporation; Espoo, Finland], flumazenil [Anexate®, 0.5 mg/kg; Hameln Pharma; Hameln, Germany] and nalaxon [Narcan®, 1.2 mg/kg; Hospital Pharmacy; Rotterdam, The Netherlands]. Anaesthetic and antagonistic agents were administered intraperitoneally, in a total volume of 175 and 250 µL, respectively.

Anti-tuberculosis therapy

The anti-tuberculosis drugs and dosage schedules used for treatment of the TB infected mice were according to the WHO guidelines.[2,10] Treatment was continued during 26 weeks (according to standard regimen) and consisted of a 9-week initial phase followed by a 17-week continuation phase. During the initial phase, animals received a combination of isoniazid [25 mg/kg; Hospital Pharmacy; Rotterdam, The Netherlands], rifampicin [10 mg/kg; Rifadin, Aventis Pharma B.V., Hoevelaken, The Netherlands] and pyrazinamide [150 mg/kg; P7136, Sigma Chemical Co, St. Louis, MO]. Agents were administered once daily, 5 days a week, subcutaneously in the neck, to avoid potential damage following long-term, daily oral gavage. As the bioavailability of both rifampicin and pyrazinamide, after oral administration is 100%, and for isoniazid this is 90%, proper correction in this respect was made for the subcutaneous administration of isoniazid. In the continuation phase, only isoniazid and rifampicin were administered in the same frequency and dose. To simulate patient non-adherence, a treatment regimen of only 13 weeks (9 weeks initial phase, followed by only 4 weeks continuation phase) was applied.

The therapeutic efficacy of both treatment regimens was assessed using various microbiological, pathophysiological and immunological parameters. To this aim mice were dissected at indicated time points during the treatment period and 13 weeks after termination of treatment, in order to detect potential relapse of TB infection in the post-treatment period. Determination of viable Mtb counts in infected organs and blood. Mice (n=4 per time point) were sacrificed at indicated time points by CO_2 exposure. In mice sacrificed during treatment, administration of anti-tuberculosis drugs was stopped 72 hrs before dissection, in order to minimize carry-over of the anti-tuberculosis drugs onto the sub-culture plates. A blood sample was taken via a (transcutaneous) cardiac puncture and a protease inhibitor [P8340, Sigma Chemical Co, St. Louis, MO] added to the blood sample to a final concentration of 5%. The lung, spleen and liver were removed and homogenized [Polytron, Kinematica, Luzern, Switzerland] in 2 mL of PBS containing a final concentration of 5% protease inhibitor for 10 sec at 30,000 rpm at room temperature. With this method, intra- and extracellular Mtb were recovered. To further prevent carry-over of anti-tuberculosis drugs (if still present in the tissues) onto the subculture plates, tissue homogenate suspensions and blood were centrifuged at 14,000xg for 10 min, and pellets were re-suspended in PBS. Samples were serially diluted in PBS and plated onto 7H10 agar supplemented with 10 % OADC. The plates were incubated for 21 days at 37^0 C and 5% CO_2 before colonies were counted.

Histopathological examination of infected lung

The histopathological changes in infected tissues during the course of the infection were determined by sacrificing the animals (n=3) at indicated time points, using an overdose of pentobarbital [Nembutal®, A.U.V, Cuijk, The Netherlands]. In situ, the lung was re-expanded

using ethanol absolute [Riedel-de Haën, Seelze, Germany] administered through a 22-gauge mouse gavage-feeding needle with a 1.25 mm diameter. The re-expanded lung was transferred to small flasks containing ethanol absolute, and stored for a minimum of 24 hrs and a maximum of 72 hrs at room temperature. After fixation, the lung lobes were separated. The tissues were subsequently dehydrated in ethanol absolute three times for 1 hr, in 100% xylene [Sigma Chemical Co, St. Louis, MO] three times for 1 hr and finally immersed three times in paraffin [Richard-Allen Scientific, Kalamazoo, MI] at 65^0C for 1 hr. The paraffin-embedded tissues were cut into 4 µm sections and one in every 7 cuts was taken for haematoxylin-eosin (HE) staining. A pathologist, blinded to the experimental condition, examined the HE-stained sections under a microscope. In these slides, the average size of granulomas and the percentage of lung surface affected by pneumonia were (semi-quantitatively) determined using a NanoZoomer Digital Pathology system (Hamamatsu Photonics K.K, Hamamatsu City, Japan) and score as described by Hernandez-Pando et al.[11]

## Immunohistochemical examination of infected lung

 The cytokine expression in infected lung tissue, during the course of infection was determined. The paraffin-embedded tissue samples used for histopathology were subsequently cut in 4 µm sections, which were immunohistochemically stained following various steps, being deparaffinization by 5 min incubation in 100% xylene, three times washing in 100% xylene, three times washing in xylol-ethanol (50:50), three times washing in ethanol 96%, and finally submersion in distilled water for 2 min. Quenching of endogenous peroxidase was achieved by incubation of the sections in a mixture of 3% H_2O_2 [Sigma Chemical Co, St. Louis, MO] in methanol [Biosolve, Westford, MA] for 30 min and five times washing in HCN-Tween 20 0.01% (HCN = Hepes 2.383gr [Sigma Chemical Co, St. Louis, MO], NaCl 8.766gr [Merck, Frankfurt, Germany] and $CaCl_2$ 0.2958gr [Merck, Frankfurt, Germany] per litre). Aspecific blocking was done with either goat- or rabbit serum (depending on the antigen used) diluted in HCN-Tween 20 0.01%, according to manufacturer's protocol [Vectastain® Elite ABC kit; Vector Laboratories, Burlingame, CA] without exposure to light for 30 min, after which the samples were washed five times with HCN-Tween 20 0.01%. The specific antibody binding was achieved by incubation of the samples with 200 µL biotin-labelled rabbit- or goat polyclonal antibodies against IL-2 (sc-7896), IL-4 (sc-1260), IL-10 (sc-1783), IL-12B p40 (sc-1283), IFN-γ (sc-9344) or TNF-α (sc-1351), all purchased from Santa Cruz Biotechnology [CA, USA] and diluted 1/100 in PBS. Bound antibodies were detected using the Vectastain® Elite ABC kit [Vector Laboratories, Burlingame, CA] according to manufacturer's protocol. The secondary antibody-stained sections were finally counterstained using haematoxylin.

Cytokine concentrations in infected lung homogenates and serum

 The cytokine concentrations were assessed at indicated time points, in samples of lung homogenate and serum, of the sacrificed animals (n=3). Samples were preserved with 5% prote-

ase inhibitor, stored at -80⁰C and cytokines were determined using the Cytometric Bead Array (CBA)-assay [CBA-flex kit, cat. no. 558266, Becton, Dickinson and Company, Franklin Lakes, NJ]. In this assay a sequence of spectrally distinct particles, which are coated with different capture antibodies was used. These particles capture specific cytokines from the samples and after this primary binding, a secondary (fluorescent) antibody was used for labelling. The samples were characterised by detection of fluorescence (to quantify cytokine binding) and flow cytometric analysis (to designate the specific cytokine). The cytokine concentrations were calculated with a sandwich format assay (plotting sample results against a standard curve). The CBA-assay generates data that are analogous to those from ELISA-based assays; however, with the CBA-assay multiple cytokine concentrations can be detected and quantified in one single sample. In addition, with this technique only a limited sample volume of 50 μL is required. In order to run the CBA in a non-tuberculosis laboratory and to prevent interference of tissue residue during the test, the samples were filtered before the CBA assay. We used a 10 μm in-tube filter [Vectaspin 10 μm, Whatman, Maidstone, UK] as a prefilter and a secondary 0.2 μm in-tube filter [Vectaspin 0.2 μm, Whatman, Maidstone, UK] as a sterilisation filter, before analyzing. The 10 μm in-tube prefilter was filled with 200 μL of the defrosted sample and centrifuged at 7,500x*g* for 10 min at room temperature. The filtered fluid was free of tissue residue and transferred to the 0.2 μm in-tube sterilisation filters. After centrifugation at 7,500x*g* for 10 min at room temperature, the sample was free of Mtb. The CBA-assay was performed according to the manufacturer's protocol. In brief: 50 μL of the samples and of the standard dilutions were incubated with 50 μL capture beads for 1 hr, in a 96-wells filter plate at room temperature. Subsequently, 50 μL phycoerythrin (PE) detection reagent, consisting of fluorescent PE-conjugated anti-mouse IL-2, IL-4, IL-10, IL-12, TNF-α or IFN-γ was added, and incubated (protected from light) for 1 hr at room temperature. After incubation the sample was measured using a flow cytometry instrument [FACS-scan, Becton, Dickinson and Company, Franklin Lakes, NJ] and results were analyzed using CBA software. Cytokine concentrations for each sample were determined by interpolation from the standard curve.
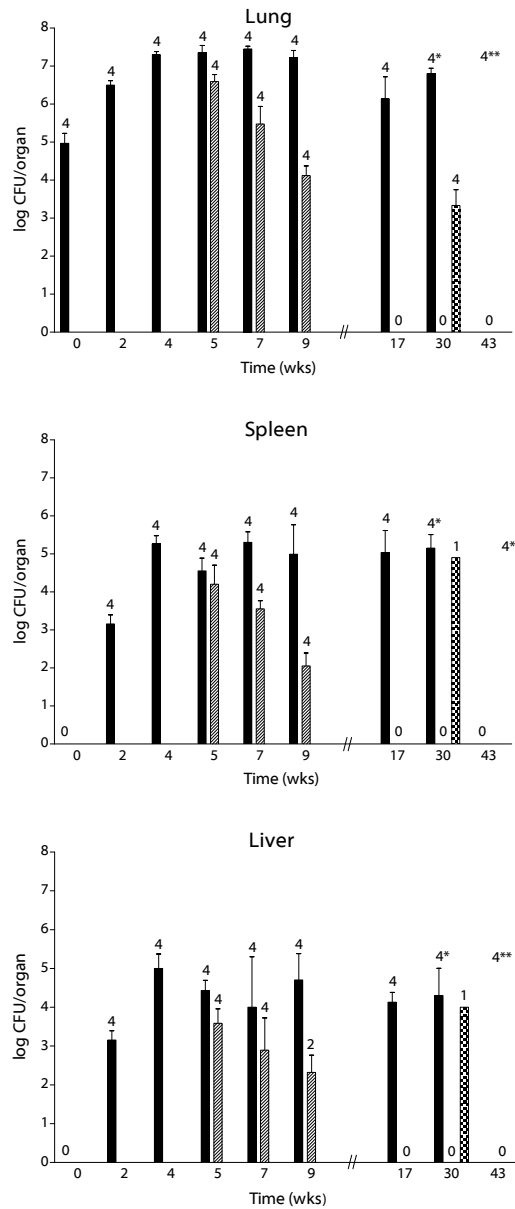
Figure 1. TB infection in mice and efficacy of standard therapy for 26 weeks (diagonally striped bars) or therapy for 13 weeks only (chequered bars). TB infected untreated mice (black bars). Therapy was started 4 weeks after inoculation of Mtb and consisted of isoniazid, rifampicin and pyrazinamide during 9 weeks, followed by an additional 4 or 17 weeks of isoniazid and rifampicin. Results are expressed as means ± SD (error bars) of the colony forming units (CFU) per organ, n = 4 per time point. Numbers above bars are the numbers of culture-positive mice out of 4 mice. * 2 out of 4 untreated mice died due to TB before time point. ** 4 out of 4 untreated mice died due to TB before time point.

RESULTS

Mouse model of TB infection

Intratracheal inoculation of 9 5x10^4 Mtb resulted in pulmonary TB in all mice. Dissemination of Mtb to extra-pulmonary sites, including spleen and liver, at a later stage of the infection, was observed. At 24 hrs after inoculation, Mtb organisms (5 8x10^4; range 4 7-8 9x10^4) were exclusively recovered from the lung, as at that time no Mtb was detected in the extra-pulmonary sites or blood (figure 1). The Mtb load increased exponentially in the lung over
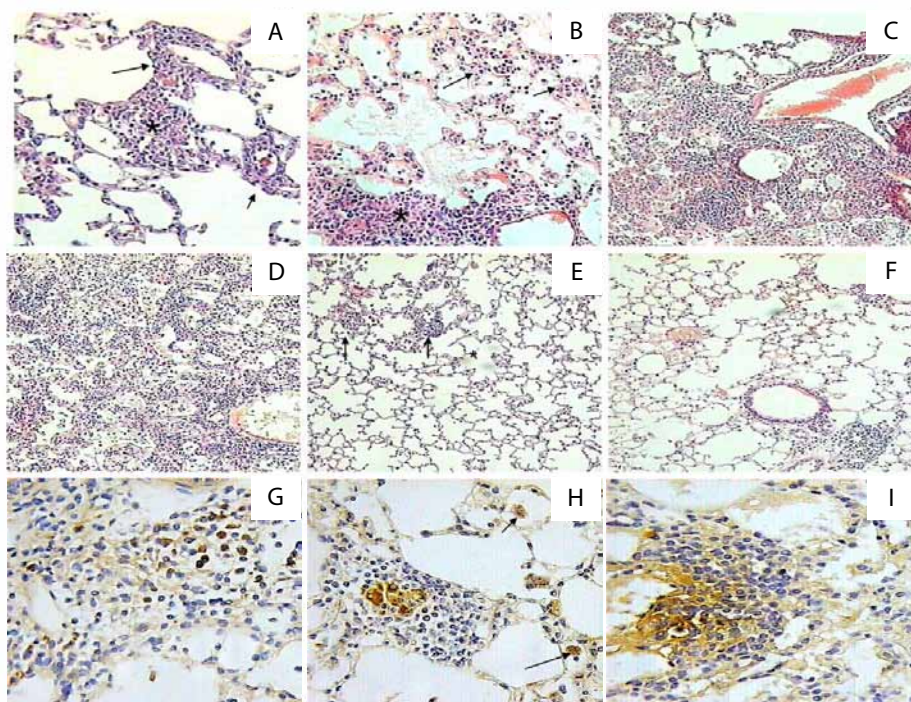
Figure 2. Representative lung histopathology **(A-D)** and cytokine expression by immunohistochemistry **(G-I)** in TB infected untreated mice. Lung histopathology of mice treated with standard therapy for 26 weeks **(E-F)**. **(A)** (400x), after 2 weeks of infection, perivascular inflammation (arrows) and well-formed granulomas (asterisk) were distinctive histological features. **(B)** (400x), after 4 weeks of infection, pneumonic patches (asterisk) and widening of alveolar-capillary interstitium due to inflammatory infiltrate were seen (arrows). **(C)** (100x), after 17 weeks of infection extensive lung pneumonia was observed. **(D)** (100x), after 30 weeks of infection, numerous foamy macrophages in the pneumonic areas were observed. **(E)** (100x), after 13 weeks of therapy, only small granulomas (arrows) were present and pneumonia was not observed. **(F)** (100x), after 26 weeks of therapy only lymphocyte cuffs around venules were observed without pneumonia or granulomas. **(G)** (1000x), after 4 weeks of infection, granuloma showed numerous IFN-γ positive cells. **(H)** (1000x), after 4 weeks of infection, activated macrophages in granulomas and in alveolar spaces (arrows) exhibited strong TNF-α expression. **(I)** (1000x), after 30 weeks of infection, numerous IL-4 positive lymphocytes were seen in granulomas.

time and extra-pulmonary sites became infected 2 weeks after inoculation of Mtb into the lung. All blood cultures were positive for Mtb at 4 weeks after infection with an average of 0 7x10^3 CFU/mL (data not shown). After this acute phase of infection the numbers of Mtb in the different organs stabilized and only some mice revealed positive blood cultures at low Mtb densities. From the time point that the maximum bacterial load in the different organs was reached, untreated mice became increasingly sick over time, as reflected by their loss of body weight and poor health-associated behaviour. Untreated mice died or became moribund (resulting in euthanasia) between 22 and 38 weeks after infection.

Histopathological examination of the lung after 2 weeks of infection revealed mild inflammatory infiltrate, consisting of lymphocytes and macrophages, located around blood vessels, bronchioles and in the alveolar-capillary interstitium (figure 2A). Well-constituted granulomas became apparent near blood vessels or the bronchial walls and in the alveolar network. Many macrophages located in the interstitium, alveolar lumina and granulomas, showed morphology characterized by the occurrence of large cells with abundant and compact cytoplasm and enlarged nuclei with marginal chromatin on the inner part of the nuclear membrane and an apparent nucleolus. After 4 weeks of infection, small patches of pneumonic lesions were seen. These areas were characterized by alveolar lumina occupied by lymphocytes, macrophages, occasional neutrophils and clumps of apparently coagulated or precipitated eosinophilic proteins (figure 2B). These pneumonic areas progressively increased in untreated mice, producing extensive lung consolidation after 17 weeks of infection (figure 2C), exhibiting focal areas of necrosis, thick lymphocyte-rich cuffs around blood vessels and hyperplastic lymphoid tissue associated with bronchial walls. After 30 weeks of infection, massive pneumonia was seen, alveolar spaces showed many large, foamy macrophages with numerous cytoplasmic vacuoles and small nuclei (figure 2D). Occasionally, multi-nucleated giant cells were observed in the alveolar areas. Semi-quantitative determination of the percentage of lung surface occupied by granulomas revealed an increase in the average and total granuloma size during the progression of the acute phase (figure 3A). The surface occupied by granulomas peaked after 5 weeks of infection and decreased from that time point. After 9 and 17 weeks of infection, there were hardly any granulomas detectable in the lung. Also the percentage of lung area consisting of pneumonic lesions increased during the course of infection up to 75% at 30 weeks after infection (figure 3B). At that time mortality of mice was observed.

Immunological evaluation of the infection progression was done in two different ways. The presence and concentration of specific cytokines in serum and lung homogenates as measured by the CBA were determined. In addition, the lung sections were immunohistochemically stained to reveal in situ cytokine expression in the lung. With respect to the cytokines circulating in serum and present in lung homogenates, the most prominent cytokine
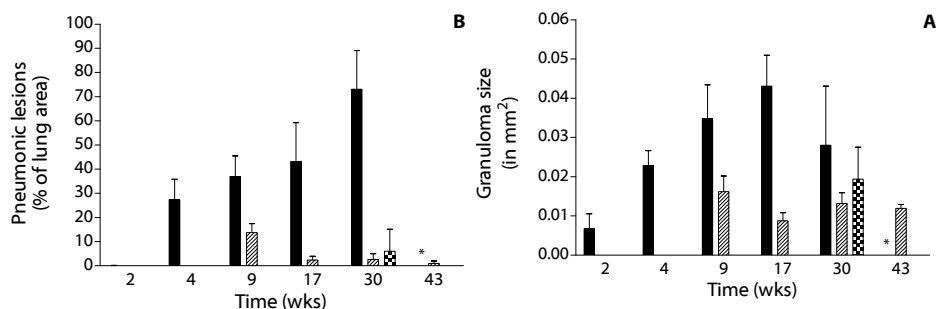
Figure 3. Lung histopathology in terms of granuloma size en percentage pneumonic lesions during the course of infection. **(A)** The average size of granulomas in the lung. **(B)** Areas of the lung, consisting of pneumonic lesions as percentage of total lung surface. TB infected untreated mice (black bars). Mice treated with the standard therapy for 26 weeks (diagonally striped bars) or therapy for 13 weeks only (chequered bars). Therapy was started 4 weeks after inoculation of Mtb and consisted of isoniazid, rifampicin and pyrazinamide during 9 weeks, followed by an additional 4 or 17 weeks of isoniazid and rifampicin. Results are expressed as means ± S.D (error bars), n = 3 per time point. From each mouse, 5 lung lobes were examined. * 4 out of 4 untreated mice died due to TB before time point.

observed during the murine TB was IFN-γ. During the course of infection, the IFN-γ levels in lung homogenates and serum rose quickly and reached a peak concentration 4 weeks after infection (figure 4A). This indicates a strong Th-1 response during the acute phase of the infection. In the first weeks of the chronic phase of infection the IFN-γ levels decreased and subsequently reached a plateau level. The second prominent cytokine in the course of TB in this model was TNF-α. Elevated concentration levels of TNF-α were observed in lung homogenates and serum in the acute phase and these levels remained high during the chronic phase of infection (figure 4B). IL-4 levels were also increased in the lung homogenates and serum at 4 weeks after infection but in much lower concentrations compared to IFN-γ and TNF-α (figure 4C). Also, the cytokine concentration profiles of IL-2, IL-10 and IL-12 were relatively low during the infection progression (data not shown).

Immunohistochemical staining showed numerous IFN-γ expressing cells with the morphology of activated lymphocytes located in granulomas after 2 and 4 weeks of infection (figure 2G), and in the inflammatory infiltrate located in the alveolar-capillary interstitium and around the venules and bronchi. The granulomas at week 2 and week 4 showed numerous activated (foamy) macrophages with strong TNF-α expression(figure 2H). Alveolar macrophages near to these granulomas and in the pneumonic areas also showed immunoreactivity against TNF-α (figure 2H). After 30 weeks of infection, lymphocytes located in the pneumonic areas and in granulomas frequently expressed IL-4 (figure

Efficacy of anti-tuberculosis drugs

Therapy was started at 4 weeks after inoculation of Mtb, at the time of the apparent switch from the acute to the chronic phase of the infection, as illustrated by stabilization of the

Mtb load in the infected organs and the histopathological findings. As shown in figure 1 the administration of the combination of isoniazid, rifampicin and pyrazinamide, resulted in a rapid decline in Mtb load in the infected organs. After 1 week of therapy the numbers of Mtb in lung, spleen and liver had significantly decreased by 81%, 93% and 60%, respectively, compared to start of therapy. Within 5 weeks of therapy a further rapid significant decrease in Mtb load was obtained in lung, spleen and liver. Blood was always sterile. After 13 weeks of therapy, viable Mtb could not be cultured from the infected organs. When anti-tuberculosis drugs were continued for a total of 26 weeks, complete elimination of Mtb from the infected organs was achieved in all mice, as evidenced by the absence of relapse of infection 13 weeks after termination of therapy. In contrast, when after 13 weeks of therapy the treatment with anti-tuberculosis drugs was stopped, 13 weeks later relapse of infection was observed in all mice (figure 1). At that time, numbers of Mtb in the lung of all mice had increased again up to $1.4x10^3$ (range $1.0-6.8x10^3$), whereas in 1 out of 4 mice bacterial numbers in the spleen and liver had increased to numbers not significantly different from the untreated controls.

Histopathological examination of the lung during therapy revealed that animals treated with anti-tuberculosis drugs, showed striking morphological changes, compared to the untreated animals (as described above). After 13 weeks of therapy only few and small pneumonic patches were observed with middle sized granulomas (figure 2E), while after 26 weeks of therapy, only occasionally granulomas and thick lymphocytes cuffs were observed. Patches of pneumonia were absent at this stage (figure 2F). At week 43 (13 weeks after the 26 weeks treatment period) histopathological evaluation of the lung revealed similar tissue morphology as seen at week 30. (data not shown).

The quantitative histopathological examination during infection revealed prevention of extension of granulomas and pneumonic lesions during therapy for 26 weeks (figure 3). When after 13 weeks therapy was stopped, the average granuloma sizes increased (figure 3A) and also the total numbers of granulomas increased (data not shown), indicating a strong progression of infection. Also the percentage of lung area consisting of pneumonic lesions at week 30 was on average somewhat increased (figure 3B).

Regarding the cytokine expression, the IFN-γ concentrations in lung homogenates and serum which in untreated mice remained at a stable level until 30 weeks after infection, significantly decreased in mice receiving 26-weeks therapy (figure 4A). At the end of the 26-weeks therapy IFN-γ concentration in lung homogenates and serum had returned to the normal low values. The effect of therapy on the TNF-α level was less prominent. Though there was a decrease in TNF-α concentration in lung homogenates following therapy, this cytokine remained elevated until the end of the 26-weeks therapy. The therapy-induced decrease in TNF-α concentration was not seen in serum. There was no significant change in of IL-4 levels in serum following therapy, except that in lung homogenates IL-4 concentrations were significantly
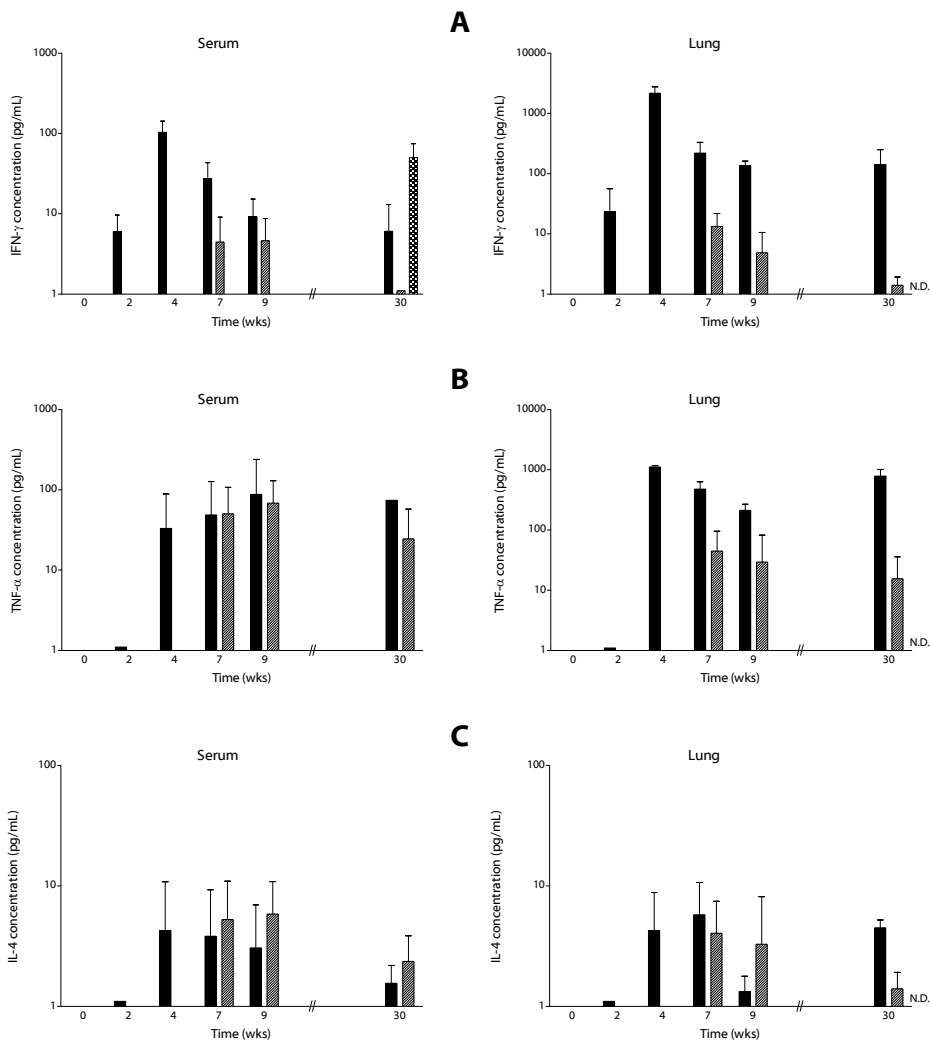
Figure 4. Concentrations of cytokines, in lung homogenates and serum during the course of infection. **(A)** IFN-γ. **(B)** TNF-α. **(C)** IL-4. TB infected untreated mice (black bars). Mice treated with the standard therapy for 26 weeks (diagonally striped bars) or therapy for 13 weeks only (chequered bars). Therapy was started 4 weeks after inoculation of Mtb and consisted of isoniazid, rifampicin and pyrazinamide during 9 weeks, followed by an additional 4 or 17 weeks of isoniazid and rifampicin. Results are expressed as means ± S.D (error bars) of cytokine concentration in pg/mL, n = 5 per time point at weeks 4, 7 and 9 and n = 3 per time point at weeks 2 and 30. N.D. = Not determined.

decreased at the end of the 26-weeks therapy. Regarding the cytokines IL-2, IL-10 and IL-12, the low concentrations of these cytokines assessed in lung homogenates and serum, did not allow evaluation of the effect of therapy on their presence (data not shown). Since the IFN-γ concentration in serum showed a good correlation with the treatment efficacy, serum IFN-γ concentrations were measured in animals receiving only 13-weeks of therapy, showing relapse of infection in the post-treatment period. A rapid increase in IFN-γ concentration in serum was found at week 30, the end of the relapse period. This showed that the increase in CFU and histopathology damage was nicely reflected in an increase in IFN-γ concentrations in both lung homogenates and serum.

DISCUSSION

In TB patients, only a few parameters are available to monitor infection progression and therapy response. These parameters include: sputum smear, chest X-ray and general clinical and laboratory infection parameters. At present it is not clear whether the cytokine profile in serum or bronchoalveolar-lavage (BAL) fluid might be indicative and can be used as parameter. The role of cytokines in the host defence during TB was demonstrated in various studies in TB patients, showing levels of IFN-γ, TNF-α, IL-4, IL-6 and IL-10 in serum, BAL fluid as well as in pleural fluid. It is not clear whether these changes in cytokine expression are related to the infection progression and therapy response (and by that) possibly are useful markers.[3-7] Monitoring cytokine levels in BAL fluid is hindered by the fact that the collection of BAL fluid from patients is an invasive procedure and is susceptible to inter-procedure variations. As a result, routine use of cytokine determinations from BAL fluid seems to be inappropriate. The use of serum cytokine levels as a reflection of the cytokine levels in infected lung tissue might be more appropriate. In the present study the value of cytokine levels in serum for monitoring infection progression and therapy efficacy was investigated in an experimental TB model in mice. At various intervals during infection and during therapy including the post-treatment period, cytokine levels in serum were determined and evaluated with respect to the in situ cytokine expression in the infected lung at that moment. Also the fluctuation in serum cytokine levels in relation to the success of therapy or failure of therapy followed by relapse of infection was assessed.

Regarding the course of cytokine levels in serum and BAL-fluid of TB patients, Verbon *et al.* and Morosini *et al.*[4,5] showed that during active TB, circulating IFN-γ levels were elevated compared to healthy control groups, whereas IL-4 levels were low. Therefore, use of cytokines as a diagnostic tool in TB patients was previously proposed by Küpeli *et al.* In their study, the TNF-α concentration in BAL-fluid appeared to be a useful tool to discriminate between smear-negative TB patients and healthy persons.[3] However, these studies were performed in

relatively small groups of patients and had the disadvantage that cytokine concentrations were difficult to match to TB-infection stage. The standard deviation of cytokine levels in TB-patients, all in different stages of their infection, hinders proper interpretation of the correlation of infection phase and cytokine level. Animal models enabling such comparative studies can overcome these disadvantages and may provide further insight.

Our experimental TB model in BALB/c mice being characterized with respect to infection progression, immune response and validated with respect to therapy outcome appears to simulate human TB. Also relapse of infection in the post-treatment period was evaluated. We used an inoculum of 9.5×10^4 CFU H37Rv to obtain a progressive disease with mortality of mice only late in the course of infection, enabling proper evaluation of efficacy of currently-used standard therapy, as well as novel therapeutic approaches in TB in future studies. We infected the mice via the respiratory route, to simulate human infection, and applied intratracheal instillation of Mtb to avoid potential variable deposition of the microorganisms in the lung.[12] The infection progressively developed and after 4 weeks the Mtb load in the lung had reached a maximum. From that time mycobacteria persisted for at least 30 weeks, indicating a chronic phase of the infection. Dissemination of Mtb to extra-pulmonary sites, such as spleen and liver, was observed from 2 weeks after infection. Blood cultures of infected mice were positive only during the initial acute phase of infection. The animals became increasingly sick over time and started dying 22 weeks after infection, due to the intensity of the inflammatory response and subsequently tissue damage.

Immunological characterization of the initial phase of Mtb infection in the mice revealed predominantly an IFN-γ driven T-helper cell-1 (Th-1) immune response, here CD4-Th1 cells as well as NK cells are involved, which is also seen in humans.[13,14] The acute initial phase shifted to a T-helper cell-2 (Th-2) driven immune response resulting in stabilization of the Th-1 response and thus preventing early mortality of mice. This balance of the Th-1 and Th-2 response during TB infection is a characteristic feature of TB. The mortality rate due to TB infection in the BALB/c mice is relatively low compared to various other mouse strains.[14] The difference is likely due to the apparent two-phase-reaction of BALB/c mice to Mtb, leading to a chronic progressive character of the infection. Immunological examination of the infected lung in the first 4 weeks of the infection showed the pro-inflammatory cytokines (e.g. IFN-γ and TNF-α) were predominant in the lung. The histopathological feature of the infected lung in this acute phase of the infection was the formation of granulomas. Immunohistochemical staining of the lung sections revealed that the granulomas had numerous IFN-γ producing lymphocytes, indicating the strong Th-1 character of this response. The area of the lung occupied by granulomas and the average granuloma seize reached a peak at the end of the acute phase. At the same time the concentration of free IFN-γ in the lung homogenates and serum also reached a peak. Besides IFN-γ the, (immuno-) histopathological characterization

of the acute phase of the infection revealed activated macrophages, expressing high levels of TNF-α in the lung and these macrophages have remained during the chronic phase of infection. High levels of TNF-α were also found in the lung homogenates and serum, which increased rapidly and remained high during the chronic phase of infection.

After the acute phase of infection we observed that the immune response changed from a Th-1 derived acute infection to a chronic reaction, characterized by expression of anti-inflammatory cytokines, such as IL-4.[16] Histopathologically the chronic phase of the infection was characterized by the development of pneumonic lesions, visualized by intra alveolar presence of neutrophils, leukocytes and plasma proteins, and were related to the Th-2 response. The histopathological changes in the lung corresponded with the load of persistent Mtb, and the mortality of mice. Immunohistochemical staining of the lung sections revealed that late in the chronic phase of the infection, numerous lymphocytes expressing IL-4 were seen in the lung. However this increase in IL-4 levels during the infection progression was just moderately observed in the lung homogenates and serum and as such did not provide additional information on the infection progression.

Next, it was investigated whether success or failure of therapy was reflected in terms of changes in cytokine levels in serum. The anti-tuberculosis therapy applied, consisted of the standard combinations of currently used anti-tuberculosis drugs and was administered at time schedules according to the WHO guidelines.[2,10] Rosenthal *et al.* and Lalande et al, have demonstrated that with the dosages used in the present study, the plasma area under the concentration-time curve AUC obtained in mice were similar to human plasma AUC.[8,17] The anti-tuberculosis therapy was started at 4 weeks after infection, when patches of pneumonic lesions were already observed and established infection was confirmed by stabilization of the Mtb load in the infected organs and TB characteristic histopathological findings. Therapeutic efficacy was established in terms of a rapid decrease in Mtb load in lung, spleen and liver. It was demonstrated that full 26-weeks duration of therapy is of primary importance in obtaining complete cure. Although after a therapy duration of only 13 weeks Mtb could not be cultured from the infected organs, relapse of infection occurred in the 13 weeks post-treatment period, probably initiated by very low numbers of persistent dormant mycobacteria in the infected organs. The therapeutic results obtained in the present study are in agreement with those of Nuermberger *et al.* [18] who administered the anti-tuberculosis drugs orally via gavage in BALB/c mice infected via the aerosol route. They started therapy at 19 days after infection, and at that time the Mtb load in the lung was similar compared to the Mtb load in the lung at 4 weeks after infection in our model.

We demonstrated that a decrease of cytokine concentration in serum resulting from effective therapeutic intervention was clearly observed for IFN-γ, but not for TNF-α or IL-4. The increase in Mtb load in infected organs and histopathological damage in the lung was nicely reflected

by an increase in IFN-γ concentrations in serum. Successful therapeutic intervention resulted in decreasing Mtb load and limited tissue damage, as well as in decrease in IFN-γ in serum and during therapy failure, IFN-γ concentrations in serum increased again. The dynamics of the IFN-γ concentration in serum before, during and after therapy, as observed in this experimental study, may be considered as a tool to monitor infection progression and success or failure of therapy in patients under anti-tuberculous therapy. Verbon *et al.* demonstrated that IFN-γ levels in patients suffering from active TB were elevated in serum compared to healthy controls and declined during and after treatment.[5] Our data obtained in mice are in agreement with the clinical data from Verbon, and suggest that the absence of a shift in IFN-γ levels, after starting therapy could be indicative for non-effective treatment, for example due to drug resistance of Mtb.

In summary, the serum cytokine IFN-γ accurately reflected the IFN-γ response at the primary, pulmonary infection site. Fluctuations in serum IFN-γ showed a good correlation with infection progression, successful therapeutic outcome and therapy failure following non-appropriate therapy. In this way, the serum IFN-γ concentration might be a useful immunological parameter to follow the presence of an early therapy response and to prevent unnoticed treatment failure due to resistance. The therapy efficacy in an individual TB patient can be monitored, thus contributing to a successful treatment-outcome.

ACKNOWLEDGEMENTS

REFERENCES

1. World Health Organization. Global Tuberculosis Control, WHO report 2008, Geneva
2. World Health Organization. The Global plan to stop TB 2006-2015, Actions for life, WHO and Stop TB Partnership 2006, Geneva
3. Kupeli E, Karnak D, Beder S. *et al.* Diagnostic Accuracy of Cytokine Levels (TNF-alpha, IL-2 and IFN-gamma) in Bronchoalveolar Lavage Fluid of Smear-Negative Pulmonary Tuberculosis Patients. Respiration 2008; 75:73-8
4. Morosini M, Meloni F, Marone Bianco A. *et al.* The assessment of IFN-gamma and its regulatory cytokines in the plasma and bronchoalveolar lavage fluid of patients with active pulmonary tuberculosis. Int J Tuberc Lung Dis 2008; 7:994-1000
5. Verbon A, Juffermans N, van Deventer S. *et al.* Serum concentrations of cytokines in patients with active tuberculosis and after treatment. Clin Exp Immunol 1999; 115:110-3
6. Ilonidis G, Parapanisiou E, Anogeianaki A. *et al.* Interleukin -1-beta (IL-1-beta), interleukin 6 (IL-6) and tumor necrosis factor (TNF) in plasma and pleural fluid of pneumonia, lung cancer and tuberculous pleuritis. J Biol Regul Homeost Agents 2006; 20:41-6
7. Doherty M, Wallis R, Zumla A. *et al.* Biomarkers for tuberculosis disease status and diagnosis. Curr Opin Pulm Med 2009; 15:181-7
8. Rosenthal I, Zhang M, Williams K. *et al.* Daily dosing of rifapentine cures tuberculosis in three months or less in the murine model. PLoS Med 2007; 4:1931-9
9. Betts J, Dodson P, Quan S. *et al.* Comparison of the proteome of *Mycobacterium tuberculosis* strain H37Rv with clinical isolate CDC 1551. Microbiology 2000; 146:3205-3216
10. Blumberg H, Burman W, Chaisson R. *et al.* American Thoracic Society/Centers for Disease Control and Prevention/Infectious Diseases Society of America: treatment of tuberculosis. Am J Respir Crit Care Med 2003; 167:603-62
11. Hernández-Pando R, Pavón L, Arriaga K. *et al.* Pathogenesis of tuberculosis in mice exposed to low and high doses of an environmental mycobacterial saprophyte before infection. Infect Immun 1997; 65:3317-27
12. Bakker-Woudenberg I. Experimental models of pulmonary infection. J Microbiol Methods 2003; 54:295-313
13. Barnes P, Vankayalapati R. Th1 and Th2 Cytokines in the Human Immune Reponse to Tuberculosis, in Tuberculosis and the Tubercle Bacillus first edition, S.T. Cole, K.D. Eisenach, D.N. McMurray, W.R. Jacobs jr. eds. American Society for Microbiology (ASM) press, Washington, 2005; 489-96
14. Hopewell P, Jasmer R. Overview of Clinical Tuberculosis in Tuberculosis and the Tubercle Bacillus first edition S.T. Cole, K.D. Eisenach, D.N. McMurray, W.R. Jacobs jr. eds American Society for Microbiology (ASM) press, Washington, 2005; 15-32
15. Keller C, Lauber J, Blumenthal A. *et al.* Resistance and susceptibility to tuberculosis analysed at the transcriptome level: lessons from mouse macrophages. Tuberculosis (Edinb) 2004; 84:144-58
16. Hernández-Pando R, Orozcoe H, Sampieri A. *et al.* Correlation between the kinetics of Th1, Th2 cells and pathology in a murine model of experimental pulmonary tuberculosis. Immunology 1996; 89:26-33
17. Lalande V, Truffot-Pernot C, Paccaly-Moulin A. *et al.* Powerful bactericidal activity of sparfloxacin (AT-4140) against *Mycobacterium tuberculosis* in mice. Antimicrob Agents Chemother 1993; 37:407-13
18. Nuermberger E, Yoshimatsu T, Tyagi S. *et al.* Moxifloxacin-containing regimen greatly reduces time to culture conversion in murine tuberculosis. Am J Respir Crit Care Med 2004; 169:421-26

Chapter 3

Course of murine tuberculosis and response to first-line therapy depends on route of infection and inoculum size

J.E.M. de Steenwinkel, M.T. ten Kate, G.J. de Knegt, H.A. Verbrugh, A. van Belkum, R. Hernandez-Pando, I.A.J.M. Bakker-Woudenberg

ABSTRACT

Objective

In the search for novel anti-tuberculosis (TB) drugs, numerous potential drugs are being screened *in vitro*. In animal models promising, novel anti-TB drugs are assessed in terms of toxic side effects and comparative therapeutic efficacy. Mice are frequently used and experimental infections are established in different ways. In the present study it is investigated to what extent the route of *Mycobacterium tuberculosis* inoculation is a determinant in the pathogenesis of TB and the therapeutic outcome. Results will contribute to insight into the translational value of TB models used for preclinical studies.

Design

TB in mice was established through intratracheal or intravenous Mtb inoculation. The efficacy of a 26-weeks therapy was evaluated; including assessment of relapse of infection 13 weeks post treatment.

Results

It was shown that the course of TB and the therapeutic response, in terms of histopathological characteristics and Mtb load, in lung and extra-pulmonary organs is substantially different and dependent on the route of infection applied and the inoculum size used.

Conclusion

When evaluating the comparative therapeutic potential of novel anti-TB drugs or drug treatment schedules investigated in different studies, it should be noted that the route of infection applied and inoculum size used influence the course of murine TB and the therapeutic response to the standard first-line TB drug regimen.

BACKGROUND

Tuberculosis (TB) remains a major cause of morbidity and mortality worldwide. *Mycobacterium tuberculosis* (Mtb) has now infected about one third of the world's population of which eight to nine million develop TB. Over one and a half million patients die annually as a result of TB.[1] In order to reduce this enormous burden of disease, development of new anti-TB drugs or improvement in use of current anti-TB drugs is needed. To facilitate the development of new anti-TB drugs, libraries of small molecules and natural products are being screened for their activity against Mtb and previously identified crucial targets of Mtb are being explored to design new inhibiting molecules.[2] Numerous novel anti-TB drugs are being tested for their *in vitro* capacity to kill Mtb under different culture conditions. Only a small selection of them will proof to be active *in vitro* and will be further explored in animal models representing a dynamic test system in which the therapeutic antimicrobial effect depends on many factors. In animal models potential toxic side effects of promising, novel anti-TB drugs can be estimated in terms of toxicity assessed by body weight, discomfort score of mice and by liver- and kidney-function tests. Mice are frequently used in TB research, and experimental infections are established in different ways. The merits of animal models are that they enable comparative therapeutic studies at similar conditions of severity and duration of infection, which is difficult in patients due to different underlying conditions. However, the limitations of animal models among which the artificial induction of infection, differences in bacterial virulence and immunological host response, and differences in pharmacokinetics and toxic side effects, should be emphasized. As a result, comparative therapeutic studies in animal TB models may only serve as a basis for therapy trials in TB patients.[3]

In mice, TB infection is mostly established by pulmonary or intravenous inoculation of Mtb. It is expected that the route of Mtb inoculation is an important determinant in the pathogenesis of the lung infection, and the dissemination. In the present study the course and pathogenesis of TB infection in lung and extra-pulmonary sites in relation to the route of infection, and the response to TB therapy is investigated. Mice were infected through the intratracheal (IT) or intravenous route (IV).

The efficacy of standard first-line therapy for 26 weeks was evaluated during therapy and after a 13-weeks period post therapy to assess relapse of TB infection. The Mtb load in the lung and extra-pulmonary organs and their histopathological characteristics were used as parameters.

MATERIALS AND METHODS

Bacterium

Mtb strain used was H37Rv (ATCC 27294). Mycobacteria were cultured on Middlebrook 7H10 agar and incubated for 21 days, as described previously.[4]

Animals

Specified pathogen-free female BALB/c mice were obtained from Charles River (Les Oncins, France). At the day of infection, animals were 10-12 weeks old and weighted 20-25 grams. Experimental protocols adhered to the rules specified in the Dutch Animal Experimentation Act and the published Guidelines on the Protection of Experimental Animals by the Council of the EC. The Institutional Animal Care and Use Committee of the Erasmus MC approved present protocols.

Infection

Intratracheal inoculation was performed as previously described.[4] In short, mice were infected by intratracheal instillation of a volume of 40 µL of Mtb suspension containing 9.5×10^4 CFU. Intravenous inoculation was performed by intravenous injection of 0.2 mL of an Mtb suspension containing 1.5×10^7 CFU via the tail vein.

Anti-TB therapy

The anti-TB drugs dosage and schedules used in our mouse TB model were derived from current clinical guidelines.[5-6] A combination of isoniazid, rifampicin and pyrazinamide, in human-pharmacokinetic-equivalent doses [7-8] was administered, as described previously.[4] In short, treatment was started at 4 weeks after inoculation, when patches of pneumonic lesions were observed and established infection was confirmed by stabilization of the Mtb load and TB-characteristic histopathological findings.[4] Treatment was continued during 26 weeks consisting of a 9-week initial phase followed by a 17-week continuation phase. During the initial phase, animals received a combination of isoniazid [25 mg/kg], rifampicin [10 mg/kg] and pyrazinamide [150 mg/kg]. In the continuation phase, only isoniazid and rifampicin were administered. Agents were administered once daily, 5 days a week.

Determination of viable Mtb counts in infected organs and blood. At all indicated time points mice (n=4 per time point) were sacrificed by CO_2 exposure. The lung, spleen and liver were removed aseptically and processed as described previously.[4] In short, blood samples were taken via cardiac puncture and the entire organs were removed and homogenized each in 2 mL PBS. To prevent carry-over of anti-TB drugs, therapy was stopped 72 hours before sacrificing the mice. Tissue homogenate suspensions were centrifuged at 14,000xg for 10 min, and pellets were re-suspended in 2 ml PBS. From the undiluted tissue homogenate and the 10-fold serial dilutions of the homogenate, samples of 200 µl were plated onto solid medium.

Assessment of relapse of infection

The amount of viable Mtb counts in lung, spleen, liver and blood of mice (n=4) was assessed 13 weeks after termination of anti-TB therapy. Relapse was defined as Mtb positive cultures of infected organs, while immediately after termination of therapy, organs were Mtb culture negative.

Histopathological examination of infected organs

Histopathological changes in lung, liver and spleen during the course of the infection were determined by sacrificing the animals (n=3) at indicated time points and processed as described previously.[4] Paraffin-embedded tissues were cut into 4 μm sections from which one in every 7 cuts was used for haematoxylin-eosin staining. A pathologist, blinded to the experimental conditions, examined 4 slides of each tissue.

RESULTS

Course of TB infection after IT or IV inoculation

At 4 weeks after IT or IV inoculation infection had developed, and a similar Mtb load was achieved in the lung being a median of $2.4x10^7$ CFU [range, $2.9x10^6$-$5.5x10^7$] and $1.5x10^7$ CFU [range, $7.5x10^6$-$2.9x10^7$] in the IT-infected mice and IV-infected mice, respectively. However, at that time histopathological changes in infected lung tissue of the IT-infected mice versus the IV-infected mice were clearly different.

In IT-infected mice, lung sections showed a limited number of pneumonia patches with areas of lung consolidation (figure 1A, asterisk), constituted by lymphocytes and numerous activated macrophages in the alveolar lumina with fibrilar material that correspond to coagulated plasmatic protein. Also, mild inflammatory infiltrates around bronchial and blood vessel walls and middle size well-formed compact granulomas were seen (figure 1A, arrow). Mtb load in the liver of the IT-infected mice was $6.3x10^4$ CFU and liver sections showed a large number of large, well-formed granulomas which were randomly dispersed (figure 1B). The spleen load of the IT-infected mice was $1.4x10^5$ CFU. Histopathology of the spleen exhibited mild white pulp hyperplasia without granulomas (figure 1C).

In contrast to the lung of IT-infected mice, at the same time-point of 4 weeks after infection the lung of IV-infected mice already showed extensive pneumonia and large granulomas on histopathological evaluation (figure 1G). The liver of the IV-infected mice showed an Mtb load of $2.6x10^7$ CFU and numerous, large granulomas were seen particularly near to central veins as well as accentuated Kupffer cell hyperplasia (figure 1H). Mtb load in the spleen of the IV-infected mice was $4.0x10^6$ CFU. Histopathological evaluation revealed accentuated macrophage hyperplasia in the marginal zone with numerous large granulomas (figure 1I, arrows).

At 17 weeks after IT infection Mtb load in the lung was 2.5×10^6 CFU. Histopathological evaluation showed more pronounced changes and extensive fibrosis with numerous plasma cells around blood vessels and extensive pneumonia (figure 1D). Mtb load in the liver was 1.6×10^4 CFU, and histopathology revealed numerous middle-sized and large granulomas (figure 2E, arrows). Mtb load in the spleen was 2.0×10^5 CFU and histopathological evaluation showed extensive hyperplasia of splenic white pulp (figure 1F).

In comparison to IT-infected mice, at the same time-point of 17 weeks after infection, the lung of the IV-infected mice had an Mtb load of 1.6×10^7 CFU. The corresponding histopathology of the lung showed extensive pneumonia, abundant interstitial fibrosis (figure 1J, asterisk) and numerous multinucleated giant cells and foamy cells were seen (figure 1J). The liver had an Mtb load of 1.5×10^7 CFU, and the histopathology of the liver consisted of large granulomas (figure 1K, asterisk) and extensive inflammatory infiltrate in the portal areas (figure 1K, arrow). Mtb load in the spleen was 1.6×10^7 CFU. Histopathological evaluation revealed numerous well-formed granulomas in the red pulp (figure 1L, arrows).

At 30 weeks after IT infection Mtb load in the lung was 3.5×10^6 CFU and histopathology of the lung was equivalent to that of 17 weeks after IT infection. Mtb load in the liver was 1.6×10^4 CFU. No significant change of histopathological damage had occurred, compared to 17 weeks after IT infection. The spleen had an Mtb load of 1.3×10^5 CFU and on histopathological examination the amount of hyperplasia was slightly increased (pictures not shown).

IV-infected mice all died between 23 and 30 weeks of infection. So, Mtb load or histopathology at 30 weeks after IV infection could not be evaluated. From 30 weeks of infection onwards the IT-infected mice became increasingly sick over time, and at 43 weeks all animals had died.

Therapeutic efficacy of standard first-line therapy

Therapy response was assessed in terms of decrease in Mtb load in lung, liver and spleen at the indicated time-points and success of therapy was defined as elimination of the Mtb load from infected organs and prevention of relapse of TB. Decreases in Mtb load in the different organs were expressed in figure 2.

After 13 weeks of therapy in the IT-infected mice Mtb elimination was achieved in lung, liver and spleen. However, in the IV-infected mice within 13 weeks, only the lung was Mtb-culture negative but longer therapy duration was needed to eliminate Mtb from liver and spleen. After 26 weeks of therapy, also liver and spleen from the IV-infected mice were Mtb-culture negative. Whereas in IT-infected mice relapse of infection at 13 weeks after termination of therapy did not occur, in IV-infected mice relapse of infection in all organs was observed in all mice at that time point (figure 2).
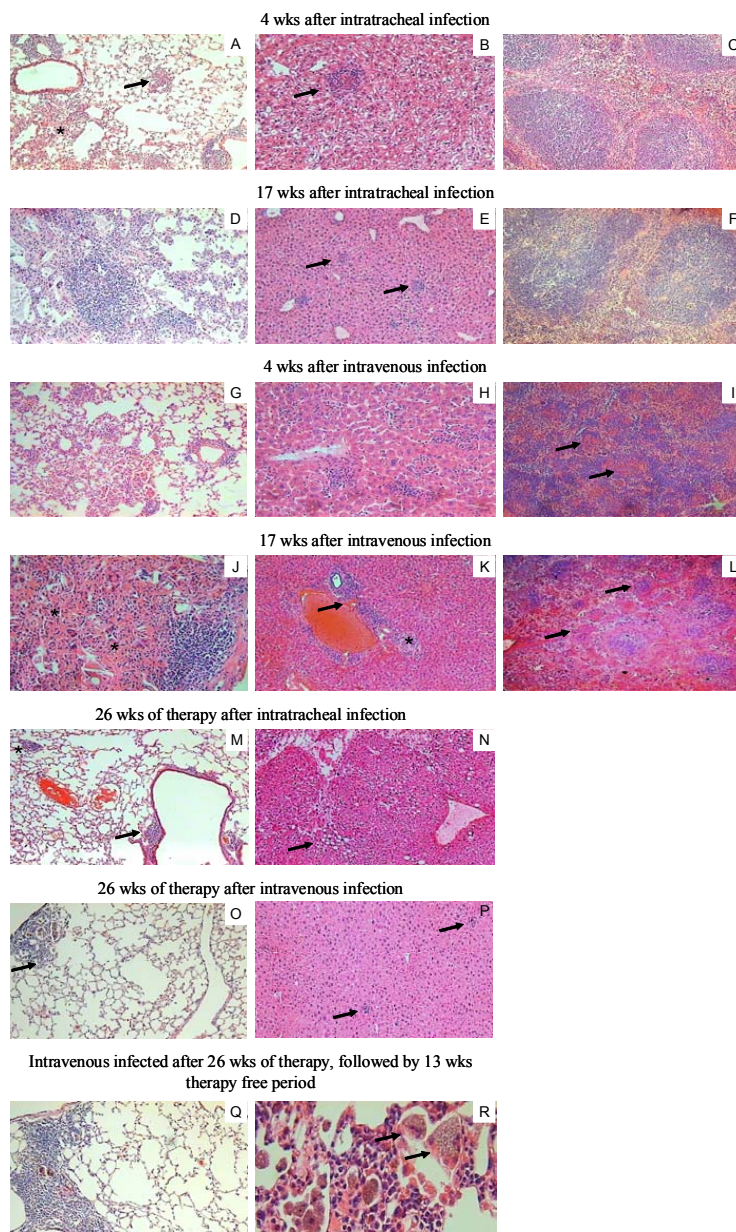
Figure 1. Representative histopathological features in lung, liver and spleen of intratracheal (IT) or intravenous (IV) TB infected mice. Histopathology is shown at 4 weeks after IT infection, in the lung **(A)** (200x), liver **(B)** (200x) and spleen **(C)** (200x); at 17 weeks after IT infection, in the lung **(D)** (200x), liver **(E)** (200x) and spleen **(F)** (200x); at 4 weeks after IV infection, in the lung **(G)** (200x), liver **(H)** (200x) and spleen (I) (200x); at 17 weeks after IV infection, in the lung **(J)** (200x), liver **(K)** (200x) and spleen **(L)** (200x); after 26 weeks of therapy in the IT-infected mice, in the lung **(M)** (200x) and liver (**N**) (200x); after 26 weeks of therapy in the IV-infected mice, in the lung **(O)** (200x) and liver **(P)** (200x); and after 26 weeks of therapy in the IV-infected mice followed by a therapy-free period of 13 weeks, in the lung **(Q)** (200x) and **(R)** (400x).

The histopathological examination of infected tissues of the mice treated with anti-TB drugs still revealed significant histological changes. After 26 weeks of therapy, the lung of the IT-infected mice exhibited some hyperplasia of the lymphoid tissue associated to bronchial wall (figure 1M, arrow) and small granulomas (figure 1M, asterisk). In the same animals, the liver showed complete elimination of granulomas and scarce chronic inflammatory infiltrate in portal areas, whereas some animals showed microvesicular steatosis (figure 1N, arrow). The spleen revealed stable white pulp hyperplasia. IV-infected mice, however, showed after 26 weeks of therapy, foamy macrophages and giant multinucleated cells with foamy cytoplasm located at small pneumonic patches in the lung (figure 1O, arrow). The liver still exhibited numerous small granulomas (figure 1P, arrows). The spleen showed mild hyperplasia in the white pulp, but no granulomas (picture not shown).

At 13 weeks after termination of therapy (at week 43) the IT-infected mice showed complete absence of pneumonia and granulomas in the lung, and only revealed residual hyperplasia of lymphoid tissue associated to bronchial mucosa. Liver and spleen showed a complete absence of granulomas or hyperplasia (pictures not shown). At the same time-point the IV-infected mice showed a relapse of infection. In their lung sections pneumonic patches constituted by lymphocytes and macrophages with foamy cytoplasm were seen (figure 1Q). These foamy cells and some activated cells showed erythrophagocytosis with cytoplasmic haematic pigment (hemosiderin) (figure 1R). At this time point, liver sections revealed many middle size granulomas and mild inflammation in the portal areas, and spleen sections showed hyperplastic white pulp without granulomas (pictures not shown).

Intratracheal infection

Intravenous infection

Lung

Lung

Liver

Liver

Spleen

Spleen
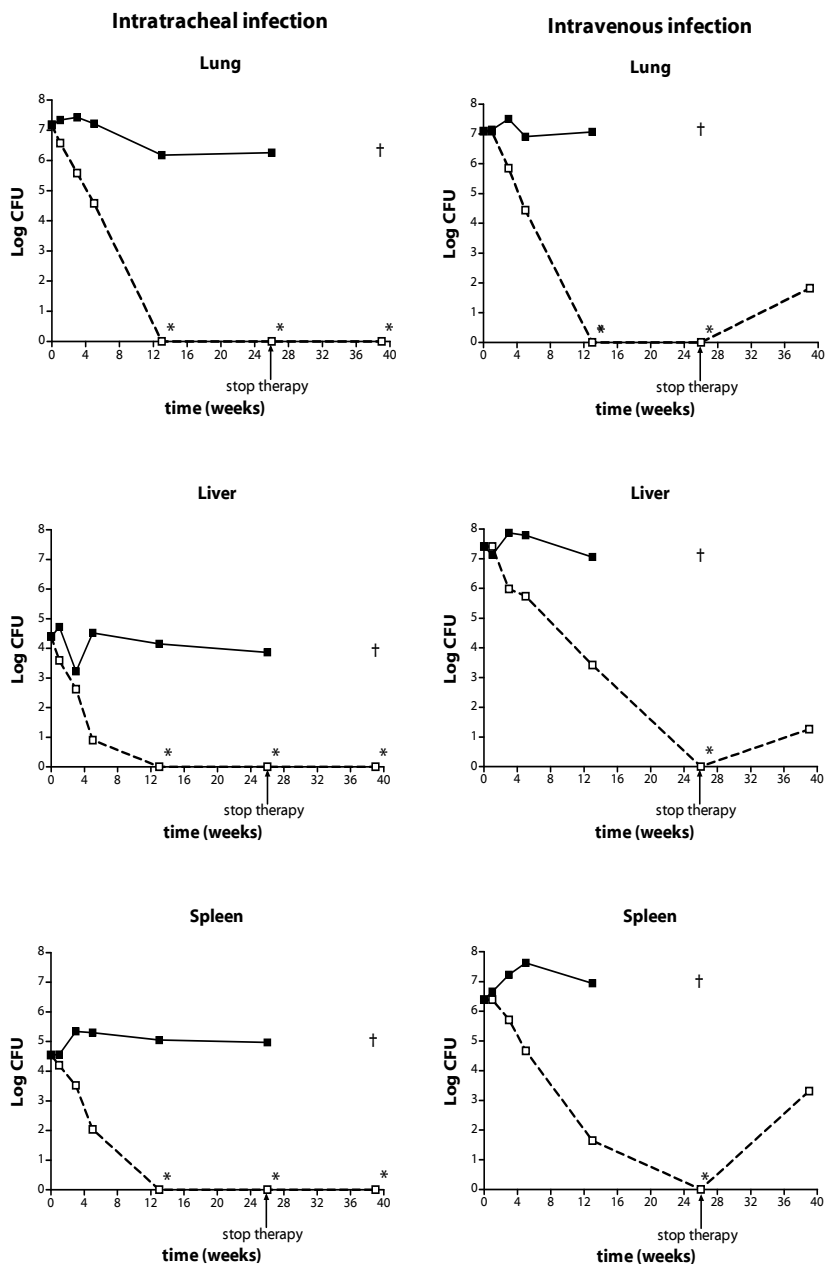
Figure 2. Efficacy of standard first-line therapy for 26 weeks in intratracheal- or intravenous infected TB mice (□).Untreated TB infected control mice (■). Start of therapy, at 4 weeks after infection, is indicated in the graphs as time zero. Mice were sacrificed at various intervals during therapy, and after termination of 26-weeks therapy (indicated in the graph). In order to determine relapse of infection, mice were sacrificed at 13 weeks after termination of therapy. Results are expressed in mycobacterial numbers in the infected organs of mycobacterial culture-positive mice. * All mice were mycobacterial culture-negative. † 4 out of 4 untreated mice died due to TB infection before indicated time point.

DISCUSSION

In the present study it is demonstrated that the pathogenesis of TB infection, monitored by Mtb cultures and histopathology of infected lung and extra-pulmonary organs, depends on the "Porte d'entrée" of Mtb and the inoculum size used. Various studies have been published on histopathological characterisation of different stage of TB in experimental models of TB. Cardona *et al.* compared various mouse strains, which differ in their susceptibility to TB, in an aerosol infection model.{Cardona, 2003 #266} Whereas North *et al.* described the difference in pathogenesis of TB in aerosol-infected mice versus intravenously-infected mice.[10-11] Similar to the experimental set-up in the present study, North *et al.* applied different Mtb inocula (relatively low numbers of Mtb for aerosol infection compared to the numbers of Mtb for intravenous infection), in order to achieve similar Mtb load in the lung. In the present study, the realization of a similar Mtb load in the lung for IV-infected and IT-infected mice resulted in a higher extra-pulmonary load in the IV-infected animals compared to the IT-infected animals. This probably contributed to the observed increased time-period before extra-pulmonary organs became culture negative in the IV-infected animals. In addition, differences in immune response following IV infection versus IT infection may add to differences in Mtb clearance from the various organs. Although in IV-infected animals the Mtb load in liver and spleen was similar to the load in the lung, different Mtb killing rate in these organs following therapy was observed, which might be related to differences in pathology and Mtb clearance capacity of these organs.

More recently, in a comparative study De Groote *et al.* used three different infection models and two mouse species, and evaluated these different models in efficacy studies with different anti-TB drugs regimens.[12] They found that a TB infection, established through the intravenous route showed a delayed treatment effect and a higher relapse rate of infection, compared to a respiratory infection model established through aerosol. In our study, we showed that a respiratory infection model of TB established through intratracheal inoculation also showed a different therapeutic response in terms of bacterial killing and relapse rate, compared to the intravenously infected mice. In this way, our results are in agreement with the results of De Groote *et al.* and add a third method to establish TB infection, which was shown to influence the course of TB and therapeutic response. Whereas we focused on the standard first-line therapy regimen, De Groote *et al.* showed that additionally to the standard first-line therapy regimen, when using other therapy regimens the observed differences related to the infection model remained standing.[12] The comparative histopathology of the lungs of the IT-infected mice versus the IV-infected mice revealed more inflammation and tissue damage (pneumonia) in IV-infected animals despite slightly lower Mtb burden than in IT-infected mice after 4 weeks of infection. Considering the early high Mtb load in the spleen of IV-infected mice, it is possible that higher lymphocyte activation occurs in this organ followed by extensive cellular migration

to the lung tissue, producing more rapid death of the IV-infected animals by a combination of active Mtb growth and immunopathology (e.g. inflammation, fibrosis) in the lungs.

The dependency of the bacterial killing kinetics of the standard first-line therapy on the route of infection is a relevant issue, as novel anti-TB drugs such as moxifloxacin, PA-824, TMC207, SQ-109 and SQ-641 have been investigated for their therapeutic potential in different animal models of TB. [13-16] These studies evaluating the most promising new anti-TB drugs are conducted either in models of respiratory infected mice (moxifloxacin and PA-824) or in models of intravenously infected mice (TMC207, SQ-109 and SQ-641).

The present study shows that in both IT-infected mice and IV-infected mice the standard first-line therapy of 26 weeks seemed effective. However, all IV-infected mice showed relapse of infection. Probably the Mtb clearance in the infected organs following the 26-weeks therapy was not sufficient due to severe tissue damage. The therapy failure in the IV-infected mice, in contrast to the IT-infected mice, was reflected in differences in the histopathological characteristics. At the end of the 26-weeks therapy IV-infected mice still exhibited lung and liver damage, although Mtb could not be cultured from both organs. The pneumonic lesions in the lung and granulomas in the liver further increased during the post-therapy period. These patches of pneumonia and liver granulomas might provide a unique environment for dormant Mtb which can not be cultured from these tissues at the end of therapy. However, after termination of therapy, regrowth of Mtb from these infection sites occurred. In this respect, interesting observations were described by Dhillon *et al.*[17] He showed that focal residual pneumonic lesions were rich in foamy macrophages, specific cell population of late tuberculous lesions characterized by its high cytoplasmic lipid content, which favour persistence of non-replicating bacilli after chemotherapy that can reactivate and resume Mtb growth.

Summarizing, in the present study the mouse model of TB through the natural respiratory route, mimicking human TB infection, showed an evident inflammatory acute phase of infection, followed by a progressive chronic phase of infection. The model was validated in terms of therapeutic successful outcome, with the rational time point for start of therapy at four weeks after infection, at transition of the acute to the chronic phase of infection. Relapse of infection in the post-therapy period did not occur. This in contrast to our data obtained in the mouse model of TB infection through the intravenous route. It is concluded that the course of infection in an animal TB model and the therapeutic response to the standard first-line therapy, in terms of pathogenesis and Mtb load in the lung and extra-pulmonary sites, is substantially dependent on the route of infection applied and the inoculum size used. Related to this, we suggest that when clinicians are evaluating the comparative therapeutic potential of novel anti-TB drugs investigated in different animal studies, they should be aware that the route of infection applied and inoculum size used influence the course of murine TB and the therapeutic response to the standard first-line TB drug regimen.

REFERENCES

1.   World Health Organization. Global tuberculosis control 2009: epidemiology, strategy and financing. WHO/HTM/TB/2009. 411. Geneva, Switzerland: WHO, 2009: 1–314.

2.   Palomino J C, Ramos D F, da Silva P A. New anti-tuberculosis drugs: strategies, sources and new molecules. Curr Med Chem 2009; 16: 1898–1904.

3.   Bakker-Woudenberg I A. Experimental models of pulmonary infection. J Microbiol Methods 2003; 54: 295–313.

4.   de Steenwinkel J E, De Knegt G J, Ten Kate M T, *et al*. Immunological parameters to define infection progression and therapy response in a well-defined tuberculosis model in mice. Int J Immunopathol Pharmacol 2009; 22: 723–734.

5.   Blumberg H M, Burman W J, Chaisson R E, *et al.* American Thoracic Society/Centers for Disease Control and Prevention/Infectious Diseases Society of America: treatment of tuberculosis. Am J Respir Crit Care Med 2003; 167: 603–662.

6.   Stop TB Partnership and World Health Organization. Global Plan to Stop TB 2006–2015. Geneva, Switzerland: WHO, 2006: 1–172.

7.   Lalande V, Truffot-Pernot C, Paccaly-Moulin A, *et al.* Powerful bactericidal activity of sparfloxacin (AT-4140) against *Mycobacterium tuberculosis* in mice. Antimicrob Agents Chemother 1993; 37: 407–413.

8.   Rosenthal I M, Zhang M, Williams K N, *et al*. Daily dosing of rifapentine cures tuberculosis in three months or less in the murine model. PLoS Med 2007; 4: e344.

9.   Cardona P J, Gordillo S, Diaz J, *et al*. Widespread bronchogenic dissemination makes DBA/2 mice more susceptible than C57BL/6 mice to experimental aerosol infection with *Mycobacterium tuberculosis*. Infect Immun 2003; 71: 5845–5854.

10.   North R J. *Mycobacterium tuberculosis* is strikingly more virulent for mice when given via the respiratory than via the intravenous route. J Infect Dis 1995; 172: 1550–1553.

11.   North R J, LaCourse R, Ryan L. Vaccinated mice remain more susceptible to *Mycobacterium tuberculosis* infection initiated via the respiratory route than via the intravenous route. Infect Immun 1999; 67: 2010–2012.

12.   De Groote M A, Gilliland J C, Wells C L, *et al*. Comparative studies evaluating mouse models used for efficacy testing of experimental drugs against *M. tuberculosis*. Antimicrob Agents Chemother 2011; 55: 1237–1247.

13.   Ibrahim M, Truffot-Pernot C, Andries K, *et al*. Sterilizing activity of R207910 (TMC207)-containing regimens in the murine model of tuberculosis. Am J Respir Crit Care Med 2009; 180: 553–557.

14.   Nikonenko B V, Reddy V M, Protopopova M, *et al*. Activity of SQ641, a capuramycin analog, in a murine model of tuberculosis. Antimicrob Agents Chemother 2009; 53: 3138–3139.

15.   Nuermberger E, Tyagi S, Tasneen R, *et al*. Powerful bactericidal and sterilizing activity of a regimen containing PA-824, moxifloxacin and pyrazinamide in a murine model of tuberculosis. Antimicrob Agents Chemother 2008; 52: 1522–1524.

16.   Rosenthal I M, Zhang M, Almeida D, *et al*. Isoniazid or moxifloxacin in rifapentine-based regimens for experimental tuberculosis? Am J Respir Crit Care Med 2008; 178: 989–993.

17.   Dhillon J, Dickinson J M, Sole K, *et al*. Preventive chemotherapy of tuberculosis in Cornell model mice with combinations of rifampicin, isoniazid, and pyrazinamide. Antimicrob Agents Chemother 1996; 40: 552–555.

Chapter 4

Tuberculosis mimicking ileocecal intussusception in a 5-month-old girl

J.E.M. de Steenwinkel, G.A. Driessen, M.H. Kamphorst-Roemer
A.G.M. Zeegers, A. Ott, M. van Westreenen

ABSTRACT

A 5-month-old girl was diagnosed with tuberculosis, mimicking ileocecal intussusception. The mother of the patient was later diagnosed with renal tuberculosis attributable to the same (unique) *Mycobacterium tuberculosis* strain. Possibly, that transmission occurred by aspiration or ingestion of infected amniotic fluid or urine, which could occur before or during birth. This case illustrates that tuberculosis can mimic other common diseases and, therefore, can be a difficult diagnosis to make. Because respiratory infection was very unlikely in this case, congenital tuberculosis or postnatal infection via infected urine or breast milk should be in the differential diagnosis. In this article, we focus on different (non-respiratory) transmission routes of *Mycobacterium tuberculosis* and give a short review of the recent literature on congenital tuberculosis.

INTRODUCTION

Worldwide there are an estimated 2 billion *Mycobacterium tuberculosis* (Mtb) infected persons, of whom 8.8 million developed tuberculosis (TB) in 2003.[1] This is in sharp contrast with the just over 300 reported cases of congenital tuberculosis (CTB). In 1994, Cantwell revised the diagnostic criteria as set by Beitzke and set the "Cantwell criteria" (table 1).[2]

The first symptoms of CTB typically occur within 3 months of birth. In most cases, onset of the disease is in the second half of the first month.[3-4] The presenting signs and symptoms are often non-specific, mimicking other more common diseases. Cantwell *et al.* described the most prevalent symptoms (table 1).

We describe a 5-month-old child suspected to have an ileocecal intussusception, who appeared to have miliary TB. This is an apparent example of the diverse and difficult ways TB can present. Because CTB should be in the differential diagnosis in such cases, we focussed on the different (non-respiratory) transmission routes of Mtb and the literature on CTB.

A	"Cantwell" diagnostic criteria for congenital tuberculosis*	
(1)	lesions present in the first week of life	
(2)	a primary hepatic complex or caseating hepatic granulomas	
(3)	tuberculous infection of the placenta or maternal genital tract	
(4)	exclusion of the possibility of postnatal transmission by thorough investigation of contacts, including the infant's hospital attendants, and by adherence to existing recommendations for treating infants exposed to tuberculosis.	
B	Symptom or Sign	No. (%) of patients
(a)	Hepatosplenomegaly	22 (76)
(b)	Respiratory distress	21 (72)
(c)	Fever	14 (48)
(d)	Lymphadenopathy	11 (38)
(e)	Abdominal distension	7 (24)
(f)	Lethargy or irritability	6 (21)
(g)	Ear discharge	5 (17)
(h)	Papular skin lesions	4 (14)

Table 1. The Cantwell criteria. * Cantwell *et al.* [2] described diagnostic criteria to differentiate congenital tuberculosis **(A)**. At least one of these criteria (1-4) must be present, together with a (culture) proven tuberculosis, in order to make the diagnosis congenital tuberculosis. The presenting symptoms of congenital tuberculosis are very divers and differ in percentage of occurrence **(B).**

CASE REPORT

A 5-month-old girl presented at a primary care hospital with a 5-day history of non-bloody diarrhoea. The patient had started vomiting two days previous to admission and had sub-sequently developed a distended abdomen. She had developed a fever one day prior to admission.

The patient was the first child of an Indonesian mother and Dutch father and was born in the Netherlands. The mother became pregnant spontaneously after several failed attempts of *in vitro* fertilization. Pregnancy and delivery were uneventful. Mother was HIV, HBsAg and syphilis negative.

On physical examination, she appeared moderately ill, with a temperature of 37,5°C, pulse rate of 150/min, and respiratory rate of 30/min. She had a distended abdomen with sparse bowel sounds. The liver was slightly enlarged without splenomegaly. A non-tender mass was palpable in the right lower abdominal quadrant. Initial laboratory examination showed: Hb 6,9 mmol/L, leucocytes $22,1x10^9$/L with 43% granulocytes and 19% band-forms, and a CRP of 286 mg/L. The abdominal radiograph was normal, but the ultrasound showed a crescent-in-doughnut sign or "multiple-concentric-ring-sign", which was compatible with the initial diagnosis of ileocecal intussusception. There were no signs of appendicitis or abdominal abscesses. In an attempt to correct the intussusception with hydrostatic pressure, a barium enema was performed, which revealed a complete obstruction at ileocecal level. After the procedure, the patient developed a more distended abdomen, with deterioration of the clinical condition, metabolic acidosis and hyponatremia. She was subsequently referred to the intensive care unit of our tertiary care hospital.

Because of suspected intestinal ischemia or bowel perforation, a laparotomy was performed. This showed an inflammatory process in the ileocecal region with multiple adhesions, but indications for an intussusception or enlarged mesenteric lymph nodes were absent. Mainly in that region, the visceral and parietal peritoneum were covered with multiple white-greyish nodules with a diameter of 2-5 mm. Auramine staining of multiple biopsies was mycobacteria positive. Culture of the nodules, ascites and gastric aspirate yielded Mtb.

CT-thorax showed miliary lesions throughout the lungs. Retrospectively, these fine lesions were already present on the preoperative chest radiograph, but unnoticed at that time. The CT-cerebrum and lumbar puncture excluded the presence of tuberculous meningitis. On reti-noscopy a few choroidal tubercles were visible. The Tuberculin Skin Test (TST) was negative initially, but became positive one month later.

Treatment was initiated with intravenous rifampicin and ciprofloxacin. Within one week, the patient was able to take oral medication, so treatment switched to oral rifampicin, isoniazid, ethambutol and pyrazinamide. Isoniazid was discontinued when the Mtb strain showed resistance to isoniazid. Pyrazinamide was stopped after 2 months and treatment with rifampicin and ethambutol was continued for another 7 months. She fully recovered.

The TST of the father measured 22 mm; nonetheless his chest radiograph was normal. Since he did not have signs of active TB, he was diagnosed with a latent TB. The initial treatment was isoniazid but changed to rifampicin for 4 months when the strain, isolated from the child appeared to be isoniazid-resistant.

The mother, aged 30 immigrated to the Netherlands at the age of 22. She was not Bacille Calmette-Guérin (BCG) vaccinated. The TST, on arrival in the Netherlands, showed an induration of 18 mm. The chest radiograph showed a small pleural adhesion and calcification suspect for primary TB complex. The mother was not treated but followed for 2 years, by half-yearly chest radiographs, which remained unchanged.

After diagnosing TB in the child, we advised the mother to consult an internist and gynaecologist to evaluate the presence of extra-pulmonary TB. However, the mother refused further examination, but when she developed fever and backache, investigations showed right-sided hydronephrosis. The pyelum was drained by nephrostomy and urine samples showed acid-fast rods and PCR confirmed Mtb.

At that time, it became apparent that the mother had consulted a gynaecologist because of fertility problems. An abdominal ultrasound, at that time, showed calcification in the right ovary and tube. The mother refused further analysis of the ovarian lesions and no final diagnosis was made

Because the child's Mtb strain was isoniazid-resistant, the mother received 2 months rifampicin, ethambutol and pyrazinamide followed by 7 months rifampicin and ethambutol. After 2 months, when infection parameters had normalised, nephrectomy of the right kidney was performed. Histopathology analysis revealed extended granulomatous inflammation and caseous necrosis of the kidney. The strain recovered from the mother's urine sample had the same Restriction Fragment Length Polymorphism (RFLP)-pattern as the strain isolated from the child (figure 1). These two strains together form cluster 7195 and are unique in the Netherlands. The exclusive RFLP-pattern is indicative for the transmission of the Mtb strain from the mother to the child.[5] Since the RFLP-pattern is unique in the Netherlands, one can argue that the TB infection of the mother took place in another country or before RFLP analysis was done on all Mtb strains in the Netherlands.

NLA000500898	7195	Daughter
NLA000501250	7195	Mother
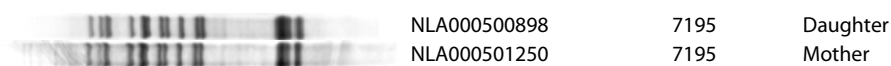
Figure 1. The IS6110 restriction fragment length polymorphism (RFLP) analysis of the *Mycobacterium tuberculosis* strains isolated from the daughter (NL A 000500898) and the mother (NL A 00501250) showed to be identical. These 2 strains are unique for the Netherlands.

According to the Dutch guidelines for contact and source tracing, the investigation of extra pulmonary TB patients focuses on the identification of a possible infectious source case. During these investigations by the Municipal Health Service, it became apparent that none of the 16 examined contacts (including the grandparents) had pulmonary TB. Ten of these contacts were examined with a TST. As mentioned above, the father of the child was the only person with a positive TST and thus treated for latent TB. Since there was no case of active (contagious) TB found, respiratory infection of the child became unlikely. This finding, together with similar and unique RFLP-pattern of the strains isolated from the mother and child, directed the differential diagnosis strongly to neonatal or CTB.

DISCUSSION

To our knowledge, this is the first report of TB mimicking an intussusception. Only after laparotomy the suspected intussusception became manifest as TB. Probably the obstruction of the bowel, that caused the symptoms, was due to the inflammatory process and the multiple adhesions. Because of the acute presentation, there was no substantial diagnostic delay in this patient, in contrast with many other cases with a gradual increase of symptoms. This diagnostic delay is of great importance, since it is an important determinant of poor disease outcome.[3-4]

The atypical presentation might lead to underestimation of the incidence of TB, especially in settings with inadequate access to health care and diagnostic facilities and undiagnosed TB or CTB, might be the cause of some unexplained infant-death.[6]

The Royal Netherlands Tuberculosis Association (KNCV) registers the incidence of TB in the Netherlands. In their surveillance report on the incidence of TB from 1996-2005, they showed that the incidence of TB in children between 0 and 14 years of age, is on average 3.0 per 100.000 (range 1.7-3.9).[7] Since CTB is a rare presentation of TB, there is no specific registration of CTB and therefore correct incidence number is difficult to give. In the literature there is only one Dutch case of CTB described in the last 50 years.[4]

Extra-pulmonary TB, like genitourinary TB, occurs more often in developing countries, probably due to poorer treatment of pulmonary TB. About 20 percent of TB patients develop extra-pulmonary symptoms, 20-40 percent of those involve the genitourinary system.[8] Most genitourinary TB cases are the result of haematogenous spread of mycobacteria from the primary pulmonary focus to the kidney and female genital organs. Genital TB often results in infertility. Consequently, the likelihood of vertical transmission decreases when the female genital organs are involved.

Possible routes of infection in-utero are haematogenous spread through the umbilical vein or ingestion of infected amniotic fluid. Transmission during labour is possible through direct contact with an infected birth canal or ingestion of infected amniotic fluid or urine. Non-respiratory infection after birth can be by ingestion of infected urine (which is highly contagious) from an infected carrier and is possible when appropriate precautions are not taken.

The best prevention of transmission is to treat the mothers during pregnancy. Treatment of the (extra-) pulmonary TB of the pregnant women should be started as soon as possible, to guarantee the best treatment outcome.[9] The place of isoniazid in this treatment is still under debate, because the prevention of TB might result in isoniazid-induced hepatitis, which increases the death rate of the unborn child. Other (new) medication enabling the treatment of (latent) TB without isoniazid possible could solve this problem.[9]

Another route of infection is via infected mother milk, though accurate risk analysis on this matter is missing. One can argue that women with a high Mtb burden, who even have the bacteria in their blood, are at risk to transmit the disease this way. Also when there are extra-pulmonary caseous lesions in the breast, the possibility of transmission is increased. Therefore, when a child is suspect for TB, without a liable route of respiratory infection, breast examination of the mother is indicated.

In CTB, the route of transmission directs the presentation and pattern of infection.[2-3] Intra-uterine infection via the umbilical vein typically results in a primary complex in the liver.[10] It is known that, infection by aspiration or ingestion may give a primary infection in the lung or gut, and direct inoculation onto fragile epithelia even e.g. in the middle ear.[11] Postnatal transmission of TB by inhalation of the bacteria is the most frequent mode, giving a primary complex in the periphery of the lung. In adults only a minority of Mtb infected persons develop active infection. In children this proportion is not exactly known but considered to be higher because of an immature immune response. Therefore TB will also more easily disseminate in young children.[11] Nonetheless, in neonates, possibly protective immunity of the mother could help to prevent development of active TB. This protective immunity through placental transmission of active elements of the immune system such as transfer-factors

might explain some cases of delayed CTB onset.[12] Immature immune response of infants also explains a reduced value of the TST. For that reason, in case of suspected CTB, specific staining and cultures of gastric aspirates, urine and cerebral spinal fluid are mandatory. In addition aspirates and/or biopsies from affected organs are required. Furthermore, cerebral and thoraco-abdominal CT-scan or MRI and fundoscopy are essential to detect dissemination. To confirm congenital transmission, a thorough evaluation of possible sources of TB is necessary, including evaluation for maternal genitourinary TB.

To further understand the difficulties of CTB, a literature review on the "recent" publications related to CTB provides the following observations. Singh *et al.* described in 2007, four different cases of TB in young infants, all presented with divers, aspecific symptoms.[13] Of these four cases, only one was classified as a CTB, due to the early onset of disease and the absence of an index patient at the time of presentation. In the CTB case, the mother of the child (like in our case) presented herself with neurological complains due to multiple tuberculomas one week after the TB diagnosis of the child. Singh *et al.* argue that it might be better to use the term perinatal TB instead of CTB or neonatal TB, because that differentiation is only of epidemiological importance and can be difficult.

Nicolaidou *et al.* reported a classical case of CTB in 2005. They described a 1-month-old baby that was infected by endometrial TB during pregnancy. The mother did not have any symptoms during pregnancy, had no history of TB and remained with a normal chest radiograph. The only sign of possible infection was a positive TST. This lack of symptoms is seen more often. In about 75 percent of the cases of CTB, the pregnant women remained asymptomatic during the extra-pulmonary TB and as a result were misdiagnosed.[4,14] Again this case showed that CTB can present itself like a more common infection and delay in the correct therapy can be the result.[3] Therefore, when a child does not respond to broad-spectrum antibiotics and supportive treatment, CTB should be in the differential diagnosis and unless a high index of suspicion is maintained the diagnosis can be missed.[13,15]

The similarity of strains, active genitourinary TB in the mother and absence of another source of TB, which is one of the Cantwell criteria's, supports our hypothesis that transmission occurred pre- or perinatally. Unfortunately, no endometrial biopsies were performed and therefore we cannot exclude intra-uterine exposure. Furthermore postnatal transmission of Mtb via breast milk or infected urine of the mother cannot be excluded. Nonetheless we hypothesise that in our case transmission of mycobacteria occurred by ingestion of infected urine during delivery, because of the massive renal infection of the mother and the possible high risk of exposure to the infected urine, during labour. Since our patient was almost five months (136 days) on presentation, far above the average of previously reported cases

of CTB, we would like to illuminate that clinicians should consider CTB in their differential diagnosis even after the age of 3 months.

In conclusion, our case demonstrates that TB can present in a non-specific way. To our knowledge this is the first report of TB in an infant that is mimicking an intussusception. The way of infection of this child, where aerogenic infection is very unlikely, can be aspiration or ingestion of infected amniotic fluid, urine or breast milk, which could have taken place before, during or after birth.

ACKNOWLEDGEMENT

REFERENCES

1. World Health Organization (WHO). Global Tuberculosis Database 2005.
2. Cantwell M, Shehab Z, Costello A, Sands L, Green W, Ewing E, Jr., *et al.* Brief report: congenital tuberculosis. N Engl J Med 1994; 330(15):1051-4
3. Mazade M, Evans E, Starke J, Correa AG. Congenital tuberculosis presenting as sepsis syndrome: case report and review of the literature. Pediatr Infect Dis J 2001; 20(4):439-42
4. Hageman J, Shulman S, Schreiber M, Luck S, Yogev R. Congenital tuberculosis: critical reappraisal of clinical findings and diagnostic procedures. Pediatrics 1980; 66(6):980-4
5. Kiers A, Drost A, van Soolingen D, Veen J. Use of DNA fingerprinting in international source case finding during a large outbreak of tuberculosis in The Netherlands. Int J Tuberc Lung Dis 1997; 1(3):239-45
6. Kumar R, Gupta N, Sabharwal A, Shalini. Congenital tuberculosis. Indian J Pediatr 2005; 72:631-3
7. Erkens C, Kalisvaart N, Slump E, Šebek M, van Soolingen D. 'Tuberculose in Nederland 2005', Surveillancerapport over de tuberculose situatie in Nederland. KNCV Tuberculosefonds 2007
8. Lenk S, Schroeder J. Genitourinary tuberculosis. Curr Opin Urol 2001; 11(1):93-8.
9. Smith KC. Congenital tuberculosis: a rare manifestation of a common infection. Curr Opin Infect Dis 2002; 15(3):269-74
10. Berk D, Sylvester K. Congenital tuberculosis presenting as progressive liver dysfunction. Pediatr Infect Dis J 2004; 23(1):78-80
11. Skevaki C, Kafetzis D. Tuberculosis in neonates and infants: epidemiology, pathogenesis, clinical manifestations, diagnosis, and management issues. Paediatr Drugs 2005; 7(4):219-34
12. Fabre R, Perez T, Aguilar L. *et al.* Transfer factors as immunotherapy and supplement of chemotherapy in experimental pulmonary tuberculosis. Clin Exp Immunol 2004; 136(2):215-23
13. Singh M, Kothur K, Dayal D, Kusuma S. Perinatal tuberculosis a case series. J Trop Pediatr 2007; 53(2):135-8
14. Abughali N, Van der Kuyp F, Annable W, Kumar ML. Congenital tuberculosis. Pediatr Infect Dis J 1994; 13(8):738-41
15. Chen A, Shih S. Congenital tuberculosis in two infants. AJR Am J Roentgenol 2004; 182(1):253-6

Chapter 5

Dynamics of Interferon-Gamma Release Assay and cytokine profiles in blood and respiratory tract specimens from mice with tuberculosis and the effect of therapy

J.E.M. de Steenwinkel, G.J. de Knegt, M.T. ten Kate, H.A. Verbrugh, T.H. Ottenhoff, I.A.J.M. Bakker-Woudenberg

ABSTRACT

There are limitations on diagnostic methods to differentiate between active and latent tuberculosis (TB), and the prediction of latent progression to TB disease is yet complex. Traditionally, tuberculosis-specific host immune response was visualized using the tuberculin skin test. Nowadays, IFN-γ release assays (IGRA) provide a more specific and sensitive tool, by which exposure to Mtb could be determined. However, the merit of IGRA in diagnosing active TB is yet unclear.

We adapted IGRA for use in mice, and quantifying bead-based flow cytometry techniques were used to assess cytokine profiles during the course of untreated infection and to investigate the value of IGRA and cytokines as biomarkers for therapy response.

High variability of IGRA results during progression of active TB infection related to various phases of infection was obtained. However, a significant decrease in IGRA results and in levels of IFN-γ, IL-17, IP-10 or MIG was observed and appeared to be associated with successful therapy.

This outcome does not support the value of IGRA to accurately diagnose active TB or to monitor infection progression. However, IGRA proved to be a useful biomarker to monitor therapy success. In addition, different cytokines might serve as biomarkers.

INTRODUCTION

Diagnosing tuberculosis (TB) remains complex and challenging. Differentiating between latent TB infections (LTBI) and active TB is of vital importance. Various tools for diagnosing TB are available. First, there is detection of *Mycobacterium tuberculosis* (Mtb) in sputum and other fluids (e.g. microscopic determination of bacilli, culture or amplification of Mtb-specific genome parts). Second, recognition of TB can be made in terms of disease presentation (e.g. patient anamnesis or chest radiography) or detection of a TB-specific host immune response (e.g. tuberculin skin test (TST) or interferon gamma (IFN-γ) release assays (IGRA). A limitation of the gold standard, that is, Mtb culture, is that it may take as long as 6 weeks, so more rapid detection of TB is needed. Therefore, numerous studies have been performed to identify biomarkers to detect TB infection, among which IGRA as potential biomarker.[1-4] The dynamics of IGRA during the course of untreated TB in not yet clear. The goal of the present study was to provide further insight in this respect and to investigate the value of IGRA as a biomarker to monitor therapy response.

IGRA are *in vitro* tests detecting an immune response to Mtb-specific antigens. IGRA was introduced in the last decade as replacement of the TST and should provide more specific test results in LTBI without cross-reactivity after a Bacillus Calmette-Guérin vaccination.[5] Currently, two different IGRA are available, QuantiFERON-TB Gold (QFT; Cellestis Ltd, Carnegie, Victoria, Australia) and T.SPOT. TB ELISpot (ELISpot; Oxford Immunotec, Abingdon, UK). Both tests are based on quantitative measurement of IFN-γ production by peripheral blood cells after stimulation with the Mtb-specific peptides early-secreted antigenic target-6 (ESAT-6) and culture filtrate protein-10 (CFP-10). Both IGRA showed excellent specificity that is unaffected by earlier BCG vaccination.[5] Several studies showed that T-SPOT.TB was more sensitive than QFT or TST.[2,5] An important annotation to these findings is the absence of a gold standard to diagnose LTBI. Nevertheless, the CDC recommended that QFT can be used in all circumstances in which TST was used, including contact investigations, evaluation of recent immigrants, and sequential-testing surveillance programs for infection control.[6] This advice is incorporated in many national guidelines. At present the merit of IGRA for diagnosing active TB, additionally to their use in diagnosing LTBI, is still under debate.

From clinical studies the additional value of using respiratory samples next to blood samples for IGRA is not (yet) clear. It is hypothesized that an IGRA performed in a sample from the primary site of infection (e.g. the lungs) might differentiate between active TB and LTBI. In patients bronchoalveolar lavage fluid or pleural fluid is used in such a way.[7] In the present study we also addressed this matter, by comparing respiratory sample IGRA results with blood IGRA results. Additionally, we assessed the cytokine/ chemokine profile in serum samples from mice at the acute and chronic phases of TB infection and during therapy and investigated

the diagnostic value of 17 immunological markers using a multiplex panel of bead-labelled cytokine and chemokine receptors.

In order to provide further insight into the dynamics of IGRA we adapted IGRA for use in our murine TB model.[8] A mouse model enables investigation of the value of this new test during the acute phase and chronic phase of infection and during standardized, well-controlled therapy. In animal models comparative studies at similar conditions of severity and duration of infection and therapy exposure can be performed, which is difficult in patients due to different underlying clinical conditions.[9]

MATERIALS AND METHODS

Animals

Specified pathogen-free female BALB/c mice, obtained from Charles River (Les Oncins, France) were infected at 10–12 weeks of age, as described previously.[8] The experimental protocols adhered to the rules specified in the Dutch Animal Experimentation Act and the published Guidelines on the Protection of Experimental Animals by the Council of the EC. The Institutional Animal Care and Use Committee of the Erasmus MC Rotterdam approved the present protocols.

Infection

Mice were infected through intratracheal instillation of a 40-μL suspension containing 9.4×10^4 CFU Mtb (H37Rv), as previously described.[8]

Anti-tuberculosis drugs

Therapy was administered from 4 weeks after the infection onwards. The therapeutic regimen consisted of a combination of isoniazid, rifampicin and pyrazinamide during the initial phase of 9 weeks, followed by a combination of isoniazid and rifampicin during 4 weeks, as described previously.[8] Anti-tuberculosis drugs were administered in human pharmacokinetic-equivalent doses.[10-11]

Interferon-gamma release assay

Peptides ESAT-6 / CFP-10 were synthesized by Pepscan (Pepscan Therapeutics, Lelystad, The Netherlands). Blood samples were obtained from sacrificed mice by cardiac puncture at indicated time points. In mice receiving therapy, administration of anti-tuberculosis drugs was stopped 72 h before dissection. Within 15 minutes of collection of blood, the heparinized samples were diluted five times using a mixture of RPMI 1640 medium (BioWhittaker–Cambrex, East Rutherford, New Jersey, USA) enriched with 2 mM Lglutamine (Invitrogen,

Carlsbad, CA, USA), 100 units of 100 µg/ml penicillin-streptomycin solution (Invitrogen), 10% heat-inactivated fetal calf serum (Invitrogen) and β-mercaptoethanol 0.002‰ (Sigma M7522, Sigma Chemical, St. Louis, MO, USA). Samples were divided into three portions, and stimulated with either concanavalin A (Invitrogen) in a final concentration of 10 µg/ml (positive control) or with enriched RPMI 1640 medium (negative control) or with a peptide mixture of ESAT-6 and CFP-10 (Pepscan) both in a final concentration of 0.25, 0.5, 1 or 2 µg/ml (Mtb-specific antigen response). After incubation for 24, 48, 72 or 96 hrs, at 37°C and 5% CO_2, 50 µl of the supernatant was used to assess the IFN-γ concentration in duplicate, employing the Mouse IFN-γ ELISA-kit II according to the manufacturers protocol (Becton Dickinson, Franklin Lakes, NJ, USA) and a Bio-Rad Elisa Reader model 680 (Bio-Rad Laboratories, Veenendaal, the Netherlands). To prepare lung cell suspensions from sacrificed mice the lungs were aseptically removed and processed using a cell strainer with 70 µm nylon mesh (Becton Dickinson). Cell suspensions were subsequently processed according to the protocol described for blood.

Cytokine / chemokine concentrations in EDTA plasma

Quantification of cytokines / chemokines was performed using a bead-based flow cytometry technique (xMap; Luminex Corporation, Austin, TX, USA). The mouse soluble cytokine receptor multiplex panel used (Millipore Corporation, Billerica, MA, USA), consisted of a beadlabelled cytokine receptor against the following biomarkers: GM-CSF, IFN-γ, IL-1β, IL-2, IL-4, IL-6, IL-10, IL-12 (p40), IL-13, IL-17, IP-10, M-CSF, MCP-1, MIG, MIP-1α, MIP-1β and TNF-α. Tests were performed according to manufacturers protocol. Samples were tested in duplicates. Results in median fluorescence intensity (MFI) values were converted to pg/mL using MILLIPLEX Analyst software (Millipore) and subsequently averaged. Statistical analysis was performed using a two-tailed, unpaired Mann-Whitney test. Only statistically significant (p-value ≥0.05) changes in cytokine concentrations were presented.

RESULTS

Adaptation and interpretation of IGRA in mice with untreated TB infection

To optimize IGRA for use in our mouse TB model, in blood samples obtained from phosphate buffered saline (PBS)-inoculated control mice and TB-infected mice at different ages, the optimum concentration of antigens ESAT-6 and CFP-10 peptides and the optimum time period of incubation were determined. In blood from TB-infected mice a maximum IFN-γ production after stimulation with 1 µg/ml of each peptide was found and optimum time of antigen exposure was 72 h (data not shown). IFN-γ production level resulting from exposure of blood to Mtb-specific antigens minus IFN-γ concentrations present in the negative controls was used as final read-out of the test and referred to as IGRA results, similar to the evaluation of IGRA results obtained in human blood.

At week four of the TB infection, six individual mice were investigated; different responses were obtained (figure 1). A distinct pattern per mouse was observed. Three out of six mice showed that a high response in the positive control (figure 1d) also showed a high response on Mtb-specific antigens stimulation (figure 1b) and a high response in the negative control (figure 1a). These mice still showed a high IGRA result (figure 1c). Three out of six mice showed overall lower responses.

IGRA in blood during the course of untreated TB infection in mice

Dynamics in immune response, expressed in IGRA results during the course of infection, are shown in figure 2. In the acute phase of TB, the positive control response was present at week 1 and remained at a certain level (figure 2b). However, IGRA results were not observed at week 1, but were significantly induced at week 3 and week 4 (figure 2a). At the beginning of the chronic phase of the TB infection, IGRA results dropped dramatically between week 4 and week 9 (figure 2a), whereas positive control response did not decrease (figure 2b). In order to determine sequestration, IGRA were performed in suspensions of lung cells from infected mice at 4, 9 and 17 weeks of infection. High IGRA results in lung cell suspensions were observed at 4 weeks of infection, reflecting high activity of lung T-cells upon stimula-
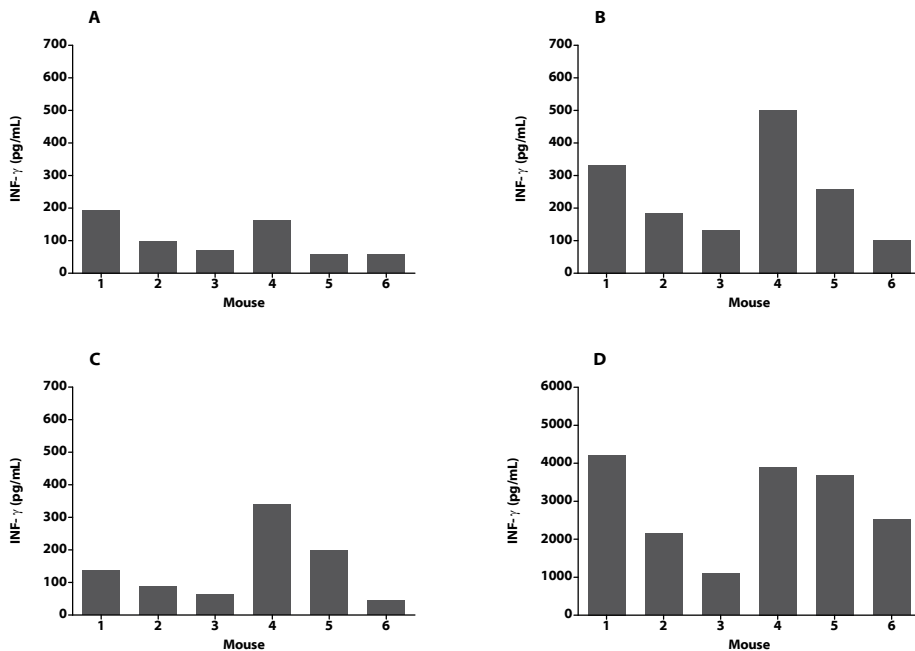
Figure 1. IFN-γ production in blood from six individual mice at 4 weeks after untreated TB infection. Blood samples were processed in IGRA. **(A)** Negative controls. **(B)** Mtb-specific-antigens responses after stimulation with ESAT-6 and CFP-10. **(C)** IGRA results (Mtb-specific antigens responses minus the negative controls). **(D)** Positive controls. Data shown are mean IFN-γ concentrations of measurements in duplicate.
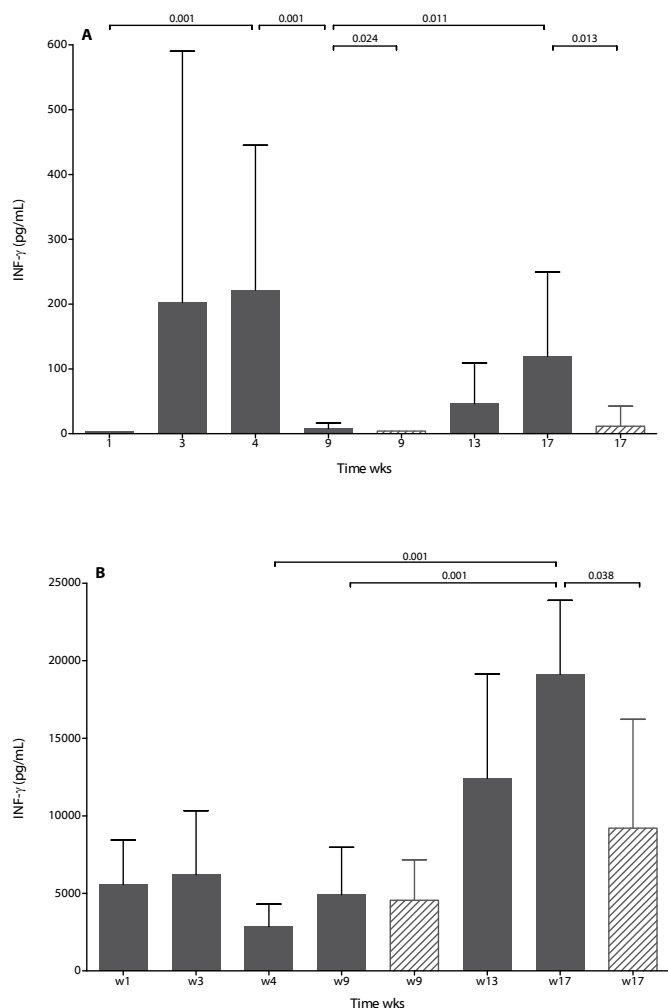
Figure 2 IFN-γ production in blood from mice (n=7) during the course of untreated TB infection and TB-infected mice receiving therapy. Blood samples were processed in IGRA. Mice without therapy (dark gray bars) and mice receiving therapy (diagonally striped bars). **(A)** IGRA results (Mtb-specific-antigens responses minus the negative controls). **(B)** Positive controls. Data shown are mean IFN-γ concentrations of measurements in duplicate. The whiskers represent the standard deviation (SD). Statistical significance if present (p-value ≤0.05) is indicated.

tion with Mtb-specific-antigens (data not shown). During the course of infection IGRA results in lung cells observed at week 4 decreased 15-fold at week 9 and another 1.5-fold at week 17 (data not shown). From 9 weeks after infection onwards IGRA results in blood gradually and significantly increase until 15-fold response at week 17 compared to 9 weeks of infection (figure 2a). Interestingly, also positive control response increased 4-fold in that period (figure 2b).

IGRA in blood of TB-infected mice receiving therapy

IGRA results in blood from mice both after 5 weeks and after 13 weeks of therapy were significantly decreased compared to untreated TB-infected mice (figure 2a). Positive control response did not significantly change after 5 weeks of therapy, but was lower after 13 weeks of therapy (figure 2b). When, after 13 weeks, the therapy was stopped, IGRA results did not increase again at 6 weeks after termination of therapy. Even at 13 weeks after therapy termination, when relapse of TB infection in terms of increased numbers of Mtb in the lung and Histopathological changes was observed [8], IGRA results remained low (data not shown).

Cytokine or chemokine profile in plasma during the course of untreated TB infection in mice and TB-infected mice receiving therapy

Five of the 17 cytokines and chemokines assessed showed a dynamic profile with significant changes during infection progression or following therapy (figure 3). IFN-γ concentration in blood reached a maximum at 4 weeks after infection. During the chronic phase of infection IFN-γ concentration significantly decreased. As found for IFN-γ also IL-17 and IP-10 showed an initial increase, which resulted in peak concentrations at 4 weeks after infection, followed by a decrease from that time. Dynamics of TNF-α concentration showed a somewhat different pattern, with increased concentrations from week 4 onwards. MIG concentrations during the course of the untreated infection were constant.

In mice receiving therapy, concentrations of IFN-γ, IL-17, IP-10 and MIG were decreased after 5 weeks of therapy, which was also observed after 13 weeks of therapy except for IFN-γ. Decreased levels of TNF-α were only observed after 13 weeks of therapy (figure 3).
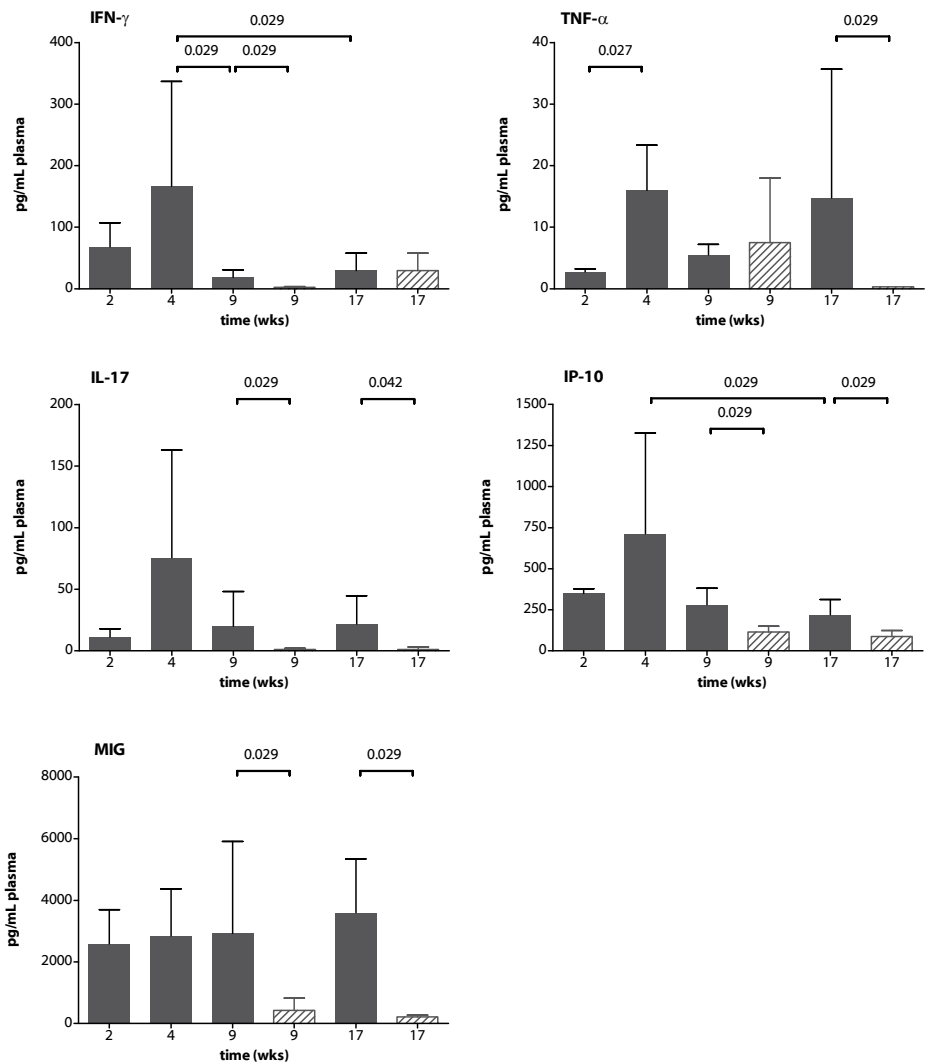
Figure 3: Concentrations of cytokines or chemokines in plasma from mice (n=4) during the course of untreated TB infection and TB-infected mice receiving therapy: mice without therapy (dark gray bars) and mice receiving therapy (diagonally striped bars). Data shown are mean concentrations of cytokines or chemokines of measurements in duplicate. The whiskers represent the standard deviation (SD). Statistically significance if present (p-value ≤0.05) is indicated.

DISCUSSION

In this study the dynamics of IGRA in TB infection and the effect of therapy were investigated in a mouse model. To this aim IGRA was optimized for use in mice. We observed a variety in IGRA responses between individual mice, which might be explained by differences in phase of TB infection in these mice and hence the number of reactive T-cells in blood. In a previous study, we showed that around 4 weeks after Mtb inoculation, the acute phase of infection progresses into the chronic phase.[8] At that time point mouse to mouse variation in T-cell response can be expected. Unfortunately, T-cell numbers in blood of TB-infected mice could not be determined, since the fluorescence-activated cell sorting technique using Mtb infected blood samples could not be performed at our institute due to safety regulations.

Dynamics in immune response expressed in IGRA results during TB showed a very slow start, which might be due to T-regulatory cell activity in the initial phase of infection, as described by Shafiani et al.[11] However, a significant increase in IGRA results was observed up to 4 weeks after infection. The observed fall in IGRA results at 9 weeks after inoculation suggests that this might be due to migration of specific T-cells to the lung and/or due to strong regulation. IGRA results in lung cell suspensions during the active phase of infection showed indeed peak values at 4 weeks after infection. These data are in concordance with the study of Arko-Mensah et al.[1], showing that increased levels of (free) IFN-γ in the respiratory tract correlated with active pulmonary TB in mice. However, our observation that IGRA results in lung T-cells decreased after 4 weeks of infection (data not shown) discarded the hypothesis that migration of T-cells to the lung was responsible for decreased IGRA results in blood. Possibly the decline in IGRA result might be due to down-regulation of T-cells.[12] It may also be related to the IFN-γ depressing capacity of Mtb during the active infection, by inhibiting IFN-γ receptor signalling, as demonstrated in a study of Sahiratmadja et al.[13] The observed increase in IGRA results and positive results from 9 weeks of infection onwards might reflect an increase in cellularity associated with severity of disease in mice during the advanced phase of TB.

The data obtained in this animal model of TB do not support the value of IGRA in blood to diagnose active TB. IGRA responses are highly variable according to various phases of active infection and might lead to false negative results during active TB. These findings are in line with a recent review by Hooper et al., who concluded that there is inadequate evidence to support the use of IGRA in the diagnosis or exclusion of active pleural TB in patients.[14]

However, the data of the present study suggest that IGRA might be a useful biomarker to monitor therapy response. Our results are in line with the findings obtained by Lee et al, demonstrating that IGRA results decreased after successful treatment.[15]. In our experimental TB model, it was also demonstrated that, next to IFN-γ, also IL-17 and IP-10 as cytokines in

the pro-inflammatory reaction cascade, might be adequate markers indicative for successful therapy. The results of the dynamics of free IFN-γ concentrations as a biomarker during the different phases of infection are in concordance with results earlier described in other studies.[8,16] However, it should be noted that the free IFN-γ concentration level in blood is also influenced by other factors not related to the TB infection. The TNF-α concentrations also revealed a strong increase during the acute phase of infection and sustained high concentrations throughout the chronic phase of infection. MIG concentrations showed no dynamics during the course of infection but revealed to be an adequate marker in therapy effect and in that perspective might contribute to proper follow-up of patients starting anti-TB therapy. These results indicate that besides IFN-γ also the pro-inflammatory cytokines like IL-17, IP-10, TNF-α and MIG are adequate biomarkers in the acute phase of infection. Recruiting T-cells, macrophages and neutrophils have a strong Th-1 reaction in this phase. In the present TB model changes in cytokine concentrations can be related to the TB infection. It should be realised that changes in pro-inflammatory cytokines can be caused by many other factors. However, the use of these cytokines to measure therapy efficacy seems achievable when using two paired samples taken before the start of therapy and after 3 weeks.

To our knowledge, only Beamer *et al.* reported studies on the use of IGRA in a mouse TB model. They showed that IGRA results from blood samples after exposure to Mtb-specific-antigens reflected IGRA results in lung cells.[17] They observed that a low IFN-γ response to Mtb-specific-antigens was associated with elevated risk of severe disease, compared to high responders. Their study using various mouse strains demonstrated that the course of TB was different and dependent on the mouse strain used, which is also reflected in their IGRA results.[17]

Summarizing, the present study demonstrates a limited value of IGRA to monitor infection progression or even to detect active TB infection. These animal data do not support use of IGRA as an accurate diagnostic tool for active TB. By contrast, the value of IGRA in monitoring therapy response in the acute phase of TB infection is demonstrated. This may indicate that IGRA can be an adequate biomarker for therapy failure due to Mtb resistance. Also, a decrease in plasma concentrations of IFN-γ, IL-17, IP-10 or MIG was associated with successful therapy. As it is known that in TB patients the concentrations of cytokine biomarkers can be influenced by other non-TB-related factors, IGRA as a TB-specific biomarker is preferable to be used for monitoring therapy efficacy in TB patients.

REFERENCES

1. Arko-Mensah J, Rahman M, Julian E. *et al.* Increased levels of immunological markers in the respiratory tract but not in serum correlate with active pulmonary mycobacterial infection in mice. Clin Microbiol Infect 2009; 15: 777-86

2. Diel R, Loddenkemper R, Nienhaus A. Evidence based comparison of commercial interferon-gamma release assays for detecting active tuberculosis -- a meta-analysis. 2010 Apr; 137(4):952-6

3. Jiang J, Shi H, Liang Q. *et al.* Diagnostic value of interferon-gamma in tuberculous pleurisy: a metaanalysis. Chest 2007; 131:1133-41

4. Lange C, Pai M, Drobniewski F. *et al.* Interferon-gamma release assays for the diagnosis of active tuberculosis: sensible or silly? Eur Respir J 2009; 33:1250-3

5. Pai M, Zwerling A, Menzies D. Systematic review: T-cell-based assays for the diagnosis of latent tuberculosis infection: an update. Ann Intern Med 2008; 149: 177-84

6. National Tuberculosis Controllers A, Centers for Disease Control and P. Guidelines for the investigation of contacts of persons with infectious tuberculosis. Recommendations from the National Tuberculosis Controllers Association and CDC. MMWR Recomm Rep 2005; 54: 1-47

7. Jafari C, Thijsen S, Sotgiu G. *et al.* Bronchoalveolar lavage enzyme-linked immunospot for a rapid diagnosis of tuberculosis: a Tuberculosis Network European Trialsgroup study. Am J Respir Crit Care Med 2009; 180:666-73

8. De Steenwinkel J, De Knegt G, Ten Kate M. *et al.* Immunological parameters to define infection progression and therapy response in a well-defined tuberculosis model in mice. Int J Immunopathol Pharmacol 2009; 22:723-34

9. Bakker-Woudenberg IA. Experimental models of pulmonary infection. J Microbiol Methods 2003; 54:295-313

10. Rosenthal I, Zhang M, Williams K. *et al.* Daily dosing of rifapentine cures tuberculosis in three months or less in the murine model. PLoS Med 2007; 4:e344

11. Shafiani S, Tucker-Heard G, Kariyone A. *et al.* Pathogen-specific regulatory T cells delay the arrival of effector T cells in the lung during early tuberculosis. J Exp Med 2010; 207:1409-20

12. Joosten S, van Meijgaarden K, Savage N. *et al.* Identification of a human CD8+ regulatory T cell subset that mediates suppression through the chemokine CC chemokine ligand 4. Proc Natl Acad Sci USA 2007; 104:8029-34

13. Sahiratmadja E, Alisjahbana B, de Boer T. *et al.* Dynamic changes in pro- and anti-inflammatory cytokine profiles and gamma interferon receptor signaling integrity correlate with tuberculosis disease activity and response to curative treatment. Infect Immun 2007; 75:820-9

14. Hooper C, Lee Y, Maskell N. Interferon-gamma release assays for the diagnosis of TB pleural effusions: hype or real hope? Curr Opin Pulm Med 2009; 15:358-65

15. Lee S, Lee C, Yim J. Serial interferon-gamma release assays during treatment of active tuberculosis in young adults. BMC Infect Dis 2010; 10:300

16. Gonzalez-Juarrero M, Kingry L, Ordway D. *et al.* Immune response to *Mycobacterium tuberculosis* and identification of molecular markers of disease. Am J Respir Cell Mol Biol 2009; 40:398-409

17. Beamer G, Flaherty D, Vesosky B. *et al.* Peripheral blood gamma interferon release assays predict lung responses and *Mycobacterium tuberculosis* disease outcome in mice. Clin Vaccine Immunol 2008; 15:474-83

Chapter 6

Relapse of tuberculosis versus primary tuberculosis; course, pathogenesis and therapy in mice

J.E.M. de Steenwinkel, G.J. de Knegt, M.T. ten Kate, H.A. Verbrugh,
R. Hernandez-Pando, P.J.M. Leenen, I.A.J.M. Bakker-Woudenberg

ABSTRACT

Relapse of tuberculosis (TB) is defined as re-emergence of clinical symptoms after stopping anti-TB treatment, while this treatment appeared effective initially. Relapse of TB can occur in patients that are therapy-compliant, but the risk of relapse of is dramatically increased when patients are non-compliant. Additionally, the probability of antibiotic resistance is higher in those patients who have a relapse of TB and thus longer treatment is recommended. Further insight in the pathogenesis of relapsing TB could provide a basis for future treatment improvement. In the present study, using a murine TB model, we assessed the differences between primary TB and relapse of TB in terms of mycobacterial load in infected organs, (immuno-) histopathology, and plasma cytokine concentrations. Compared to primary TB, in relapse of TB we observed a lower mycobacterial load in lung, spleen and liver at the phase of established infection. Also the levels of TNF-α, IFN-γ, IL-6, MIG/CXCL9, IP-10/CXCL10 and IL-17 were significantly lower. It was observed that in relapse of TB memory Th-1 cells were locally and systemically expanded and congregated in the lung, permitting an efficient control of Mtb growth. Treatment response in relapse of TB is as good as the treatment response in primary TB; thereby no supportive evidence could be given for the recommended longer treatment duration in case of relapse of TB.

INTRODUCTION

Tuberculosis (TB) remains an infectious disease that requires extremely lengthy treatment.[1] A number of studies are ongoing to reduce treatment duration using new TB drugs while preserving treatment efficacy.[2] However, the current (minimal) six-month therapy leads to many problems, among which the high proportion of patients failing to adhere to the TB treatment.[3] As a result of this non-compliance (non-adherence) of patients, especially in TB-HIV co-infected patients there seems to be an increased risk of therapy failure, resulting in relapse of infection and/or development of resistance.[3-6] These potential problems were among the driving forces to enrol patients in Directly Observed Therapy (DOT) programmes.[7]

Recurrent TB infection should be divided into relapse of infection and re-infection, which are two fundamentally independent forms of TB infection.[8] Re-infection occurs in endemic areas where there is high incidence of TB in a crowded population (such as prisons and townships), with limited coughing hygiene and high vulnerability to infection due to malnutrition and HIV infection.[3-4] Thus, re-infection is an infection caused by a new (exogenous) strain of *Mycobacterium tuberculosis* (Mtb). In contrast, relapse of TB infection is recurrence of an untreated or inadequately treated TB infection, with the same (endogenous) Mtb strain.

Regarding the therapy of re-infection versus relapse of infection a different approach is needed. Re-infection of TB can be considered as a new primary infection allowing standard regimens to be started. This re-infection occurs often, partly because patients that had TB once have a strongly increased risk of developing TB when they are re-exposed.[9] In contrast to re-infection with TB, relapse of TB infection carries an increased risk of infection due a resistant variant of their original mycobacterial strain persisting after inadequately-treated primary TB infection, and re-growing during the relapse period.[10] As a consequence, the recommended treatment for relapsing TB infection is an 8-month re-treatment regimen, consisting of 2 months of isoniazid, rifampin, pyrazinamide, ethambutol and streptomycin followed by 1 month of isoniazid, rifampin, pyrazinamide and ethambutol and finally 5 months of isoniazid, rifampin and ethambutol.[7]

The present study was performed to investigate the course and pathogenesis of relapse of TB versus primary TB. In our mouse TB model we induced relapse of TB by administration of suboptimal TB therapy to mice with primary TB infection, in this respect closely mimicking non-compliance of patients.[11] Parameters to characterize the course of TB infection were quantitative mycobacterial cultures from infected organs, histopathology in infected organs and cytokine profile in blood. In addition, we investigated differences in therapy response of mice with primary TB versus mice with relapse of TB.

MATERIALS AND METHODS

Bacterial culture

Mtb strain H37Rv (ATCC 27294) was used. Bacterial suspensions were cultured in Middlebrook 7H9 broth (Difco Laboratories, Detroit, MI, USA), supplemented with 10% oleic acid-albumin-dextrose-catalase enrichment (OADC, Baltimore Biological Laboratories, Baltimore, MD, USA), 0.5% glycerol (Scharlau Chemie S.A, Sentmenat, Spain) and 0.05% Tween 20 (Sigma Chemical Co, St. Louis, MO, USA), under shaking conditions at 96 rpm at 37⁰C. Mtb suspensions were stored at -80°C. Cultures on solid media were grown on Middlebrook 7H10 agar (Difco), supplemented with 10% OADC for 21 days at 37°C with 5% CO_2.

Primary TB, relapse of TB, and treatment with anti-TB drugs

Experimental TB in mice was established via infection using the respiratory route, as described previously.[11] In short, TB drugs dosage and schedules used were derived from current clinical guidelines.[12-13] Isoniazid, rifampin and pyrazinamide, in human pharmacokinetic-equivalent doses [14-16] were administered, as described previously.[11] In short, treatment of primary TB was started at 4 weeks after Mtb inoculation, when patches of pneumonic lesions were observed and established infection was confirmed by stabilization of the Mtb load in infected organs and TB-characteristic histopathological findings [11]. Treatment consisted of a 9-week initial phase followed by a 4- or 17-week continuation phase. During the initial phase, animals received a combination of isoniazid [25 mg/kg], rifampin [10 mg/kg] and pyrazinamide [150 mg/kg]. In the continuation phase, animals continued with isoniazid and rifampin. Agents were administered subcutaneously once daily, 5 days a week. In mice with primary TB, treated for 13 weeks only, relapse of TB infection occurred in all mice at the end of the 13-weeks post-treatment period. At that time point the treatment of relapse of TB was started and continued for 26 weeks.

Determination of viable Mtb counts in infected organs and blood

At indicated time points mice (n=4 per time point) were sacrificed by CO_2 exposure. The lung, spleen and liver were removed aseptically and processed as described previously.[11] Blood samples were taken via cardiac puncture and the entire organs were removed and homogenized in 2 mL PBS. From the undiluted tissue homogenate and the 10-fold serial dilutions of the homogenate, samples of 200 µl were plated onto solid medium for CFU counting after 3 weeks of incubation of the subculture plates.

Selection of drug-resistant Mtb

In order to detect the presence of drug-resistant Mtb mutants, samples from infected tissue homogenates were cultured on rifampin-containing and isoniazid-containing solid media. The concentrations of rifampin and isoniazid in the subculture plates were 4-fold the "critical

concentration", and were 4 mg/L rifampin, 0.8 mg/L isoniazid. Resistant Mtb colonies, able to grow on this media, were characterized using the GenoType® MTBDR*plus* assay (Hain Lifescience GmbH, Nehren, Germany), to detect the most common mutations.[17]

Assessment of relapse of TB infection

The number of CFU in lung, spleen and liver of mice (n=4) was assessed 13 weeks after termination of TB treatment. Relapse of was defined as Mtb-positive organ cultures, while immediately after termination of treatment organs were Mtb culture-negative.

Histopathological examination of infected organs

Histopathological changes in lung, liver and spleen during the course of the (un-)treated infection were determined by sacrificing the animals (n=3) at indicated time points, as described previously.[11] Paraffin-embedded tissues were cut into 4 μm sections from which one in every 7 cuts was used for haematoxylin-eosin staining. A pathologist, blinded to the experimental conditions, examined 4 slides of each tissue. The same paraffin-embedded material prepared for the histopathological studies was used to determine the local cytokine production by immunohistochemistry. Lung sections from infected mice were de-paraffinized and maintained in HCN buffer (Hepes, NaCl and CaCl$_2$). Sections were washed with HCN + 0.05% Tween 20, and the endogenous peroxidase activity was blocked with 6% H$_2$O$_2$ dissolved in PBS + 0.1% sodium azide and incubated for 1 hour. After blocking with normal swine sera, tissue sections were incubated with primary antibodies overnight at 4ºC at optimal dilutions, which had been determined previously. We used primary antibodies against TNF-α (rabbit polyclonal IgG, 281 clone H-156, sc-8301, Santa Cruz Biotechnology), IFN-γ (goat polyclonal IgG, clone D-17, sc- 9344, Santa Cruz Biotechnology), and IL-4 (goat polyclonal IgG, Santa Cruz Biotechnology). Secondary biotinylated antibodies (anti-rabbit-biotin IgG or anti-goat-biotin IgG) were used to detect the binding of the primary antibodies. Finally, HPR-conjugated avidin and 3,3-diaminobenzidine (DAB)/hydrogen peroxide were used to develop the reaction. Tissue sections were counterstained with haematoxylin.

Cytokine- / chemokine concentrations in blood

At week 4, 9 and 17 of primary TB and relapse of TB blood was obtained from mice, and from EDTA-blood plasma samples were prepared. Quantification of cytokines / chemokines was performed using a bead-based flow cytometry technique (xMap; Luminex Corporation, Austin, TX, USA). Mouse soluble cytokine receptor multiplex panel used (Millipore Corporation, Billerica, MA, USA), consisted of bead-labelled cytokine receptor against following biomarkers; granulocyte colony-stimulated factor (G-CSF), interferon gamma (IFN-γ), interleukin (IL)-1β, IL-2, IL-4, IL-6, IL-10, IL-12 (p40), IL-13, IL-17, IFN-γ-induced protein-10 (IP-10/CXCL10), macrophage colony-stimulated factor (M-CSF), monocyte chemoattractant protein-1 (MCP-1/CCL2), macrophage induced by IFN-γ (MIG/CXCL9), murine macrophage inflammatory

protein-1α (MIP-1α), MIP-1β and tumor necrosis factor alpha (TNF-α). Tests were performed according to manufacturer's protocol. Samples were tested in duplicates. Results in median fluorescence intensity (MFI) values were converted to pg/mL using MILLIPLEX Analyst software (Millipore) and subsequently averaged.

Statistical analysis

CFU counts were log10 transformed before analysis. The CFU counts and serum cytokine levels of the primary TB groups of mice and relapse of TB groups of mice were averaged and subsequently compared using two-tailed, unpaired Mann-Whitney test with Bonferroni correction (GraphPad Prism 5).

RESULTS

Primary TB – non-compliance treatment – relapse of TB

As shown in figure 1 during the primary TB infection Mtb loads in lung, spleen and liver increased respectively up to $2.1x10^7$ [1.4 - $3.7x10^7$], $0.3x10^5$ [0.2 - $1.0x10^5$] and $0.6x10^5$ [0.2 - $1.3x10^5$] cfu/organ at week 4. TB treatment was started at week 4 and resulted in a decrease in Mtb load. After 13 weeks (week 17) treatment was stopped, and from that time point relapse of TB infection occurred in all mice. At week 22 the relapse of TB had resulted in an Mtb load of $0.7x10^3$ [0.1 – $1.6x10^3$] in the lung, 0 [0 – 95] in the spleen and 0 [0 – 0] in the liver. At week 30 (13 weeks post-treatment) the relapse of TB was established at a plateau level and the mean Mtb numbers had increased up to $1.2x10^4$ [0.7 – $4.1x10^4$], 5 [0 – $4.5x10^4$] and 0 [0 – $3.6x10^2$] in the lung, spleen and liver, respectively, and remained at this level up to week 56.

Mtb load in primary TB and relapse of TB

The mycobacterial load in lung, spleen and liver during relapse of TB was significantly lower than in the primary TB (p-value = <0.0001, two-tailed, unpaired Mann-Whitney) (figure 1). About half of the mice with relapse of TB developed extra-pulmonary TB. In none of the relapsed animals rifampin-resistant or isoniazid-resistant Mtb mutants were cultured from the infected organs.

Histopathology in primary TB and relapse of TB

Histopathological evaluation of the relapse of TB showed chronic inflammatory infiltrates around medium size blood vessels and in airways wall and, at a later stage, pneumonic patches in coexistence with middle size granulomas. In contrast, primary infection was histologically characterized by progressive pneumonia. More specific, in mice with primary TB extensive areas of pneumonia and middle size granulomas were seen after 4 weeks of infection (figure 2A). After 30 weeks of primary TB there was a more extensive alveolar pa-

Lung

Spleen

Liver
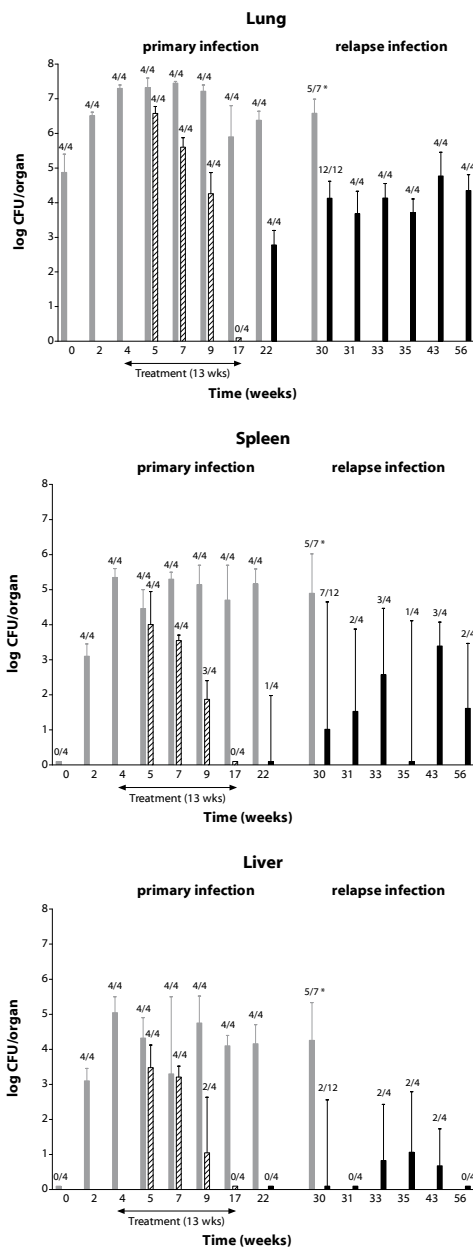
Figure 1: Mycobacterial load in infected organs in untreated mice with primary TB (gray bars) and in untreated mice with relapse of TB (black bars). Relapse of TB developed in mice with a primary TB infection that were treated for only 13 weeks (diagonally striped bars). Results are expressed as median ± range (error bars) of the colony forming units (CFU) per organ, n = 4 per time point. Numbers above bars are the numbers of culture-positive mice out of 4 mice. * 2 out of 7 untreated mice died due to TB before time point. Note that mycobacterial loads were significantly lower (p<0.001) during relapse of TB compared to primary TB.
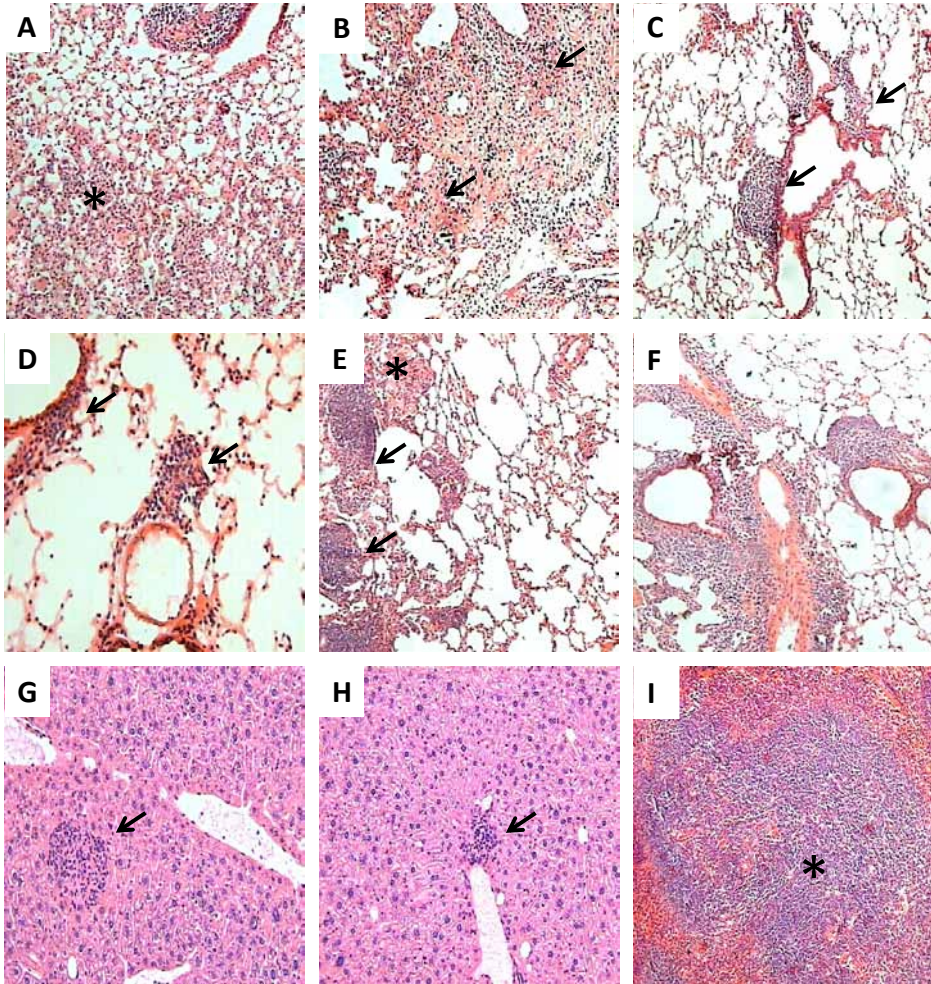
Figure 2: Representative histopathological features in lung tissue of untreated primary TB **(A-D)** or relapse of TB **(E-F)**, in liver tissue of untreated primary TB **(G)** or relapse of TB **(H)** and in spleen tissue of untreated relapse of TB **(I)**. **(A)** Large areas of pneumonia (asterisk) in the lung were observed 4 weeks after the infection. **(B)** Larger area of pneumonia with extensive fibrosis (arrows) occurred at week 30 of the primary infection. **(C)** 5 weeks of primary TB treatment resulted pneumonia disappearance, only peribronchial and perivascular lymphocytic nodules (arrows) are seen. **(D)** Only mild inflammatory infiltrate in the wall of bronchi and blood vessels (arrows) was observed at 26 weeks of treatment of the primary TB. **(E)** Start of the relapse of TB showed big nodules constituted by lymphocytes and macrophages in the wall of airways and blood vessels (arrows) with patches of pneumonia (asterisk). **(F)** Increased lymphocytic nodules around bronchi and blood vessels were seen in the lung of the relapse of TB, at week 43. **(G)** Mild size granuloma (arrow) in the liver at week 4 of the primary TB. **(H)** Small granuloma (arrow) in the liver at the start of the relapse of TB (week 30); note the numerous hepatocytes with large and hyperchromatic nucleus or binucleation, which correspond to regenerative changes. **(I)** Extensive white pulp hyperplasia (asterisk) in the spleen at 26 weeks of treatment of relapse of TB (week 56). All images have an original magnification of 200 times.

thology in coexistence with interstitial fibrosis (figure 2B). Immunohistochemistry analysis of the pneumonic areas revealed IFN-γ positive lymphocytes (figure 3A), in coexistence with numerous IL-4 positive lymphocytes (figure 3B) and TNF-α positive macrophages (figure 3C). In contrast, 5 weeks of treatment of primary TB resulted in an evident decrease of pneumonia in coexistence with granulomas with activated macrophages which showed strong TNF-α immunostaining (figure 3F) and distinctive middle size cuffs of lymphocytes around blood vessels and airways (figure 2C). The majority of these cells were positive for IFN-γ (figure 3D). Also some IL-4 positive cells around blood vessels and airways were observed (figure 3E). After 26 weeks of treatment of primary TB the lung histology was almost normal, only small cuffs of lymphocytes, many of them IFN-γ positive, with occasional plasma cells and scar IL-4 positive lymphocytes around venules or bronchi were seen (figure 2D).

At the start of relapse of TB (week 30) large inflammatory cuffs constituted by lymphocytes and distinctive activated macrophages, without apparent alveolar pathology were seen around blood vessels and airways (figure 2E). At week 5 of the relapse of infection, these cuffs of inflammatory cells were bigger and coexisted with middle size granulomas, numerous activated macrophages and small pneumonic patches. The untreated relapse of infection induced even bigger perivascular or peribronchiolar nodules consisting of lymphocytes and activated macrophages, and small patches of pneumonia with numerous activated macrophages at week 43 (figure 2F) and week 56. Many of the lymphocytes around blood vessels and bronchial walls were IFN-γ positive (figure 3G), and highly TNF-α immunoreactive macrophages were present in granulomas and in the interstitial inflammatory infiltrate (figure 3I). Fewer and weakly IL-4 positive cells in the perivascular inflammatory infiltrate of the lung were observed (figure 3H).

The histological analysis of the spleen of mice with primary TB showed extensive and diffuse hyperplasia of the white pulp at week 4 and week 30, while during relapse of TB extensive white pulp hyperplasia was present and numerous plasma cells were observed around arterioles and in the red pulp (not shown).

Regarding the liver, animals after 4 weeks of primary TB showed occasional middle size randomly located granulomas and diffuse Kupffer cell hyperplasia (figure 2G). After 30 weeks of infection, there were more and larger granulomas, Kupffer cell hyperplasia and some portal areas with mild inflammatory infiltrate essentially populated by lymphocytes. However, at the start of relapse of TB, the mice showed smaller granulomas surrounded by hepatocytes with large and hyperchromatic nuclei or two nuclei compatible with regenerative cells.
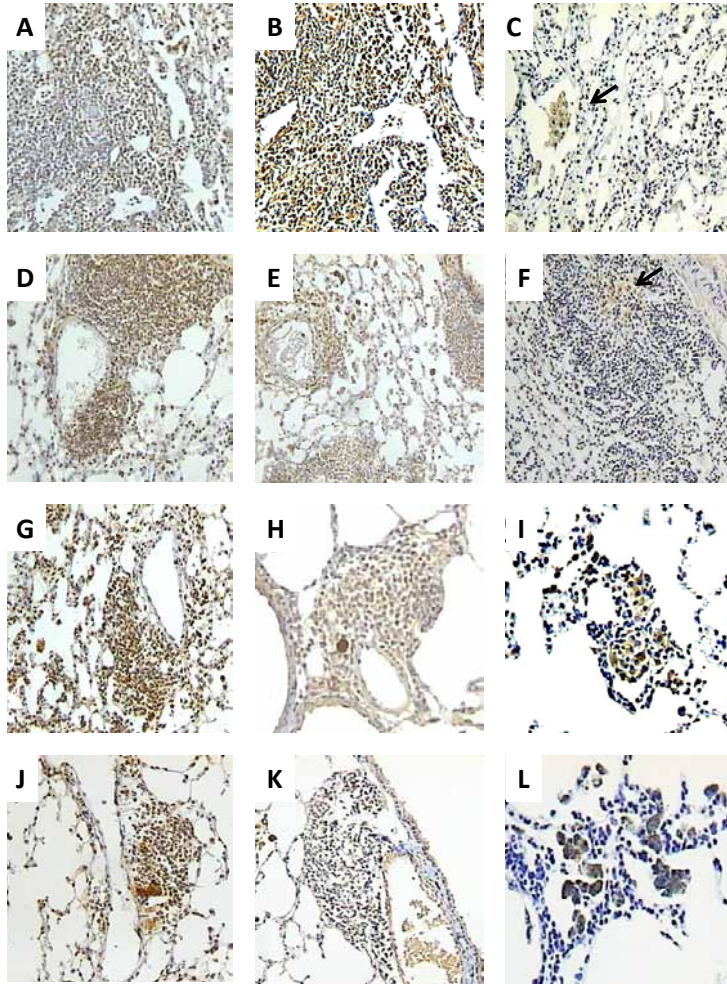
Figure 3: Representative immunohistochemical features in lung tissue of untreated primary TB at week 30 **(A-D)**, treated primary TB at week 9 **(E-F)**, untreated relapse of TB at week 35 **(G-I)** and treated relapse of TB at week 56 **(J-L)**. Lung tissue was immunostained with anti-IFN-γ **(A, D, G, J)**, anti-IL-4 **(B, E, H, K)** or anti-TNF-α **(C, F, I, L)**, respectively. Lungs of mice with 30 weeks of primary TB infection showed **(A)** moderate amount of IFN-γ immunostained cells in the pneumonic areas, **(B)** numerous amounts of IL-4 positive cells in the same lungs and **(C)** a 'scar' of TNF-α immunostained macrophages (arrow). Lungs of mice with primary TB that had been treated for 5 weeks showed **(D)** numerous IFN-γ immunostained cells in the inflammatory infiltrate around blood vessels, **(E)** some IL-4 immunostained cells around blood vessels and airways and **(F)** macrophages immersed in the pneumonic areas showed TNF-α immunostaining (arrow). Lungs of mice with relapse of TB, at week 35, showed **(G)** perivascular cuffing with numerous and strongly IFN-γ immunostained cells, **(H)** fewer and weak IL-4 immunostained cells in the perivascular inflammatory infiltrate and **(I)** middle size granuloma shows immunostained TNF-α macrophages. In the lungs of mice with relapse of TB and 26 weeks of retreatment we observed **(J)** perivascular inflammatory infiltrate with numerous IFN-γ immunostained cells, **(K)** a 'scar' of IL-4 positive cells in the perivascular inflammation and **(L)** alveolar activated macrophages that showed TNF-α immunostaining. All images have an original magnification of 200 times.
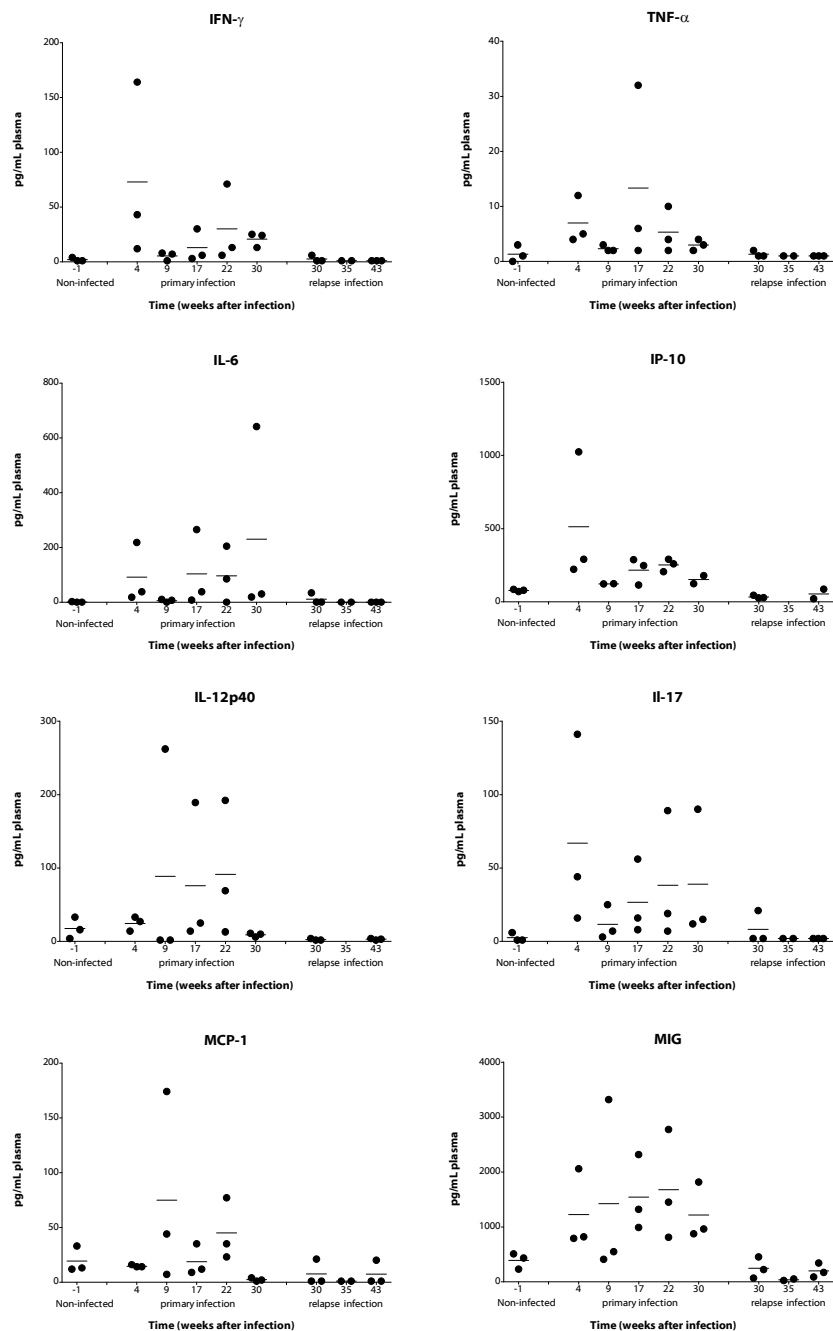
Figure 4: Concentrations of cytokines or chemokines in plasma from mice during the course of untreated primary TB, untreated relapse of TB and in uninfected mice. Data are represented for individual mice with indicated mean (n=3 per time point).

Cytokines / chemokines in primary TB and relapse of TB

Plasma cytokine profiling during the course of primary TB versus the course of relapse of TB revealed significantly (p ≤0.003, two-tailed, unpaired Mann-Whitney) different levels for 6 of the 17 cytokines (figure 4). The cytokines TNF-α (p-value = 0.0002), IFN-γ (p = 0.0005), IL-6 (p = 0.003), MIG/CXCL9 (p = 0.0002), IP-10/CXCL10 (p = 0.002) and IL-17 (p = 0.0009) were significantly lower during the relapse of TB compared to the primary TB (figure 4). Whereas only a trend of lower concentration at the relapse of TB compared to the primary TB was observed for IL-12p40 (p = 0.005) and MCP-1/CCL2 (p = 0.01). The data showed that cytokine levels in all cases are significantly higher in primary TB compared to relapse of TB. In relapse of TB, the circulating cytokine and chemokine levels generally do not exceed the levels observed in non-infected mice (data not shown).

Treatment response in primary TB and relapse of TB

The data in figure 5 represent the response to a 26 weeks treatment in mice with primary TB and mice with relapse of TB in terms of mycobacterial load of lung, spleen and liver. From the start of treatment (time zero) a decline of the Mtb load in the lungs was observed. After 13 weeks of treatment (week 13) a similar efficacy in terms of sterilization of the infected organs was observed in primary TB as well as relapse of TB. Due to the fact that the mycobacterial loads in the spleen and liver of the relapsed animals were very low or even undetectable in some of the animals (figure 1), the efficacy of treatment could not be assessed or adequately be compared to mice with primary TB. After 26 weeks of treatment (week 26) in primary TB as well as relapse of TB all organ cultures were negative. Relapse of infection at 13 weeks after termination of the 26 weeks of treatment (week 39) did never occur, indicating that a 26-weeks treatment period was completely successful in both primary TB and relapse of TB (figure 5).

Histopathology in relapse of TB during treatment

Mice with relapse of TB started re-treatment at week 30. In the lungs of the re-treated mice at week 35 and 43, well constituted granulomas with activated macrophages, small patches of pneumonia with numerous activated macrophages and multinucleated giant cells were observed (data not shown). After 26 weeks of re-treatment slight perivascular and peribronchiolar inflammatory cuffing was observed, with small granulomas and small patches of pneumonia. Almost all the lymphocytes around blood vessels were IFN-γ positive (figure 3J), while activated macrophages exhibited strong TNF-α immunoreactivity (figure 3L). Additionally, only few IL-4 positive cells were observed in the perivascular inflammation areas (figure 3K).
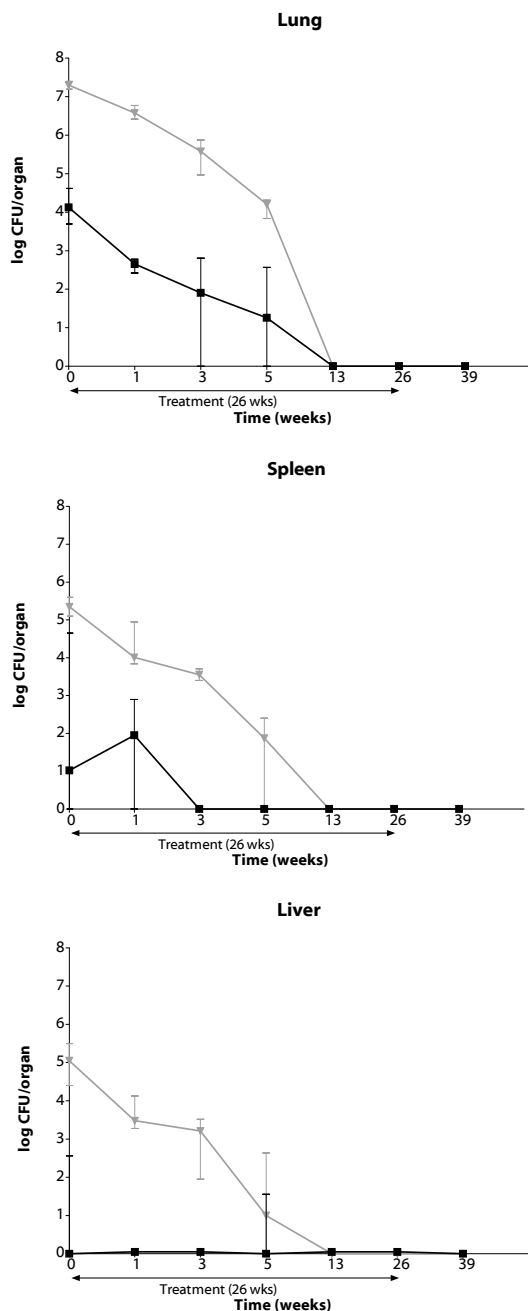
Figure 5: Efficacy of standard TB treatment administered for 26 weeks in mice with primary TB (□ with gray line) and in mice with relapse of TB (■ with black line). Start of therapy is indicated in the graphs as time zero. Mice were sacrificed at various intervals during treatment and at 13 weeks after termination of treatment (week 39). Results are expressed as median ± range (error bars) of the colony forming units (CFU) per organ, n = 4 per time point.

In the liver of mice with relapse of TB, after 13 weeks of treatment, occasional middle size granulomas were seen, while 26 weeks of treatment induced numerous hepatocytes with regenerative changes, as well as focal steatosis and occasional small granulomas (figure 2H).

In the spleen of mice with relapse of TB extensive white pulp hyperplasia and numerous plasma cells around arterioles and in the red pulp were observed. These histological features remained evident after re-treatment for 26 weeks (week 56, figure 2I).

DISCUSSION

In the present study we investigated the characteristic features of primary TB versus relapse of TB in a murine model closely mimicking the natural human TB infection. The most prominent phenomenon we observed was the substantially lower mycobacterial load in infected organs without significant fluctuation during relapse of infection compared to the primary infection. In addition, mice with relapse of TB showed no signs of illness, and none of the mice died.

The analysis of the inflammatory mediator profile in plasma during the course of primary TB versus relapse of TB revealed for 8 of 17 tested cytokines and chemokines a significant difference at the moment of established infection for both. A likely explanation for this observation is that in relapse of TB the mycobacterial loads in infected organs are approximately 1000-fold lower than in primary TB. Relapse of TB, like primary TB, was not confined to the lung, but frequently disseminated. However, the host response locally resulting from exposure of parenchymal and host defence cells to mycobacterial products including cytokine and chemokine production by activated cells, apparently do not permeate into the circulation in case of relapse of TB. Analysis of the immunohistochemistry characteristics in primary TB showed predominance of IFN-γ positive lymphocytes in the perivascular nodules as well as in the hyperplastic lymphoid tissue associated to bronchial mucosa, in coexistence with strong TNF-α immunostained activated macrophages distributed in the alveolar-capillary interstitium and granulomas. Thus, in contrast with the low concentrations in plasma of these protective cytokines during relapse of TB, in the lung numerous IFN-γ and TNF-α immunostained cells were located in the perivascular and peribronchial inflammatory infiltrates as well as in granulomas where even macrophages were intensely IFN-γ positive. This suggests that during primary TB and anti-TB treatment numerous Th-1 cells were activated while in relapse of TB many memory Th-1 cells are locally and systemic expanded and congregated in the lung, permitting an efficient control of mycobacterial growth. After the completion of successful anti-TB treatment in relapse of TB, only small perivascular cuffs and mild hyperplasia of bronchus-associated lymphoid tissue (BALT) remained with clear predominance of IFN-γ positive cells.

In primary TB the mediator profiles of infection in plasma showed some remarkable trends over time. The inflammatory 'driver' cytokines TNF-α, IFN-γ and IL-6 all displayed a biphasic pattern, with elevated levels early in the phase of chronic infection (week 4), and significant reduction to lower levels during the established infection stage at week 9. Subsequently, the cytokine levels rose again at later time points during infection. A similar pattern was found for systemic IL-17 and IP-10/CXCL10 levels. Production of IP-10/CXCL10 is strongly induced by IFN-γ, while IL-17 can be produced by the same T cells in TB.[18] Production of the chemokine MIG/CXCL9 is also strongly stimulated by IFN-γ, but this showed no decrease at week 9. The circulation of IL-12p40 and MCP-1/CCL2 showed a different development over time. Both were not found to be elevated at the start of the chronic phase of infection, week 4, but only observed at later stages of infection. Interestingly, both IL-12 and MCP-1/CCL2 are induced by IL-4 in mononuclear phagocytes, and MCP-1/CCL2 is also produced by Th2 cells rather than Th1 cells. Together, this further emphasizes that, in primary TB in mice the initial peak of Th1 polarization at week 4 is followed and balanced by activation of Th2 cells at week 9, which is in concordance with our previous histopathological observations.[11]

In relapse of TB the decreased levels of several cytokines and thus reduced chemotaxis of inflammatory cells might indicate that the less severe manifestation of untreated infection in relapse of TB is a result of an improved host reaction.

A few notes of caution on the interpretation of the histopathological findings are justified. First, relatively large differences were noted between cytokine profiles in different animals. This is remarkable, especially since the mycobacterial counts in infected organs showed relatively small inter-individual variation. This diversity probably relates to the fact, already stated above, that systemic levels of mediators are only derivatives of inflammatory processes that occur locally in the various infected organs, in particular the lung. Specific conditions in individual animals may strongly influence the level to which these processes are reflected in the levels of cytokines and chemokines in blood. This is further strengthened by the finding that levels of different mediators in individual animals show no clear correlation, i.e. there are no evident high or low responders identifiable within the cohort.

Considering treatment efficacy in relapse of TB, this study showed that the standard treatment of 26 weeks using human pharmacokinetic-equivalent dosage resulted in therapeutic efficacy that was similar, in terms of decrease of mycobacterial load, to that observed in primary TB.[11] In addition, the 26 weeks treatment of relapse of TB did not result in a second relapse of TB. These data do not provide evidence that relapse of TB should be treated longer than the standard 6 months course, an approach recommended by the WHO.[7] The therapeutic success of the standard therapy regimen in relapse of TB is finding is noteworthy, since a difference in treatment response in relapse of TB versus primary TB would be expected

as a consequence of the low regrowth of the mycobacteria in relapse of TB that might be associated with low susceptibility to anti-TB drugs.[19] A recent review article by van der Werf *et al.*[10] provided further evidence that treatment non-compliance carries the risk of becoming resistant. However, throughout the treatment period and the post-treatment period of primary TB and relapse of TB, rifampin or isoniazid-resistant Mtb mutants were never selected.

In conclusion, the present study shows that the course of relapse of TB and primary TB are different in terms of mycobacterial load in infected organs, circulating cytokine levels and histopathology. This is possibly due to an improved host reaction in relapse of TB. Although in relapse of TB the increase in mycobacterial load in the infected organs is slow and limited reflecting a low metabolic-active mycobacterial population, the 6 months standard anti-TB regimen is sufficient to achieve a curative therapy in relapse of TB. Emergence of drug resistance during and after treatment of relapse of TB did not occur.

REFERENCES

1. American Thoracic S, Cdc, Infectious Diseases Society of A. Treatment of tuberculosis. MMWR Recomm Rep 2003; 52:1-77.
2. Koul A, Arnoult E, Lounis N, Guillemont J, Andries K. The challenge of new drug discovery for tuberculosis. Nature 2011; 469:483-90.
3. Castelnuovo B. A review of compliance to anti tuberculosis treatment and risk factors for defaulting treatment in Sub Saharan Africa. Afr Health Sci 2010; 10:320-4.
4. Amuha MG, Kutyabami P, Kitutu FE, Odoi-Adome R, Kalyango JN. Non-adherence to anti-TB drugs among TB/HIV co-infected patients in Mbarara Hospital Uganda: prevalence and associated factors. Afr Health Sci 2009; 9 Suppl 1:S8-15.
5. Oxlade O, Schwartzman K, Pai M, Heymann J, Benedetti A, Royce S, Menzies D. Predicting outcomes and drug resistance with standardised treatment of active tuberculosis. Eur Respir J 2010; 36:870-7.
6. Xue He G, van den Hof S, van der Werf MJ, Guo H, Hu YL, Fan JH, Zhang WM, Tostado CP, Borgdorff MW. Inappropriate tuberculosis treatment regimens in Chinese tuberculosis hospitals. Clin Infect Dis 2011; 52:e153-6.
7. WHO. Treatment of Tuberculosis guidelines, fourth edition. WHO Library Cataloguing-in-Publication Data 2010; WHO/HTM/TB/2009.420.
8. Lambert ML, Hasker E, Van Deun A, Roberfroid D, Boelaert M, Van der Stuyft P. Recurrence in tuberculosis: relapse of or re-infection? Lancet Infect Dis 2003; 3:282-7.
9. Verver S, Warren RM, Beyers N, Richardson M, van der Spuy GD, Borgdorff MW, Enarson DA, Behr MA, van Helden PD. Rate of re-infection tuberculosis after successful treatment is higher than rate of new tuberculosis. Am J Respir Crit Care Med 2005; 171:1430-5.
10. van der Werf MJ, Langendam MW, Huitric E, Manissero D. Multidrug resistance after inappropriate tuberculosis treatment: a meta-analysis. Eur Respir J 2012; 39:1511-9.
11. de Steenwinkel JE, de Knegt GJ, Ten Kate MT, van Belkum A, Verbrugh HA, Hernandez-Pando R, van Soolingen D, Bakker-Woudenberg IA. Immunological parameters to define infection progression and therapy response in a well-defined tuberculosis model in mice. Int J Immunopathol Pharmacol 2009; 22:723-34.
12. Blumberg HM, Burman WJ, Chaisson RE, Daley CL, Etkind SC, Friedman LN, Fujiwara P, Grzemska M, Hopewell PC, Iseman MD, Jasmer RM, Koppaka V, Menzies RI, O'Brien RJ, Reves RR, Reichman LB, Simone PM, Starke JR, Vernon AA, American Thoracic Society CfDCaPatIDS. American Thoracic Society/Centers for Disease Control and Prevention/Infectious Diseases Society of America: treatment of tuberculosis. Am J Respir Crit Care Med 2003; 167:603-62.
13. Centers for Disease C, Prevention. Emergence of *Mycobacterium tuberculosis* with extensive resistance to second-line drugs--worldwide, 2000-2004. MMWR Morb Mortal Wkly Rep 2006; 55:301-5.
14. Grosset J. The sterilizing value of rifampicin and pyrazinamide in experimental short-course chemotherapy. Bull Int Union Tuberc 1978; 53:5-12.
15. Lalande V, Truffot-Pernot C, Paccaly-Moulin A, Grosset J, Ji B. Powerful bactericidal activity of sparfloxacin (AT-4140) against *Mycobacterium tuberculosis* in mice. Antimicrob Agents Chemother 1993; 37:407-13.
16. Rosenthal IM, Zhang M, Williams KN, Peloquin CA, Tyagi S, Vernon AA, Bishai WR, Chaisson RE, Grosset JH, Nuermberger EL. Daily dosing of rifapentine cures tuberculosis in three months or less in the murine model. PLoS Med 2007; 4:e344.

17. Hillemann D, Rusch-Gerdes S, Richter E. Evaluation of the GenoType®MTBDR*plus* assay for rifampin and isoniazid susceptibility testing of *Mycobacterium tuberculosis* strains and clinical specimens. J Clin Microbiol 2007; 45:2635-40.

18. Jurado JO, Pasquinelli V, Alvarez IB, Pena D, Rovetta AI, Tateosian NL, Romeo HE, Musella RM, Palmero D, Chuluyan HE, Garcia VE. IL-17 and IFN-gamma expression in lymphocytes from patients with active tuberculosis correlates with the severity of the disease. J Leukoc Biol 2012; 91:991-1002.

19. Chao MC, Rubin EJ. Letting sleeping dos lie: does dormancy play a role in tuberculosis? Annu Rev Microbiol 2010; 64:293-311.

Chapter 7

Time-Kill Kinetics of anti-tuberculosis drugs, and emergence of resistance, in relation to metabolic activity of *Mycobacterium tuberculosis*

J.E.M. de Steenwinkel, G.J. de Knegt, M.T. ten Kate, A.van Belkum, H.A. Verbrugh, K. Kremer, D. van Soolingen, I.A.J.M. Bakker-Woudenberg

ABSTRACT

Objectives

The pharmacodynamics of tuberculosis (TB) treatment should be further explored, to prevent emergence of resistance, treatment failure and relapse of infection. The diagnostic drug susceptibility tests guiding TB therapy investigate metabolically active *Mycobacterium tuberculosis* (Mtb) isolates under static conditions and as such are not informative with respect to the time–kill kinetics of anti-TB drugs and the emergence of resistance in metabolically lowly active or even dormant Mtb cells.

Methods

In vitro, the killing capacity of rifampicin, isoniazid, ethambutol and amikacin regarding the degree of killing, killing rate and selection of resistant mutants was investigated in metabolically highly active versus metabolically lowly active Mtb cells.

Results

Isoniazid showed rapid and high killing capacity towards highly active mycobacteria, but due to the emergence of resistance could not eliminate the Mtb. Efflux pump-mediated isoniazid resistance was predominant. Rifampicin revealed a relatively slow and time-dependent killing capacity, but achieved elimination of all mycobacteria. Ethambutol was not bactericidal. Amikacin showed a high and extremely rapid killing activity that was not time dependent and could eliminate all mycobacteria. Exposure of lowly active Mtb populations to isoniazid, rifampicin or amikacin led to the emergence of resistant mutants. Compared with the highly active mycobacteria, elimination of the susceptible lowly active mycobacteria required a 64-fold increased isoniazid concentration and a 4-fold increased rifampicin concentration, whereas amikacin was equally effective irrespective of the metabolic state of the mycobacteria.

Conclusions

The anti-TB drugs differ significantly regarding their time-kill kinetics. In addition, the metabolic state of Mtb significantly affects its susceptibility to antimicrobials, with the exception of amikacin. Optimization of dosage of anti-TB drugs is required to achieve maximum drug concentrations at the site of infection in order to maximize reduction in Mtb load and to minimize the emergence and selection of resistance.

INTRODUCTION

Tuberculosis (TB) remains one of the most important preventable infectious diseases world-wide. With over two billion persons latently infected with *Mycobacterium tuberculosis* (Mtb) worldwide, nine million patients with active TB diagnosed each year and almost two million deaths due to this disease annually, TB is a major cause of mortality and morbidity.[1] Although the incidence of TB is stabilizing, from a worldwide perspective the prevalence is still rising. Improvement in TB treatment is urgently needed, since the global spread of drug-resistant TB is being observed.[1,2] Optimal dosing and treatment duration, which is of the utmost importance to obtain maximum efficacy and to prevent resistance, has not been fully established. Although the usefulness of new drugs is evaluated,[3] more efficient use of the available drugs could be a more realistic short-term goal. This may also serve the development of combined regimens of conventional and new drugs. For optimization of current treatment regimens, regarding dose and duration, insight into the dynamics of the activity of the anti-TB drugs is of critical importance. The *in vitro* drug susceptibility tests currently used are not informative in this way, as they provide only endpoint data obtained after a continuous 2-4 week drug exposure of the Mtb isolate. In this respect *in vitro* tests do not simulate the *in vivo* situation, being a static equilibrium, where the pharmacokinetic curve reflects fluctuating drug concentrations.4 Moreover, besides the degree of killing the rate of killing is also highly clinically significant, but this is not measured in current susceptibility assays.

Clinical experience is that inadequate exposure to anti-TB drugs may result in the emergence of resistant mycobacteria.[5,6] However, the mechanism by which resistance is induced is not always known. The term "phenotypic drug resistance" is used to indicate drug-tolerant mycobacteria that exhibit reduced susceptibility to anti-TB drugs without known genetic mutations. Phenotypic drug resistance might, for instance, be due to increased efflux pump activity, porin loss, permeability decrease or drug-modifying enzymes, resulting in reduced intracellular drug concentrations.[7-9] "Genotypic drug resistance" indicates resistance associated with known mutations in the genome of Mtb and relates to known levels of resistance.

In this study we aimed to visualize the concentration-dependent and time-dependent killing capacity of relevant, currently used anti-TB drugs towards Mtb and the emergence of resistance in relation to the metabolic state (growth phase) of the Mtb population. In the present study, the drug concentrations are also static; however, by using a wide range of concentrations and assessment of Mtb killing at different time-points during drug exposure (instead of an endpoint assay), insight is provided into the dynamic killing capacity of fluctuating drug concentrations. This knowledge will contribute to a better understanding of the time-kill kinetics of anti-TB drugs and the emergence of resistance, and as such may help to optimize the use of these drugs.

MATERIALS AND METHODS

Mtb cultures

The Mtb strain used was H37Rv, a clinical isolate and reference strain nowadays commonly used *in vitro* as well as in animal TB models. The MICs determined as described by the CLSI (formerly the NCCLS) document M24-A10 were 0.125 mg/L for rifampicin, 0.125 mg/L for isoniazid, 8 mg/L for ethambutol and 2 mg/L for amikacin. Mtb suspensions were cultured in Middlebrook 7H9 broth (Difco Laboratories, Detroit, USA), supplemented with 10% oleic acid-albumin dextrose catalase enrichment (OADC; Baltimore Biological Laboratories, Baltimore, MD, USA), 5% glycerol (Scharlau Chemie, Sentmenat, Spain) and 0.05% Tween 20 (Sigma Chemical Co., St Louis, USA), under shaking conditions at 96 rpm at 378C. Vials with Mtb suspensions were stored at -80^{0}C. Cultures on solid medium were grown on Middlebrook 7H10 agar (Difco), supplemented with 10% OADC for 21 days at 37^{0}C with 5% CO2. Metabolic activity of highly active/low-density and lowly active/high-density Mtb cultures The metabolic activity of Mtb in cultures was assessed by measuring the adenosine-5'-triphosphate (ATP) level using the firefly luciferase bioluminescence assay.[11] With a luminometer, light emission, which is proportional to the ATP concentration in Mtb, was quantified. The microbial ATP kit HS (BioThema AB, Dalarö, Sweden) was used according to the recommendations of the manufacturer.[12]

Anti-TB drugs

Rifampicin, isoniazid, ethambutol and amikacin were purchased from Sigma Chemical Co. (I-3377, R-3501, E-4630 and A-3650). Dilutions of anti-TB drugs were prepared according to the recommendations of the manufacturers.

Concentration- and time-dependent bactericidal activity of anti-TB drugs

Mtb vials were defrosted and used to generate Mtb cultures in the early logarithmic phase of growth and at a density of 5×10^5 cfu/mL (range $4–6 \times 10^5$), as confirmed by quantitative plate counts. These cultures were exposed to each of the individual anti-TB drugs at 2-fold increasing concentrations, ranging from 0.0005 mg/L to 256 mg/L, in 125 mL Erlenmeyer flasks (Corning Costar, Cambridge, MA, USA) for 6 days at 37^{0}C, under shaking conditions at 96 rpm. On days 1, 2, 3 and 6, samples of 500 mL were taken for cfu counting, provided the Mtb suspensions did not show visible aggregation, as from aggregated Mtb cultures accurate cfu counts could not be established. Log cfu values were plotted against time (in days) to obtain time–kill curves. In order to prevent drug carry-over, samples were washed once by centrifugation at 14000 g for 10 min and resuspended in medium without anti-TB drugs. The washed suspensions were serially diluted in PBS and plated onto antibiotic-free 7H10 agar supplemented with OADC. After 21 days of incubation at 37^{0}C and 5% CO_2 cfu values were determined.

Selection of drug-resistant Mtb

In order to detect drug-resistant Mtb, in the highly active/low-density culture, the samples taken after 6 days of exposure to each of the individual anti-TB drugs at concentrations ranging from 0.0005 mg/L to 1024 mg/L were cultured on anti-TB drug-containing 7H10 agar plates. The concentrations of the drugs in the subculture plates were 4-fold the 'critical' concentrations of the agents,[10] i.e. 4 mg/L rifampicin, 0.8 mg/L isoniazid, 20 mg/L ethambutol and 20 mg/L amikacin. Only the drug-resistant Mtb were able to grow on these drug-containing subculture plates, whereas both susceptible and drug-resistant Mtb showed growth on the subculture plates without anti-TB drugs.

Detection of drug-resistant Mtb in the lowly active/high-density culture after 6 days of drug exposure was performed using the same selection method as described earlier. The high-density/late-log-phase culture containing 0.9×10^8 cfu/mL (range $0.3–1.3 \times 10^8$ cfu/mL) was obtained after 4 days of incubation of the early-log-phase culture in the absence of anti-TB drugs at 37^0C.

Characterization of drug-resistant mutants

Occurrence of phenotypic drug resistance caused by induction of efflux pumps was investigated by plating the samples from the anti-TB drug-exposed cultures not only onto agar plates containing anti-TB drugs but also onto agar plates containing a combination of anti-TB drugs and 20 mg/L reserpine (R0875-16; Sigma Chemical Co.), a known efflux pump inhibitor.[7,8] In our assay we confirmed that the presence of 20 mg/L reserpine alone in the agar plates did not affect the growth of H37Rv (data not shown). From plates containing anti-TB drug and 20 mg/L reserpine, 10 colonies were picked randomly and investigated for known drug resistance-associated mutations (genotypic resistance).

From the isoniazid-resistant mycobacteria obtained from the highly active/low-density culture exposed to 64 mg/L isoniazid, the stability of resistance was also explored by repeated culture in isoniazid-free medium. To this aim the BACTEC MGIT-960TM system (Becton Dickinson & Co., Franklin Lakes, NJ, USA) was used. Two colonies picked from the isoniazid/reserpine-containing agar plates were each resuspended in 600 mL of Middlebrook 7H9 medium and cultured in an MGIT™ control tube (isoniazid-free medium), in a 0.2 mg/L isoniazid-containing MGIT™ tube and in a 1.0 mg/L isoniazid-containing MGIT™ tube. The time to positivity of each of these three tubes was registered. The mycobacteria from the positive control tube (without isoniazid) subsequently underwent further stability control, by inoculating a new set of MGIT™ tubes containing isoniazid-free medium, medium containing 0.2 mg/L isoniazid and medium containing 1.0 mg/L isoniazid. This procedure was repeated for a total of five times. The percentage of isoniazid-resistant organisms in the total Mtb population was assessed and it was investigated whether isoniazid genotypic resistance could be detected.

From the drug-resistant Mtb isolates obtained, 10 colonies were randomly picked from the reserpine-containing plates and investigated for the presence of genotypic resistance. The GenoType® MTBDR*plus* assay (Hain Lifescience GmbH, Nehren, Germany) was used to detect the most common mutations in *rpoB* conferring rifampicin resistance and those in *katG* and *inhA* leading to isoniazid resistance.[13] The GenoType® MTBDR*plus* assay (Hain Lifescience GmbH) was used to detect mutations in the *rrs* gene related to amikacin resistance.[14] Both assays were performed according to the manufacturer's recommendations.

In addition to the GenoType® MTBDR*plus* assay to detect mutations in the *katG* gene, deletion of the *katG* gene (so-called Δ*katG*) was also determined, described by Bergval *et al.*[15] In short, 10 colonies grown on 7H10 agar containing 0.4 mg/L isoniazid were selected and DNA was prepared. Primer sets specific for *katG* codon 315 and for *katG* codon 463 were used in a PCR assay using a GeneAmp® PCR system 9700 (Applied Biosystems, Nieuwerkerk aan den IJssel, The Netherlands). Isolates were scored Δ*katG* if one or both of the PCR products were absent.

RESULTS

Metabolic activity of Mtb by growth phase

We differentiated between 'metabolically highly active' and 'metabolically lowly active' Mtb as as-sessed by determination of the amount of ATP per viable Mtb. The highly active/low density Mtb population increased from the start of the experiment with 5.0×10^5 cfu/mL to 0.9×10^8 cfu/mL on day 3. The active metabolism during the 3 day period was reflected by a 6-fold increasing ATP con-tent per cfu, being 1.5×10^{-18} mol ATP/cfu (range $1.4\text{-}1.6\times10^{-18}$) at the beginning of the experiment and 0.9×10^{-17} mol ATP/cfu (range $0.7\text{-}1.2\times10^{-17}$) on day 3. From day 4 onwards the ATP content per cfu was lower and remained at a constant level of 4.7×10^{-18} mol ATP/cfu (range $2.8\text{–}7.4\times10^{-18}$), reflecting metabolically lowly active mycobacteria showing a constant but reduced metabolism.

Time-Kill Kinetics of anti-TB drugs towards highly active/low-density Mtb

In the absence of anti-TB drugs, the density of the Mtb H37Rv culture increased from 5.0×10^5 cfu/mL at the start of the experiment to 5.7×10^6 cfu/mL on day 1, 3.6×10^7 cfu/mL on day 2 and 1.1×10^8 cfu/mL on day 3. On day 6 the Mtb suspension was aggregated due to increased density of mycobacteria and as a result appropriate quantification of the non-drug exposed Mtb on day 6 could not be performed. The time–kill kinetics of rifampicin, isoniazid, eth-ambutol and amikacin on the highly active Mtb cultures are shown in figures 1 and 2. The data shown in the figures ranged from the concentrations that proved ineffective (identical growth compared with the control) up to 256 mg/L.

Rifampicin

Isoniazid
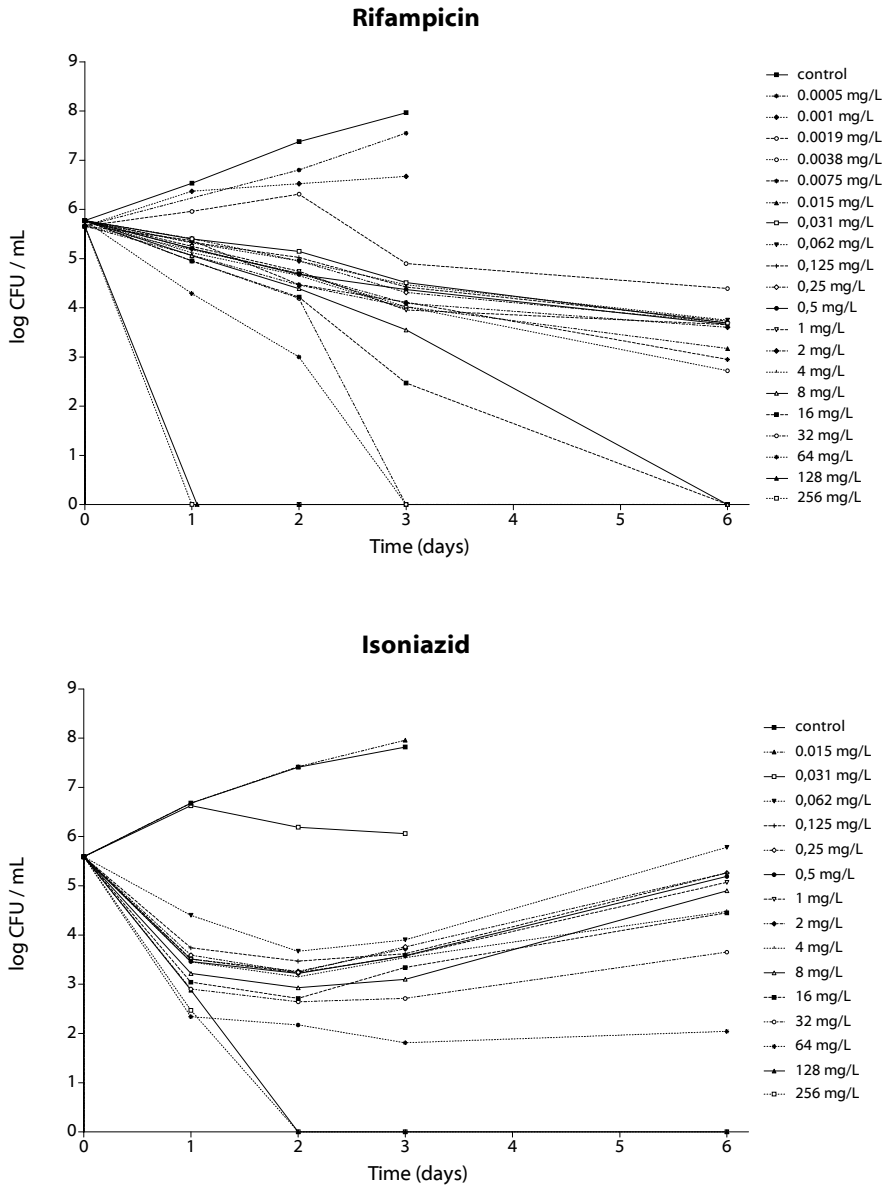
Figure 1. Concentration- and time-dependent bactericidal effect of anti-TB drugs on metabolically active Mtb strain H37Rv. Cultures of Mtb at low density in the early logarithmic phase of growth (5×10^5 cfu/mL) were exposed to rifampicin or isoniazid at 2-fold increasing concentrations for 6 days at 37^{0}C. After 1, 2, 3 and 6 days of exposure, quantitative cultures were performed on subculture plates without anti-TB drugs. Due to aggregation of the mycobacteria in the culture, at 6 days of exposure to some of the low concentrations, accurate cfu counts could not be performed.
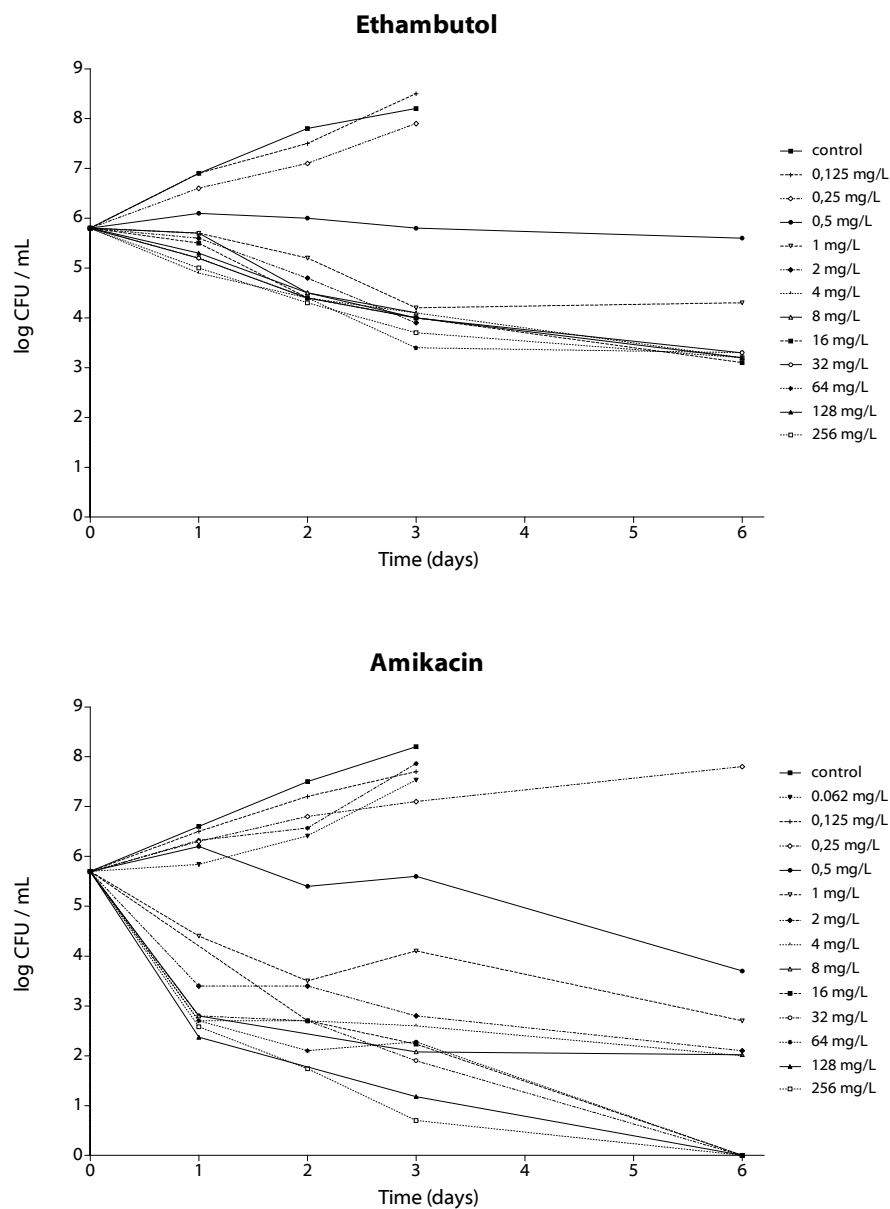
Figure 2. Concentration- and time-dependent bactericidal effect of anti-TB drugs on metabolically active Mtb strain H37Rv. Cultures of Mtb at low density in the early logarithmic phase of growth (5×10^5 cfu/mL) were exposed to ethambutol or amikacin at 2-fold increasing concentrations for 6 days at 37^0C. After 1, 2, 3 and 6 days of exposure, quantitative cultures were performed on subculture plates without anti-TB drugs. Due to aggregation of the mycobacteria in the culture, at 6 days of exposure to some of the low concentrations, accurate cfu counts could not be performed.

	Lowest concentration (mg/L) resulting in ≥**99%** killing at various time points during exposure to anti-TB drug			
	day 1	day 2	day 3	day 6
rifampicin	128	64	8	0.031
isoniazid	0.125	0.062	0.125	32
ethambutol	>256	>256	64	2
amikacin	2	1	2	0.5

Table 1. Concentration-dependent bactericidal effect (≥99% killing) over time of anti-TB drugs towards highly active/low-density Mtb strain H37Rv. Cultures of Mtb strain H37Rv (5×10^5 cfu/mL) were exposed to rifampicin, isoniazid, ethambutol or amikacin at 2-fold increasing concentrations for 6 days at 37^0C. After 1, 2, 3 and 6 days of exposure, quantitative cultures were performed on plates without anti-TB drugs.

Rifampicin showed clear concentration-dependent killing activity, which was also strongly time dependent. At a high concentration of 128 mg/L, ≥99% killing was achieved within 1 day of exposure. A moderate concentration of 8 mg/L was needed to achieve ≥99% killing after 3 days of exposure (table 1) and this concentration eliminated Mtb after 6 days of exposure (figure 1).

Isoniazid also showed concentration-dependent killing activity, which was more rapid compared with rifampicin (figure 1). At a low concentration of 0.125 mg/L, ≥99% of the Mtb was killed within only 1 day of exposure (table 1). Within 2 days of exposure a 2-fold lower concentration killed ≥99%; however, from that time onwards the number of cfu in the Mtb cultures increased again. This regrowth of Mtb was observed over a wide range of isoniazid concentrations, and was caused by the development of an isoniazid-resistant Mtb subpopulation. After 6 days of drug exposure, a concentration of 32 mg/L was needed to achieve ≥99% Mtb killing (table 1). Only at a concentration of ≥128 mg/L was the expansion of isoniazid-resistant mycobacteria completely prevented (table 2).

Ethambutol showed moderate killing activity that was almost independent of its concentration, and not time dependent (figure 2). Even at the highest concentration of 256 mg/L, Mtb could not be fully eliminated. The concentrations of ethambutol needed to achieve ≥99% killing were >256 mg/L on day 1, >256 mg/L on day 2, 64 mg/L on day 3 and 2 mg/L on day 6 (table 1).Amikacin showed strong concentration-dependent killing capacity and a high killing rate (figure 2). Killing of ≥99% after 1 day was achieved at a concentration of only 2 mg/L. To achieve ≥99% killing after 6 days of exposure, a modest decrease in concentration of only 4-fold was required (table 1), indicating that the killing activity of amikacin was largely independent of time of exposure to this agent. The amikacin concentration needed for 100% elimination of Mtb after 6 days of exposure was only 16 mg/L (figure 2 and table 2).

Selection of drug-resistant mutants in highly active/low-density Mtb
In the highly active Mtb population, drug-resistant mutants were only observed after exposure to isoniazid and not after exposure to the other anti-TB drugs. Isoniazid concentrations

	Lowest concentration (mg/L) resulting in **100% killing** after 6 days of exposure to anti-TB drugs					
	Mtb highly active / low-density			Mtb low active / high density		
	susceptible mycobacteria	resistant mycobacteria	genotypic mutation [a]	susceptible mycobacteria	resistant mycobacteria	genotypic mutation [a]
rifampicin	8	-	-	32	512	*rpoB*
isoniazid	4	128	Δ*katG* [b]	256	512	Δ*katG* [b]
ethambutol	>1024	-	-	>1024	-	-
amikacin	16	-	-	8	512	*rrs*

Table 2. Elimination (100% killing) of susceptible or resistant Mtb strain H37Rv by anti-TB drugs, in relation to metabolic activity of the mycobacteria. Cultures of Mtb strain H37Rv at low density (5×10^5 cfu/mL) or at high density (1×10^8 cfu/mL) were exposed to rifampicin, isoniazid, ethambutol or amikacin at 2-fold increasing concentrations for 6 days at 37^0C. After 6 days of exposure, quantitative cultures were performed on plates without anti-TB drugs and plates containing 4 mg/L rifampicin, 0.8 mg/L isoniazid, 20 mg/L ethambutol or 20 mg/L amikacin.
[a] Detection of mutations in *rpoB* for rifampicin, *katG* and *inhA* for isoniazid and *rrs* for amikacin.
[b] Δ*katG* indicates that the *katG* gene was (partly) deleted.

of ≥4mg/L resulted in equal numbers of mycobacteria on the subculture plates without anti-TB drugs and the drug-containing subculture plates, whereas ≥128 mg/L resulted in elimination of all mycobacteria, including the resistant Mtb. The isoniazid concentrations within which resistant mutants were selected ranged from 0.031 up to 64 mg/L, whereas in a concentration window between 4 and 64 mg/L isoniazid equal numbers of mycobacteria on the subculture plates without anti-TB drugs and the drug-containing subculture plates were cultured. Surprisingly, genotypic characterization revealed no mutations in *inhA* or *katG*, as assessed by the GenoType® MTBDR*plus* assay. However, using the *katG* gene PCR, according to Bergval et al,[15] a deletion of the *katG* gene was demonstrated in two of the 10 isolates tested.

Additional differentiation between phenotypic and genotypic isoniazid-resistant isolates demonstrated that only 1.9% of the isoniazid-resistant mycobacteria that were selected after 22 days of exposure to 64 mg/L were able to grow in the presence of the efflux pump inhibitor. This suggests that the majority of the isoniazid-resistant population represents efflux pump-mediated phenotypic drug resistance. Twenty colonies that were picked from the isoniazid-reserpine-containing plates for genetic characterization revealed no mutations in the *inhA* or *katG* genes using the GenoType® MTBDR*plus* assay. However, deletion of (a part of) the *katG* gene was demonstrated in two out of eight isolates tested.

The stability of the isoniazid-resistant mutants was demonstrated by subculture of two mutant isolates in MGIT™ medium without isoniazid, with 0.2 mg/L isoniazid or with 1.0 mg/L isoniazid. Mutants showed similar growth rates in all media. This indicates that the isoniazid resistance was conserved even without isoniazid pressure, suggesting that genotypically resistant mu-

tants were present. The genetic characterization of the isoniazid-resistant mutants that after sub-culturing consecutively for five times remained stable revealed no mutations in the *inhA* or *katG* gene, as assessed by the GenoType® MTBDR*plus* assay. However, in these stable genotypically resistant mutants, a deletion of a part of the *katG* gene was observed in one out of two.

Selection of drug resistant mutants in low active / high density Mtb

In the low active Mtb population, drug resistant mycobacteria were selected during exposure to rifampicin, isoniazid and amikacin, but not during exposure to ethambutol.

After rifampicin exposure, selection of resistant mutants was only observed in a rifampicin concentration window between 32 and 256 mg/L. Resistant mycobacteria did not emerge at the concentration of ≥512 mg/L. Analysis of 10 rifampicin-resistant colonies showed an altered *rpoB* gene sequence. Eight colonies had a mutation at codon 526 of the *rpoB* gene; six of these had the His526Tyr mutation and two had an unknown mutation at this position. One colony exhibited the Ser531Leu mutation and the remaining colony had an unknown mutation at codon 531 or 533 (table 2).

After isoniazid exposure also resistant Mtb were observed. Isoniazid concentrations of ≥256 mg/L resulted in equal numbers of mycobacteria on the subculture plates without anti-TB drugs and the drug-containing subculture plates, whereas ≥512 mg/L resulted in elimination of all mycobacteria, including the resistant Mtb. The analysis of these isoniazid-resistant mycobacteria revealed no mutations in the *inhA* or *katG*, as assessed by the GenoType® MTBDR*plus* assay (table 2). Using the *katG* gene analysis, in three of the 10 isolates, a (partial) deletion of the *katG* gene was observed.

Exposure to ethambutol did not result in selection of resistant Mtb. At the concentration of 4 mg/L multiplication of Mtb up to high levels resulting in aggregation of the Mtb suspension was prevented, and ≥99.9% killing of Mtb was obtained, whereas full elimination of Mtb was not achieved (table 2). Continuation of ethambutol exposure up to 10 days did not result in further decrease of Mtb numbers (data not shown).

Exposure to amikacin did result in resistant Mtb. Selection of only resistant mutants was found within an amikacin concentration window between 8 and 256 mg/L. Amikacin concentrations of ≥8 mg/L resulted in equal numbers of mycobacteria on the subculture plates without anti-TB drugs and the drug-containing subculture plates, whereas ≥512 mg/L resulted in elimination of all mycobacteria, including the resistant Mtb. Ten amikacin-resistant mutants were investigated and revealed a mutation in the *rrs* gene at codon 1401 (Ala1401Gly) (table 2).

DISCUSSION

The ideal anti-TB drug should exhibit a high killing rate, resulting in a rapid decrease in Mtb load and, hence, a reduced risk of spreading the disease and development of resistance. Also the bactericidal activity of the anti-TB drug against mycobacteria at low growth rate is important, as deep-seated Mtb in tissues during dormant state probably exhibit low metabolic activity, and may be more difficult to eliminate.[16] Moreover, attainable tissue concentrations of anti-TB drugs at the infectious foci are important; they may be too low with the current dosing regimes. It is expected that suboptimal concentrations of anti-TB drugs facilitate the emergence of resistance by allowing enrichment and amplification of resistant Mtb subpopulations.[5,6]

All first line drugs currently used to treat TB have a long history of clinical use. However, their pharmacodynamics are yet to be fully elucidated and there are indications that improvement of dosage could be of great value. The results of the present study provide additional insight in the *in vitro* killing dynamics of the anti-TB drugs, with respect to the degree of killing (concentration dependence), the rate of killing (time dependence) and the selection of phenotypic and/or genotypic resistant mutants. Furthermore, the metabolic activity (growth phase) of the Mtb population was taken into account. To our knowledge this is the first study in which the cornerstone anti-TB drugs isoniazid and rifampicin, as well as ethambutol and amikacin have been investigated in this way.

Isoniazid and rifampicin differed strongly with respect to their killing rate of metabolically active mycobacteria. Noticeably, isoniazid showed extremely rapid and completely concentration-dependent killing. In contrast, rifampicin revealed relatively slow and strongly time-dependent killing. This evident difference in dynamics of the bactericidal activity between isoniazid and rifampicin is in concordance with therapeutic results obtained in studies in TB patients investigating the early bactericidal activity (EBA) of anti-TB drugs, assessed by the decline of viable Mtb in consecutive sputum samples during the initial days of therapy.[17] Also the EBA studies show the rapid killing of mycobacteria by isoniazid. Whereas in the present study a rapid and high killing capacity of isoniazid towards highly active mycobacteria was demonstrated, isoniazid could not eliminate all mycobacteria, due to emergence of resistant mutants. This indicates that EBA studies in humans have a very limited predicting value relating to the sterilizing activity of anti-TB drugs.

Compared to isoniazid, the EBA of rifampicin was demonstrated to be substantially less.[17] Based on this observation the essential therapeutic role of rifampicin is thought to be during the continuation phase of the TB treatment, where rifampicin is responsible for sterilization.[7] Also in the present study, a slow and time-dependent killing activity of rifampicin was observed as well as elimination of the highly active Mtb population, provided adequate concentrations of rifampicin were available. We concluded that our *in vitro* data support the concepts of a

biphasic action of isoniazid and rifampicin against Mtb. Isoniazid plaid the most eminent role in the first phase of treatment, whereas rifampicin became of importance in the second phase of TB treatment. As a result, one could contemplate increasing dosing of isoniazid to accelerate the time to sputum-smear conversion. Increasing dosing of rifampicin to generate a faster sterilizing effect may result in the possibility of reduced total treatment duration.

The cessation of Mtb killing after three and four days of isoniazid exposure and resistance development were also observed in the studies of Gumbo *et al.* who investigated the bactericidal activity of isoniazid in an *in vitro* pharmacodynamic model in which Mtb strain H37Rv was exposed to isoniazid concentration-time profiles encountered in TB patients.[7] Gumbo *et al.* demonstrated, as we now confirmed, that the Mtb population remaining at the time bactericidal activity ceased represented an isoniazid-resistant sub-population. We characterized the isoniazid-resistant mutants that were selected from the highly active Mtb population in the present study. Within a broad isoniazid concentration range only isoniazid-resistant mycobacteria were cultured. We concluded that the majority of the isoniazid-resistant mutants found are not due to genetic mutations in known drug resistance-associated genes. As such, they are not identified as genotypic resistant mycobacteria. We demonstrated that this resistance was efflux-mediated, by the use of the efflux pump inhibitor reserpine. Efflux pump inhibitors were also applied in the studies of Viveiros *et al.*[8] and Colangeli *et al.*[18] who examined their role in isoniazid resistance in Mtb. Their studies suggested that efflux pump inhibitors can reverse the mycobacterial tolerance to isoniazid and that even high-level resistance to isoniazid can be induced in isoniazid-susceptible Mtb strains by the induction of a reserpine-sensitive efflux mechanism.[8,18] Gumbo *et al.* also have found in their pharmacodynamics model that isoniazid resistance is partly due to single point mutations in the *katG* gene and is partly the result of an efflux pump mechanism.[7] All these findings, including our data, indicate there may be a role for efflux pump inhibitors in treatment of TB, as they also have proven potency to treat MDR-TB.[19]

The emergence of resistant mutants during exposure to the anti-TB drugs in relation to the metabolic activity of the mycobacteria was also explored in the present study. Whereas in the highly active Mtb population resistant mutants were only observed after exposure to isoniazid, in the low active Mtb population selection of resistant mutants was found after exposure to isoniazid, rifampicin or amikacin. Selection of resistant Mtb is primarily expected from the high density Mtb population in view of the mutation frequency. As for isoniazid the mutation frequency is known to be relatively high compared to the other drugs, selection of isoniazid-resistant mutants from the low density population is not surprising. Again the isoniazid-resistant genotypic mutants were difficult to characterize, but we conclude that the minority of genotypically resistant mutants was characterized by deletion of the *katG* gene, whereas the majority of isoniazid-resistant genotypic mutants remained unclassified. The rifampicin-

resistant mutants on the other hand, all exhibited mutations in their *rpoB* gene. Whereas, compared to highly active bacteria, for elimination of low active Mtb a 64-fold higher isoniazid concentration was needed, for rifampicin only a 4-fold increase in concentration was required. It is therefore concluded that rifampicin is superior to isoniazid with respect to killing of Mtb with a low metabolic activity. This supports the existing concepts on the role of rifampicin in TB therapy.[20,21] We also found that the killing of isoniazid-resistant or rifampicin-resistant mutants required extremely high drug concentrations. As to achieve such high drug concentrations at the site of infection is expected to be impossible, it is important to avoid selection of resistant mutants. Our data underline the need to optimize the dosage schedule of anti-TB drug in order to achieve the maximum-attainable drug concentration that results in maximum reduction in Mtb load, and in this way to minimize the selection of resistant mutants.

Ethambutol exhibited a primarily bacteriostatic activity. Not even at 1024 mg/L for six days ethambutol killed all mycobacteria. This confirms the limited efficacy of ethambutol on active multiplying Mtb and the poor efficacy on the low active Mtb subpopulation, as also seen in other studies.[17, 22,23] It is clear that the primary role of ethambutol in the treatment of TB is to minimize the risk of emergence of resistance towards the other anti-TB drugs administered.

Amikacin displayed a concentration-dependent, rapid bactericidal activity. Interestingly, complete elimination of highly active Mtb compared to low active Mtb required similar amikacin concentrations, indicating that amikacin is effective irrespective of the growth phase and metabolic state of the Mtb cells. In this respect, amikacin was superior to the other agents. However, as with isoniazid resistance and rifampicin resistance, for killing of amikacin-resistant mutants extremely high drug concentrations are required.

In conclusion, the classes of anti-TB drugs differ substantially with respect to the dynamics of their mycobactericidal effect. In addition, these drugs are significantly different in their capacity to kill metabolically low active Mtb. This might be an important observation as the deep-seated, low-active or dormant mycobacteria in the infected tissues are probably responsible for relapse of TB. Also the risk of selection of resistance is strongly dependent on the class of drug used and on the growth phase (metabolic activity) of the Mtb. With respect to isoniazid, phenotypic resistance is the dominant resistance type, and reserpine-inhibitable efflux pumps might play a role as a mechanism contributing to this phenotypic resistance. However clinical relevance should be further evaluated. In genotypic isoniazid-resistant Mtb as yet unknown genetic mutations contribute to isoniazid resistance. The present study indicates that increasing rifampicin and/or amikacin dosing resulting in enhanced anti-TB drug concentration at the site of infection, may significantly improve the therapeutic outcome of TB.

ACKNOWLEDGEMENTS

REFERENCES

1. WHO. World Health Organization: Global Tuberculosis Control 2009; Epidemiology, Strategy and Financing. WHO Library Cataloguing-in-Publication Data 2009: 1-314.
2. Wright A, Zignol M, Van Deun A. *et al.* Epidemiology of antituberculosis drug resistance 2002-07: an updated analysis of the Global Project on Anti-Tuberculosis Drug Resistance Surveillance. Lancet 2009; 373: 1861-73.
3. Ginsberg A. Emerging drugs for active tuberculosis. Semin Respir Crit Care Med 2008; 29: 552-9.
4. Davies GR, Nuermberger E. Pharmacokinetics and pharmacodynamics in the development of anti-tuberculosis drugs. Tuberculosis (Edinb) 2008; 88 Suppl 1: S65-74.
5. Zhao X, Drlica K. A unified anti-mutant dosing strategy. J Antimicrob Chemother 2008; 62: 434-6.
6. Drlica K, Zhao X. Mutant selection window hypothesis updated. Clin Infect Dis 2007; 44: 681-8.
7. Gumbo T, Louie A, Liu W. *et al.* Isoniazid's bactericidal activity ceases because of the emergence of resistance, not depletion of *Mycobacterium tuberculosis* in the log phase of growth. J Infect Dis 2007; 195: 194-201.
8. Viveiros M, Portugal I, Bettencourt R. *et al.* Isoniazid-induced transient high-level resistance in *Mycobacterium tuberculosis*. Antimicrob Agents Chemother 2002; 46: 2804-10.
9. Louw G, Warren R, Gey van Pittius N. *et al.* A balancing act: efflux/influx in mycobacterial drug resistance. Antimicrob Agents Chemother 2009; 53: 3181-9.
10. Woods G, Brown-Elliot B, Desmond E. *et al.* Susceptibility testing of mycobacteria, nocardiae, and other aerobic actinomycetes. Approved standard. National Committee for Clinical Laboratory Standards 2003; M24-A, volume 23: 1-69.
11. Lundin A. Use of firefly luciferase in ATP-related assays of biomass, enzymes, and metabolites. Methods Enzymol 2000; 305: 346-70.
12. Prioli R, Tanna A, Brown I. Rapid methods for counting mycobacteria--comparison of methods for extraction of mycobacterial adenosine triphosphate (ATP) determined by firefly luciferase assay. Tubercle 1985; 66: 99-108.
13. Hillemann D, Rusch-Gerdes S, Richter E. Evaluation of the GenoType®MTBDR*plus* assay for rifampicin and isoniazid susceptibility testing of *Mycobacterium tuberculosis* strains and clinical specimens. J Clin Microbiol 2007; 45: 2635-40.
14. Hillemann D, Rusch-Gerdes S, Richter E. Feasibility of the GenoType MTBDRsl assay for fluoroquinolone, amikacin-capreomycin, and ethambutol resistance testing of *Mycobacterium tuberculosis* strains and clinical specimens. J Clin Microbiol 2009; 47: 1767-72.
15. Bergval I, Schuitema A, Klatser P. *et al.* Resistant mutants of *Mycobacterium tuberculosis* selected *in vitro* do not reflect the *in vivo* mechanism of isoniazid resistance. J Antimicrob Chemother 2009; 64: 515-23.
16. Mitchison D, Coates A. Predictive *in vitro* models of the sterilizing activity of anti-tuberculosis drugs. Curr Pharm Des 2004; 10: 3285-95.
17. Donald P, Diacon A. The early bactericidal activity of anti-tuberculosis drugs: a literature review. Tuberculosis (Edinb) 2008; 88 Suppl 1: S75-83.
18. Colangeli R, Helb D, Sridharan S. *et al.* The *Mycobacterium tuberculosis* iniA gene is essential for activity of an efflux pump that confers drug tolerance to both isoniazid and ethambutol. Mol Microbiol 2005; 55: 1829-40.
19. Amaral L, Boeree M, Gillespie S. *et al.* Thioridazine cures extensively drug-resistant tuberculosis (XDR-TB) and the need for global trials is now! Int J Antimicrob Agents 2010; 35: 524-6.

20. Herbert D, Paramasivan C, Venkatesan P. *et al.* Bactericidal action of ofloxacin, sulbactam-ampi-cillin, rifampicin, and isoniazid on logarithmic- and stationary-phase cultures of *Mycobacterium tuberculosis*. Antimicrob Agents Chemother 1996; 40: 2296-9.

21. Mitchison D. Antimicrobial therapy of tuberculosis: justification for currently recommended treatment regimens. Semin Respir Crit Care Med 2004; 25: 307-15.

22. Mitchison D. Role of individual drugs in the chemotherapy of tuberculosis. Int J Tuberc Lung Dis 2000; 4: 796-806.

23. Rastogi N, Labrousse V, Goh K. In vitro activities of fourteen antimicrobial agents against drug susceptible and resistant clinical isolates of *Mycobacterium tuberculosis* and comparative intracel-lular activities against the virulent H37Rv strain in human macrophages. Curr Microbiol 1996; 33:167-75.

Chapter 8

Rifampicin-induced transcriptome response in rifampicin-resistant *Mycobacterium tuberculosis*

G.J. de Knegt, O. Bruning, M.T. ten Kate, M. de Jong, T.M. Breit,
H.A. Verbrugh, I.A.J.M. Bakker-Woudenberg, J.E.M. de Steenwinkel

ABSTRACT

Objectives

Tuberculosis (TB) is still a major life-threatening infectious disease, within which especially the rise of multidrug resistant TB (MDR-TB) is currently worrying. This study focuses on mechanisms of development of rifampicin resistance, since rifampicin seems to play an important role in the development of MDR-TB.

Methods

To provide further insight in rifampicin resistance, we performed a genome-wide transcriptional profile analysis for *Mycobacterium tuberculosis* using microarray technology and qRT-PCR analysis. A rifampicin-susceptible H37Rv wild type (H37Rv-WT) and a rifampicin-resistant progeny H37Rv strain with a H526Y mutation in the *rpoB* gene (H37Rv-H526Y) were exposed to several concentrations of rifampicin, to define the effect of rifampicin on the transcription profile.

Results

Our study showed that there are rifampicin resistance-dependant differences in response between both Mtb strains. Gene clusters associated with efflux, transport and virulence were altered in the rifampicin-resistant H37Rv mutant compared to the rifampicin-susceptible H37Rv-WT strain after exposure to rifampicin.

Conclusions

The small gene cluster Rv0559c-Rv0560c in the H37Rv-H526Y strain showed a remarkable up-regulation in the microarray analysis and qRT-PCR results and appeared to be dependent on rifampicin concentration and time of exposure. Therefore this study suggests that Rv0559c and Rv0560c play a pivotal role in rifampicin resistance of Mtb. Further investigation of Rv0559c and Rv0560c is needed to reveal function and mechanism of both genes that were triggered upon rifampicin exposure.

INTRODUCTION

Tuberculosis (TB) is one of the major life-threatening infectious diseases. In 2011, with 8.8 million new cases reported, TB was responsible for the death of 1.5 million people, equal to 4100 deaths a day.[1] Due to a considerable increasing rate of isoniazid and rifampicin resistance among strains of *Mycobacterium tuberculosis* (Mtb) and the poor treatment outcome of multidrug resistant (MDR)-TB treatment,[1] more insight in the development of MDR-TB is needed. The World Health Organization estimated that world wide 3.3% of all new TB cases in 2009 were MDR-TB[2] and over 85% of rifampicin-resistant clinical isolates are also resistant to isoniazid.[3] Our study focused on rifampicin-induced transcriptome responses in rifampicin-susceptible and rifampicin-resistant Mtb strains, since rifampicin seems to play a driving role in the development of MDR-TB.

Resistance can either be intrinsic or acquired via genotypic changes. Mtb is intrinsically resistant to a wide range of antimicrobial compounds due to the unusually low permeability of the bacterial outer membrane.[4] Additionally, Mtb can become resistant to rifampicin via various routes. Genotypic resistance towards rifampicin is caused for almost 95% by target alteration due to non-synonymous single nucleotide polymorphisms (nsSNP).[5] The nsSNP, which primarily occurs in an 81 base pair region in the *rpoB* gene, known as the rifampicin resistance-determining region (RRDR), results in several changes in the β-subunit of RNA polymerase. Due to these changes, rifampicin is less competent to bind to the β-subunit of RNA polymerase,[5-6] resulting in Mtb mutants that are less susceptible or resistant to rifampicin. Recently, Siu *et al.* showed two new mutations in the *rpoB* gene outside the RRDR that also resulted in rifampicin resistance.[7] Another form of genotypic resistance is for example porin loss by mutations in genes encoding porin proteins leading to decreased cell wall permeability.[8] Resistance can also be caused by efflux pump activity. Efflux pump-induced drug extrusion will result in suboptimal intracellular drug concentrations.[9-11] The activity of efflux pump genes and transporter genes can be actively induced by rifampicin at the level of gene expression.[12]

To define the effect of rifampicin on the transcription profile, we performed a genome-wide transcriptional profile analysis for Mtb exposed to rifampicin using microarray technology. We compared the transcription profiles of an isogenic pair of rifampicin-susceptible and rifampicin-resistant Mtb strains, to provide further insight in the influence of rifampicin resistance on overall gene expression upon rifampicin exposure.

MATERIALS AND METHODS

Bacterial culture and drug treatment

The two Mtb strains used were: a H37Rv wild type (H37Rv-WT) strain and a progeny H37Rv strain with a H526Y mutation in the *rpoB* gene (H37Rv-H526Y). The minimum inhibitory concentration (MIC) for rifampicin (Rifadin®, Aventis Pharma B.V, Hoevelaken, the Netherlands) was determined and was 0.25 mg/L for the H37Rv-WT strain and 512 mg/L for the H37Rv-H526Y strain, using CLSI guidelines.

Mtb suspensions were taken from a frozen stock, thawed and cultured in Middlebrook 7H9 broth (Difco Laboratories, Detroit, MI, USA), supplemented with 10% oleic acid-albumin-dextrose-catalase enrichment (OADC, Baltimore Biological Laboratories, Baltimore, MD, USA), 0.5% glycerol (Scharlau Chemie S.A, Sentmenat, Spain) and 0.05% Tween 20 (Sigma-Aldrich, St. Louis, MO, USA), under shaking conditions at 96 rpm at 37°C. After 6 days of growth cultures of H37Rv-WT were exposed to 0.063 mg/L and 0.25 mg/L rifampicin, and cultures of H37Rv-H526Y to 128 mg/L and 512 mg/L rifampicin. These rifampicin concentrations represent ¼x MIC and 1x MIC of rifampicin for both strains. In the controls solvent was added. The Mtb suspensions were cultured to late log-phase, prior to addition of rifampicin. Samples were collected 30 minutes and 12 hours after exposure to rifampicin, or solvent.

RNA extraction

RNA was isolated using a FastPrep-24 with a FastRNA® Pro Blue Kit (MP Biomedicals, Irvine, CA, USA). To remove residual DNA, RNA samples were treated with RNase-free DNase (Ambion, Austin, TX, USA) and were purified using the RNeasy MiniElute Clean-up Kit (Qiagen Benelux, Venlo, the Netherlands), all according to the manufacturers protocol. The amount of RNA was measured using the NanoDrop ND-1000 (Thermo Scientific, Wilmington, DE, USA) and the integrity was investigated with the 2100 BioAnalyzer (Agilent Technologies Inc., Santa Clara, CA, USA) using a RNA Nano 6000 kit (Agilent Technologies) yielding RIN-values ≥ 8.9.

Labelling protocol

Per test sample, 5 µg total RNA together with 1 µg random octamers (Biolegio, Nijmegen, the Netherlands) in 4.5 µl was heated to 65°C for 10 min to denature the RNA and was allowed to cool in an ice-water bath for 10 min. This 4.5 µl was supplemented to 10 µl with a first strand mastermix. The mastermix contained final concentrations of 50 mM Tris-Cl (pH 8.3), 3 mM $MgCl_2$, 75 mM KCl, 200 mM Raffinose (Sigma-Aldrich), 0.015% Triton X-100, 30 ng Actinomycin-D (Sigma-Aldrich), 0.01M DTT, 0.5 mM dGAC, 0.35 mM dUTP, 0.15 mM dUTP-Cy3 (test) or dUTP-Cy5 (common reference) (GE Healthcare, Hoevelaken, the Netherlands) and 200U SuperScript-II (Life Technologies, Bleiswijk, the Netherlands). The mixture was incubated for 2 min at 25°C, 120 min at 42°C and 15 min at 70°C. Finally, 1.5 µl of 2.5M NaOH

was added to hydrolyze the remaining RNA upon heating for 10 min at 70°C. 8.5 µl 2M MOPS was added for neutralization and the labeled cDNA was purified with the E.Z.N.A. MicroElute RNA Clean-up Kit (Omega Biotek, Norcross, GA, USA). Dye incorporation and cDNA yield was measured on the NanoDrop ND-1000 yielding 2-2.5 µg per sample and a FOI >8 pmol/µg. The common reference was made by an equimolar pool of the test samples (5 µg per sample) and subsequently labeled as the test samples with Cy5 incorporation.

Microarray hybridization and scanning

Each hybridization mixture was made up from 500 ng test (Cy3) and 500 ng common reference (Cy5) material. Hybridization mixtures were prepared as described in the Agilent Two-Color Microarray-Based Gene Expression Analysis guide version 5.5 (G4140-90050, Agilent technologies) without the inclusion of the RNA fragmentation mixture. Mtb whole genome arrays were supplied by the Bacterial Microarray Group at St. George's Hospital, University of London. Hybridization samples were loaded onto 8x15k Mtb microarrays (Design ID: 027543, Agilent Technologies) and hybridized for 17 hours at 65°C. Afterwards the slides were washed and scanned (20 bit, 5 µm resolution) in an ozone-free room with the Agilent G2505C scanner as described in the Agilent G4140-90050 guide. Data were extracted with Feature Extraction (v10.7.3.1, Agilent Technologies) with the GE2_107_Sep09 protocol for two-color Agilent microarrays.

Microarray data processing

The raw data from all arrays were subjected to multiple quality control checks, i.e. visual inspection of the microarray scans, testing against criteria for foreground and background signals, testing for consistent performance of the labeling dyes, checking for spatial effects through pseudo-color plots, and inspection of pre- and post-normalized data with box plots, ratio-intensity (RI) plots and PCA plots. These checks revealed significant position effects on a slide. Subsequently, within-array normalization was performed using LOESS. Between-array normalization was run on the Cy3-channel by summarizing the intensity values of the probes in a probe set using the robust multi-array average (RMA) algorithm. The study (basically a three-factorial design) was subjected to 2 types of contrast analyses using mixed linear models with coefficients for slide-position and sample isolation day (both random) and each experimental group (fixed), to determine differential gene expression between ¼x MIC, 1x MIC of rifampicin and non-exposure, per genotype and time-point and also to determine differential gene expression between the H37Rv-H526Y and H37Rv-WT per MIC treatment and time-point.[13-14] For hypothesis testing, a Fs test was used and correction of the resulting P-values for false discoveries was done according to Storey and Tibshirani.[15-16] All data handling was performed using R-2.11.1 (http://www.R-project.org) and Bioconductor (www.bioconductor.org) software. Microarray data are available via an open access database.

		H37Rv-WT							
		¼ x MIC RIF (0.06 mg/L)				1 x MIC RIF (0.25 mg/L)			
	Total nr.	30 min		12 h		30 min		12 h	
Functional class	on array	Up	Down	Up	Down	Up	Down	Up	Down
1: Virulence, detoxification and adaption	216	0	0	0	1	0	0	5	5
2: Lipid metabolism	270	0	0	0	0	0	0	10	10
3: Information pathways	241	0	0	0	0	0	0	5	5
4: Cell-wall and cell processes	762	0	0	0	0	0	0	24	24
5: Stable RNAs	0	0	0	0	0	0	0	0	0
6: Insertion sequences and phages	101	0	0	0	0	0	0	1	6
7: PE and PPE proteins	165	0	0	0	0	0	0	5	8
8: Intermediary metabolism and respiration	920	0	0	0	0	0	0	28	30
9: Proteins of unknown function	13	0	0	0	0	0	0	1	1
10: Regulatory proteins	194	0	0	0	0	0	0	3	10
11: Conserved hypothetical proteins	1005	0	0	0	0	0	0	22	50
Total	3887	0	0	0	1	0	0	104	149

		H37Rv-H526Y							
		¼ x MIC RIF (128 mg/L)				1 x MIC RIF (512 mg/L)			
	Total nr.	30 min		12 h		30 min		12 h	
Functional class	on array	Up	Down	Up	Down	Up	Down	Up	Down
1: Virulence, detoxification and adaption	216	0	0	0	0	1	1	8	4
2: Lipid metabolism	270	0	0	0	3	0	2	5	4
3: Information pathways	241	0	0	0	0	0	0	4	1
4: Cell-wall and cell processes	762	7	0	8	0	9	1	13	7
5: Stable RNAs	0	0	0	0	0	0	0	0	0
6: Insertion sequences and phages	101	0	0	0	0	0	0	0	0
7: PE and PPE proteins	165	0	0	0	1	0	0	2	3
8: Intermediary metabolism and respiration	920	1	1	1	1	2	0	14	10
9: Proteins of unknown function	13	0	0	0	0	0	0	0	0
10: Regulatory proteins	194	1	0	2	0	2	0	16	0
11: Conserved hypothetical proteins	1005	1	0	2	1	4	1	13	10
Total	3887	10	1	13	6	18	5	75	39

Table 1. Numbers of differentially expressed genes assessed by microarray analysis, classified to their function in H37Rv-WT and H37Rv-H526Y after 30 minutes and 12 hours exposure to ¼x MIC and 1x MIC of rifampicin.

qRT-PCR analysis

Reverse transcriptase was performed with 50 ng of total RNA of each sample using a Reverse Transcriptase Core kit (Eurogentec, Seraing, Belgium). Primers were designed using Primer-BLAST (NCBI) and primer sequences are shown in table 3. Quantitative Real-Time PCR (qRT-PCR) was performed with a 7500 Fast Real-Time PCR System (Applied Biosystems, Bleiswijk, the Netherlands) using a MESA FAST qRT-PCR MasterMix Plus for SYBR® Assay Low ROX (Eurogentec). The relative fold induction level of each transcript was obtained by ΔΔCt analysis and was performed on duplicate biological samples that were assayed in duplicate. For quantitative results sigA was used for normalization.

Expression levels after 12h exposure to 1x MIC of Rifampicin

					¼x MIC RIF (128 mg/L)		1x MIC RIF [512 mg/L] [qPCR]		
Condition	**Rv number**	**Gene**	**Funct. Cat.**	**Description**	**30 min**	**12 h**	**30 min**	**12 h**	**12 h**
Up-regulation	Rv0251c	hsp	1	Heat shock protein hsp (heat-stress-induced ribosome-binding protein a)	1.0	2.7	1.5	10.9	[3.9]
	Rv0450c	mmpL4	4	Probable conserved transmembrane transport protein mmpl4	1.8	3.3	4.7	6.8	[1.1]
	Rv0451c	mmpS4	4	Probable conserved membrane protein mmps4	2.1	3.8	4.4	5.3	[1.7]
	Rv0452	Rv0452	10	Possible transcriptional regulatory protein	2.9	5.1	6.4	5.0	[1.3]
	Rv0559c	Rv0559c	4	Possible conserved secreted protein	9.3	13.3	18.9	18.1	[40.0]
	Rv0560c	Rv0560c	8	Possible benzoquinone methyltransferase (methylase)	52.9	98.3	72.7	137.1	[242.6]
	Rv0676c	mmpL5	4	Probable conserved transmembrane transport protein mmpl5	22.6	11.6	34.6	26.0	[6.4]
	Rv0677c	mmpS5	4	Possible conserved membrane protein mmps5	14.5	8.0	34.7	18.3	[8.5]
	Rv0678	Rv0678	11	Conserved hypothetical protein	16.0	6.9	31.5	25.2	[9.1]
	Rv0711	atsA	8	Possible arylsulfatase atsa (aryl-sulfate sulphohydrolase) (arylsulphatase)	-1.1	1.2	1.8	5.5	[3.7]
	Rv1216c	Rv1216c	4	Probable conserved integral membrane protein	2.1	5.7	4.2	8.4	[1.5]
	Rv1217c	Rv1217c	4	Probable tetronasin-transport integral membrane protein abc transporter	3.0	4.6	7.2	8.7	[1.9]
	Rv1218c	Rv1218c	4	Probable tetronasin-transport atp-binding protein abc transporter	2.7	4.0	8.5	7.2	[1.6]
	Rv1219c	Rv1219c	10	Probable transcriptional regulatory protein	1.7	4.4	1.9	6.4	[1.4]
Down-regulation	Rv0096	PPE1	7	Ppe family protein	1.0	-6.0	1.4	-9.9	[-2.1]
	Rv0097	Rv0097	8	Possible oxidoreductase	1.0	-6.1	1.4	-9.0	[-2.6]
	Rv0098	fcoT	2	Probable fatty acyl coa thioesterase type iii fcot	1.0	-6.3	1.1	-12.7	[-2.6]
	Rv0099	fadD10	2	Possible fatty-acid-coa ligase fadd10 (fatty-acid-coa synthetase) (fatty-acid-coa synthase)	-1.0	-6.6	1.1	-10.5	[-1.3]
	Rv0100	Rv0100	11	Conserved hypothetical protein	1.0	-3.9	-1.0	-6.0	[-1.5]
	Rv0101	nrp	2	Probable peptide synthetase nrp (peptide synthase)	1.2	-3.2	1.0	-5.0	[-1.1]

Table 2. Fold change of 20 exclusively differentially-expressed genes in H37Rv-H526Y after 30 minutes and 12 hours exposure to ¼x MIC and 1x MIC of rifampicin determined with microarray analysis. qRT-PCR results obtained after 12 hours exposure to 1x MIC of rifampicin are shown between brackets.

Gene	Annotation	Forward primer	Reverse primer
Rv0096	*PPE1*	CAGCAGCTGGCAGGGAACCG	AGCTCTGCTGGGGTGGGCAT
Rv0097		TCCGTCTCCGCGGGAGTTCA	ATGCCAGAACGCGCCGGTTT
Rv0098	*fcoT*	ACACCGACTTGACGCCCTGC	TGGCGCTGTACTGTGCGTCG
Rv0099	*faD10*	GATGGCATCGGCCCTACCGC	CCGGTGTTCACCCAGCCGTC
Rv0100		CGCCGTCTGCGACGTGTTGTA	GGCCAATCGGGACGGCAGTT
Rv0101	*nrp*	ATTCCTGGCCGCTCTGCACG	GCACCGTATGCCGCACCAGT
Rv0251c	*hsp*	GCTGCGCCTGAGTTTCGGCT	TCATTCCGCCGCTCGTTCCG
Rv0450c	*MmpL4*	GTCGCTGCTCATCGCCAAGGG	CGCCATCCATCGCCGCACTA
Rv0451c	*MmpS4*	CACGGTAGCACCGCTCCATCG	GATCCGCGGCTTCTTCGGCTC
Rv0452		AACGGCTGTCGCAGGTCGTG	AGCTGCTCGCATACCGTGCC
Rv0559c		CGCCCACATGCTCAGGGCAG	GGCGTTGACGGCGATGCGTA
Rv0560c		GTGTCCCCGTTCGGCCAGTG	GGAGGGAGTCCGACCGCCAT
Rv0676c	*MmpL5*	CCAACGGCACACCGAGGGTC	CAGGACCGGGAGTCGGCGTA
Rv0677c	*MmpS5*	GCCATCGACGGTGATTCGGCA	GACCTCGACGCCAAGCCACAG
Rv0678		TCCGGGCAATGGCCGAACTG	GTCCTCTCCGGTTCGCTGGC
Rv0711	*atsA*	GCCCGACAAGCCGTGGTTCA	TGTCGGGTGGCACGATCCCT
Rv1216c		GCACGCGCTCAGCACCATCA	AGCACCACGATTGGCCCCAC
Rv1217c		CGAACGTCACGCCGTCGGAA	CGCTGTACCTGCTCGGCTCG
Rv1218c		TCGCACAGCGCTTCGGTCTC	GCGCGCACCTACTCCAAGGG
Rv1219c		CGGCGCGTACTCCTTCGTCC	AACGACCCGACCACCTGGCT
Rv2703	*sigA*	GTCGGAGGCCCTGCGTCAAG	AGGCCAGCCTCGATCCGCTT

Table 3. Primer sequences as used in the quantitative reverse transcriptase-PCR analysis.

RESULTS

Mtb growth

H37Rv-WT and H37Rv-H526Y at a density of 7.4×10^5 [$4.3 – 9.9 \times 10^5$] CFU/mL were cultured. After 6 days both cultures had increased up to 3.1×10^7 [$2.1 – 4.0 \times 10^7$] CFU/mL. Both strains showed identical growth patterns. At day 6, rifampicin was added and quadruple cultures were exposed to either solvent or rifampicin concentrations at ¼x MIC or 1x MIC for each strain. After 30 minutes and 12 hours exposure the control growth of both strains reached 3.9×10^7 [$3.0 – 5.0 \times 10^7$] CFU/mL and 2.5×10^7 [$1.9 – 2.8 \times 10^7$] CFU/mL respectively. Exposure to ¼x MIC of rifampicin led in both strains to similar CFU counts being 3.0×10^7 [$2.1 – 4.1 \times 10^7$] after 30 minutes and 2.1×10^7 [$1.5 – 3.1 \times 10^7$] after 12 hours exposure. Exposure to 1x MIC of rifampicin led in both strains also to similar CFU counts being 3.1×10^7 [$2.8 – 3.4 \times 10^7$] after 30 minutes and 2.3×10^7 [$1.2 – 3.1 \times 10^7$] after 12 hours exposure.

Microarray analysis

After microarray analysis, all genes that responded to rifampicin (FDR p-values ≤ 0.05), at each time point were categorized and the associated distribution between functional categories is displayed in table 1. Of the total number of up-regulated genes upon rifampicin exposure, 4 genes were up-regulated in both strains and of the total number of down-regulated genes

upon rifampicin exposure, 2 genes were down-regulated in both strains. In H37Rv-WT no genes were induced after 30 minutes exposure to ¼x MIC and 1x MIC of rifampicin. After 12 hours exposure to ¼x MIC of rifampicin, Rv1397c (*vapC10*) encoding a possible toxin was found down-regulated, a 12 hour exposure to 1x MIC of rifampicin resulted in 104 up-regulated genes and 149 down-regulated genes. After 12 hours exposure to 1x MIC of rifampicin *vapC10* was also down-regulated which was stronger compared to exposure to ¼x MIC.

The H37Rv-H526Y showed more response upon rifampicin exposure compared to the H37Rv-WT. Exposure to ¼x MIC of rifampicin resulted in 10 up-regulated genes and 1 down-regulated gene after 30 minutes, and 13 up-regulated genes and 6 down-regulated genes after 12 hours. Exposure to 1x MIC of rifampicin resulted in 18 up-regulated and 5 down-regulated genes after 30 minutes and 75 up-regulated and 39 down-regulated genes after 12 hours. Under all conditions in the H37Rv-H526Y strain nine genes were found up-regulated. Of all these genes, 20 genes were selected that showed in at least 2 conditions differential expression ≥ 4 fold (14 genes) or ≤ ¼ fold (6 genes) in H37Rv-H526Y and not in H37Rv-WT upon exposure to rifampicin (table 2). From the 14 ≥ 4 fold up-regulated genes, 8 appeared to be involved in cell wall and cell processes (Rv0450c, Rv0451c, Rv0559c, Rv0676c, Rv0677c, Rv1216c, Rv1217c and Rv1218c), 2 encode proteins involved in intermediary metabolism and respiration (Rv0560c and Rv0711), 2 encode regulatory proteins (Rv0452 and Rv1219c), 1 is associated with virulence, detoxification and adaption (Rv0251c), and 1 encodes a conserved hypothetical protein (Rv0678). Of the 6 down-regulated genes, 3 encode proteins that are involved in lipid metabolism (Rv0098, Rv0099 and Rv0101), 1 belongs to the PPE family proteins (Rv0096), 1 encodes a protein involved in intermediary metabolism and respiration (Rv0097), and 1 encodes a conserved hypothetical protein (Rv0100).

qRT-PCR confirmation

Aliquots of the RNA from rifampicin-treated and control samples were also used for qRT-PCR analysis. The samples obtained after 12 hours 1x the MIC of rifampicin exposure, were compared with the 12 hours control samples; *sig*A was used for normalization. Results of the ΔΔCt analysis are in agreement with the microarray data. The direction of change was in concurrence by both qRT-PCR and microarray analysis for all samples. However, the fold change determined by qRT-PCR is different from that determined by the microarray analysis as shown in table 2 and figure 1. Another ΔΔCt analysis of independent RNA samples showed that the direction of change was in agreement by both qRT-PCR and microarray analysis for 70% of the samples. However, in general gene-expression levels are lower compared to the microarray analysis and to the expression levels obtained from the first qRT-PCR experiment. Of the 20 genes that were up-regulated in at least two conditions in the microarray analysis, only Rv0559c and Rv0560c were found strongly and constantly up-regulated in both qRT-PCR experiments in H37Rv-H526Y compared to H37Rv-WT.
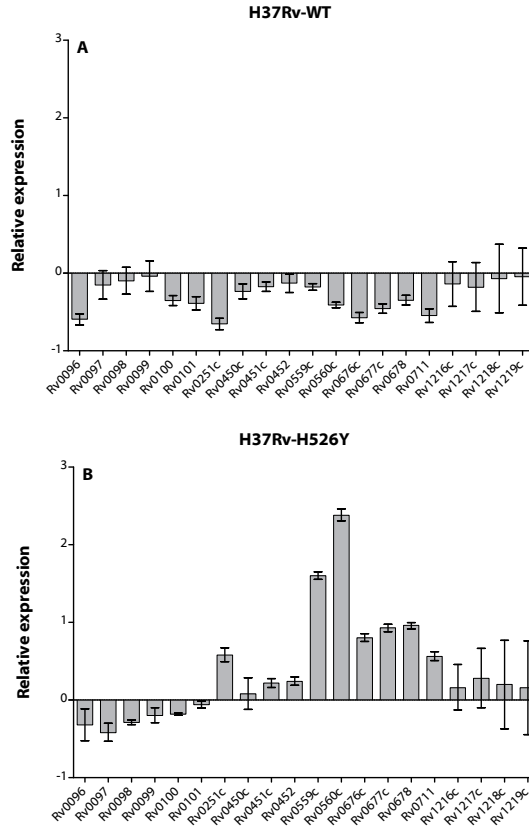
Figure 1. Differentially expressed genes assessed by quantitative Real-Time PCR (qRT-PCR). The relative gene expression of H37Rv-WT **(A)** and H37Rv-H526Y **(B)** assessed with qRT-PCR and normalised to sigA after 12 hours of exposurse to 1x MIC of rifampicin

DISCUSSION

We have investigated differences in rifampicin-induced gene responses between rifampicin-susceptible and rifampicin-resistant Mtb strains using microarray analysis and qRT-PCR. At ¼x MIC of rifampicin exposure more genes are differentially expressed in H37Rv-H526Y than H37Rv-WT, whereas at 1x MIC of rifampicin and long exposure this is reversed. These results show that the rifampicin-susceptible and rifampicin-resistant Mtb strain have an altered response upon rifampicin exposure.

Using qRT-PCR we assessed if biological duplicates showed similar up-regulation. This revealed that one cluster of genes (Rv0559c-Rv0560c) was strongly up-regulated in all experiments after exposure to rifampicin in the H37Rv-H526Y. These results were confirmed in a second qRT-PCR experiment in which expression of Rv0559c and Rv0560c was also highly

up-regulated in the H37Rv-H526Y strain compared to the H37Rv-WT strain (data not shown). The Rv0559c gene encodes a protein with an unknown function. However, a previous study of Denkin *et al.* showed that Rv0559c is also induced upon salicylate exposure.[17] Rv0560c is also induced by salicylate and probably encodes a benzoquinone methyltransferase.[17-18] Schuessler *et al.* showed that Rv0559c and Rv0560c have slow induction kinetics after exposure to salicylate and that gene expression is increasing over time.[19] Our results are in agreement with these findings, since our microarray data also revealed that up-regulation of Rv0559c and Rv0560c is time-dependent and rifampicin concentration-dependent. The data showed an increase in expression of Rv0560c between 30 minutes and 12 hours of rifampicin exposure. An increased expression was also observed for both genes comparing exposure to rifampicin at ¼x MIC and 1x MIC. Sun *et al.* suggested that Rv0559c, Rv0560c and Rv0561c are located within the same operon,[18] and Schuessler *et al.* showed that only Rv0559c and Rv0560c are regulated by the same promoter. In our microarray analysis we did not find a significant up-regulation of Rv0561c after rifampicin exposure in the H37Rv-H526Y strain, which is in concordance with earlier observations by Schuessler *et al.* In all, our study provides further evidence that Rv0559c and Rv0560c are potentially involved in (rifampicin) resistance and thereby further investigation on the function of the proteins they encode for is appropriate.

We have also found 4 other distinct clusters of genes and 2 different genes differently expressed between both strains after 12 hours of exposure to 1x MIC of rifampicin. The first cluster of Rv0096 to Rv0101 is strongly down-regulated in the H37Rv-H526Y strain upon 12 hours of rifampicin exposure. The other clusters, Rv0450c to Rv452, Rv0676c to Rv678 and Rv1216c to Rv1219c are strongly up-regulated in the H37Rv-H526Y. None of these clusters are induced in the H37Rv-WT in response to rifampicin exposure. Genes of the Rv0096-Rv0101 operon encode a PPE protein family member (Rv0096), a putative oxidoreductase of the *tfdA* dioxygenase family (Rv0097), a type III thioesterase (Rv0098), a fatty acid AMP ligase (Rv0099), an acyl carrier protein (Rv0100) and a nonribosomal peptide synthase (Rv0101). These genes seem to be co-regulated by a two-component regulatory system (*senX3-regX3*)[20] and are involved in biosynthesis of Phthiocerol Dimycocerosate (PDIM).[21] PDIM is part of the lipid-rich content of the mycobacterial cell envelop and is associated with an increased Mtb virulence.[22-23] Interestingly, no down-regulation was found after microarray analysis for Rv2942 (*MmpL7*), which is also involved in the transport of PDIMs.[24] So, upon rifampicin exposure, down-regulation of this virulence-associated operon in the H37Rv-H526Y is observed. Thus a possible direct linkage between loss of fitness and mutations in the RRDR region is given.

Another gene, up-regulated after 12 hours of exposure to 1x MIC of rifampicin in the H37Rv-H526Y is Rv0251c, which is associated with stress response.[25] The up-regulation of stress-

related genes after exposure to rifampicin seems a logic event. However with these results, an exact gene is known and thus a more precise study can be conducted to unravel the exact function of Rv0251c in Mtb and thereby provide a possible drug-target.

Furthermore, two up-regulated gene clusters being Rv0450c to Rv452 and Rv0676c to Rv678 were found. Both clusters consist of genes of the MmpL (Mycobacterial membrane protein Large) family, of the MmpS (Mycobacterial membrane protein Small) family and a gene with unknown function. The MmpL proteins belong to the group of resistance, nodulation and cell division proteins (RND) and are associated with drug efflux.[26] The RND family is a group of multidrug resistance pumps that recognize and mediate the transport of a great diversity of compounds and has been well-documented in Gram-negative bacteria. However, Domenech *et al.* concluded in their study that these MmpL genes seem to play a limited role in anti-TB drug resistance in Mtb.[26] *MmpL4* (Rv0450c) and *MmpL5* (Rv0676c) are transcriptional coupled with *MmpS4* and *MmpS5*, these smaller genes are predicted to encode proteins with one transmembrane domain. Still, little is known about the MmpS family. In *Mycobacterium smeg-matis MmpS4* (Rv0451c) is associated with glycopeptidolipid biosynthesis and export cell surface glycolipids.[27] In our experiments, the up-regulation of Rv0450c to Rv0452 is almost constant in all conditions tested. Our data showed that the response of Rv0676c to Rv0678 is higher after 30 minutes of exposure to both rifampicin concentrations compared to 12 hours of rifampicin exposure. This suggests that Rv0676c to Rv0678 are early response genes. *MmpL5* and *MmpS5* (Rv0677c) are associated with efflux pump-related azole resistance in Mtb and are regulated by Rv0678.[28] Milano *et al.* showed that Rv0678 has almost 50% homology with the well-characterized *MarR* of *Escherichia coli*,[28] this family of regulatory proteins plays an important role in of the development of antibiotic resistance.[29] Based on the already known function of MmpL and MmpS genes and the up-regulation found in the microarray analysis it is likely that in Mtb *MmpL4*, *MmpS4*, *MmpL5* and *MmpS5* are involved in rifampicin efflux out of the cell. This indicates that although previous studies showed no crucial role for some of the proteins they encode for in drug resistance, the up-regulation of these genes upon rifampicin exposure is a genuine phenomenon and thereby might possess a target for future drug efflux inhibition.

Rv0711 (*atsA*) encodes for a possible arylsulfatase but knowledge about *atsA* is very limited in Mtb. The knowledge about the up-regulated gene cluster Rv1216c-Rv1219c in the H37Rv-H526Y is also very limited. Rv1216c and Rv1217c encode for probable integral membrane proteins. Rv1218c encodes an ABC transporter and previous studies suggest an important role for this gene product in mediating efflux to a wide variety of compounds.[30-31] However Balganesh *et al.* showed that the MIC of rifampicin is not influenced in Rv1218c knock-out mutants.[30] This suggests that Rv1218c is not primarily involved in regulation of the intracel-lular concentration of rifampicin. In our rifampicin-resistant H37Rv-H526Y mutant however,

Rv1218c is strongly up-regulated, which implies an association between up-regulation of Rv1218c and rifampicin resistance. Rv1219c probably encodes for a transcriptional regulatory protein but further function and regulation is unknown.

To conclude, our results show that several interesting gene clusters associated with efflux, transport and virulence show an altered response in the rifampicin-resistant H37Rv mutant compared to the rifampicin-susceptible H37Rv wild type strain upon exposure to rifampicin. Not all genes could be completely confirmed with qRT-PCR. Although the directions of change were identical, fold changes appeared in general to be lower in qRT-PCR. This lack of concurrence between methods for genes exhibiting low levels of change has been reported by several others.[32-35] In the present paper we show by microarrays and qRT-PCR experiments that Rv0559c and Rv0560c are strongly rifampicin-inducible. This indicates that the induction of both genes is dependent on concentration of rifampicin and exposure time. Therefore this study suggests that Rv0559c and Rv0560c play a pivotal role in rifampicin resistance of Mtb. Further investigation on the exact function and regulation of Rv0559c and Rv0560c is needed to understand the mycobacterial mechanisms that are triggered upon rifampicin exposure.

REFERENCES

1.   WHO. Global tuberculosis control 2011.
2.   WHO. Global tuberculosis control 2010.
3.   Drobniewski FA, Wilson SM. The rapid diagnosis of isoniazid and rifampicin resistance in *Mycobacterium tuberculosis*--a molecular story. J Med Microbiol 1998;47:189-96.
4.   Jarlier V, Nikaido H. Mycobacterial cell wall: structure and role in natural resistance to antibiotics. FEMS Microbiol Lett 1994;123:11-8.
5.   Telenti A, Imboden P, Marchesi F, Lowrie D, Cole S, Colston MJ, Matter L, Schopfer K, Bodmer T. Detection of rifampicin-resistance mutations in *Mycobacterium tuberculosis*. Lancet 1993;341:647-50.
6.   Huitric E, Werngren J, Jureen P, Hoffner S. Resistance levels and *rpoB* gene mutations among *in vitro*-selected rifampin-resistant *Mycobacterium tuberculosis* mutants. Antimicrob Agents Chemother 2006;50:2860-2.
7.   Siu GK, Zhang Y, Lau TC, Lau RW, Ho PL, Yew WW, Tsui SK, Cheng VC, Yuen KY, Yam WC. Mutations outside the rifampicin resistance-determining region associated with rifampicin resistance in *Mycobacterium tuberculosis*. J Antimicrob Chemother 2011;66:730-3.
8.   Stephan J, Mailaender C, Etienne G, Daffe M, Niederweis M. Multidrug resistance of a porin deletion mutant of Mycobacterium smegmatis. Antimicrob Agents Chemother 2004;48:4163-70.
9.   da Silva PE, Von Groll A, Martin A, Palomino JC. Efflux as a mechanism for drug resistance in *Mycobacterium tuberculosis*. FEMS Immunol Med Microbiol 2011.
10. Gupta AK, Katoch VM, Chauhan DS, Sharma R, Singh M, Venkatesan K, Sharma VD. Microarray analysis of efflux pump genes in multidrug-resistant *Mycobacterium tuberculosis* during stress induced by common anti-tuberculous drugs. Microb Drug Resist 2010;16:21-8.
11. Louw GE, Warren RM, Gey van Pittius NC, McEvoy CR, Van Helden PD, Victor TC. A balancing act: efflux/influx in mycobacterial drug resistance. Antimicrob Agents Chemother 2009;53:3181-9.
12. Louw GE, Warren RM, Gey van Pittius NC, Leon R, Jimenez A, Pando RH, McEvoy CR, Grobbelaar M, Murray M, van Helden PD, Victor TC. Rifampicin Reduces Susceptibility to Ofloxacin in Rifampicin Resistant *Mycobacterium tuberculosis* through Efflux. Am J Respir Crit Care Med 2011.
13. Wolfinger RD, Gibson G, Wolfinger ED, Bennett L, Hamadeh H, Bushel P, Afshari C, Paules RS. Assessing gene significance from cDNA microarray expression data via mixed models. J Comput Biol 2001;8:625-37.
14. Smyth GK. Linear models and empirical bayes methods for assessing differential expression in microarray experiments. Stat Appl Genet Mol Biol 2004;3:Article3.
15. Cui X, Hwang JT, Qiu J, Blades NJ, Churchill GA. Improved statistical tests for differential gene expression by shrinking variance components estimates. Biostatistics 2005;6:59-75.
16. Storey JD, Tibshirani R. Statistical significance for genomewide studies. Proc Natl Acad Sci U S A 2003;100:9440-5.
17. Denkin S, Byrne S, Jie C, Zhang Y. Gene expression profiling analysis of *Mycobacterium tuberculosis* genes in response to salicylate. Arch Microbiol 2005;184:152-7.
18. Sun Z, Cheng SJ, Zhang H, Zhang Y. Salicylate uniquely induces a 27-kDa protein in tubercle bacillus. FEMS Microbiol Lett 2001;203:211-6.
19. Schuessler DL, Parish T. The promoter of Rv0560c is induced by salicylate and structurally-related compounds in *Mycobacterium tuberculosis*. PLoS One 2012;7:e34471.
20. Parish T, Smith DA, Roberts G, Betts J, Stoker NG. The senX3-regX3 two-component regulatory system of *Mycobacterium tuberculosis* is required for virulence. Microbiology 2003;149:1423-35.

21. Hotter GS, Wards BJ, Mouat P, Besra GS, Gomes J, Singh M, Bassett S, Kawakami P, Wheeler PR, de Lisle GW, Collins DM. Transposon mutagenesis of Mb0100 at the ppe1-nrp locus in Mycobacterium bovis disrupts phthiocerol dimycocerosate (PDIM) and glycosylphenol-PDIM biosynthesis, producing an avirulent strain with vaccine properties at least equal to those of M. bovis BCG. J Bacteriol 2005;187:2267-77.

22. Hotter GS, Collins DM. Mycobacterium bovis lipids: virulence and vaccines. Vet Microbiol 2011;151:91-8.

23. Wang F, Langley R, Gulten G, Wang L, Sacchettini JC. Identification of a type III thioesterase reveals the function of an operon crucial for Mtb virulence. Chem Biol 2007;14:543-51.

24. Camacho LR, Constant P, Raynaud C, Laneelle MA, Triccas JA, Gicquel B, Daffe M, Guilhot C. Analysis of the phthiocerol dimycocerosate locus of *Mycobacterium tuberculosis*. Evidence that this lipid is involved in the cell wall permeability barrier. J Biol Chem 2001;276:19845-54.

25. Stewart GR, Newton SM, Wilkinson KA, Humphreys IR, Murphy HN, Robertson BD, Wilkinson RJ, Young DB. The stress-responsive chaperone alpha-crystallin 2 is required for pathogenesis of *Mycobacterium tuberculosis*. Mol Microbiol 2005;55:1127-37.

26. Domenech P, Reed MB, Barry CE, 3rd. Contribution of the *Mycobacterium tuberculosis* MmpL protein family to virulence and drug resistance. Infect Immun 2005;73:3492-501.

27. Deshayes C, Bach H, Euphrasie D, Attarian R, Coureuil M, Sougakoff W, Laval F, Av-Gay Y, Daffe M, Etienne G, Reyrat JM. *MmpS4* promotes glycopeptidolipids biosynthesis and export in Mycobacterium smegmatis. Mol Microbiol 2010;78:989-1003.

28. Milano A, Pasca MR, Provvedi R, Lucarelli AP, Manina G, Ribeiro AL, Manganelli R, Riccardi G. Azole resistance in *Mycobacterium tuberculosis* is mediated by the *MmpS5-MmpL5* efflux syste*M. tuberculosis* (Edinb) 2009;89:84-90.

29. Nikaido H. Multiple antibiotic resistance and efflux. Curr Opin Microbiol 1998;1:516-23.

30. Balganesh M, Kuruppath S, Marcel N, Sharma S, Nair A, Sharma U. Rv1218c, an ABC transporter of *Mycobacterium tuberculosis* with implications in drug discovery. Antimicrob Agents Chemother 2010;54:5167-72.

31. Balganesh M, Dinesh N, Sharma S, Kuruppath S, Nair AV, Sharma U. Efflux pumps of *Mycobacterium tuberculosis* play a significant role in antituberculosis activity of potential drug candidates. Antimicrob Agents Chemother 2012;56:2643-51.

32. Wurmbach E, Yuen T, Sealfon SC. Focused microarray analysis. Methods 2003;31:306-16.

33. Rajeevan MS, Vernon SD, Taysavang N, Unger ER. Validation of array-based gene expression profiles by real-time (kinetic) RT-PCR. J Mol Diagn 2001;3:26-31.

34. Ding Y, Xu L, Jovanovic BD, Helenowski IB, Kelly DL, Catalona WJ, Yang XJ, Pins M, Bergan RC. The methodology used to measure differential gene expression affects the outcome. J Biomol Tech 2007;18:321-30.

35. Morey JS, Ryan JC, Van Dolah FM. Microarray validation: factors influencing correlation between oligonucleotide microarrays and real-time PCR. Biol Proced Online 2006;8:175-93.

Chapter 9

Drug susceptibility of *Mycobacterium tuberculosis* Beijing genotype, association with MDR-TB

J.E.M. de Steenwinkel, M.T. ten Kate, G.J. de Knegt, K. Kremer, R.E. Aarnoutse,
M.J. Boeree, H.A. Verbrugh, D. van Soolingen, I.A.J.M. Bakker-Woudenberg

ABSTRACT

To determine differences in the ability of *Mycobacterium tuberculosis* strains to withstand anti-tuberculosis drug treatment, we compared the activity of anti-tuberculosis drugs against susceptible Beijing and East-African/Indian genotype Mtb strains. Beijing genotype strains showed high rates of mutation within a wide range of drug concentrations, possibly explaining this genotype's association with multidrug-resistant tuberculosis.

INTRODUCTION

The emergence of *Mycobacterium tuberculosis* (Mtb) resistance to anti-tuberculosis (anti-TB) drugs is a major public health challenge that is threatening World Health Organization targets set for the elimination of TB).[1] Approximately 500,000 cases of multidrug-resistant TB (MDR-TB) are diagnosed annually, but the true magnitude of the MDR-TB problem is not known because adequate laboratory tools are lacking. Multiple factors contribute to low cure rates, treatment failures, and relapses: poor-quality guidance regarding treatment, HIV co-infection, transmission of resistant forms of TB, underdeveloped laboratory services, and unavailability of alternative drug treatments. However, the evolution of Mtb is an additional factor that presumably fuels the worldwide problem of emerging resistance. The Beijing genotype is significantly associated with drug resistance [2-6], especially in geographic areas where prevalence of resistance to anti-TB drugs is high, and it is associated with recent TB transmission.[2-6] There are also indications that the population structure of Mtb in areas with a high prevalence of anti-TB drug resistance is changing rapidly toward an increase in Beijing genotype strains.[2,6-8]

The World Health Organization target rates for detecting and curing TB in Vietnam have been met; however, the rate of TB infection is not decreasing as expected.[4-5]. Earlier in this country, the Beijing genotype was strongly correlated with MDR-TB and treatment failures.[9] Extensive molecular epidemiologic studies showed that the Beijing and East-African/Indian (EAI) genotypes are predominating in Vietnam; each lineage causes ≈40% of the TB cases. According to the single-nucleotide polymorphism typing described by Hershberg *et al.* [10], the Beijing genotype is a representative of the modern lineage, and the EAI genotype is believed to represent an evolutionary lineage more closely related to the common ancestor of the Mtb complex.

We compared the *in vitro* activity of anti-TB drugs against susceptible Beijing and EAI Mtb isolates from Vietnam and determined the *in vitro* mutation frequency of these strains during drug exposure. We also determined time-kill kinetics of anti-TB drugs and assessed the emergence of resistant mutants and the concentration range within which resistant mutants and no susceptible mycobacteria were selected. The concentration at which resistant mutants did not emerge (the mutant prevention concentration) was also ascertained. By using this approach, we established an *in vitro* model for determining differences in the ability of Mtb strains to resist anti-TB drug treatment.

THE STUDY

Results of a liquid culturing system (BD BACTEC MGIT 960 System; BD Diagnostics, Sparks, MD, US) (for details, see the Technical Appendix) showed that all 5 Beijing and 5 EAI genotype strains were susceptible to isoniazid, rifampicin, moxifloxacin (MXF), and amikacin (AMK). MICs were determined by using the agar proportion method [11], which showed that ranges were small for the Beijing and EAI genotype strains; isoniazid: 0.062–0.125 mg/L, rifampicin: 0.125–1 mg/L, MXF: 0.125–0.5 mg/L and AMK: 0.5–2 mg/L. Duplicate values showed only minor differences.

We determined the mutation frequencies of the Beijing and EAI genotype strains by using previously defined critical drug concentrations of 1 mg/L for isoniazid, rifampicin, and MXF and 5 mg/L for AMK (11,12) (for details, see the Technical Appendix). The mutation frequencies of the Beijing and EAI genotype strains were similar for isoniazid, MXF, and AMK, but they were significantly different for rifampicin (1.6×10^{-5} to 5.4×10^{-3} for Beijing strains vs. 6.3×10^{-8} to 3.8×10^{-4} for EAI strains; p = 0.003, unpaired Mann-Whitney test) (table 1; figure 1). Because rifamycin drugs are widely used to treat TB, the difference in the mutation frequencies of Beijing and EAI genotype strains for rifampicin is a major finding.

For Beijing genotype strains, the increase in mutation frequency during exposure to rifampicin could be due to described missense mutations in the mut genes.[13] Such mutations in the mut genes can change the DNA repair mechanism; as a consequence, the frequency of resistant mutant formation might increase. However, a direct correlation between the occurrence of particular mutations in mut genes and altered mutation frequency has not been proven. Furthermore, Werngren and Hoffner [14] found an equal mutation frequency for Beijing (3.6×10^{-8}) and non-Beijing (4.4×10^{-8}) genotypes. A possible explanation for the discrepancy in findings might be the concentration of rifampicin used in the subculture plates. In our study, the critical concentration

		Mutation Frequency								
	Beijing genotype strains					East-African/Indian genotype strains				
	1585	1607	2115	2121	2145	1627	1606	1592	1596	2113
INH	5.7×10^{-6}	8.6×10^{-6}	7.3×10^{-6}	6.8×10^{-5}	9.1×10^{-4}	3.7×10^{-6}	8.7×10^{-6}	1.8×10^{-5}	3.9×10^{-5}	1.3×10^{-5}
	6.2×10^{-6}	1.4×10^{-5}	1.1×10^{-5}	2.9×10^{-4}	5.0×10^{-4}	6.5×10^{-6}	1.6×10^{-4}	2.6×10^{-5}	2.8×10^{-5}	4.1×10^{-5}
RIF	3.0×10^{-3}	1.5×10^{-3}	1.0×10^{-3}	2.9×10^{-5}	1.6×10^{-5}	4.1×10^{-6}	3.8×10^{-4}	3.0×10^{-4}	1.4×10^{-5}	6.7×10^{-8}
	4.3×10^{-3}	5.4×10^{-3}	9.2×10^{-5}	1.9×10^{-4}	5.5×10^{-5}	2.8×10^{-6}	2.7×10^{-5}	2.4×10^{-5}	3.9×10^{-6}	6.3×10^{-8}
MXF	4.3×10^{-8}	6.9×10^{-8}	1.0×10^{-8}	1.1×10^{-7}	7.9×10^{-8}	9.3×10^{-9}	3.2×10^{-8}	9.9×10^{-8}	1.7×10^{-7}	1.5×10^{-8}
	6.1×10^{-8}	2.4×10^{-7}	4.3×10^{-8}	1.6×10^{-7}	1.0×10^{-7}	1.5×10^{-7}	1.0×10^{-7}	4.5×10^{-8}	2.0×10^{-7}	1.0×10^{-7}
AMK	2.3×10^{-8}	8.6×10^{-8}	1.4×10^{-8}	9.3×10^{-8}	7.6×10^{-7}	5.6×10^{-8}	7.5×10^{-9}	9.4×10^{-8}	3.7×10^{-8}	4.4×10^{-8}
	3.2×10^{-8}	3.0×10^{-7}	2.8×10^{-8}	1.1×10^{-7}	1.1×10^{-6}	4.5×10^{-9}	1.5×10^{-9}	1.5×10^{-9}	3.2×10^{-7}	3.3×10^{-7}

Table 1: Mutation frequency *Mycobacterium tuberculosis* genotype strains originating from Vietnam, by anti-tuberculosis drug, determined in duplicate.
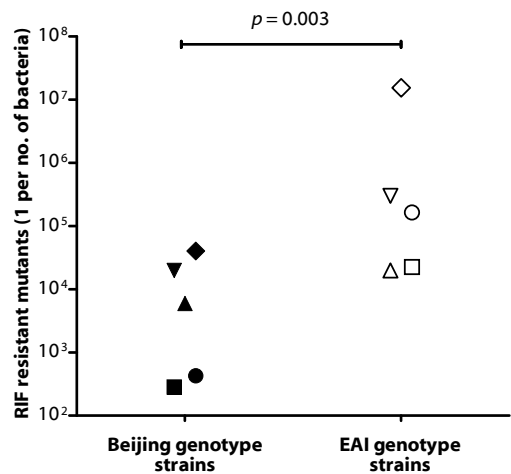
Figure 1. Frequency of rifampicin (RIF)-resistant mutants in *Mycobacterium tuberculosis* Beijing and East-African/Indian (EAI) genotype strains (5 strains each) originating from Vietnam. Mutation frequencies were determined in duplicate. Statistical analysis was performed by using an unpaired Mann-Whitney test.

of 1 mg/L rifampicin was used [11], whereas Werngren and Hoffner used a concentration of 2 mg/L rifampicin. In addition, Werngren and Hoffner compared the Beijing and non-Beijing genotypes of several genotype families, whereas we compared Beijing and EAI genotype strains that were selected from the same tuberculosis-endemic area and during the same period.

We determined the time-kill kinetics of rifampicin toward 2 strains with significantly different mutation frequencies: Beijing-1585 (3.7×10^{-3} [3.0×10^{-3} and 4.3×10^{-3}, duplicates]) and EAI-1627 (3.5×10^{-6} [2.8×10^{-6} and 4.1×10^{-6}, duplicates]). Cultures with low and high

	Lowest concentration (mg/L) resulting in killing of Mtb after various time points during RIF exposure							
	Beijing-1585				EAI-1627			
	≥99% killing		100% killing		≥99% killing		100% killing	
	low density †	high density ‡	low density §	high density ¶	low density †	high density ‡	low density §	high density ¶
Day 1	8	ND	256	ND	8	ND	32	ND
Day 3	1	0.008	64	1024	0.125	0.03	8	32
Day 6	0.001	0.008	2	64	0.001	0.06	1	2

Table 2. Concentration- and time-dependent bactericidal effect of rifampicin toward *Mycobacterium tuberculosis* genotypes in low- and high-density cultures. Cultures were exposed to RIF at 2-fold increasing concentrations for 6 days at 37°C; at indicated time-points, subcultures were performed on solid media for counting. Low, low-density culture; high, high-density culture; ND, not determined.
†   Density of 5.1×10^5 CFU/mL
‡   Density of 4.4×10^6 CFU/mL
§   Density of 6.8×10^5 CFU/mL
¶   Density of 3.0×10^6 CFU/mL
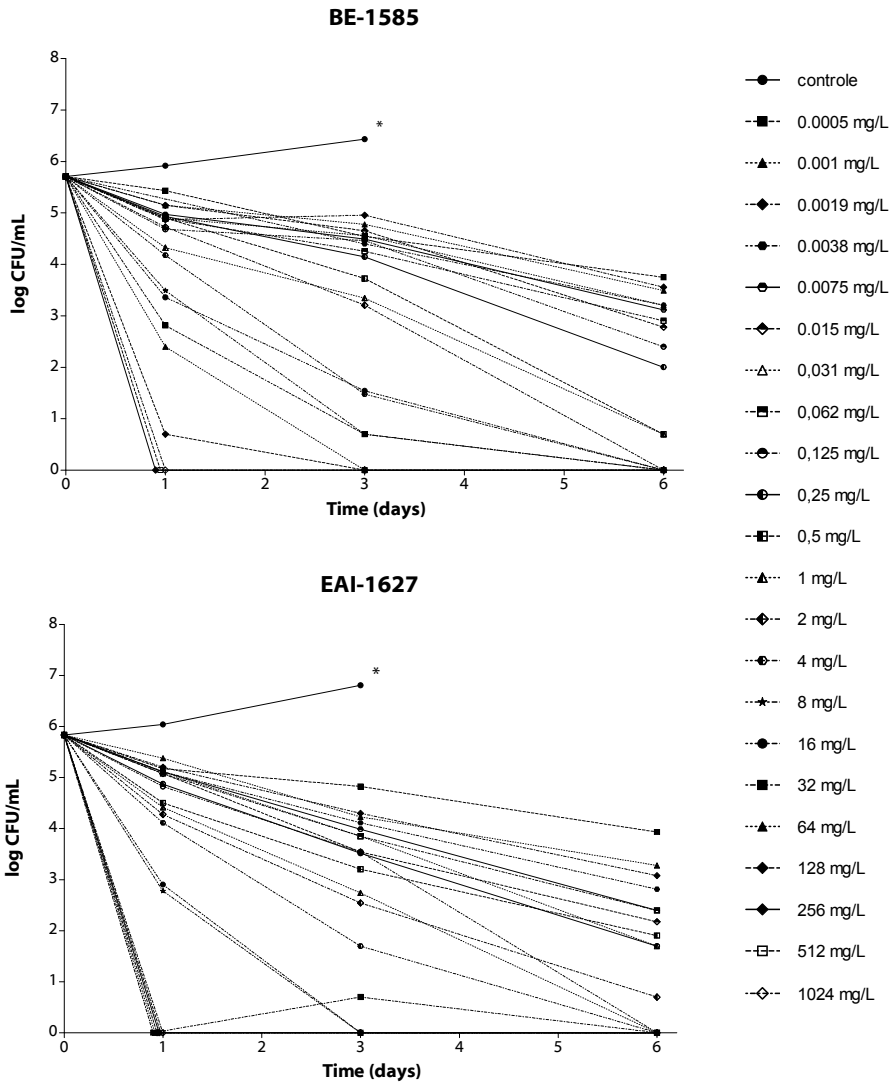
BE-1585

EAI-1627

Figure 2. Concentration- and time-dependent bactericidal effect of rifampicin (RIF) towards low density cultures of Mtb BE-1585 (5.1×10^5 cfu/mL) and Mtb EAI-1627 (6.8×10^5 cfu/mL). Cultures were exposed to rifampicin at 2-fold increasing concentrations for 6 days at 37°C. After 1, 3 or 6 days of exposure subcultures on solid media were performed for cfu-counting. * = Due to complete outgrowth of the mycobacteria at 6 days of exposure aggregation had occurred and accurate cfu counting could not be performed.

densities of Beijing-1585 and EAI-1627 were investigated as described.[15] Rifampicin showed strong time- and concentration-dependent activity toward low-density cultures of the 2 strains (figure 2). Low concentrations of rifampicin were needed to achieve >99% Mtb killing; differences between Beijing-1585 and EAI-1627 were minor (table 2). However, to achieve 100% killing, especially for Beijing-1585, rifampicin concentrations had to be increased substantially (table 2). Compared with the low-density culture for Beijing-1585, a substantial increase in rifampicin concentrations was needed to achieve 100% killing of the high-density culture (table 2). This finding may be relevant in the clinical context because high-density mycobacteria populations are expected to exist in infected tissues of TB patients.

Rifampicin-resistant mutants did not emerge in low-density cultures of Beijing-1585 and EAI-1627. However, rifampicin-resistant mutants were selected at relatively high numbers from high-density Beijing-1585 cultures compared with high-density EAI-1627 cultures. In Beijing-1585 cultures, exposure to rifampicin concentrations of 2–32 mg/L selected resistant mutants only; this was not observed in EAI-1627 cultures. Analysis of rifampicin-resistant Beijing mutants showed the following altered *rpoB* gene sequences: CAC•GAC (H526D), CAC•TAC (H526Y), and TCG•TTG (S531L), as assessed by using the GenoType®MTBDR*plus* (Hain Lifescience, Nehren, Germany) assay (for details, see the Technical Appendix).

For 3 of the 4 anti-TB drugs, the difference in the range of mutant prevention concentrations for the Beijing and EAI genotype strains was small; isoniazid: 128–256 mg/L, RIF: 256–1,024 mg/L and MXF: 2–8 mg/L. The mutant prevention concentration for AMK was >1,024 mg/L for all strains tested.

Conclusions

We showed that the currently used anti-TB drug susceptibility assays do not discriminate between the *in vitro* susceptibility, as determined by the methods used in this study, of the Mtb Beijing and EAI genotype strains. We also showed that the determination of mutation frequencies might be more informative than results of anti-TB drug susceptibility assays. For rifampicin, mutation frequencies in Beijing genotype strains were high compared with those in EAI genotype strains, and the selection of rifampicin-resistant mutants among Beijing strains, but not EAI strains, occurred within a wide range of rifampicin concentrations. In addition, the killing capacity of rifampicin toward the Beijing genotype is dependent on the density of mycobacteria: high concentrations of rifampicin are required to achieve 100% killing of high-density Beijing genotype populations but not of high-density EAI genotype populations. These *in vitro* characteristics might contribute to the less favourable treatment outcome of Beijing genotype TB infections and their significant association with drug re-sistance. Our findings demonstrate the need for anti-TB drug treatments that will prevent

resistance among Mtb Beijing genotype TB cases, and they suggest that the development of genotype-specific TB therapy might be justified.

ACKNOWLEDGMENTS

TECHNICAL APPENDIX

Bacteria

The 10 Mtb strains used in this study were all clinical isolates from Vietnam of which five represented the Beijing genotype and five the East-African/Indian (EAI) genotype. Strains were stored at the National Tuberculosis Reference Laboratory (RIVM, Bilthoven, the Netherlands) as Beijing VN 2002-1585 (Beijing-1585), VN 2002-1607, VN 1998-2115, VN 1998-2121 and VN 1998-2145, and EAI VN 2002-1627 (EAI-1627), VN 2002-1606, VN 2002-1592, VN 2002-1596 and VN 1998-2113. A subculture of strain Beijing-1585 (known as strain VN+) was previously subjected to genome sequencing described by Schürch *et al.* (Infection, Genetics and Evolution 2011; 11:587–597). The Mtb strains in this study were selected on basis of their diverse genotyping results, as determined by using spoligotyping and IS6110 restriction fragment length polymorphism (RFLP) typing according to the internationally standardized methods (Kamerbeek *et al.* J Clin Microbiol. 1997; 35(4):907-14 and van Embden *et al.* J Clin Microbiol. 1993; 31(2):406-9). The genotypes of the strains were defined as either Beijing or EAI according to their characteristic spoligotypes, following the well-accepted genotype definitions described by Kremer *et al.* (J. Clin Microbiol. 2004; 42(9)4040-9) and Brudey *et al.* (BMC Microbiol. 2006; 6:6-23). Comparison of the five different RFLP patterns of the five Beijing strains of this study to those of Beijing strains that were subjected to single nucleotide polymorphism (SNP) typing previously performed by Schürch *et al.* (submitted for publication) showed that strains VN 2002-1585 and VN 1998-2121 represent the typical Beijing SNP type and that strains VN 2002-1607, VN 1998-2115, and VN 1998-2145 represent an intermediate Beijing SNP type. The EAI strains showed RFLP patterns with either two (VN 2002-1596) or one copy of IS6110. However, the four 1-copy strains could be discriminated on basis of the molecular weight of the IS6110 containing RFLP fragment and/or their spoligo pattern.

Cultures

Mtb suspensions were cultured in Middlebrook 7H9 broth (Difco Laboratories, Detroit, MI, USA), supplemented with 10% oleic acid-albumin-dextrose-catalase enrichment (OADC, Baltimore Biological Laboratories, Baltimore, MD, USA), 0.5% glycerol (Scharlau Chemie S.A, Sentmenat, Spain) and 0.05% Tween 20 (Sigma Chemical Co, St. Louis, MO, USA), under shaking conditions at 96 rpm at 37^0C. Vials with Mtb suspensions were stored at -80°C. Cultures on solid media were grown on Middlebrook 7H10 agar (Difco), supplemented with 10% OADC and 0.5% glycerol for 28-35 days at 37°C with 5% CO_2. The exact incubation time was dependent on the growth rate of the Mtb genotype strain investigated.

Anti-TB drugs

The anti-TB drugs assayed were isoniazid (Hospital Pharmacy; Rotterdam, The Netherlands), rifampicin (Rifadin®, Aventis Pharma B.V, Hoevelaken, The Netherlands), moxifloxacin (MXF,

Avelox®, Bayer Schering Pharma A.G, Berlin, Germany) and amikacin (AMK, Hospira Benelux BVBA, Brussels, Belgium). Dilutions of the drugs were prepared according to the recommendations of the manufacturers.

Susceptibility testing (MGIT)

The Mtb genotype strains were subjected to the MGIT drug susceptibility testing at the National Tuberculosis Reference Laboratory using the BACTEC MGIT-960 system™ (Becton, Dickinson and Company, Franklin Lakes, NJ, US) liquid culturing system for isoniazid, rifampicin, AMK and MXF susceptibility (Woods *et al.* National Committee for Clinical Laboratory Standards M24-A, volume 23; 2003; 18:1-69).

Minimal inhibitory concentration (MIC)

To determine the MIC of the Mtb genotype strains we used the agar proportion method as described by the Clinical and Laboratory Standards Institute (CLSI) (Woods *et al.* National Committee for Clinical Laboratory Standards M24-A, volume 23; 2003; 18:1-69). Colonies grown on solid media were suspended in broth using glass beads and vortexing during 4 min. The suspension was left for 30 minutes, after which the supernatant was taken and set to an optical density of McFarland standard 1. Using broth, a 1:10 dilution of this Mtb suspension was plated onto solid media containing serial, twofold dilution concentrations of anti-TB drug. After incubation the degree of growth was assessed. The MIC was defined as the lowest concentration of anti-TB drug that resulted in >99% growth inhibition. MIC determinations were performed in duplicate.

Mutation Frequency (MF)

Determination of the MF of the Mtb genotype strains was performed using the critical concentrations of the anti-TB drug, being 1 mg/L for isoniazid, 1 mg/L for rifampicin, 5 mg/L for amikacin and 1 mg/L for moxifloxacin, as defined by the CLSI (Woods *et al.* National Committee for Clinical Laboratory Standards M24-A, volume 23; 2003; 18:1-69) and Gumbo *et al.* (Antimicrob Agents Chemother. 2010; 54(4):1484-91). Starting from a high density (concentrated) Mtb culture (~1x10^{10} cfu), serial dilutions of the Mtb suspension were plated onto solid media without drugs and onto solid media containing the "critical concentration" of the respective anti-TB drugs. After incubation, the total numbers of colony forming units (cfu) and numbers of resistant mycobacteria were counted and the MF was calculated. MF were determined in duplicate. In order to assess the stability of the resistant mutants isolated from the anti-TB drug-containing solid media, 10 colonies were randomly picked and plated onto solid media without anti-TB drug. After incubation, these colonies were plated to check for re-growth on solid media containing the "critical concentration" of the same anti-TB drug.

Time-Kill Kinetics

For Beijing-1585 and EAI-1627 a time-kill kinetic assay for rifampicin was performed. The concentration- and time-dependent bactericidal activity of the anti-TB drug was determined as described previously (de Steenwinkel *et al*. J Antimicrob Chemother. 2010; 65(12):2582-9). In short, Mtb cultures at low density or at high density were exposed to rifampicin at 2-fold increasing concentrations, ranging from 0,5 µg/L to 256 mg/L for six days at 37⁰C. On days 1, 3 and 6, samples were taken for cfu counting provided that the Mtb suspension did not show visible aggregation.

Selection of drug resistant Mtb

During the time-kill kinetic assay for Beijing-1585 and EAI-1627 the selection of resistant mutants was performed. In order to detect drug-resistant Mtb in the low density or the high density cultures, the samples taken after six days of exposure to rifampicin were cultured on rifampicin-containing solid media. The concentration of rifampicin in the solid media was 4-fold the "critical concentration" (4 mg/L rifampicin). Resistant Mtb colonies, able to grow on this medium, were characterized using the GenoType® MTBDR*plus* assay (Hain Lifescience GmbH, Nehren, Germany), to detect the most common mutations in *rpoB* gene conferring rifampicin-resistance (J Clin Microbiol. 2007; 45(8):2635-40).

Mutant Prevention Concentration (MPC)

The MPC of the Mtb genotype strains was determined using the protocol as described by Drlica *et al*. (J Antimicrob Chemother. 2003; 52(1):11-7) and Goessens *et al*. (J Antimicrob Chemother. 2007; 59(3):507-16). In short, from a high density (concentrated) Mtb culture approximately 10^{10} cfu was plated onto solid medium containing 2-fold increasing concentrations of anti-TB drug, ranging from 64 mg/L to 1024 mg/L for isoniazid, rifampicin or amikacin and from 1 mg/L to 32 mg/L for moxifloxacin. The MPC was defined as the lowest concentration of anti-TB drug in the solid medium, which prevented growth of Mtb.

REFERENCES

1. World Health Organization. Multidrug and extensively drug-resistant TB (M/XDR-TB): 2010 global report on surveillance and response. WHO Library Cataloguing-in-Publication Data 2010.

2. European Concerted Action on New Generation Genetic M, Techniques for the E, Control of T. Beijing/W genotype *Mycobacterium tuberculosis* and drug resistance. Emerg Infect Dis 2006; 12: 736-43.

3. Parwati I, van Crevel R, van Soolingen D. Possible underlying mechanisms for successful emergence of the *Mycobacterium tuberculosis* Beijing genotype strains. Lancet Infect Dis 2010; 10:103-11.

4. Buu TN, Huyen MN, Lan NN *et al. Mycobacterium tuberculosis* genotype and case notification rates, rural Vietnam, 2003-2006. Emerg Infect Dis 2009; 15:1570-7.

5. Buu TN, Huyen MN, Lan NT *et al.* The Beijing genotype is associated with young age and multidrug-resistant tuberculosis in rural Vietnam. Int J Tuberc Lung Dis 2009; 13:900-6.

6. van der Spuy GD, Kremer K, Ndabambi SL *et al.* Changing *Mycobacterium tuberculosis* population highlights clade-specific pathogenic characteristics. Tuberculosis (Edinb) 2009; 89:120-5.

7. Anh DD, Borgdorff MW, Van LN *et al. Mycobacterium tuberculosis* Beijing genotype emerging in Vietnam. Emerg Infect Dis 2000; 6:302-5.

8. Cowley D, Govender D, February B *et al.* Recent and rapid emergence of W-Beijing strains of *Mycobacterium tuberculosis* in Cape Town, South Africa. Clin Infect Dis 2008; 47:1252-9.

9. Lan NT, Lien HT, Tung le B *et al. Mycobacterium tuberculosis* Beijing genotype and risk for treatment failure and relapse, Vietnam. Emerg Infect Dis 2003; 9:1633-5.

10. Hershberg R, Lipatov M, Small PM *et al.* High functional diversity in *Mycobacterium tuberculosis* driven by genetic drift and human demography. PLoS Biol 2008; 6:e311.

11. Woods GL, Brill MR, Brown-Elliot BA *et al.* Susceptibility testing of mycobacteria, nocardiae, and other aerobic actinomycetes. Approved standard-second edition. Clinical and Laboratory Standards Institute 2011; M24-A2, volume 26: 1-61.

12. Gumbo T. New susceptibility breakpoints for first-line antituberculosis drugs based on antimicrobial pharmacokinetic/pharmacodynamic science and population pharmacokinetic variability. Antimicrob Agents Chemother 2010; 54:1484-91.

13. Ebrahimi-Rad M, Bifani P, Martin C *et al.* Mutations in putative mutator genes of *Mycobacterium tuberculosis* strains of the W-Beijing family. Emerg Infect Dis 2003; 9:838-45.

14. Werngren J, Hoffner SE. Drug-susceptible *Mycobacterium tuberculosis* Beijing genotype does not develop mutation-conferred resistance to rifampicin at an elevated rate. J Clin Microbiol 2003; 41:1520-4.

15. de Steenwinkel JE, de Knegt GJ, ten Kate MT *et al.* Time-Kill Kinetics of anti-tuberculosis drugs, and emergence of resistance, in relation to metabolic activity of *Mycobacterium tuberculosis*. J Antimicrob Chemother 2010; 65:2582-9.

Chapter 10

Consequences of non-compliance on therapy efficacy and emergence of resistance in murine tuberculosis caused by the Beijing genotype

J.E.M. de Steenwinkel, M.T. ten Kate, G.J. de Knegt, H.A. Verbrugh, R.E. Aarnoutse, M.J. Boeree, M.A. den Bakker, D. van Soolingen, I.A.J.M. Bakker-Woudenberg

ABSTRACT

Despite great effort of health organizations worldwide in fighting tuberculosis (TB), morbidity and mortality is not declining as expected. One of the reasons is related to the evolutionary development of *Mycobacterium tuberculosis* (Mtb), in particular the Beijing genotype strains.

In a previous study, we showed the association between Beijing genotype and an increased mutation frequency for rifampicin. In this study we use a Beijing genotype strain and an East-African/Indian genotype strain, to investigate in our mouse TB model whether the higher mutation frequency observed in a Beijing genotype strain is associated with treatment failure particularly during non-compliance therapy.

Both genotype strains showed a high virulence in comparison to Mtb strain H37Rv, resulting in a highly progressive infection with rapid lethal outcome in untreated mice. Full-compliance treatment was effective without relapse of TB irrespective the infecting strain, showing similar decrease of Mtb load in infected organs, and similar histopathological changes. Non-compliance treatment, simulated by a reduced duration and dosing frequency resulted in relapse of infection. Relapse rates were correlated with the level of non-compliance and were identical for Beijing infection and East-African/Indian infection. However, in only Beijing-infected mice isoniazid-resistant mutants were selected at the highest level of non-compliance. This is in line with the substantial selection of isoniazid-resistant mutants *in vitro* in a wide isoniazid concentration window observed for the Beijing strain and not for the EAI strain.

These results suggest that genotype diversity of Mtb may be involved in emergence of resistance and indicates that genotype-tailor-made treatment should be investigated.

INTRODUCTION

Resistance to anti-tuberculosis (TB) drugs is rapidly emerging worldwide [1] with nearly half a million cases of multidrug resistant TB (MDR-TB) recorded annually. The majority of MDR-TB is found in Former Soviet Union States and Asia.[1] The true magnitude of resistance problem may be much greater, as in most high TB prevalence settings laboratory service is underdeveloped and resistance cannot be adequately detected. Moreover, in almost all countries worldwide, extensively drug resistant TB (XDR-TB) has also been reported [2] and there are already publications on the emergence of totally drug resistant TB (TDR-TB), e.g. in Iran and India.[3] Because only a minority of MDR-TB cases can currently be treated according to the guidelines of the WHO, resistant TB may increasingly become an untreatable disease, although there is hope that new drugs may force a major improvement in this situation within some years.[4]

There are multiple factors known that underlie the development of resistance to anti-TB drugs, like unregulated availability of anti-TB drugs, poor quality of drugs, unprofessional prescription, non-compliance, malabsorption in certain subpopulations and large inter-individual variability in pharmacokinetics of anti-TB drugs, and host genetic factors. The combination and/or relative impact of factors that eventually lead to resistance emergence are not well understood. However, non-compliance is generally considered to be the most relevant factor leading to resistance in TB treatment.[1, 5-6] A recent addition to the determinants of resistance is a bacterial one. Particular strains seem more prone to develop resistance and/or be transmitted as MDR-TB. For instance, at multiple geographical sites, the Beijing genotype has been correlated with MDR and XDR-TB.[7-8] In Europe Beijing strains are significantly associated with transmission of resistance.[9-10] But also in Vietnam, Beijing strains have been correlated with MDR-TB, treatment failures and relapses after initially curative treatment in multiple studies.[11-13] Whereas the East-African/Indian (EAI) genotype strains are not associated with these problems. Still both Beijing and EAI genotypes are predominant in Vietnam, both lineages cause about 40% of the TB cases. For this reason, in a recent study we selected strains of these both lineages and compared their intrinsic *in vitro* susceptibility and determined their mutation frequency regarding the development of resistance to four different anti-TB drugs.[14] The results revealed that for the Beijing genotype bacteria a much higher dosage of rifampicin was required to achieve a 100% killing and that two out of five Beijing strains exhibit a remarkably high frequency of mutations conferring rifampicin resistance.[14] These data underline the importance of the use of different Mtb strains in preclinical experimental studies using animal models, as stated by de Groote *et al.* [15] They recommend the use of different Mtb strains in the confirmation of treatment efficacy results of novel drugs in the translational phase, in order to strengthen the likelihood of success of novel drug regimens that advance forward into clinical trials.[15]

In the present paper we studied the impact of non-compliance and the role of Mtb strains as risk factors for the emergence of resistance to TB treatment. More specifically, we investigated in a well-established mouse TB model [16] whether the consequences of suboptimal treatment, simulating non-compliance in patients, would be more pronounced in the outcome of TB caused by a Beijing genotype strain in comparison to TB caused by an EAI genotype strain. The results obtained may help explanation the large differences in treatment success in Vietnam in patients infected by Beijing versus those infected by EAI genotype bacteria.

MATERIALS AND METHODS

Bacterial strain

The two Mtb strains used were clinical isolates obtained from Vietnam one of the Beijing genotype and one of the EAI genotype, as described previously.[14] The strains were provided by the National Tuberculosis Reference Laboratory (Bilthoven, the Netherlands), where they were labelled as Beijing VN 2002-1585 (Beijing-1585) and EAI VN 2002-1627 (EAI-1627) and were cultured as described previously.[17]

Infection model

Specified pathogen-free female BALB/c mice were obtained from Charles River [Les Oncins, France]. The experimental protocols adhered to the rules specified in the Dutch Animal Experimentation Act (1977) and the published Guidelines on the Protection of Experimental Animals by the Council of the EC (1986). The Institutional Animal Care and Use Committee of the Erasmus MC Rotterdam approved the present protocols. Mice were infected through intratracheal inoculation followed by inhalation, as described previously.[16] The inoculum of Mtb used for infection contained 1.3×10^5 cfu [range $1.2 - 1.3 \times 10^5$] of Beijing-1585 and 0.6×10^5 cfu [range $0.5 – 0.7 \times 10^5$] of EAI-1627.

Drug dosing and anti-TB treatment

The mice receiving compliance therapy were treated with dosage and schedules of anti-TB drugs derived from current clinical guidelines. Isoniazid (Hospital Pharmacy; Rotterdam, The Netherlands), rifampicin (Rifadin®, Aventis Pharma B.V, Hoevelaken, The Netherlands) and pyrazinamide [150 mg/kg; P7136, Sigma Chemical Co, St. Louis, MO] were administered in human pharmacokinetic-equivalent doses, as described previously.[16] Treatment was started at 2 weeks after infection. The duration of full-compliance treatment was 26 weeks, consisting of a 9-week initial phase followed by 17-week continuation phase. During the initial phase, animals received a combination of isoniazid [25 mg/kg], rifampicin [10 mg/kg] and pyrazinamide [150 mg/kg]. In the continuation phase, animals received isoniazid and rifampicin. Agents were administered subcutaneously once daily, five days per week. In

the non-compliance treatment drugs were administered for treatment duration of only 13 weeks (9 weeks isoniazid, rifampicin and pyrazinamide, followed by 4 weeks of isoniazid and rifampicin), simulating premature discontinuation in patients (defaulting). Also underdosing was simulated by applying a reduced frequency of dosing; mice received treatment either five days per week, or three days per week, or once a week. In the non-compliance treatment, the daily doses were identical to the compliance treatment.

Therapeutic efficacy

Parameters for therapeutic efficacy were (1) Mtb load in pulmonary and extra-pulmonary organs and emergence of drug resistance, (2) clinical signs of illness of mice, (3) relapse of infection during the 3 months post-treatment period, (4) histopathological characterization in the infected organs and (5) cytokine concentrations in blood. Treatment success was defined as elimination of the Mtb load from infected organs and prevention of TB relapse after 13 weeks post-treatment.

Therapeutic efficacy – Mtb load in pulmonary and extra-pulmonary organs and emergence of drug resistance

At indicated time points the Mtb load in infected organs was assessed. Mice (n=4 per time point) were sacrificed by CO_2 exposure. Subsequently, lung, spleen and liver were removed aseptically and homogenized each in 2 mL PBS, samples were centrifuged and washed with PBS to prevent carry-over of anti-TB drugs. From the undiluted tissue homogenate and 10-fold serial dilutions samples of 200 µl were plated onto 7H10 agar. To detect the presence of drug-resistant Mtb mutants, subcultures on rifampicin-containing or isoniazid-containing plates were also performed. The concentrations of rifampicin and isoniazid in the subculture plates were 4-fold the "critical concentration", i.e. 4 mg/L for rifampicin and 0.8 mg/L for isoniazid.[18] Colonies of drug-resistant Mtb were characterized using the GenoType® MTBDR*plus* assay (Hain Lifescience GmbH, Nehren, Germany), to detect the most common mutations.[19]

THERAPEUTIC EFFICACY – CLINICAL SIGNS OF ILLNESS OF MICE

The behaviour of mice was monitored daily, as prescribed by the animal ethical committee. Clinical parameters were the body weight assessed 3 times per week and evaluation of a discomfort score was performed 5 times per week. Mice that displayed severe signs of illness were euthanized by CO_2 exposure.

### Therapeutic efficacy – relapse of infection

Mtb load in the lung, spleen and liver of mice (n=4) were assessed 13 weeks after termination of TB treatment. Relapse was defined as Mtb-positive organ cultures, while immediately after termination of treatment organ cultures were Mtb-negative. Emerging drug-resistant Mtb mutants were characterized.

### Therapeutic efficacy – histopathological changes of infected organs

Lung, spleen and liver from sacrificed animals (n=3) at indicated time points (at weeks 1 and 2 of the untreated infection, at weeks 3, 5, 7, 15 and 28 during treatment and in weeks 28 and 41 post-treatment) were processed as described previously.[16] In brief, standard 4 μm haematoxylin-eosin stained sections were prepared from ethanol fixed, paraffin wax embedded lung, spleen and liver tissues. Additionally, a Ziehl-Neelsen staining was performed to detect acid-fast bacilli. Histopathological analysis was performed on tissues from untreated infected mice, from infected mice receiving compliance treatment and from mice receiving non-compliance treatment once per week for 13 weeks.

Therapeutic efficacy – cytokine levels in blood

Blood samples were obtained by cardiac puncture from mice at week 2 (start treatment), from compliance treated mice at week 28 and 41 and from non-compliance treated mice (treatment once dose a week for 13 weeks) at week 15 and 28. Plasma samples were prepared from EDTA-blood. Quantification of cytokines was performed using a bead-based flow cytometry technique (xMap; Luminex Corporation, Austin, TX, USA). A milliplex map mouse cytokine, 31-plex was used (Millipore Corporation, Billerica, MA, USA) consisting of bead-labelled cytokine receptor against the following biomarkers; Eotaxin, G-CSF, GM-CSF, IFN-γ, IL-10, IL-12 (p40), IL-12 (p70), IL-13, IL-15, IL-17, IL-1α, IL-1β, IL-2, IL-2, IL-4, IL-5, IL-6, IL-7, IP-10, KC-like, LIF, LIX, M-CSF, MCP-1, MIG, MIP-1α, MIP-1β, MIP-2, RANTES, TNF-α and VEGF. Tests were performed according the manufacturers' protocol. Samples were tested in duplicate. Results in median fluorescence intensity (MFI) values were converted to pg/mL using MILLIPLEX Analyst software (Millipore) and subsequently averaged.
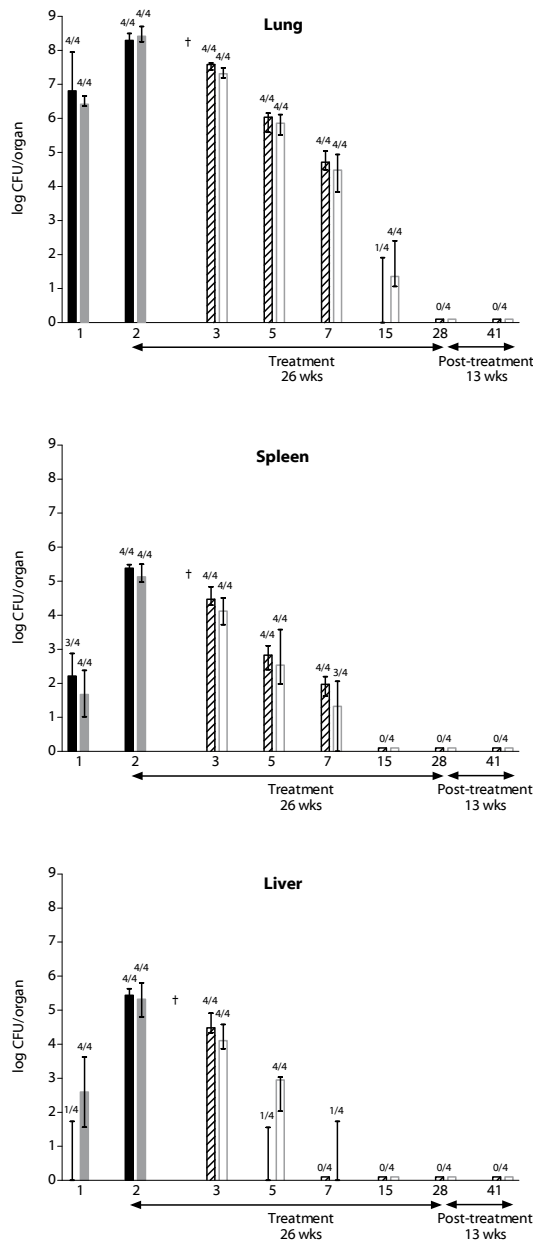
Figure 1. TB infection and efficacy of compliance treatment in mice infected with Beijing-1585 or EAI-1627. The mycobacterial load in lung, spleen and liver of the untreated mice, infected with Beijing-1585 (black bars) or EAI-1627 (gray bars). Mice receiving therapy started 2 weeks after infection and continued for 26 weeks are indicated for the BE-1585 (diagonally stripped bars) and for the EAI-1627 (open bars). Results are expressed as median ± range (error bars) of the colony forming units (CFU) per organ, n = 4 per time point. Numbers above bars are the numbers of culture-positive mice out of total numbers of mice at that time point. † = 4 out of 4 untreated mice died due to TB infection before this time point.
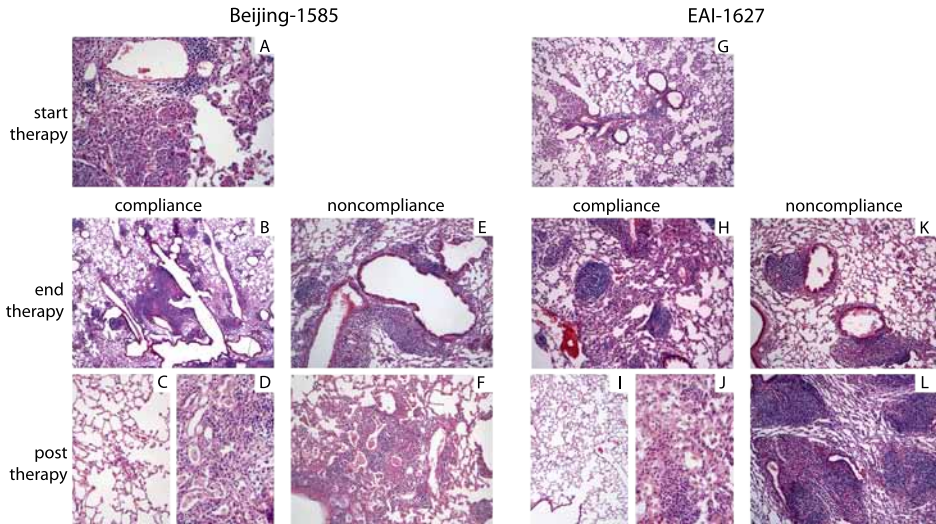
Figure 2. Histology. Lung tissue from mice infected with Beijing-1585 or EAI-1627. **(A-E)** mice infected with Beijing-1585. **(F-J)** mice infected with EAI-1627. **(A, F)** week 2, start of treatment. **(B, G)** week 28, end of compliance treatment. **(D, I)** week 15, end of non-compliance (once per week) treatment. **(C, H)** week 41, 13 weeks post-compliance treatment. **(E, J)** week 28, 13 weeks post-non-compliance (once per week) treatment. **(A)** (original magnification 100x)**:** Extensive intra-alveolar accumulation of histiocytes is observed, with a peri-bronchiolar lymphocytic component. [Ziehl-Neelsen (ZN) staining revealed numerous acid-fast bacilli; not shown] **(B)** (25x)**:** Peri-bronchiolar infiltrates, predominantly composed of lymphocytes are seen, admixed with a minor histiocytic component. **(C)** (50x)**:** Scattered sparse lymphocytic foci are observed. **(D)** (50x)**:** A moderately dense peri-bronchiolar predominantly lymphocytic infiltrate is present, no intra-alveolar or interstitial inflammation is seen. **(E)** (100x)**:** A combination of an intra-alveolar histiocytic infiltrate is present with a moderately dense peri-bronchiolar lymphocytic component; the pattern is similar, however less extensive to the pattern observed in **(A)**. [Sparse acid-fast bacilli are observed in ZN staining]. **(F)** (50x)**:** Intra-alveolar histiocytes are seen with a centri-lobular distribution, combined with a minor lymphocytic component. [ZN staining reveal numerous acid-fast bacilli; not shown]. **(G)** (50x)**:** A mild to moderately dense lymphocyte predominant infiltrate is present; a mild increase in alveolar macrophages is also seen. **(H)** (50x)**:** Moderate to dense peri-bronchiolar infiltrates are present, mainly composed of lymphocytes. **(I)** (50x)**:** A mild to moderately dense peri-bronchiolar lymphocytic infiltrate is present. **(J)** (25x)**:** A dense lympho-histiocytic infiltrate is present. [Sparse acid-fast bacilli are observed in ZN staining].

RESULTS

Course of untreated TB infection

As shown in figure 1, progressive TB infection caused by Beijing-1585 or EAI-1627 in untreated mice resulted in similar Mtb load in the lung from week 1 after infection, which increased at week 2 up to 8.7×10^7 [0.6 - 1.4×10^8] cfu Beijng-1585 and 1.2×10^8 [0.8 - 2.2×10^8] cfu EAI-1627. In the third week of untreated infection caused by either strain all mice died or became moribund, as evidenced by their discomfort score and body weight loss (data not shown).

At week 2 histological analysis of lung tissue from untreated mice infected with either strain showed predominantly centrilobular inflammatory infiltrates composed of lymphocytes and histiocytes. The infiltrates were dense and located within the alveoli, sparing the interstitium (figure 2A and 2F). No differences were observed between the Beijing-1585 or EAI-1627-infected mice at this stage.

Cytokine profile in plasma at week 2 revealed no significant different levels in any of the cytokines between mice infected with Beijing-1585 and mice infected with EAI-1627. In both infections the levels of IL-17, IP-10, MIG, TNF-α and IFN-γ were elevated compared to uninfected mice (data not shown). As untreated mice died in week 3, their cytokine levels could not be assessed at later time points. Therefore the dynamics of these cytokines in untreated infections could not be assessed further.

Therapeutic efficacy of compliance treatment

As shown in figure 1, the therapeutic efficacy of compliance treatment as measured by decreases in Mtb load was similar for the Beijing-1585-infected mice and the EAI-1627-infected mice. The liver was the first organ that became culture-negative, followed by the spleen and finally the lung. After 26 weeks of treatment all organs of the Beijing-1585 and EAI-1627 infected mice were culture-negative. Importantly, drug-resistant Mtb mutants were never selected from these mice receiving full compliance treatment.

Relapse assessment after the additional 13 weeks post treatment period, revealed that relapses of infection did not occur. From 2-4 weeks of treatment onwards, the discomfort score and weight of the mice in both Beijing-1585 and EAI-1627-infected mice were at the level of the uninfected control mice (data not shown).

During full-compliance treatment, lung tissue from the mice infected with Beijing-1585 initially showed an increase of compact fields of epithelioid histiocytes, which in later stages decreased in intensity (figure 2B). Almost complete resolution at week 41 (26 weeks therapy followed by 13 weeks post-treatment) with only sparse peri-bronchiolar infiltrates was ob-

Beijing-1585 genotype

EAI-1627 genotype
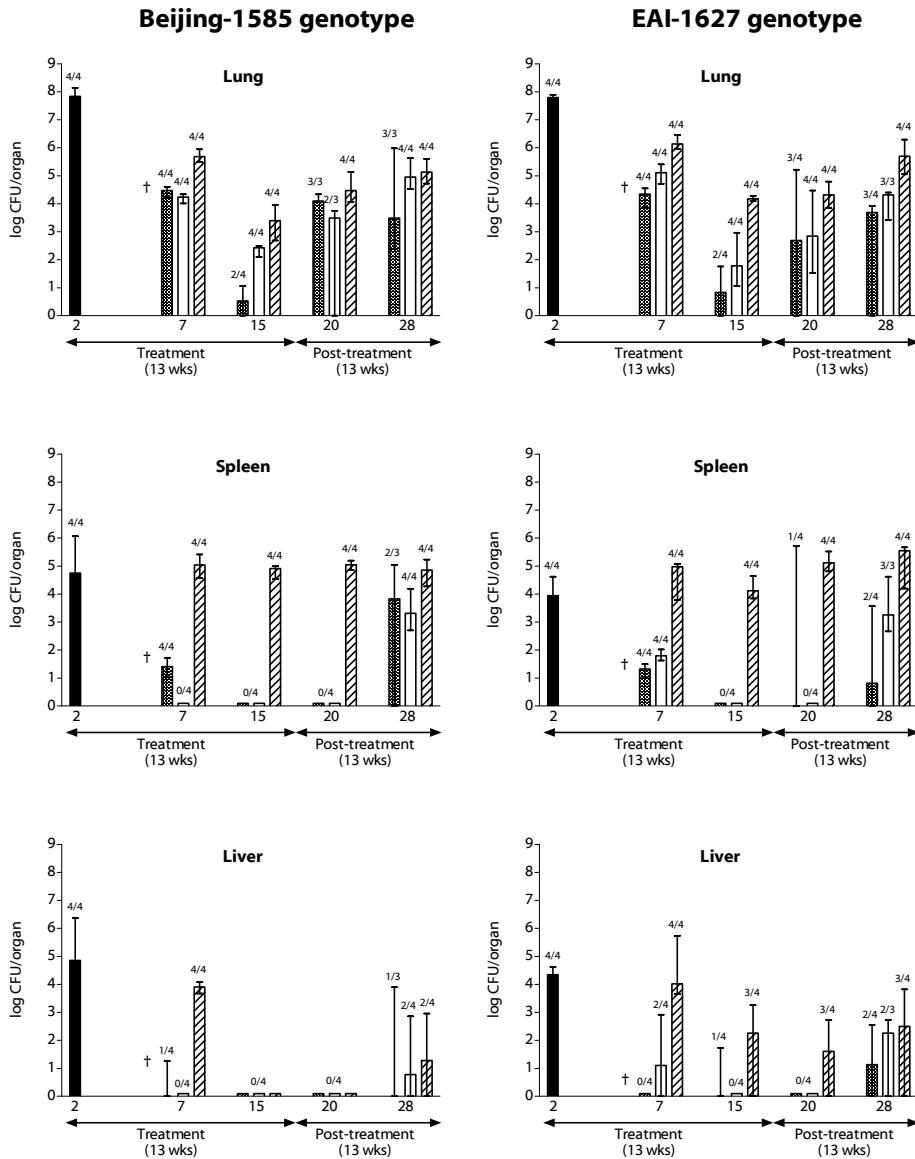
Figure 3. TB infection and efficacy at non-compliance treatment in mice infected with Beijing-1585 or EAI-1627. The mycobacterial load in lung, spleen and liver of the untreated mice (black bars). Therapy started 2 weeks after infection continued for 13 weeks. Mice received treatment five times per week (chequered bars), three times per week (open bars) or once per week (diagonally stripped bars). Results are expressed as medians ± range (error bars) of the colony forming units (CFU) per organ, n = 4 per time point. Numbers above bars are the numbers of culture-positive mice out of total numbers of mice at that time point. † = 4 out of 4 untreated mice died due to TB before this time point.

served. Mice infected with EAI-1627 (figure 2H) showed essentially similar histopathological characteristics as the Beijing-1585-infected mice (figure 2C). During full-compliance treatment the infiltrate diminished to a mild peri-bronchiolar exclusively lymphocytic pattern (figure 2G).

Cytokine profile in plasma during the course of Beijing-1585 infection or EAI-1627 infection showed elevated levels of IL-17, IP-10, MIG, TNF-α and IFN-γ at week 2, which decreased upon start therapy. After 13 weeks of therapy, the levels of these 5 cytokines were back to baseline. No differences in cytokine patterns or the height of the cytokine levels were observed when comparing the Beijing-1585 with EAI-1627 infected mice (data not shown). In the 13 weeks post-treatment period, the cytokines patterns did not change compared to week 28 (end of treatment, data not shown).

Therapeutic efficacy at non-compliance treatment

The non-compliance treatment of mice consisted of only 13 weeks treatment at various dosing frequencies. Results are shown in figure 3. Treatment for five days per week resulted in relapse of infection in all Beijing-1585-infected and EAI-1627-infected mice at 13 weeks post-treatment. At the end of treatment (week 15) half of the mice were Mtb culture-negative in the lung (two out of four mice, for both Beijing-1585 and EAI-1627). However, at 13 weeks post-treatment all mice relapsed and the Mtb load in the lung was 1.4×10^3 [$1.1 \times 10^2 – 4.2 \times 10^5$] cfu Beijing-1585 and 2.2×10^3 [$0 – 3.7 \times 10^3$] cfu EAI-1627 at week 28. Reduction of treatment frequency to 3 days per week resulted in Mtb culture-positive lungs after 13 weeks of treatment in all Beijing-1585-infected and all EAI-1627-infected mice, whereas the spleen- and liver cultures were negative. The Mtb load in the lung at the end of treatment (week 15) was 1.2×10^2 [$0.6 – 1.4 \times 10^2$] cfu Beijing-1585 and 28 [$5 – 4.0 \times 10^2$] cfu EAI-1627. At 13 weeks post-treatment all mice showed regrowth of Mtb, resulting in a Mtb load in the lung of 3.9×10^4 [$0.2 – 1.9 \times 10^5$] cfu Beijing-1585 and 9.0×10^3 [$0.1 – 1.1 \times 10^4$] cfu EAI-1627 at week 28. Finally, treatment of mice once per week revealed culture-positive lungs and spleens after 13 weeks in all Beijing-1585-infected and all EAI-1627-infected mice. The Mtb load in the lung at the end of treatment (week 15) was 1.7×10^3 [$0.2 – 4.0 \times 10^3$] cfu Beijing-1585 and 6.5×10^3 [$5.4 – 8.3 \times 10^3$] cfu EAI-1627. After the 13 weeks post-treatment period all mice showed relapse of infection, resulting in a Mtb load in the lung of 6.2×10^4 [$0.2 – 1.8 \times 10^5$] cfu Beijing-1585 and 2.7×10^5 [$0.5 – 8.6 \times 10^5$] cfu EAI-1627 at week 28. Mice receiving the non-compliance treatment once per week showed a very high Mtb load throughout the entire course of infection, especially in the spleen. During non-compliance treatment significant differences in the efficacy of any treatment modality were not observed between the Beijing-1585-infected and EAI-1627-infected mice.

Remarkably, only in the Beijing-1585-infected mice, receiving non-compliance treatment once per week for 13 weeks isoniazid-resistant Mtb mutants were selected from lungs and

spleens of all mice, at week 20 and week 28. Isoniazid-resistant mutants at week 20 repre-sented 2.2% [range, 0.3-6.4] of the total Mtb load in the lung, and 1.9% [0.7-2.6] of the Mtb load in the spleen. At week 28, isoniazid-resistant Mtb mutants represented, 1.7% [1.2-3.4] in the lung and 5.1% [3.4-18.5] in the spleen. In the livers selection of resistant Mtb mutants was not observed. The selection of resistance was not observed in Beijing-1585-infected mice receiving non-compliance treatment three times per week or five-times per week for 13 weeks nor in any of the EAI-1627-infected mice receiving non-compliance treatment. Further analysis of the isoniazid-resistant Mtb mutants selected from the lung at week 20 and week 28 showed that the minimal inhibitory concentration of isoniazid was 128 mg/L. Genotypic analysis revealed no mutations in the *katG* or *inhA* genes.

Lung tissue of mice infected with Beijing-1585 and receiving non-compliance treatment once per week, initially showed a minor lymphocytic infiltrate (week 15) without epithelioid histiocytes (figure 2D), which became more dense at week 28 and was associated with a mild histiocytic component (figure 2E). In the EAI-1627-infected mice receiving the same non-compliance treatment, the infiltrate initially decreased at week 15 (figure 2I) but became more widespread and denser at week 28 (figure 2J).

Cytokine levels in plasma from mice during the non-compliance treatment once per week showed that the levels were similar to that of the mice receiving full-compliance treatment. However, during the relapse of infection the cytokines IP-10, MIG and TNF-α reappeared above the base-line level (data not shown). The cytokine levels of Beijing-1585-infected and EAI-1627-infected animals were highly similar.

DISCUSSION

From previous studies in Vietnam, it is known that TB patients infected with an Mtb Beijing genotype strain have a poorer outcome than patients infected with an EAI genotype strain. However, no satisfactory explanation for this observed phenomenon is yet available. Recently, we have shown in *in vitro* studies that Beijing genotype strains have an increased mutation frequency for rifampicin, compared to EAI genotype strains.[14] Also a relatively large window of rifampicin concentrations within which rifampicin resistant Mtb mutants were selected, was observed in the Beijing genotype. In the present study it is investigated whether the high mutation frequency for rifampicin observed in only Beijing genotype strains is associated with treatment failure in Beijing infection. We compared the treatment efficacy in a mouse model of TB caused by the Beijing-1585 strain or the EAI-1627 strain. The mutation frequency for rifampicin in Beijing-1585 and EAI-1627 strain were 3.7×10^{-3} and 3.5×10^{-6}, respectively.[14]

The genotype of Mtb may influence different aspects of the infection. One hypothesis is that the Beijing genotype strain might exhibit mechanisms that modulate the immune response by the host; as such having an advantage over other Mtb strains.[20-21] Elaborating on this hypothesis, when mass vaccination with the bacillus Calmette-Guérin (BCG) was introduced in TB endemic areas, the Beijing genotype could use this advantage over other strains and spread more easily.[20] In the present study in unvaccinated mice, a potential advantage of the Beijing genotype over the EAI genotype was not observed. It was shown that both Beijing-1585 and EAI-1627 are equal in pathogenic capacity in the progression of TB. In both infections the untreated animals died or became moribund within 3 weeks after infection. Also a similar increase in Mtb load in infected organs during the first two weeks was observed. In addition, the histopathological damage inflicted was equivalent and the changes in cytokine levels during the course of untreated infection were similar for both strains. Moreover, the cytokine profile of both strains were in line with previously described cytokine levels in our murine TB model caused by the Mtb strain H37Rv.[22] The H37Rv strain is a clinical isolate and nowadays the strain most commonly used in studies *in vitro* as well as in animal models. Nonetheless, the Beijing-1585 and EAI-1627 strains show an increased virulence in the course of TB compared to the H37Rv strain. In a previous study, we showed that H37Rv-infected mice survived for at least 22 weeks.[16] The increased virulence of the Beijing genotype is in accordance with previously described studies [8, 23-24] The high virulence of the EAI genotype in our mouse TB model is consistent with the fact that EAI strains, similar to the Beijing strains, do very frequently cause disease in Vietnam (40% of the TB patients).[11, 13] In contrast to the Beijing strains, the EAI-strains in Vietnam are negatively correlated with resistance, and in the previous studies [14] and the present study in mice we found clues to explain this.

A very prominent observation is that the treatment efficacy in conditions mimicking compliance is similar for Beijing-1585-infected and EAI-1627-infected mice; both Mtb load in infected organs

and cytokine levels in blood were equivalent. This finding suggests that if treatment is applied adequately therapy should be successful without differences in causative infecting strain. Another factor contributing to the emergence of MDR-TB might be variability in pharmacokinetics of anti-TB drugs among patients. Gumbo *et al.* predicted in their hollow fiber studies for both bactericidal and sterilizing effect, that approximately 1% of TB patients with full-compliance therapy would still develop MDR-TB due to interindividual variability in pharmacokinetics of anti-TB drugs, causing low drug concentrations in a subset of patients.[25] The variability in pharmacokinetics is less distinct in inbred mice as used in our TB-model. As a consequence differences in pharmacokinetics of anti-TB drugs could not be investigated in the present study.

The consequences of non-compliance were mimicked in the present study to evaluate this relevant factor in the emergence of resistance in TB treatment. It was demonstrated that an increasing level of non-compliance led to reduced Mtb killing in the lung, as well as the spleen and liver at the end of the 13 weeks treatment period. The compliance-dependent results obtained in Beijing-infected and EAI-infected mice are strikingly identical. The only difference found between with Beijing-1585 infection and the EAI-1627 infection was the selection of isoniazid-resistant Mtb mutants. These resistant mutants were selected only in the Beijing infection and only in mice relapsing from the most severe non-compliance condition (once per week treatment). In EAI-infected mice at non-compliance condition resistant mutants Mtb were never found, although treatment response at non-compliance condition was similar in EAI infection and Beijing infection. Similar observational data are obtained in clinical studies in endemic areas [11-13]. As a result the present model could serve in future studies to further unravel the mechanism(s) by which Beijing genotype strains facilitate the selection of resistant mutants. Whereas, in a previous *in vitro* study we showed that the Beijing genotype strains exhibit an increased mutation frequency for rifampicin,[14] in Beijing infection *in vivo* no selection of rifampicin-resistant mutants was observed. In contrast, isoniazid-resistant mutants were found. Given the fact that in patients isoniazid-resistance is most often observed and is regarded as precursor for MDR-TB, our *in vivo* results are well in line with clinical reality. Possibly, an increase in isoniazid dosage could prevent the selection of isoniazid-resistant Beijing mutants, and thereby prevent the formation of MDR-TB. Further studies to explore this hypothesis are needed.

In conclusion, this study shows that the genotypic diversity of Mtb in terms of selection of resistant mutants occurred not only *in vitro* but also in our *in vivo* mouse TB model. Resistant Mtb mutants were selected only in Beijing-infected mice during severe non-compliance treatment. This might justify genotype-tailor-made therapy.

REFERENCES

1. WHO. Global tuberculosis control 2011, Annual Report WHO. WHO Library Cataloguing-in-Publication Data 2011:1-258

2. WHO. Towards universal access to diagnosis and treatment of multidrug-resistant and extensively drug-resistant tuberculosis by 2015, WHO progress report 2011. WHO Library Cataloguing-in-Publication Data 2011:1-127

3. Velayati A, Masjedi M, Farnia P. *et al.* Emergence of new forms of totally drug-resistant tuberculosis bacilli: super extensively drug-resistant tuberculosis or totally drug-resistant strains in iran. Chest 2009; 136:420-5

4. Ginsberg A. Drugs in development for tuberculosis. Drugs 2010; 70: 2201-14.

5. Sharma S, Mohan A. Multidrug-resistant tuberculosis: a menace that threatens to destabilize tuberculosis control. Chest 2006; 130:261-72

6. van den Boogaard J, Boeree M, Kibiki G. *et al.* The complexity of the adherence-response relationship in tuberculosis treatment: why are we still in the dark and how can we get out? Trop Med Int Health 2011; 16:693-8

7. European Concerted Action on New Generation Genetic M, Techniques for the E, Control of T. Beijing/W genotype *Mycobacterium tuberculosis* and drug resistance. Emerg Infect Dis 2006; 12:736-43

8. Parwati I, van Crevel R, van Soolingen D. Possible underlying mechanisms for successful emergence of the *Mycobacterium tuberculosis* Beijing genotype strains. Lancet Infect Dis 2010; 10:103-11

9. Devaux I, Kremer K, Heersma H. *et al.* Clusters of multidrug-resistant *Mycobacterium tuberculosis* cases, Europe. Emerg Infect Dis 2009; 15:1052-60

10. Devaux I, Manissero D, Fernandez de la Hoz K. *et al.* Surveillance of extensively drug-resistant tuberculosis in Europe, 2003-2007. Euro Surveill 2010; 15

11. Buu T, Huyen M, Lan N. *et al.* The Beijing genotype is associated with young age and multidrug-resistant tuberculosis in rural Vietnam. Int J Tuberc Lung Dis 2009; 13:900-6

12. Duong D, Nguyen T, Nguyen T. *et al.* Beijing genotype of *Mycobacterium tuberculosis* is significantly associated with high-level fluoroquinolone resistance in Vietnam. Antimicrob Agents Chemother 2009; 53:4835-9

13. Lan N, Lien H, Tung le B. *et al. Mycobacterium tuberculosis* Beijing genotype and risk for treatment failure and relapse, Vietnam. Emerg Infect Dis 2003; 9:1633-5

14. de Steenwinkel J, ten Kate M, de Knegt G. *et al.* The worldwide problem of multidrug resistant tuberculosis may be related to lower intrinsic susceptibility of Beijing genotype strains to anti-tuberculosis drugs. Emerg Infect Dis 2012; In press

15. de Groote M, Gruppo V, Woolhiser L. *et al.* Importance of Confirming *in vivo* Efficacy Data of Novel Antibacterial Drug Regimens against Various Strains of *Mycobacterium tuberculosis*. Antimicrob Agents Chemother 2011

16. de Steenwinkel J, de Knegt G, Ten Kate M. *et al.* Immunological parameters to define infection progression and therapy response in a well-defined tuberculosis model in mice. Int J Immuno-pathol Pharmacol 2009; 22:723-34

17. de Steenwinkel J, de Knegt G, ten Kate M. *et al.* Time-Kill Kinetics of anti-tuberculosis drugs, and emergence of resistance, in relation to metabolic activity of *Mycobacterium tuberculosis*. J Antimicrob Chemother 2010; 65:2582-9

18. Woods G, Brown-Elliot B, Desmond E. *et al.* Susceptibility testing of mycobacteria, nocardiae, and other aerobic actinomycetes. Approved standard. National Committee for Clinical Laboratory Standards 2003; M24-A, volume 23:1-69

19. Hillemann D, Rusch-Gerdes S, Richter E. Evaluation of the GenoType®MTBDR*plus* assay for rifampicin and isoniazid susceptibility testing of *Mycobacterium tuberculosis* strains and clinical specimens. J Clin Microbiol 2007; 45:2635-40

20. Abebe F, Bjune G. The emergence of Beijing family genotypes of *Mycobacterium tuberculosis* and low-level protection by bacille Calmette-Guerin (BCG) vaccines: is there a link? Clin Exp Immunol 2006; 145:389-97

21. Krishnan N, Malaga W, Constant P *et al. Mycobacterium tuberculosis* lineage influences innate immune response and virulence and is associated with distinct cell envelope lipid profiles. PLoS One 2011; 6:e23870

22. de Steenwinkel J, de Knegt G, Ten Kate M. *et al.* Dynamics of interferon-gamma release assay and cytokine profiles in blood and respiratory tract specimens from mice with tuberculosis and the effect of therapy. Eur J Clin Microbiol Infect Dis 2011

23. Hanekom M, Gey van Pittius N, McEvoy C *et al. Mycobacterium tuberculosis* Beijing genotype: a template for success. Tuberculosis (Edinb) 2011; 91: 510-23.

24. Nicol M, Wilkinson R. The clinical consequences of strain diversity in *Mycobacterium tuberculosis*. Trans R Soc Trop Med Hyg 2008; 102:955-65

25. Srivastava S, Pasipanodya J, Meek C. *et al.* Multidrug-resistant tuberculosis not due to non-compliance but to between-patient pharmacokinetic variability. J Infect Dis 2011; 204: 1951-9

Chapter 11

Optimization of the rifampicin dosage to improve the therapeutic efficacy in tuberculosis treatment, using a murine model

J.E.M. de Steenwinkel, R.E. Aarnoutse, G.J. de Knegt, M.T. ten Kate, M. Teulen, H.A. Verbrugh, M.J. Boeree, D. van Soolingen, I.A.J.M. Bakker-Woudenberg

ABSTRACT

The dosage of 10 mg/kg/day rifampicin, as currently used in the treatment of tuberculosis (TB), is not (yet) an optimal dose. Shortening of treatment duration might be achievable using an increased rifampicin dose. The objectives of the current stuy are; determination of the optimal rifampicin dosage in mice, resulting in maximum therapeutic effect including prevention of relapse of infection, and without adverse effects. Moreover, we assessed the pharmacokinetics/pharmacodynamics (PK/PD) parameters to determine the human pharmacokinetic-equivalent dose.

A murine TB infection was established using a Beijing genotype *Mycobacterium tuberculosis* strain for intratracheal bacterial instillation. We assessed dose-dependent activity of rifampicin (R) in single-drug treatment during 3 weeks. Also the maximum tolerated dosage (MTD) and PK/PD were determined. Secondly, therapeutic efficacy of a range of rifampicin dosages added to a base regimen of isoniazid (H) and pyrazinamide (Z) was assessed.

The MTD of rifampicin in the murine TB was 160 mg/kg/day. PK/PD measurement in the HR(10)Z and HR(160)Z therapy regimens showed for rifampicin a Cmax of 16.2 and 157.3 mg/L, an AU C0-24h of 132 and 1782 h*mg/L and a 24h-AU C/MIC ratio of 22 and 297, respectively. A clear dose-effect correlation was observed for rifampicin after 3-weeks single-drug treatment. Administration of HR(80)Z allowed 9-week treatment duration to be effective without relapse of infection.

Our findings indicate that the currently used rifampicin dosage in the therapy of TB is too low. In our murine TB model a rifampicin dosage of 80 mg/kg/day enabled a significant reduction in therapy duration without adverse effects.

INTRODUCTION

The current treatment of TB is long and complex, which may lead to non-adherence, inadequate response, and emergence of multidrug-resistant TB (MDR-TB) or extensively drug-resistant TB (XDR-TB).[1] As a consequence there is a need to develop a novel, shorter and simpler TB therapy. The use of current drugs can be optimised; alternative combinations can be explored possibly involving new drugs.[2-3]

The role of rifampicin, being the cornerstone drug in TB treatment is believed to be its ability to kill actively-growing as well as dormant *Mycobacterium tuberculosis* (Mtb). Unfortunately, the 10 mg/kg rifampicin dose (often 450 or 600 mg daily) as determined in the 1960s based on pharmacokinetics, toxicity and financial considerations [4], appears to be at the lower end of the dose-response curve. Early experiments in mice [5] and clinical trials performed before 1985 [6] already suggested that a higher dose of rifampicin may enhance sterilizing activity and shorten therapy duration. Currently observed failure of TB treatment has caused a resurgence of interest to increase the dosage of rifampicin in TB treatment, as reflected in an experimental study in mice, [7] a clinical study on early bactericidal activity (EBA) of high dose (20 mg/kg) rifampicin administered as single-drug therapy,[8] a small trial on pharmacokinetics and tolerability of a higher dose of rifampicin [9] and ongoing clinical trials on high dose rifampicin in pulmonary TB and in TB meningitis.[10] Recently, Rosenthal *et al.* showed in experimental TB in BALB/c mice using the Mtb strain H37Rv, that each rifamycin demonstrates a significant increase in sterilizing activity with increasing dose.[11] Of note, an increase in rifampicin dose may not only result in enhanced killing of mycobacteria and shorter therapy duration, but may also result in prevention of drug-resistance.[12-13]

In view of the apparent potential of a higher dose of rifampicin, and the wide availability and affordability of this drug in resource-poor settings, stronger evidence on the utility of higher dosage of this potent drug is needed. It is important to know what the MTD for rifampicin is and what dose increase is needed to achieve a significant reduction in therapy duration. Therefore, the current study assessed the MTD for rifampicin in mice and the effect of incremental increases in rifampicin dosages on treatment response in terms of treatment duration needed and prevention of resistance.

We focused on maximizing the rifampicin dosage aiming for reduction of therapy duration from 6 months to even 2 months in mice. As the Beijing genotype of Mtb is a major driving force in the emergence of MDR-TB in high prevalence areas [14] in which rifampicin resistance develops more readily [15], a high-mutator strain of this lineage was tested in our murine TB model.[16-17]

MATERIAL AND METHODS

Bacterial strain

The previously described Mtb genotype strain Beijing VN 2002-1585 (BE-1585) was used.[18] Susceptibility assays performed according to CLSI guidelines [19], showed MICs for rifampicin of 0.25 mg/L and for isoniazid of 0.125 mg/L, and susceptibility for pyrazinamide

Infection model

Specified pathogen-free female BALB/c mice (13-15 weeks old) were obtained from Charles River [Les Oncins, France] and infected as previously described [16]. In short, mice were exposed to intratracheal instillation of a suspension (40 µl) containing $0.7x10^5$ [0.5 – 0.8 $x10^5$] cfu of BE-1585, followed by proper inhalation.

Anti-tuberculosis treatment

Dosage and schedules of TB drugs, derived from current clinical guidelines were administered as described earlier. All treatment schedules started at 2 weeks after infection.[16] In Study 1 mice received single-drug treatment with rifampicin at various doses (10, 20, 40, 80, 160 or 320 mg/kg/day po.) for 3 weeks. In study 2 mice received a 9-week or 13-week combination therapy: during 9 weeks various doses rifampicin (10, 40, 80 or 160 mg/kg/day po.) in combination with isoniazid (25 mg/kg/day sc.) and pyrazinamide (150 mg/kg/day sc.), followed by 4 weeks (in case of 13 weeks treatment) various doses of rifampicin (10, 40, 80 or 160 mg/kg/day po.) in combination with isoniazid (25 mg/kg/day sc.).

Maximum tolerated dose (MTD)

MTD was assessed in Study 1 and was defined as the highest dose that did not cause 1) local damage at the site of injection, 2) liver and/or kidney dysfunction, identified by increase of more than 5-times the upper limit of normal (in clinical studies regular considered a measure of toxicity) for aspartate aminotransferase (AST), alanine aminotransferase (ALT), creatinine (CREAT) and blood urea nitrogen (BUN), using a Cobas° modular analyser (Roche Diagnostics, Basel, Switzerland), 3) animal death and 4) abnormal animal behavior. Clinical parameters were bodyweight (assessed 3x/week) and daily evaluation of a discomfort score.

Pharmacokinetic sampling

Pharmacokinetic parameters were assessed for rifampicin 10 mg/kg or 160 mg/kg, as single-drug treatment (Study 1) or in combination with isoniazid and pyrazinamide (Study 2) at the end of week 3, when steady-state for anti-TB drugs was expected. Blood was sampled at 5, 15, 30, 45 min and at 1½, 3, 6 and 12h post dose. At each sampling point, 3 mice were sacrificed, blood was obtained by cardiac puncture, collected in heparin tubes (Sarstedt, Nümbrecht,

Germany), and centrifuged at 11.000x*g* for 5 min to obtain plasma. Plasma samples were immediately frozen at -80°C.

Measurement of TB drugs in plasma

Total (protein-bound plus protein-unbound) concentrations of rifampicin (Study 1) and of rifampicin, isoniazid and pyrazinamide (Study 2) were measured with validated HPLC methods for human plasma that were cross validated to murine plasma. The analytical method for rifampicin was described before.[9] Total concentrations of isoniazid and pyrazinamide were measured with liquid-liquid extraction followed by Ultra Performance Liquid Chromatography (UPLC) with ultraviolet (UV) detection. Accuracy was between 99.7-119% for isoniazid and between 96.4-104.9% for pyrazinamide, depending on the concentration level. Intra-assay coefficients of variation were less than 4.5 % for isoniazid and less than 4.3% for pyrazinamide (dependent on the concentration) over the range of 0.15-15.1 mg/L isoniazid and 0.6-60.6 mg/L pyrazinamide. To measure protein-unbound rifampicin, a validated HPLC method was used based on ultrafiltration of plasma with Centrifee YM-30 tubes (Millipore, Amsterdam, the Netherlands).

Pharmacokinetic data analysis

Based on measurements in 3 mice, a geometric mean plasma concentration was calculated for each drug at each sampling point. Next pharmacokinetic curves for each drug were constructed by combining geometric mean plasma concentrations at the various sampling points. Pharmacokinetic parameters including the area under the concentration-time curve (AUC_{0-24h}), peak plasma concentration (C_{max}), time to peak plasma concentration (T_{max}) and elimination half-life ($T_{1/2}$) were assessed with non-compartmental techniques using Winnonlin, version 5.3 (Pharsight, Mountain View, California, USA). The concentration at 24 h post dose (C_{24h}) was estimated, based on the last measurable concentration (C_{last}) and elimination rate constant β using the formula $C_{24h} = C_{last} * e^{-\beta * (24-Tlast)}$.

Pharmacokinetic parameters for total (protein-bound plus protein-unbound) rifampicin and pyrazinamide and for the protein-unbound (free) fraction of rifampicin in mice were compared to data in Indonesian TB patients, assessed with the same analytical methods.[9, 20] Whereas, pharmacokinetic parameters for isoniazid in mice were compared to data from measurements in Tanzanian TB patients, which were assessed with the same analytical methods.[21]

Therapeutic efficacy

Parameters for therapeutic efficacy were; 1) animal survival; 2) elimination of Mtb in pulmonary and extra-pulmonary organs; 3) the absence of emergence of drug resistance; 4) re-growth of Mtb during 2 weeks post-treatment (Study 1), or relapse of infection during 3 months post-therapy (Study 2). Relapse was defined as Mtb-positive organ cultures, if organ cultures immediately after termination of therapy were Mtb-negative.

The Mtb load and the presence of rifampicin-resistant and isoniazid-resistant mutants were determined as described previously.[16] For genotypic characterization of resistant Mtb, the GenoType® MTBDR*plus* assay (Hain Lifescience, Nehren, Germany) was used.

Therapeutic efficacy - Statistical analysis

CFU counts of Study 1 were log10 transformed before analysis. Mean CFU counts between groups of mice were compared using one-way ANOVA (Stata 12, Stata Corporation, TX, USA).

RESULTS

Study 1

Maximum tolerated dose (MTD)

Administration of rifampicin at doses of 10, 20, 40, 80 or 160 mg/kg/day po. during 3 weeks did not result in changes in behavior of mice or in liver and kidney function tests. A dose of 320 mg/kg/day showed an increase of AST and ALT although below five-times the upper limit of normal, whereas CREAT and BUN values were not changed (data not shown). Mice receiving a dose of 320 mg/kg/day became hyperactive and unmanageable. Thus, the MTD of rifampicin was defined as 160 mg/kg/day.

Pharmacokinetic analysis

In uninfected mice the 16-fold increase in rifampicin dose from 10 to 160 mg/kg resulted in an almost proportional (15-fold) increase in exposure (AUC_{0-24h}) from 125.1 to 1854.8 h*mg/L. C_{max} increased almost 9-fold. $T_{\frac{1}{2}}$ of rifampicin at a dose of 160 mg/kg could only be estimated very roughly, as decrease in plasma concentrations was small compared to the sampling period, and it appeared to be much longer (19.2 h) than the $T_{\frac{1}{2}}$ at a dose of 10 mg/kg (4.4 h).

Efficacy of rifampicin administered as single-drug treatment

A clear dosage-effect correlation was observed for rifampicin after 3 weeks single-drug treatment (p = <0.0001, one-way ANOVA) (figure 1). Administration of 10 mg/kg/day rifampicin resulted in a Mtb load in the lung of $7.7x10^5$ [range 5-$1.x10^5$] cfu, in the spleen $9.0x10^2$ [7-$25x10^2$] cfu and in the liver $3.1x10^2$ [0.4-$20x10^2$] cfu, whereas 160 mg/kg/day rifampicin resulted in a Mtb load in the lung of $1.8x10^2$ [0.8 – $6.8x10^2$] cfu and undetectable Mtb loads in the spleen and liver. All mice survived.

With respect to regrowth of Mtb, at 2 weeks after termination of treatment with 10 mg/kg rifampicin the Mtb load increased up to $8.5x10^5$ [6–$20x10^5$] cfu in the lung, $8.0x10^4$ [3–$19x10^4$] cfu in the spleen and $4.6x10^3$ [0.5–$16x10^3$] cfu in the liver. At 2 weeks after termination of 160 mg/kg rifampicin the Mtb load in the lung had increased to $3.7x10^3$ [2.2–$4.7x10^3$] cfu and in the spleen to $1.1x10^2$ [0.1–$12x10^2$] cfu, but the liver remained culture-negative (figure 1). Rifampicin-resistant Mtb mutants were never found.

Study 2

MTD. Administration of rifampicin in combination therapy schedules HR(10)Z, HR(40)Z, HR(80)Z, and HR(160)Z during 13 or 9 weeks did not result in changes in behaviour of mice or liver- or kidney function tests.
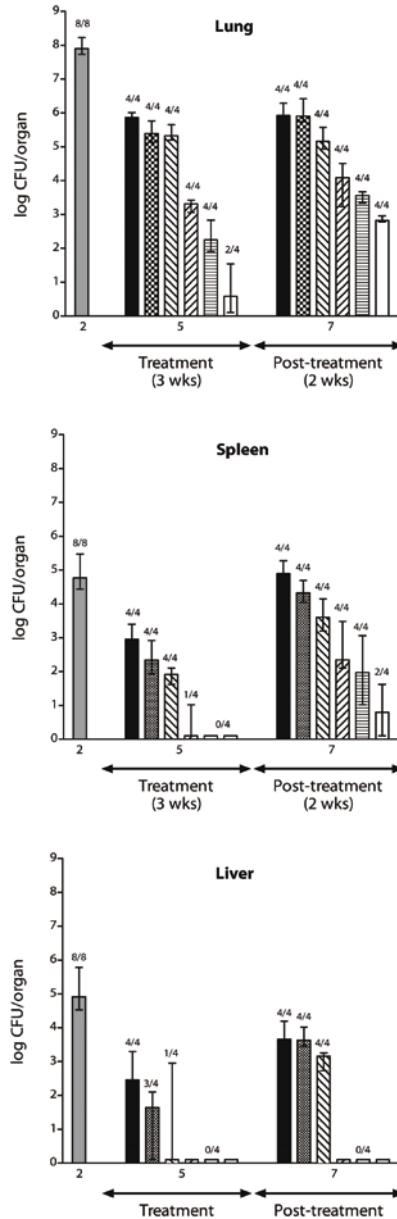
Figure 1. Effect of single-drug treatment for 3 weeks with rifampicin at various doses (10, 20, 40, 80, 160 or 320 mg/kg/day po). The Mtb load in lung, spleen and liver at the start of the treatment (gray bar) and at indicated time points (end of 3 weeks treatment and 2 weeks post-treatment). Mice received rifampicin either 10 mg/kg/day (black bars), 20 mg/kg/day (chequered bars), 40 mg/kg/day (left high diagonally striped bars), 80 mg/kg/day (right high diagonally striped bars), 160 mg/kg/day (horizontally striped bars) or 320 mg/kg/day (open bars) for a total of 3 weeks, 5 days a week. Results are expressed as median ± range (error bars) of the colony forming units (CFU) per organ, n = 4 per time point. Numbers above bars are the numbers of culture-positive mice out of total numbers of mice at that time point.

Pharmacokinetic analysis

Pharmacokinetic data for rifampicin at a dose of 10 mg/kg and 160 mg/kg in Study 1 and Study 2 were similar (table 1). This indicates that co-administration of isoniazid and pyrazinamide does not affect pharmacokinetics of rifampicin. After administration of 10 mg/kg rifampicin combined with isoniazid and pyrazinamide, samples (combined around T_{max}) yielded a total (protein bound plus protein-unbound) concentration of 15.1 mg/L and a protein-unbound concentration of 0.48 mg/L, yielding a protein-unbound (free) fraction of 3.2% (corresponding to 96.8 % protein binding).

After administration of 160 mg/kg rifampicin combined with isoniazid and pyrazinamide, the protein-unbound fraction was 2.6% at a total rifampicin concentration of 65 mg/L and 4.0% at a total concentration of 141 mg/L. This shows that protein-unbound fractions were not strongly dependent on the total concentration of rifampicin, i.e. no saturation of protein binding occurred at higher doses of rifampicin. Exposure (AUC_{0-24h}) and C_{max} of isoniazid were 23-24% lower when combined with 160 mg/kg of rifampicin compared to 10 mg/kg rifampicin. This may suggest that a strongly increased dose of rifampicin affects the exposure to the other TB drugs to a limited extent. Similarly, AUC_{0-24h} and C_{max} to pyrazinamide were 24% and 10% lower when combined with the high dose of 160 mg/kg rifampicin compared to 10 mg/kg rifampicin.

	Dose (mg/kg)	AUC_{0-24h} (h*mg/L)	C_{max} (mg/L)	T_{max} (h)	$T_{1/2}$ (h)
Study 1: rifampicin single-drug treatment					
rifampicin	10	125.1	18.5	0.5	4.4
rifampicin	160	1854.8	142.1	0.75	19.2
Study 2: rifampicin (10 mg/kg) combination therapy with isoniazid and pyrazinamide					
rifampicin	10	131.9	16.2	0.5	5.4
isoniazid	25	31.9	26.7	0.25	0.90
pyrazinamide	150	256.4	173.8	0.25	0.84
Study 2: rifampicin (160 mg/kg) combination therapy with isoniazid and pyrazinamide					
rifampicin	160	1782.3	157.3	0.25	11.1
isoniazid	25	24.2	20.7	0.25	0.61
pyrazinamide	150	194.7	156.2	0.25	0.57

Table 1. Steady-state pharmacokinetics of rifampicin, isoniazid and pyrazinamide. Study 1 (single-drug treatment with rifampicin), Study 2 (combination therapy of rifampicin, isoniazid and pyrazinamide). Results obtained are based on sampling at 5, 15, 30, 45 min and at 1.5, 3, 6 and 12h post dose. A geometric mean plasma concentration based on measurements in 3 mice was calculated for each drug at each sampling point. Data refer to total (protein-bound plus protein-unbound) concentrations. For protein-unbound (free) plasma concentrations: see text. Abbreviations: AUC_{0-24h}: area under the concentration-time curve from 0-24h post-dose, C_{max}: maximum concentration, T_{max}: time to maximum concentration, $T_{1/2}$: elimination half-life.

Pharmacokinetics in mice versus humans

For rifampicin administered to mice in a dose of 10 mg/kg (table 1) the AUC_{0-24h} is much (almost 3-fold) higher than that recorded in Indonesian TB patients [9], using the same analytical techniques (AUC_{0-24h} 132 h* mg/L in mice vs. 48.5 h*mg/L in humans). However, protein-unbound fraction for rifampicin in mice (circa 3.2%, see above) is much (also circa 3-fold) lower than protein-unbound fraction (10.3%) assessed in Indonesian TB patients.[20] implicating that, protein-unbound, active concentrations of rifampicin in mice and men are similar at the human pharmacokinetic-equivalent dose of 10 mg/kg.

AUC_{0-24h} values of pyrazinamide in mice (256.4 h* mg/L) were lower than those in Indonesian patients (472.8 h*mg/L).[21] For isoniazid administered to mice in a human pharmacokinetic-equivalent dose (table 1) the AUC_{0-24h} is higher than that in humans (AUC_{0-24h} 31.9 h* mg/L in mice vs. 11.0 h*mg/L in humans) using the same assays.[21] No protein-unbound concentrations of isoniazid or pyrazinamide were measured in the current study.

Therapeutic efficacy of rifampicin administered in combination therapy with isoniazid and pyrazinamide

Administration of HR(10)Z, HR(40)Z, HR(80)Z and HR(160)Z during 13 weeks or 9 weeks resulted in undetectable Mtb loads in all organs at the end of therapy (figure 2 and 3), with the exception of 9 weeks HR(10)Z therapy, which showed in 3 out of 4 mice positive lung cultures with a Mtb load of 46 [0.4–2.3x10^2] cfu (figure 3).

At 13 weeks after termination of 13 weeks therapy all mice receiving rifampicin 10 mg/kg/day relapsed, with a Mtb load of 8.5x10^3 [0.2–12x10^3] cfu in the lung, 0.3x10^4 [0.2–2.9x10^4] cfu in the spleen and 0.0 [0.0–3.6x10^2] cfu in the liver (figure 2). Treatment with 40 mg/kg/day rifampicin resulted in relapse of infection in 1 out of 4 mice, showing a Mtb load of 0.0 [0.0–2.9x10^5] cfu in the lung, 0.0 [0.0–2.1x10^5] cfu in the spleen and 0.0 [0.0–1.7x10^4] cfu in the liver.

At 13 weeks after termination of 9 weeks therapy, all mice receiving rifampicin 10 mg/kg/day relapsed, with an Mtb load of 5.3x10^4 [2.0–9.4x10^4] cfu in the lung, 3.5x10^4 [0.5–8.6x10^4] cfu in the spleen and 0.6x10^3 [0.0–2.2x10^3] cfu in the liver (figure 3). Treatment with 40 mg/kg/day rifampicin resulted in relapse of infection in 2 out of 4 mice, showing a Mtb load of 0.1x10^4 [0.0–1.1x10^4] cfu in the lung, 0.0 [0.0–7.4x10^1] cfu in the spleen and were culture-negative in the liver. Mice receiving isoniazid, pyrazinamide and rifampicin in a dose of 80 mg/kg/day or higher for 9 or 13 weeks did not show relapse of TB in any of the cultured organs, meaning that rifampicin dosed at 80 mg/kg (in combination with the other drugs) was the lowest dose that enabled treatment shortening to 9 weeks. Rifampicin-resistant or isoniazid-resistant Mtb mutants were never cultured.
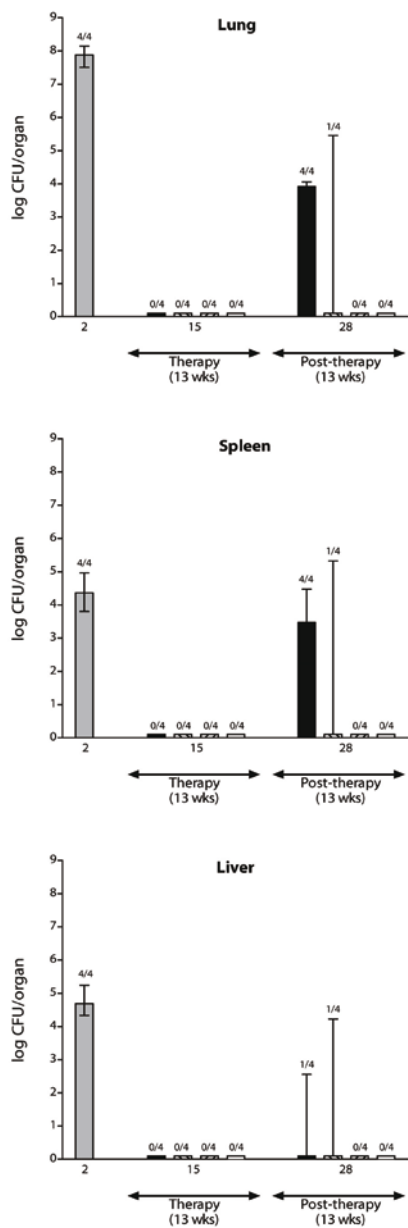
Figure 2. Therapeutic efficacy of combination therapy for 13 weeks with rifampicin at various doses (10, 40, 80 or 160 mg/kg/day po.) in combination with isoniazid (25 mg/kg/day sc. and pyrazinamide (150 mg/kg/day sc.). The Mtb load in lung, spleen and liver at the start of the therapy (gray bar) and at indicated time points (end of 13 weeks therapy and 13 weeks post-therapy). Mice received rifampicin either10 mg/kg/day (black bars), 40 mg/kg/day (left high diagonally striped bars), 80 mg/kg/day (right high diagonally striped bars) or 160 mg/kg/day (open bars) for a total of 13 weeks, 5 days a week. Results are expressed as median ± range (error bars) of the colony forming units (CFU) per organ, n = 4 per time point. Numbers above bars are the numbers of culture-positive mice out of total numbers of mice at that time point.
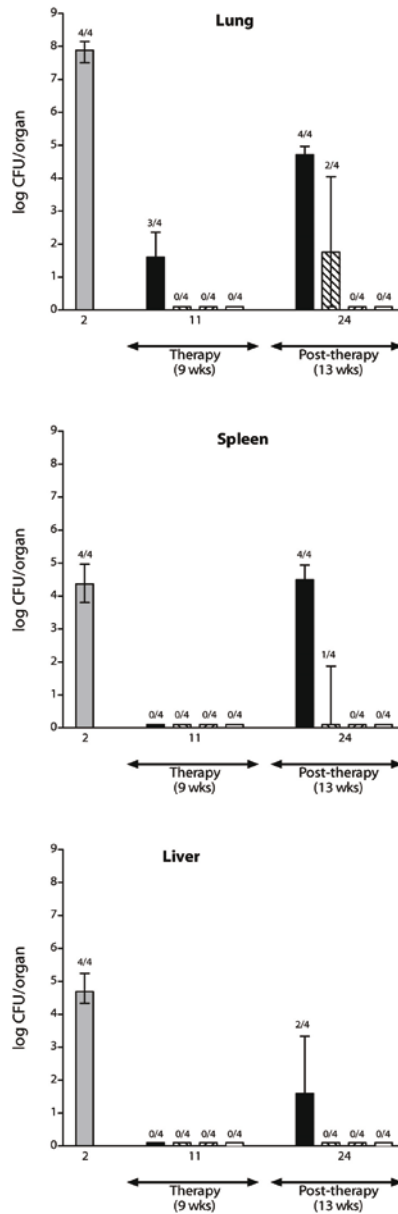
Figure 3. Therapeutic efficacy of combination therapy for 9 weeks with rifampicin at various doses (10, 40, 80 or 160 mg/kg/day po.) in combination with isoniazid (25 mg/kg/day sc. and pyrazinamide (150 mg/kg/day sc.). The Mtb load in lung spleen and liver at the start of the therapy (gray bar) and at indicated time points (end of 9 weeks therapy and 13 weeks post-therapy. Mice received either10 mg/kg/day rifampicin (black bars), 40 mg/kg/day (left high diagonally striped bars), 80 mg/kg/day (right high diagonally striped bars) or 160 mg/kg/day (open bars) for a total of 9 weeks, 5 days a week. Results are expressed as median ± range (error bars) of the colony forming units (CFU) per organ, n = 4 per time point. Numbers above bars are the numbers of culture-positive mice out of total numbers of mice at that time point.

DISCUSSION

Sufficient improvement of drug activity in the sterilizing phase of TB therapy is important to achieve reduction of treatment duration. Based on previous studies in mice, improving the sterilizing activity of rifampicin might be achieved by increasing its dosage.[5, 7, 11] Similar findings have been shown for rifapentine administered more frequently or in a higher dose in mice [11, 22] and for rifabutin.[11] However, escalation of the daily dose of rifapentine above 15 mg/kg in humans did not result in an increase of drug exposure.[23] Rifampicin is generally available, highly affordable and there is widespread experience with its clinical use; a new regimen with higher dose could be implemented quickly.

In a previous *in vitro* study we have demonstrated that Beijing genotype strains showed high rates of mutation towards rifampicin within a wide range of rifampicin concentrations, compared to the East-African/Indian genotype strains. Strains of both genotypes are highly prevalent in Vietnam, but only the Beijing genotype is associated with MDR-TB, treatment failures and relapses after curative treatment.[24] Based on our previous studies showing differences in emergence of drug-resistant mutants between different Mtb genotypes, in the present study we used a selected strain of the endemic Beijing genotype family.[17-18]

First, a strong dose-dependent activity of rifampicin in single-drug treatment was found (Study 1), which is in line with the concentration-dependent activity of rifampicin *in vitro* as we described previously.[18, 25] In addition, in combination with isoniazid and pyrazinamide (Study 2) the dose-dependency of rifampicin was again clearly visible.

Second, the MTD of rifampicin in the murine model was found to be 160 mg/kg based on aberrant behaviour of mice. We did not find gastro-intestinal problems or hepatotoxicity as dose limiting adverse events. This MTD can be interpreted as relatively high, as it is 16-fold higher than the usual dose, which is promising regarding increasing the dose in humans. In the dosage range we investigated, increasing the rifampicin dose resulted in a roughly proportional increase in AUC_{0-24h} and C_{max} in mice. This was not anticipated, as rifampicin shows non-linear pharmacokinetics in humans.[9, 26] Preliminary unpublished results of an MTD study in TB patients that currently takes place in Cape Town (www.clinicaltrials.gov NCT01392911) reveal that rifampicin doses up to 35 mg/kg are tolerated and that the pharmacokinetic parameters show a similar proportional increase in the higher dose groups (M. Boeree, personal communication).

Third, this study determined the efficacy of a range of rifampicin dosages up to the MTD. A rifampicin dose of 80 mg/kg/day in combination with isoniazid and pyrazinamide for only 9 weeks was sufficient to achieve successful therapy without relapse after 3 months

post-treatment. These results are generally in line with the observations of Rosenthal *et al.* in murine TB caused by the H37Rv strain.[11] However, results of our study and that of Rosenthal *et al.* differed in the dosage of rifampicin that resulted in relapse-free therapy. Rifampicin at 40 mg/kg/day rifampicin was sufficient to achieve a relapse-free therapy in the study of Rosenthal *et al.*[11], whereas we still observed relapse of TB in 1 out of 4 mice. This might be related to the Beijing-1585 strain, being the causative agent in our murine TB. Using this strain, which is known to be associated with treatment failures, allows a more realistic representation of the clinical situation. Importance of using different Mtb strains to assess the *in vivo* efficacy of new drug regimens has been recently emphasized by de Groote *et al.*[27].

Studies on high dose rifampicin in murine TB using different study design and in one EBA study in humans [8] suggest that an increased dose of rifampicin is associated with a fast decline of Mtb load in the lung. Thereby, one can argue that a patient treated with increased dosage of rifampicin would become sputum smear-negative in a shorter time resulting in a reduced time or risk of TB transmission. Moreover, the rapid decrease in Mtb load in the infected organs in the early stage of therapy will reduce the risk of selection of drug-resistant mutants; as we showed in a previous study, the risk of selection of resistance will increase with an increasing Mtb load and prolonged time of TB drug exposure to the Mtb population.[25] The different murine studies on the efficacy of increasing rifampicin dosages should be considered as proof-of-concept, paving the road for phase-II clinical trials. In addition, there are several studies ongoing: the aforementioned MTD study in Cape Town and a phase II study investigating 10, 15 and 20 mg/kg in 150 patients in Tanzania (www.clinicaltrials.gov NCT 00760149).

The current study in mice is also informative on the human pharmacokinetic-equivalent dose of rifampicin in mice, which is relevant for future studies in the murine TB model. The human pharmacokinetic-equivalent dose of rifampicin in mice has been designated as 10 mg/kg, i.e. similar to the dose in humans, based on data presented by Grosset *et al.*[28]. Our AUC_{0-24h} and C_{max} values in mice following administration of 10 mg/kg rifampicin until steady-state were remarkably similar to those recorded by Rosenthal *et al.*(AUC_{0-24h} 131.9 h*mg/L and C_{max} 16.2 mg/L in the current study versus AUC_{0-24h} 142.1 h*mg/L and C_{max} 13.52 mg/L in their study).[11] We noted that the AUC_{0-24h} at the presumed human pharmacokinetic-equivalent rifampicin dose was almost 3-fold higher than that recorded in Indonesian TB patients on 10 mg/kg rifampicin, while using the same bio-analytical techniques for assessment of rifampicin plasma concentrations.[9] Rosenthal *et al.* have noticed the same discrepancy and state that rifampicin exposures observed in mice overestimate those in humans. In the current study we have gone one step further and showed that this is not the case, by measuring protein-unbound rifampicin plasma concentrations. The total exposure to rifampicin at a dose of 10 mg/kg is higher in mice, but the protein-unbound fraction of rifampicin in mice is lower. Thus 10

mg/kg is the human pharmacokinetic-equivalent dose for rifampicin indeed. Importantly, increasing the dose of rifampicin up to 160 mg/kg did not result in a relevant change in protein-unbound fraction, i.e. no saturation of protein binding did occur. This means that interpretation of total AUC_{0-24h} and C_{max} values in mice is not misled by changes in protein binding.

In conclusion, the present study shows that efficacy of rifampicin in the human pharmacokinetic-equivalent dose of 10 mg/kg/day can significantly be improved, by increasing the dose to 80 mg/kg/day. This increased rifampicin dose showed no adverse effects in our murine model and enabled therapy duration of only 9 weeks to be effective. Our use of a clinically relevant strain, like the Beijing strain will improve the translational power of animal studies to TB patients and may further support the clinical studies on tolerability and efficacy of increased rifampicin doses in TB patients, currently ongoing.

ACKNOWLEDGMENTS

REFERENCES

1. van den Boogaard J, Boeree MJ, Kibiki GS *et al.* The complexity of the adherence-response relationship in tuberculosis treatment: why are we still in the dark and how can we get out? Trop Med Int Health 2011; 16: 693-8.

2. Ginsberg AM. Drugs in development for tuberculosis. Drugs 2010; 70: 2201-14.

3. van den Boogaard J, Kibiki GS, Kisanga ER *et al.* New drugs against tuberculosis: problems, progress, and evaluation of agents in clinical development. Antimicrob Agents Chemother 2009; 53: 849-62.

4. van Ingen J, Aarnoutse RE, Donald PR *et al.* Why Do We Use 600 mg of Rifampicin in Tuberculosis Treatment? Clin Infect Dis 2011; 52: e194-9.

5. Verbist L. Rifampicin activity "*in vitro*" and in established tuberculosis in mice. Acta Tuberc Pneumol Belg 1969; 60: 397-412.

6. Steingart KR, Jotblad S, Robsky K *et al.* Higher-dose rifampicin for the treatment of pulmonary tuberculosis: a systematic review. Int J Tuberc Lung Dis 2011; 15: 305-16.

7. Jayaram R, Gaonkar S, Kaur P *et al.* Pharmacokinetics-pharmacodynamics of rifampicin in an aerosol infection model of tuberculosis. Antimicrob Agents Chemother 2003; 47: 2118-24.

8. Diacon AH, Patientia RF, Venter A *et al.* Early bactericidal activity of high-dose rifampicin in patients with pulmonary tuberculosis evidenced by positive sputum smears. Antimicrob Agents Chemother 2007; 51: 2994-6.

9. Ruslami R, Nijland HM, Alisjahbana B *et al.* Pharmacokinetics and tolerability of a higher rifampicin dose versus the standard dose in pulmonary tuberculosis patients. Antimicrob Agents Chemother 2007; 51: 2546-51.

10. Crevel Rv, Ruslami R, Ganiem AR *et al.* Pharmacokinetics, safety and effectiveness of high-dose rifampicin and moxifloxacin for tuberculosis meningitis: a randomised clinical trial in Indonesia. 22nd European Congress of Clinical Microbiology and Infectious Diseases (ECCMID). London, 2012.

11. Rosenthal IM, Tasneen R, Peloquin CA *et al.* Dose-ranging comparison of rifampicin and rifapentine in two pathologically distinct murine models of tuberculosis. Antimicrob Agents Chemother 2012; 56(8):4331-40

12. Goutelle S, Bourguignon L, Maire PH *et al.* Population modeling and Monte Carlo simulation study of the pharmacokinetics and antituberculosis pharmacodynamics of rifampicin in lungs. Antimicrob Agents Chemother 2009; 53: 2974-81.

13. Gumbo T, Louie A, Deziel MR *et al.* Concentration-dependent *Mycobacterium tuberculosis* killing and prevention of resistance by rifampicin. Antimicrob Agents Chemother 2007; 51: 3781-8.

14. Parwati I, van Crevel R, van Soolingen D. Possible underlying mechanisms for successful emergence of the *Mycobacterium tuberculosis* Beijing genotype strains. Lancet Infect Dis 2010; 10: 103-11.

15. Parwati I, Alisjahbana B, Apriani L *et al. Mycobacterium tuberculosis* Beijing genotype is an independent risk factor for tuberculosis treatment failure in Indonesia. J Infect Dis 2010; 201: 553-7.

16. de Steenwinkel JE, de Knegt GJ, Ten Kate MT *et al.* Immunological parameters to define infection progression and therapy response in a well-defined tuberculosis model in mice. Int J Immunopathol Pharmacol 2009; 22: 723-34.

17. de Steenwinkel JE, ten Kate MT, de Knegt GJ *et al.* Consequences of non-compliance on therapy efficacy and emergence of resistance in murine tuberculosis caused by the Beijing genotype. Antimicrob Agents Chemother 2012; In press.

18. de Steenwinkel JE, ten Kate MT, de Knegt GJ *et al.* Drug susceptibility of *Mycobacterium tuberculosis* Beijing genotype and association with MDR TB. Emerg Infect Dis 2012; 18: 660-3.

19. Woods GL, Brill MR, Brown-Elliot BA *et al.* Susceptibility testing of mycobacteria, nocardiae, and other aerobic actinomycetes. Approved standard-second edition. Clinical and Laboratory Standards Institute 2011; M24-A2, volume 26: 1-61.

20. Aarnoutse RE, Mooren FW, Nijland H *et al.* Evaluation of protein-unbound, active concentrations of rifampicin in Indonesian tuberculosis patients. Fourth International Workshop on Clinical Pharmacology of TB Drugs. Chicago, IL USA, 2011.

21. Tostmann A, Mtabho CM, Semvua HH *et al.* Pharmacokinetics of first line tuberculosis drugs in Tanzanian tuberculosis patients. 2012.

22. Rosenthal IM, Zhang M, Williams KN *et al.* Daily dosing of rifapentine cures tuberculosis in three months or less in the murine model. PLoS Med 2007; 4: e344.

23. Dooley KE, Bliven-Sizemore EE, Weiner M *et al.* Safety and pharmacokinetics of escalating daily doses of the antituberculosis drug rifapentine in healthy volunteers. Clin Pharmacol Ther 2012; 91: 881-8.

24. Buu TN, Huyen MN, Lan NT *et al.* The Beijing genotype is associated with young age and multidrug-resistant tuberculosis in rural Vietnam. Int J Tuberc Lung Dis 2009; 13: 900-6.

25. de Steenwinkel JE, de Knegt GJ, ten Kate MT *et al.* Time-Kill Kinetics of anti-tuberculosis drugs, and emergence of resistance, in relation to metabolic activity of *Mycobacterium tuberculosis*. J Antimicrob Chemother 2010; 65: 2582-9.

26. Burman W, Gallicano K, Peloquin C. Comparative pharmacokinetics and pharmacodynamics of the rifamycin antibacterials. Clin Pharmacokinet 2001; 40:327-41.

27. De Groote MA, Gruppo V, Woolhiser LK *et al.* Importance of Confirming *in vivo* Efficacy Data of Novel Antibacterial Drug Regimens against Various Strains of *Mycobacterium tuberculosis*. Antimicrob Agents Chemother 2011.

28. Grosset J. The sterilizing value of rifampicin and pyrazinamide in experimental short-course chemotherapy. Bull Int Union Tuberc 1978; 53: 5-12.

Chapter 12

Summarizing discussion

To reduce the high mortality and/or morbidity of TB diagnostics and treatment of this infectious disease need significant of substantial improvement. However, to accomplish this enormous task and unravel the puzzle, which might result in eradication of TB, will take time and great effort from many different organisations and scientists around the world. The studies described in this thesis were aimed to add one piece to that puzzle.

The (translational) pathway of TB-drug development needs to be as short a possible without giving in on the predictive value for the clinical trials. This is not only needed to reduce the costs of TB-drug development, but also to ensure that TB remains a treatable disease. The increasing emergence and spreading of drug-resistant TB is currently threatening the status of treatable disease. Moreover, there is an increasing number of cases not only of multidrug resistant TB (MDR-TB; resistance to rifampicin and isoniazid) but also of extensively-drug resistant TB (XDR-TB; besides MDR also resistance to one of the injectable TB-drugs and one of the fluoroquinolones). The therapeutic outcome of patients with XDR-TB is very poor, even with optimal care and resources. Recently, the anxiety of the emergence of totally-drug resistant TB (TDR-TB) came true in Asia and the Middle-East. Here we have an infectious disease where medical doctors can only watch the course of infection in their patients. In a way, this is like historic time where there were no antibiotics. It is more than clear that novel treatment approaches are urgently needed.

Translational studies in animal TB models are needed as they provide the basis for the design of therapeutic clinical trials in TB patients. The animal model should be well described in histopathological and immunological characteristics, and validated in terms of therapy response under treatment compliance and treatment non-compliance conditions. Such an animal model using the H37Rv Mtb strain as infectious organism has been described in **chapter 2**

Dependent on the research question and the objectives of a study, the choice of the right translational animal model is of high importance. In **chapter 3** it is shown in mice using the H37Rv Mtb strain that the route of Mtb inoculation applied influences the course of the TB infection and the therapeutic response. It is concluded that the comparative therapeutic potential of novel anti-TB drugs in translational animal studies can only be established within the same animal model.

The diversity of different animal models is also demonstrated in the studies described in **chapter 6** where we compared the course of primary TB versus relapse of TB in mice, both caused by the H37Rv Mtb strain. We showed that the histopathological and immunological characteristics of relapse of TB resulting from treatment non-compliance during primary TB, were essentially different compared to those in primary TB. The most striking difference is

the relatively low Mtb load in the infected organs in relapse TB compared to the primary TB. It was observed that in relapse TB memory Th-1 cells were locally and systemically expanded and congregated in the lung, permitting an efficient control of Mtb growth. However, this immune response is insufficient to clear the Mtb, thereby leaving a potential infectious reservoir within the mice. This is probably also occurring in therapy non-compliant patients. Interestingly, treatment response in relapse of TB is as good as the treatment response in primary TB; so no supportive evidence could be given for the recommended longer treatment duration in case of relapse of TB.

A small side-step in this thesis is represented in the **chapters 4 and 5**, within which we discussed the difficulties of accurately diagnosing TB. The case report of the congenital TB (**chapter 4**) illustrates that TB can present in a non-specific way and thus can be very difficult to diagnose. Missing the diagnosis TB or getting it too late can have fatal implications for the patients. Therefore, numerous studies are conducted to explore the possibilities for new diagnostic tools. One of these investigated assays is the Interferon Gamma Release Assay (IGRA). The IGRA took over the field of TB screening in just a couple of years, and is in short time implemented in the clinic. Gradually it is being used not only to screen for (latent) TB, but also for diagnosing active TB. However, the value of the IGRA for diagnosing active TB is still a matter of debate. Therefore we investigated in our murine TB model the value of the IGRA during different phases of the TB infection (**chapter 5**). In murine TB no support could be found for the value of IGRA to accurately diagnose active TB or to monitor infection progression. Nonetheless, IGRA showed to be a useful biomarker to monitor therapy success in murine TB.

Besides the studies on animal model design and limitations in diagnosis, the primary research question for this thesis was: 'How can treatment of TB be improved and emergence of drug resistance in TB be reduced?'.

The currently-used diagnostic drug susceptibility tests (MGIT, MIC) guiding TB therapy, investigate metabolically active Mtb isolates under static conditions and provides an end-point measurement of only the bacteriostatic activity of the anti-TB drug. In **chapter 7** we performed Time-Kill Kinetics assays to investigate the concentration-dependent bactericidal activity of the anti-TB drugs over time and the emergence of drug-resistant mutants during drug exposure. We included the differences in metabolic state of the mycobacteria by comparing actively-growing versus slowly-growing or even dormant Mtb cells. It was observed that the anti-TB drugs differed significantly in the Time-Kill Kinetics analysis and the impact of the metabolic state of the mycobacteria to their drug susceptibility. Isoniazid showed rapid and high killing capacity towards actively-growing mycobacteria, but due to the emergence of resistance isoniazid could not eliminate Mtb. Rifampicin revealed time-dependent kill-

ing capacity, and did achieve elimination. Ethambutol was not bactericidal at all. Amikacin showed immediate and rapid killing activity which was not time-dependent.

Better knowing these anti-TB drug characteristics we could further design optimization of the dosage of anti-TB drugs in the treatment of infection. It is clear that achievement of maximum drug concentrations at the site of infection is of utmost importance in order to maximize reduction in Mtb load and in this way to minimize the emergence and selection of drug resistance. Depending on the growth phase and thereby the metabolic activity of the Mtb population, we observed selection of drug-resistant mutants for different anti-TB drugs. For rifampicin we further analysed the drug-resistant mutants by performing a micro-array analysis. Rifampicin-resistant mutants were compared to their wild type counterpart. The microarray results described in **chapter 8** have shown that several interesting gene clusters associated with molecular efflux, cell membrane transport and virulence are altered in the rifampicin-resistant H37Rv mutant compared to the rifampicin-susceptible H37Rv wild type strain upon exposure to rifampicin. We identified Rv0559c and Rv0560c being strongly rifampicin-inducible, with a high level induction based on microarray analysis and multiple qPCR experiments. Evidence was obtained that the induction of both genes is dependent on concentration of rifampicin and exposure time. We concluded that the Mtb mutant although being rifampicin-resistant, still was influenced by rifampicin exposure at different genetic levels. This may open new ways for future treatment improvement.

In **chapter 9** and **10** we focus on the mycobacterial side that drives the development of drug-resistance in TB. Certain genotype Mtb strains appear to be particularly associated with treatment failures. Therefore we investigated different endemic Mtb strains in our *in vitro* assays and *in vivo* infection, aiming for additional insight and improvement of the predictive value of these *in vitro* and ***vivo*** models. In this way the preclinical (translational) value of drug-development research might be improved. Although the approach of using clinically-relevant genotype strains in viral disease research is not new, surprisingly in the TB research field the use of endemic Mtb strains is very limited.

In **chapter 9** we compared the *in vitro* activity of anti-TB drugs against five endemic Beijing genotype strains and five East-African/Indian genotype strains that were all drug-susceptible according to the currently-used drug susceptibility tests. The Beijing genotype strains showed high rates of mutation towards rifampicin within a wide range of drug concentrations, possibly explaining this genotype's association with MDR-TB. The increased mutation frequency only observed for the Beijing genotype strains showed the relevance of the use of different genotype strains, and may contribute to further insight in the mechanisms behind the Mtb genotype-associated resistance.

To further investigate improvement of TB treatment and reduction of drug resistance in our TB infection murine model we decided to apply as infecting strains one Beijing genotype strain and one East-African Indian genotype strain instead of the in TB research traditionally-used H37Rv Mtb strain. As described in **chapter 10** both Mtb strains showed a high virulence in comparison to the H37Rv Mtb strain, resulting in a highly progressive infection with rapid lethal outcome in untreated mice. Full-compliance treatment was effective without relapse of TB irrespective the infecting strain, showing similar decrease of Mtb load in infected organs, and similar histopathological changes. Non-compliance treatment, simulated by a reduced treatment duration and reduced dosing frequency resulted in relapse of infection. Relapse rates were correlated with the level of non-compliance and were identical for Beijing infection and East-African/Indian infection. However, in only Beijing-infected mice and not in EAI-infected mice isoniazid-resistant mutants were selected at the highest level of non-compliance. This is in line with the substantial selection of isoniazid-resistant mutants *in vitro* in a wide isoniazid concentration window that we observed for the Beijing strain and not for the EAI strain. These results suggest that genotype diversity of Mtb may be involved in emergence of drug resistance and indicates that genotype-tailor-made treatment in TB should be investigated.

To improve TB treatment and reduce drug resistance there are many different approaches to achieve these goals such as the application of newly-developed drugs or novel drug combinations. Next, optimization of the dosage regimen of currently-used drugs also deserves full attention. For the last approach rifampicin is a good candidate drug, as we have shown for rifampicin *in vitro* a strong concentration- and time-dependent killing activity (**chapter 7**) and a high mutation frequency in the Beijing genotype strains (**chapter 9**). In **chapter 11** we determined the optimal rifampicin dosage in mice with Beijing genotype infection, resulting in maximum therapeutic effect including prevention of relapse of infection, and without adverse effects. We concluded that the dosage of 10 mg/kg/day rifampicin, as currently used in the therapy of TB is too low. In Beijing genotype-infected mice a rifampicin dosage of 80 mg/kg/day is far more effective without adverse effects, and enabled a significant reduction in therapy duration from 6 months to only 2 months.

MAIN FINDINGS

– A model of TB infection induced through the natural respiratory route in BALB/c mice is developed, characterized and validated in terms of therapy response under treatment compliance and treatment non-compliance conditions. **[chapter 2]**

– The evaluation of the comparative therapeutic potential of novel anti-TB drugs in translational studies in mice should be performed in the same model, as the route of infection applied influence the course of infection and therapeutic response. **[chapter 3]**

– The course of infection in mice with relapse TB is different compared to primary TB in terms of a lower Mtb load and different histopathological and immunological characteristics. However, the therapy response of the infected mice is equal irrespective relapse of TB or primary TB. **[chapter 6]**

– Based on results obtained in a murine TB model, no support can be given that there is a value of IGRA to accurately diagnose active TB or to monitor infection progression. However, IGRA showed to be a useful biomarker to monitor therapy success. **[chapter 5]**

– Anti-TB drugs differ significantly regarding their concentration-dependent time-kill kinetics. The metabolic state of Mtb significantly affects the drug susceptibility. **[chapter 7]**

– Optimization of anti-TB drugs dosage is required to achieve optimal drug concentrations at the site of infection in order to maximize reduction in Mtb load and to minimize the emergence and selection of drug-resistance. **[chapter 7]**

– Several genes associated with molecular efflux, cell membrane transport and virulence are altered in the rifampicin-resistant H37Rv mutant compared to the rifampicin-sensitive H37Rv wild type strain after exposure to rifampicin. Mtb mutants although being rifampicin-resistant, still are influenced by rifampicin exposure at different genetic levels. **[chapter 8]**

– Beijing genotype Mtb strains show high rates of mutation frequency for rifampicin within a wide range of rifampicin concentrations, possibly explaining this genotype's association with multidrug-resistant TB. **[chapter 9]**

– In mice with a Beijing genotype TB infection and mice with an East-African/Indian TB infection relapse of TB is correlated with the level of non-compliance, irrespective the infecting strain. **[chapter 10]**

– Only in Beijing-infected mice at non-compliance treatment isoniazid-resistant mutants are selected, which is in line with the selection of isoniazid-resistant mutants *in vitro* that we observe for the Beijing strain only. This suggests that genotype diversity of Mtb is involved in emergence of drug resistance and indicates that genotype tailor-made treatment should be investigated. **[chapter 10]**

– The currently used rifampicin dosage in the therapy of TB is too low. In mice with Beijing genotype TB infection an 8-fold increased rifampicin dosage is far more effective without adverse effects, and enables a significant reduction in therapy duration from 6 months to 2 months. **[chapter 11]**

FUTURE PERSPECTIVES

The *in vitro* and *in vivo* tools described in this thesis, were developed to gain insight in different aspects of *Mycobacterium tuberculosis* and TB infections, and were designed for studies to improve TB treatment and reduce drug-resistance in TB. The future perspective is to continue the studies by investigating different treatment approaches using new regimens of (combinations of) anti-TB drugs aiming for 1) substantial reduction of treatment duration, 2) prevention of selection of resistant Mtb mutants, and 3) therapeutic success in the treatment of MDR-TB.

Our recent finding that a substantially increased therapeutic efficacy is achieved by simply increasing the dosage of rifampicin opens the door to other and new ways to achieve this goal. One approach might be the addition of efflux pump inhibitors or the use of cell wall destabilizing agents that increase bacterial cell wall permeability. Both will result in increased intracellular and/or intrabacterial concentrations of anti-TB drugs. Also drugs relatively new in TB treatment like the oxazolidinones and newer fluoroquinolones should be further investigated. Combining the new drugs with efflux pumps inhibitors and/or cell wall destabilizers will possibly even further increase the therapeutic efficacy even in MDR-TB.

Next to the application of more potent (combinations of) drugs, the approach of drug targeting to the primary infected organs should be elaborated. In this respect pulmonary delivery of anti-TB drugs looks promising as it is expected to result in relatively high concentrations of anti-TB drugs in the lung without systemic toxic side effects. High anti-TB drug concentrations in the lung will effect rapid decrease of the Mtb load resulting in reduced transmission of disease as well as reduction/prevention of selection of drug-resistant mutants. By using nanocarriers containing the most potent drug combinations in pulmonary delivery we expect to further increase the therapeutic effect.

To accelerate the search for a novel treatment approach and tackle pre-clinical research barriers two important initiatives, i.e. the Critical Path to TB Drug Regimens (CPTR) and the PreDiCT-TB consortium have been founded, both being consortia of academia and pharmaceutical companies. In their approach of starting with back-validation of currently-used anti-TB drugs using existing *in vitro* and *in vivo* models in TB research, these models can be evaluated with respect to their prognostic and translational value as the drugs tested already have been used in clinical trials or even in large groups of TB patients with the clinical outcome known. The *in vitro* and *in vivo* models described in this thesis will be part of the PreDiCT-TB consortium, and in the novel treatment approaches the new anti-TB drugs developed by the pharmaceutical consortium partners will be included.

Chapter 13

Nederlandse samenvatting

Tuberculose (TBC) is een ziekte die bij veel mensen associaties en reacties zal oproepen zoals; 'uit de tijd van mijn grootouders', 'de oude kuuroorden in de Alpen' of 'betaat die ziekte nog?' De keiharde waarheid is dat TBC nog jaarlijks, wereldwijd zo'n 1.6 miljoen slachtoffers eist. Daarmee is TBC, na HIV/aids, de op één na dodelijkste infectieziekte van dit moment. Volgens schattingen van de Wereldgezondheidsorganisatie (WHO) zijn er jaarlijks zo'n 9 miljoen nieuwe gevallen van TBC, die allemaal een hoge ziektelast met zich meebrengen. De bacterie die TBC veroorzaakt is *Mycobacterium tuberculosis* (Mtb). Het is bekend dat slechts een relatief klein deel (5-10%) van de mensen die geïnfecteerd raakt met deze bacterie ook daadwerkelijk TBC ontwikkelt. Een heel groot deel van de mensen draagt de bacterie bij zich maar wordt er niet ziek van; die mensen ontwikkelen geen actieve TBC; men noemt dit dan een latente TBC infectie. De WHO schat dat ongeveer éénderde van de wereldbevolking zo'n latente TBC infectie heeft. Er is dus een enorm grote groep van mensen die mogelijk actieve TBC kunnen ontwikkelen als hun afweersysteem minder goed wordt. Dysfunctioneren van het afweersysteem kan gebeuren bij voorbeeld bij mensen die door hogere leeftijd altijd al een minder goed afweersysteem hebben of bij personen met een HIV infectie. Juist die laatste groep is in de laatste 25 jaar toegenomen en vormt een probleem voor het in de hand houden / verminderen van de wereldwijde TBC epidemie. HIV/aids en TBC gaan (helaas) hand in hand en zijn samen een dodelijke combinatie.

Naast de schrikbarend hoge cijfers van mortaliteit en morbiditeit (sterfte en ziektelast) van TBC, is er de laatste jaren een nieuw probleem bij gekomen: de resistentie voor antibiotica. In korte tijd heeft de Mtb zich weten te ontwikkelen tot een bacterie die veel minder gevoelig is voor verschillende antibiotica. De bacterie wordt dan resistent genoemd. Hoewel het arsenaal aan antibiotica waarover we beschikken groot is, is het aantal antibiotica waarmee patiënten met TBC kunnen worden behandeld redelijk beperkt. Unieke eigenschappen in de celwand van Mtb zorgen ervoor dat veel beschikbare antibiotica niet of nauwelijk werkzaam zijn.

De huidige 4 antibiotica die in combinatie als standaard therapie gegeven worden voor TBC zijn isoniazide (INH), rifampicine (RIF), pyrazinamide (PZA) en ethambutol (EMB). De duur van therapie is bij actieve TBC ten minste 6 maanden, waarbij 2 maanden INH, RIF, PZA en EMB gegeven wordt, gevolgd door 4 maanden INH en RIF. Hiermee is het een langdurige en inge-wikkelde therapie, met als gevolg dat de behandeling vaak niet volledig wordt afgemaakt. Het gevolg van deze 'therapie-ontrouwheid' is dat patiënten weer ziek worden (relaps TBC) en dat de bacterie door de onvolledig gevolgde behandeling minder gevoelig of ongevoelig (resistent) voor de antibiotica is geworden.

Al met al ziet het er naar uit dat, na de tijd van onze grootouders en de kuuroorden in de Alpen, we nu staan voor een immens probleem van TBC dat nog lang niet uit de wereld is en

waarvan de behandeling door de toenemende antibiotica resistentie wereldwijd ons voor grote problemen stelt. Het proefschrift PREDICT TB, beschrijft een aantal studies waarmee we hopen onze bijdrage te kunnen leveren aan de wetenschap aangaande TBC, opdat in de toekomst deze ziekte effectiever én in een kortere periode te behandelen is, zodat onze kleinkinderen met trots kunnen zeggen: TBC was een ziekte uit de tijd van onze grootouders!

In de **hoofdstukken 2 en 3** beschrijven we de door ons ontwikkelde TBC modellen in proefdieren (muizen). Studies in diermodellen zijn nodig om beter inzicht te krijgen in hoe verbetering kan worden verkregen in de TBC diagnostiek in het laboratorium en de behandeling van de patiënt. Bij de opzet van onze TBC modellen hebben we beoogd dat het begin en het verloop van de ziekte in de muizen zoveel mogelijk lijkt op dat in de mens, opdat we de resultaten verkregen in de muis met TBC zo goed mogelijk kunnen vertalen naar verbetering in diagnostiek en behandeling van de mens met TBC.

In **hoofdstuk 6** gaan we nog een stukje verder. Daar vergelijken we het verloop en de behandeling 'primaire TBC' ('voor het eerst verkregen TBC') met 'relaps TBC' ('het weer terugkrijgen van de TBC omdat de behandeling van de primaire TBC niet goed is geweest'). Onze studies geven inzicht in de verschillen in karakteristieken van beide vormen van de infectie en in effectiviteit van de behandeling.

Hoofdstuk 4 en 5 hebben als focus de problemen die er zijn met adequate diagnostiek van actieve TBC. Kweken van de bacterie uit opgehoest sputum van de patiënt (de gouden standaard methode) duurt lang, en de waarde van nieuwe, meer gevoelige en snellere technieken waarbij je het DNA van de bacterie aantoont (bijvoorbeeld PCR) is nog niet helder. In **hoofdstuk 4** illustreren we dit aan de hand van een moeilijke patiëntcasus met TBC, die zich presenteerde in het Sofia Kinderziekenhuis.

Ook voor de diagnostiek van latente TBC zijn er nieuwe tests en technieken in ontwikkeling. In **hoofdstuk 5** bestuderen we een van de nieuwe tests: de IGRA (Interferon Gamma Release Assay) in ons TBC diermodel. We concluderen dat in de muis de IGRA niet bruikbaar is om actieve TBC aan te tonen. Hiermee is de boodschap voor de kliniek dat de bruikbaarheid van de IGRA in de diagnostiek van actieve TBC nog moet worden onderzocht, ook al is de rol van deze test in het aantonen van latente TBC bewezen. In de muis bleek de IGRA wel een goede maat om het succes van de behandeling van TBC vast te stellen. Een goede basis om dit ook in TBC patiënten te onderzoeken.

In **hoofdstuk 7** onderzoeken we diepgaand de verschillen in werkzaamheid van de antibiotica die op dit moment worden toegepast in de behandeling van TBC. Dit is een belangrijke basis om te kunnen nadenken over en werken aan nieuwe en alternatieve vormen van be-

handeling van TBC. In het diagnostisch laboratorium wordt tot nu toe alleen in een beperkte opzet gemeten of de toegepaste antibiotica de Mtb in de groei remmen. In hoofdstuk 7 hebben wij ons verdiept in de bacteriedodende werking bij meerdere concentraties van antibiotica, en op meerdere tijdstippen gemeten. Daarbij is ook gelet op het mogelijk ontstaan van antibioticum-resistente bacteriën, en zo ja onder welke condities van blootstelling aan antibiotica dit gemakkelijk kan ontstaan. Grote verschillen worden er gevonden voor de verschillende antibiotica met betrekking tot hun concentratie-afhankelijke en tijd-afhankelijke bacteriedodende activiteit. Tevens blijkt er een sterk verschil te zijn tussen de omstandigheden waaronder er selectie van resistentie kan optreden. Dit verdiepend inzicht is van belang bij het ontwerp van nieuwe alternatieve therapieschema's.

Studies van anderen, en ook onze eigen studies (hoofdstuk 7 en 9) hebben laten zien dat rifampicine, één van de twee hoekstenen van de TBC therapie, een belangrijke rol heeft in de resistentie problematiek in TBC. Daarom hebben we ons in **hoofdstuk 8** toegespitst op rifampicine resistentie en de gevolgen die dat heeft op genetisch niveau. Het blijkt dat naast bekende resistentie genen (stukjes DNA die informatie bij zich dragen over de opbouw van de bacterie) er ook een aantal genen veranderen die coderen voor cel membraan transport, moleculaire efflux en virulentie factoren. We concluderen dat bacteriën, ook al zijn ze resistent voor rifampicine, nog steeds veranderen onder invloed van rifampicine. Mogelijk zijn deze veranderingen en de eiwitten die daarvoor verantwoordelijk zijn een doelwit voor het ontwikkelen van nieuwe geneesmiddelen.

In **hoofdstuk 9, 10 en 11** richten we ons op klinisch-relevante Mtb stammen die veel voorkomen in TBC endemische gebieden, moeilijk behandelbaar zijn, en gemakkelijk antibioticum resistentie ontwikkelen.

In **hoofdstuk 9** hebben we bacteriestammen uit de Beijing-groep die veel voorkomen en prominent geassocieerd zijn met verkrijgen van antibiotica-resistentie vergeleken met bacteriestammen uit de East-African/Indian (EAI) groep, ook veel voorkomend maar niet geassocieerd met deze resistentieproblematiek. Een opmerkelijke bevinding is dat vooral in de stammen uit de Beijing-groep de genen heel gemakkelijk en snel muteren (veranderen), wat gemakkelijk tot resistentie leidt. Het is ook een opmerkelijk brede antibioticum concentratie-reeks waarbinnen de resistentie vorming blijkt te gebeuren. Met dit laboratorium onderzoek kunnen we dus een mogelijke verklaring geven voor de in-de-bacterie gevonden associatie met resistentie in de dagelijkse praktijk.

In navolging hebben we in **hoofdstuk 10** onderzocht in het muis TBC model of het verloop van de infectie, wanneer veroorzaakt door de Beijing stam, anders is dan wanneer veroorzaakt door de EAI stam. Er blijkt geen verschil te zijn, evenmin in de effectiviteit van de behandeling

mits die volledig wordt gevolgd. Echter, in geval van een niet volwaardige behandeling (te korte duur en te weinig doses, als simulatie van een therapie-ontrouwe patient) dient de resistentie problematiek zich aan in de Beijing infectie, maar niet in de EAI infectie.

We weten dat therapie-ontrouw bij de TBC patiënt in de endemische gebieden nog altijd een realistisch gegeven is en dat nieuwe krachtige middelen (nog) niet beschikbaar zijn voor behandeling. Voor ons is het dan ook de ultieme uitdaging om, met onze verkregen kennis aangaande rifampicine, in het model van de Beijing infectie te onderzoeken wat de waarde is van intensivering van de rifampicine behandeling. Het doel van dit onderzoek, beschreven in **hoofdstuk 11**, was een succesvolle behandeling te verkrijgen met een hogere dosering van rifampicine bij een korte behandelingsduur. De resultaten laten zien dat een therapie verkorting van 6 naar 2 maanden gepermitteerd is mits een 8-voudige toename van de rifampicine dosering gegeven wordt; de behandeling die door de muizen goed wordt verdragen is succesvol, er is geen relaps van TBC 3 maanden na beëindigen van de behandeling, en er is geen ontwikkeling van resistentie.

We hopen dat met boven beschreven onderzoek we een aantal puzzelstukjes hebben aangeleverd, en dat de grote puzzel die tot eradicatie van TBC wereldwijd moet leiden verder kan worden gelegd.

Appendices

PhD Portfolio

Dankwoord

CURRICULUM VITAE

Naam:	Jurriaan Evert Mathijs de Steenwinkel
Geboortedatum:	13 mei 1977
Geboorteplaats:	Brussel
1989-1995:	VWO aan het Maerlant Lyceum in Den Haag
1996-2003:	Biomedische Wetenschappen aan de Universiteit Leiden
2000-2003:	Geneeskunde aan de Universiteit Leiden
2003-2005:	Co-schappen geneeskunde
2005-2012	Promotieonderzoek in het *Mycobacterium tuberculosis* project van de afdeling Medische Microbiologie en Infectieziekten in het Erasmus MC
2006-2012	Arts-assistent in opleiding tot arts microbiologie

Promotor:	Prof.dr. H.A. Verbrugh
Copromotor:	Dr. I.A.J.M. Bakker-Woudenberg
Research school:	Erasmus Postgraduate School Molecular Medicine

PhD ONDERWIJS

-   Molecular Medicine, Erasmus Postgraduate School: "The Animal Imaging Workshop by AMIE" (2008)
-   Molecular Medicine, Erasmus Postgraduate School: "Course: Molecular Diagnostics" (2008)
-   Molecular Medicine, Erasmus Postgraduate School: "2nd symposium and workshops on Molecular Microbiology of Infectious diseases (2008)
-   DOO, Erasmus MC, Rotterdam, Desiderius School: Module Medische Ethiek (2009)
-   DOO, Erasmus MC, Rotterdam, Desiderius School: Module Gezondheidsrecht (2010)
-   Centraal Bureau voor Schimmelcultures (CBS), Institute of the Royal Netherlands Academy of Arts and Sciences (KNAW), Utrecht, Course on Medical Mycology (2010)
-   DOO, Erasmus MC, Rotterdam, Desiderius School: Module Management (2010)
-   Boerhaave cursus / NVMM cursus, Leiden: Medische parasitologische diagnostiek (2010)
-   DOO, Erasmus MC, Rotterdam, Desiderius School: Module Samenwerking (2011)
-   Basiscursus Management voor AIOS Medische Microbiologie, NVMM (2011)

CONGRESSEN EN SEMINARS

2006

- NVMM Regionale Refereeravond Infectieziekten: "Lijninfecties en de IC, Hemato- of On-cologiepatiënten: Zelfde probleem, andere aanpak?"
- NVVM Wetenschappelijke Voorjaarsvergadering
- IUATLD 37th Union World Conference on Lung Health, Parijs, Frankrijk
- NMM Regionale Refereeravond IC, 23 november 2006, Rotterdam, Nederland

2007

- Erasmus MC, "Ruimte voor de Toekomst", Wetenschapsdag AAV 2007
- NVVM Wetenschappelijke Voorjaarsvergadering 2007
- 5th European Congress on Tropical Medicine and International Health; "Partnership and Innovation in Global Health" Amsterdam, Nederland
- KNCV Tuberculosefonds, Symposium: "Op weg naar eliminatie van TB in Nederland"
- KNCV Tuberculosefonds, Symposium: "TB in Vietnam: Can dots control TB in Asia?"
- NVMM nascholing: "MRSA-symposium: van sneldiagnostiek tot behandeling"
- Centrum voor Infectieziekten, refereeravond: "Borreliosis en de ziekte van Lyme"

2008

- 15e Symposium van de NVAMM: "Klein, kleiner, kleinst: kinderinfectiologie"
- Centrum voor Infectieziekten, refereeravond: "Hepatitis B/C"
- Erasmus MC, refereeravond Infectieziekten: "HIV: onbekend maakt onbemind"
- Erasmus MC, refereeravond Infectieziekten: "Catheter-related Bloodstream infections: Prevention, outcome and treatment"
- NVMM Wetenschappelijke Voorjaarsvergadering 2008
- Havenziekenhuis, referee avond Infectieziekten: "Parodontitis en gedissemineerde infec-ties en een niet orale manifestatie van anaërobe mondinfecties i.v.v. arteriosclerose"
- 1st International Workshop on Clinical Pharmacology of Tuberculosis Drugs
- Refereeravond Haven ziekenhuis: Mag u patiënt op reis naar de tropen? Refereeravond SDD op de Intensive Care: "SDD op de IC; een zege of een zonde?"
- Avondonderwijs Longziekten: "Immune Reconstitution Inflammatory Syndrome and TB"
- Nascholing Tropische Geneeskunde, Havenziekenhuis: Importziekte voor jong en oud.
- Rodent tissues training fluorescent diagnostics, Maasstad Ziekenhuis Rotterdam.

2009

- Infectieziekten symposium "Dokters in Debat"
- NVAMM symposium "Infectiepreventie Paniek onder controle?"
- NVMM Wetenschappelijke Voorjaarsvergadering 2009

- Infectieziekten symposium "Timing is everything"
- Wetenschapsdag MMI 2009, World Trade Center Rotterdam
- RIVM, Bilthoven, Nederlandse Tuberculose Diagnostiek Dagen

2010

- 3rd International Workshop on Clinical Pharmacology of Tuberculosis Drugs
- Klinische virologie onderwijsdag, Rotterdam, HIV
- Wetenschapsdag MMI 2010, World Trade Center Rotterdam
- NVAMM, 17e Symposium, Het lab van straks, Microbiologie in de toekomst
- Erasmus MC zorgacademie, Basis Acute Zorg: 'ABCDE Methode, BLS, AED en PBLS'

2011

- NVAMM, 18e Symposium NVAMM, Vaccinologie, Beyond trails and errors
- NVMM Wetenschappelijke Voorjaarsvergadering 2011
- 4th International Workshop on Clinical Pharmacology of Tuberculosis Drugs
- NVMM Wetenschappelijke Najaarsvergadering 2011

2012

- Desideriusschool: Implementatietraining modernisering medische vervolgopleidingen; "Implementatietraining Medische Microbiologie"
- Symposium "Therapeutic Drug Monitoring (TDM): makes a good drug better" Nascholing op het gebied van antimcobiële middelen, 19 januari 2012, Rotterdam
- Symposium on Carbapenemase-producing organisms: the beginning of the end?

ONDERWIJS

- 2006-2012: Supervisie van 2de-jaars studenten Geneeskunde tijdens het vaardigheid onderwijs in thema: Infectieziekten en immuun stoornissen.

PRESENTATIES

- IUATLD 37th Union World Conference on Lung Health, 2 november 2006 Parijs, oral presentation entitled: Mycobacteria attacked with a TROIAN-trick.
- Landelijk overleg *Mycobacterium tuberculosis* onderzoek, 9 januari 2007, RIVM, Bilthoven, oral presentation entitled: *Mycobacterium tuberculosis* research in Rotterdam.

- Voorjaarsvergadering van de Nederlandse Vereniging voor Medische Microbiologie, 16-18 april 2007 Papendaal, poster presentation entitled: Mycobacteria attacked with TROIAN-therapy.
- Junior Med School 2007, Rotterdam, oral presentation voor 6 VWO scholieren met interesse in Geneeskunde, Hoe is het om onderzoek te doen?
- VMT training dierverzorging DM III niveau, Rotterdam, oral presentation voor EDC medewerkers, BVF over de veiligheidsaspecten van het werken met *Mycobacterium tuberculosis*.
- 5th European Congress on Tropical Medicine and International Health, May 24-28, 2007 Amsterdam, The Netherlands, poster presentations entitled: Different parameters to evaluate infection progress and therapy response in mice infected with *Mycobacterium tuberculosis* and their relevance to clinical practice and will Mycobacteria fall for the TROIAN-trick?
- 1st International Workshop on Clinical Pharmacology of Tuberculosis Drugs, 15 May 2008, Toronto, Canada, oral and poster presentation, "A BALB/c mouse tuberculosis model well defined by histopathology, mycobacterial load and cytokine expression, including a simulation of relapse, to assess infection progression and therapy efficacy"
- Refereermiddag Havenziekhuis, Rotterdam 2008, oral presentation over de principes van de IGRA, Interferon Gamma Release Assays
- Boerhaave cursus / NVMM cursus, Leiden 2009, Cursus Medische parasitologische diagnostiek, oral presentation over Congenitale Toxoplasmose
- Research presentatie Mycobacteriële Werkgroep Bespreking RIVM, Bilthoven 2009, oral presentation entitled: Tuberculosis research on Endemic strains
- Erasmus MC, Research Master Infection and Immunity Summer Course II, Rotterdam 2009, oral presentation entitled: Tuberculosis: pathogenesis and therapy, research in a mouse TB model
- Haven Ziekenhuis Klinische Les, afdeling parasitologie en klinische chemie, Rotterdam 2010, Tuberculose diagnostiek, de ziekte en therapie
- 3rd Workshop on Clinical Pharmacology of TB Drugs, Boston, September 11th 2010: Time-kill kinetics of anti-tuberculosis drugs, and emergence of resistance, in relation to metabolic activity of *Mycobacterium tuberculosis*
- Workpackage presentation of the Erasmus MC on the 1st Full Consortia Meeting of PreDiCT-TB; Madrid 2011, A model-based preclinical development of anti-TB drug combinations.
- 4th International Workshop on Clinical Pharmacology of TB Drugs, 14, September 16th 2011, Chicago (USA) Rifampicin concentration effect relationships for resistance development differ between *Mycobacterium tuberculosis* genotypes,
- Project presentatie op de Kick-off meeting van het NanoNextNL-Drug Delivery programma: 13 october 2011, Utrecht.

- Emergence of multidrug resistant TB may be related to lower intrinsic susceptibility of Beijing genotype strains to rifampicin, Najaarsvergadering NVMM / VIZ 2011, 17 November 2011, Rotterdam
- New insights question the current rifampicin dose in tuberculosis treatment, Scientific Spring Meeting KNVM & NVMM 2012 Parallel session on Mycobacterial disease Tuesday 17 April 2012, Papendal

PUBLICATIES

- HLA-G transactivation by cAMP-response element-binding protein (CREB). An alternative transactivation pathway to the conserved major histocompatibility complex (MHC) class I regulatory routes. Gobin SJ, Biesta P, de Steenwinkel JE, Datema G, van den Elsen PJ. J Biol Chem. 2002 277(42):39525-31.
- Diagnosiek van leishmaniasis. de Steenwinkel JE, Verweij JJ, Gyssens IC. Ned. Tijds. Med. Microbiologie. 2005 15(3): 63-66.
- A patient with long-term, unrecognized leishmaniasis. Rabelink NM, de Steenwinkel JE, van Biezen P, van Daele PL, Gyssens IC. Ned Tijdschr Geneeskd. 2006 150(49):2715-9.
- Targeted drug delivery to enhance efficacy and shorten treatment duration in disseminated *Mycobacterium avium* infection in mice. de Steenwinkel JE, van Vianen W, Ten Kate MT, Verbrugh HA, van Agtmael MA, Schiffelers RM, Bakker-Woudenberg IA. J Antimicrob Chemother. 2007 60(5):1064-73.
- Tuberculosis mimicking ileocecal intussusception in a 5-month-old girl. de Steenwinkel JE, Driessen GJ, Kamphorst-Roemer MH, Zeegers AG, Ott A, van Westreenen M. Pediatrics. 2008 121(5):e1434-7.
- Immunological parameters to define infection progression and therapy response in a well-defined tuberculosis model in mice. de Steenwinkel JE, de Knegt GJ, ten Kate MT, van Belkum A, Verbrugh HA, Hernandez-Pando R, van Soolingen D, Bakker-Woudenberg IA. Int J Immunopathol Pharmacol. 2009 22(3):723-34.
- Time-kill kinetics of anti-tuberculosis drugs, and emergence of resistance, in relation to metabolic activity of *Mycobacterium tuberculosis*. de Steenwinkel JE, de Knegt GJ, ten Kate MT, van Belkum A, Verbrugh HA, Kremer K, van Soolingen D, Bakker-Woudenberg IA. J Antimicrob Chemother. 2010 65(12):2582-9
- Cutane scedosporiose R. Waalboer, de Steenwinkel JE, Biemans AA, Thio HB. Ned Tijdschr Dermatologie en Venerologie 2010 20(9): 573-4.
- Dynamics of interferon-gamma release assay and cytokine profiles in blood and respiratory tract specimens from mice with tuberculosis and the effect of therapy. de Steenwinkel JE, de Knegt GJ, Ten Kate MT, Verbrugh HA, Ottenhoff TH, Bakker-Woudenberg IA. Eur J Clin Microbiol Infect Dis. 2012 31(6):1195-201.

- Course of murine tuberculosis and response to first-line therapy depends on route of infection and inoculum size. de Steenwinkel JE, ten Kate MT, de Knegt GJ, Verbrugh HA, van Belkum A, Hernandez-Pando R, Bakker-Woudenberg IA. Int J Tuberc Lung Dis. 2011 15(11):1478-84.
- Drug susceptibility of *Mycobacterium tuberculosis* Beijing genotype, association with MDR-TB. de Steenwinkel JE, ten Kate MT, de Knegt GJ, Kremer K, Aarnoutse RE, Boeree MJ, Verbrugh HV, van Soolingen D, Bakker-Woudenberg IA. Emerg Infect Dis. 2012 18(4):660-3
- Consequences of non-compliance on therapy efficacy and emergence of resistance in murine tuberculosis caused by the Beijing genotype. de Steenwinkel JE, Ten Kate MT, de Knegt GJ, Verbrugh HA, Aarnoutse RE, Boeree MJ, den Bakker MA, van Soolingen D, Bakker-Woudenberg IA. Antimicrob Agents Chemother. 2012 56(9):4937-44

DANKWOORD

Dank! Dank voor het lezen van dit proefschrift en niet alleen het dankwoord. Dank voor de inspiratie en motivatie, die gediend hebben als fundament voor het schrijven van dit proefschrift. Dank voor het geschonken vertrouwen in mij en het TB onderzoek. Dank voor alle hulp met het denken over de opbouw van de studies, uitvoeren van de vele experimenten en verwerken van de resultaten. Het onderzoek had simpelweg niet kunnen gebeuren zonder deze eindeloze hulp. Dank voor het delen, drinken en halen van Brand, Hertog Jan en Jupiler, ze waren van tijd tot tijd essentieel om de vrolijke kanten te kunnen belichten. Dank voor het begrip als ik weer eens probeerde veel te veel te plannen in een dag, waardoor ik of een manuscript hopeloos te laat kwam. Maar bovenal; dank voor al het lachen, luisteren en de liefde. Als jij je bij één (of meer) van de bovengenoemde dankbetuigingen aangesproken voelt, dan klopt dit ook. Ik schreef dit dankwoord met **jou** in gedachte!